REGULATION OF ENDOCYTOSIS BY ULTRASOUND AND MICROBUBBLE TREATMENT: POTENTIAL FOR CONTROLLED CELLULAR DELIVERY OF DRUGS TO CANCER CELLS

by
Farnaz Fekri
Bachelor of Science, Ryerson University, 2014

A dissertation
presented to Ryerson University
in partial fulfillment of the
requirements for the degree of
Doctor of Philosophy
in the program of
Molecular Science

Toronto, Ontario, Canada 2019

Author's Declaration

I hereby declare that I am the sole author of this dissertation. This is a true copy of the dissertation, including any required final revisions, as accepted by my examiners.

I authorize Ryerson University to lend this dissertation to other institutions or individuals for the purpose of scholarly research. I further authorize Ryerson University to reproduce this dissertation by photocopying or by other means, in total or in part, at the request of other institutions or individuals for the purpose of scholarly research.

I understand that my dissertation may be made electronically available to the public.

Regulation of endocytosis by ultrasound and microbubble treatment: potential for controlled cellular delivery of drugs to cancer cells

Farnaz Fekri

Doctor of Philosophy, 2019

Molecular Science, Ryerson University

Abstract

The delivery of therapeutics across biological barriers is a limiting factor in achieving ideal pharmacologic responses in patients. Modulating endocytic mechanisms with targeted, clinically-relevant interventions can increase intracellular delivery across biological barriers, and improve the efficacy of drugs. Ultrasound-microbubble (USMB) is a novel targeted delivery strategy that has shown promising potential in both diagnostic and therapeutic applications. The collective behaviour of microbubbles in the acoustic field can increase the plasma membrane permeability of surrounding cells, and enhance the delivery of therapeutics across biological barriers. USMB achieves the intracellular delivery of drugs through sonoporation and modulation of endocytic pathways, but the type of endocytic pathways and the mechanisms of activation were not known. I identified that, under distinct regulations, USMB enhances the rate of both clathrin-mediated endocytosis, as well as a non-receptor-mediated pathway responsible for internalizing bulk fluid into cells. I discovered that lysosome exocytosis and acid-sphingomyelinase are required for the regulation of the clathrin-mediated pathway but not fluid-phase endocytosis following USMB treatment. Given the potential of the clathrin-independent pathway to form high capacity carries for the uptake of fluids and therapeutics into cells, I aimed to identify the molecular identity of the proteins that drive the formation of non-clathrin coated vesicles following USMB treatment. I established that flotillins contribute to the USMB-induced vesicular uptake of fluid into cells, a phenomenon that depends on palmitoyltransferase DHHC5 and the Src-family kinase Fyn. Furthermore, I confirmed that USMB treatment can enhance the

intracellular delivery of chemotherapeutic drugs such as cisplatin, and improve its therapeutic efficacy in a flotillin-dependent manner. This project established that both clathrin-mediated endocytosis and flotillin-dependent endocytosis can be modulated by clinically-relevant USMB treatments to enhance drug uptake and efficacy, revealing an important new strategy for targeted drug delivery in cancer treatment.

Acknowledgement

I would like to thank my supervisors, Dr. Costin Antonescu and Dr. Raffi Karshafian, for their unconditional support, mentorship and trust throughout my graduate career. They have truly had a profound impact on my life and have taught me not just to be a diligent scientist but to live my life with passion, compassion and kindness.

I would like to thank my graduate committee members Dr. Gupta and Dr. Kuebler for their continuous feedback and guidance. I would also like to thank Dr. Botelho, who participated in my PhD transfer committee—without his advice I would have never embarked on the journey of scientific research.

Thank you to all of the members of the Antonescu, Botelho and Karshafian labs both past and present. Special thanks to soon to be Drs. Stephen Bautista, Stefanie Lucarelli and Victoria Hipolito, who embarked on this journey with me five years ago. I could not have asked for kinder and stronger friends to stand beside me throughout this remarkable journey.

Lastly, I would like to thank my partner Pouya, my mother and father, my sisters Ferial and Farnia, and my best friend Sepideh, for without their continuous support, love, and encouragement, I would not be where I am today.

Table of Contents

Author's Declaration ***ii***

Abstract ***iii***

Acknowledgement ***v***

List of Figures ***ix***

List of Appendices ***xi***

Abbreviations ***xii***

Chapter 1 Introduction ***1***

1.1 Drug delivery strategies: a new era in cancer treatment **2**

1.2 Pharmacokinetics and drug efficacy **4**

1.3 Drug delivery strategies to improve pharmacokinetics **10**

1.3.1 Biopharmaceuticals 12

1.3.2 Liposomal drug delivery systems 13

1.3.3 Nanoparticle drug delivery systems 15

1.3.3.1 Active targeting of nanoparticles using magnetic force 16

1.3.4 Ultrasound and microbubbles 18

1.3.4.1 Ultrasound 18

1.3.4.2 Transducers 20

1.3.4.3 Natural cavitation 21

1.3.4.4 Microbubble responses in the acoustic field 23

1.3.4.5 Microbubble safety 26

1.3.4.6 The biomedical applications of microbubbles 27

1.3.4.7 Ultrasound and microbubble mechanisms of drug delivery 31

1.4 Endocytosis as the entry pathway of drugs to cells upon USMB treatment **33**

1.5 Clathrin-mediated endocytosis **35**

1.6 Clathrin-independent endocytosis **42**

1.6.1 Complexity in defining CIE highlighted by GPI-APs studies 44

1.6.2 Diversity of the molecular mechanisms of CIE subclasses 45

1.6.3 Endocytic pathway mediated by Rho family of GTPases 47

1.6.4 GEEC pathway 48

1.6.5 Caveolae-mediated endocytosis 50

1.6.6 Macropinocytosis 52

1.6.7 Flotillin-dependent endocytosis 55

1.6.7.1 Flotillin's role in endocytosis 57

1.6.7.2 Flotillins as a signalling platform 59

1.6.8 Calcium-induced massive endocytosis 60

1.6.8.1 DHHC5, a key regulator of MEND pathways 61

1.7 Membrane repair following injury activates endocytosis **66**

1.7.1 Ceramide as a modulator of endocytosis 71

1.7.2 Role of acid-sphingomyelinase in ceramide-induced endocytosis 74

1.8 Hypothesis **75**

Chapter 2 Materials and Methods ***83***

2.1 Materials **84**
2.2 Cell lines and cell culture **84**
2.3 Ultrasound treatment **84**
2.4 Inhibitor and drug treatments **85**
2.5 Plasmid and siRNA transfections **86**
2.6 CRISPR/Cas9 genome editing **87**
2.7 HRP and fluorescent dextran fluid-phase internalization assay **87**
2.8 Immunofluorescence staining **88**
2.9 Fluorescent transferrin uptake and EEA1 immunofluorescence staining **88**
2.10 Fluorescence microscopy **89**
2.11 Image analysis **90**
2.12 Immunoblotting **92**
2.13 Cell viability measurements **93**
2.14 Statistical analysis **94**
Chapter 3 Results: The mechanisms of USMB-induced clathrin-mediated endocytosis ***95***
3.1 Chapter 3 rationale **96**
3.2 USMB treatment rapidly enhances the rate of clathrin-mediated endocytosis **96**
3.3 USMB treatment alters the properties of clathrin-coated pits **97**
3.4 USMB-stimulated fluid-phase uptake is delayed relative to the onset of increased CME **99**
3.5 Lysosome exocytosis occurs after USMB treatment **100**
3.6 Vacuolin-1 inhibits USMB-stimulated reduction of cell surface TfR without affecting the enhanced fluid-phase uptake **100**
3.7 Desipramine inhibits USMB-stimulated reduction of cell surface TfR **101**
3.8 Desipramine synergizes with USMB treatment to enhance fluid-phase uptake **101**
Chapter 4 Results: USMB treatment elicits fluid uptake via flotillin-mediated pathway ***112***
4.1 Chapter 4 rationale **113**
4.2 USMB treatment triggers flotillin-dependent fluid-phase endocytosis **113**
4.3 Enhanced flotillin-dependent fluid-phase uptake induced by USMB requires DHHC5 **116**
4.4 Enhanced flotillin-dependent fluid-phase uptake induced by USMB requires Fyn **118**
4.5 Enhanced flotillin-dependent uptake induced by USMB enhances drug uptake and action **119**
Chapter 5 Discussion ***132***
5.1 USMB enhances the rate of CME and fluid-phase uptake **133**
5.2 Lysosome exocytosis upon USMB treatment **134**

5.3 Regulation of CME by USMB treatment **135**
5.4 Regulation of fluid-phase endocytosis by USMB treatment **138**
5.5 Palmitoylation of membrane proteins **139**
5.6 DHHC5-dependent control of fluid-phase endocytosis **139**
5.7 Flotillin-dependent endocytosis is tuneable by a Fyn and DHHC5 signalling pathway **142**
5.8 Enhanced endocytosis by USMB treatment is an effective strategy for targeted drug delivery **145**
Chapter 6 Future direction ***149***
6.1 Detailed mechanism of flotillin-dependent endocytosis **150**
6.2 Identifying the intracellular target of desipramine **152**
6.3 Increasing the delivery of trastuzumab using USMB and desipramine treatment **154**
Conclusion ***157***
Appendices ***160***
Bibliography ***171***

List of Figures

Figure 1.1. Different acoustic behaviours of microbubbles. 78

Figure 1.2. Endocytic pathways can be subdivided into two major categories of clathrin-dependent and clathrin-independent pathways in cells. 79

Figure 1.3. Flotillins undergo dynamic rearrangement at the plasma membrane to actively participate in cell signalling and membrane trafficking events. 80

Figure 1.4. Dynamic palmitoylation regulates the localization of proteins at the plasma membrane and can influence membrane-associated processes and signalling events. 81

Figure 1.5. Plasma membrane repair pathway involves exocytosis of lysosomes followed by the activation of compensatory endocytosis 82

Figure 3.1. USMB treatment rapidly reduces cell surface TfR levels. 103

Figure 3.2. USMB treatment enhances the rate of Transferrin uptake. 104

Figure 3.3. USMB treatment alters the properties of clathrin-coated pits 105

Figure 3.4. USMB treatment results in a delayed increase in fluid-phase internalization. 106

Figure 3.5. USMB treatment increases the cell surface abundance of the lysosomal marker LAMP1. 107

Figure 3.6. Vacuolin-1 treatment impairs the reduction in cell surface TfR levels by USMB treatment. 108

Figure 3.7. Vacuolin-1 treatment does not affect the regulation of fluid-phase endocytosis by USMB treatment. 109

Figure 3.8. Desipramine treatment impairs the reduction in cell surface TfR levels by USMB treatment. 110

Figure 3.9. Desipramine enhances the rate of fluid-phase uptake in USMB-treated cells. 111

Figure 4.1. Flotillin is required for USMB-induced fluid uptake. 123

Figure 4.2. USMB treatment regulates flotillin cell surface levels, dynamics and internalization. 124

Figure 4.3. DHHC5 is required for USMB-triggered flotillin and fluid-phase internalization. 126

Figure 4.4. USMB treatment regulates DHHC5. 127

Figure 4.5. Expression of a phosphorylation-defective mutant of DHHC5 impairs flotillin internalization elicited by USMB treatment. 128

Figure 4.6. Fyn is required for USMB-triggered flotillin and fluid-phase internalization. 129

Figure 4.7. USMB treatment enhances cisplatin-mediated DNA damage and death in breast cancer cells in a flotillin-1 dependent manner. 130

List of Appendices

Figure A3.1. Full image panels for TIRF-M images shown in Figure 3.1. 161

Figure A3.2. Diagram depicting the timing of measurements of membrane traffic used in this study. 162

Figure A3.3. Quantification of cellular fluorescence intensity, used for measurement of cell surface TfR and LAMP1, Tfn uptake and FITC-dextran uptake. 163

Figure A4.1. Flotillin knockdown and immunofluorescence detection. (A) RPE cells were transfected with siRNA targeting flotillin-1 and -2 (flotillin) or non-targeting siRNA (control). 164

Figure A4.2. DHHC5 knockdown and transfection. (A) RPE cells were transfected with siRNA targeting DHHC5 or non-targeting siRNA (control). 166

Figure A4.3. Fyn knockdown. RPE cells were transfected with siRNA targeting Fyn or nontargeting siRNA (control). 168

Figure A4.4. Flotillin knockout cells and contribution of flotillin to cell viability in USMB treated cells. 169

Abbreviations

A488-dextran
: Dextran, Alexa Fluor 488

AP-2
: adaptor protein complex 2

ARF6
: ADP-ribosylation factor 6

A-SMase
: acid-sphingomyelinase

BAR
: Bin/amphiphysin/Rvs

CCP
: clathrin-coated pit

CCV
: clathrin-coated vesicle

CDDP
: cisplatin

CIE
: clathrin-independent endocytosis

CLIC
: clathrin-independent tubulovesicular carriers

CME
: Clathrin-mediated endocytosis

CTxB
: cholera toxin B subunit

Cyst
: Cystein

DAT
: dopamine transporter

DHHC5
: palmitoyl acyl transferase 5

DMSO
: dimethyl sulfoxide

EEA1
: Early Endosome Antigen1

EGF
: epidermal growth factor

EGFR
: epidermal growth factor receptor

ER
: endoplasmic reticulum

FEME
: fast endophilin-mediated endocytosis

FITC-dextran
: fluorescein dextran

GAP
: GTPase-activating-protein

GEEC
: GPI-enriched endosomal compartments

GEF
: guanine nucleotide exchange factor

GFP
green fluorescent protein
GPCR
G protein-coupled receptor
GPI
glycosylphosphatidylinositol
GPI-APs
glycosylphosphatidylinositol-anchored proteins
GRAF1
GTPase regulator associated with focal adhesion kinase1
HRP
horseradish peroxidase
IGF-1
insulin-like growth factor 1
IL-2R
interleukin 2 receptor
LAMP-1
lysosomal-associated membrane protein-1
LDL
low-density lipoprotein
MAPK
mitogen-activated protein kinase
MEND
massive endocytic events
mPTP
mitochondrial permeability transition pore
NPC1L1
Niemann-Pick C1-like 1 protein
N-SMase
neutral sphingomyelinase
PAT
palmitoyl acyl transferases
PI(3)P
Phosphatidylinositol 3-phosphate
PI3K
phosphoinositide 3-kinase
PtdIns(3,4,5)P_3
Phosphatidylinositol (3,4,5)-trisphosphate
PtdIns(4,5)P_2
phosphatidylinositol (4,5)-bisphosphate
RPE
retinal pigment epithelium
RTK
receptor tyrosine kinase
SLO
pore-forming toxin streptolysin O
SMase
sphingomyelinase
SNARE
soluble N-ethlymaleimide-sensitive factor attachment protein receptor
SV40
simian virus 40
Tfn

iron-bound transferrin

TfR
transferrin receptor

TGN
trans-Golgi network

TIRF
internal reflection fluorescence

TIRF-M
total internal fluorescence microscopy

TNFα
tumour necrosis factor-alpha

Chapter 1 Introduction

1.1 Drug delivery strategies: a new era in cancer treatment

As a major cause of death, cancer has become the number one focus for pharmaceutical research around the world. According to cancer report, in 2006-2007, the United States alone contributed $6.5 billion in oncology research and about $2.23 billion in drug research & development, with European countries coming in second with a combined $3.0 billion of investment in cancer research (Kanavos et al., 2010). The cancer related incidence and mortality rates show no sign of slowing down, as it is estimated that by 2030, there will be 27 million new cases of cancer and 16 million cancer-related deaths worldwide. Correspondingly, R&D costs will continue to rise and are expected to reach $165 billion by 2020 (Kanavos et al., 2010).

A quick look at the annual reports of the cancer research landscape confirms that the shortcoming in finding the cure cannot be attributed to the lack of investment or effort in the field. For decades, cellular biology research has been motivated by molecular targeted therapy approaches to identify and target molecules that are over expressed or that undergo abnormalities in function. The sole focus on molecular target therapies has not been entirely successful as treatment strategy due in part to the diversity of solid tumours, mutational cross-talk, the microenvironment of the tumour itself, as well as limitations in drug delivery strategies. Instead of a sole focus on molecular target identities, it is more likely that the successful transition of a newly discovered drug into clinics and a better treatment outcome will be a combination of the molecular target identification, drug discovery, and innovations in delivery systems.

Undoubtedly, safe and effective delivery of anti-cancer drugs has remained one of the major challenges in the oncology field. These challenges have initiated the notion that designing strategies and vehicles to the ensure safe and efficient drug delivery to a particular site at the correct time is as valuable as discovering new drugs. The recognition of this reality over the past

10 years has helped to shift the focus to more advanced therapeutic strategies, such as nanoparticle-based treatments, liposomal delivery systems, and antibody-based therapeutics. The emerging field of targeted drug delivery tries to address one of the most fundamental obstacles in the drug treatment of any disease: how to target and enhance drug delivery to maximize safety, increase efficacy and improve therapeutic outcome. After all, the efficacy of the treatment does not entirely rely on the physiochemical properties of the drug, but also on the delivery strategies that control the pharmacokinetic parameters and improve the therapeutic profile of the drug.

Developing new strategies that facilitate the targeted and enhanced delivery of therapeutics across biological barriers can improve the bioavailability and effectiveness of existing drugs to achieve better treatment outcomes. Due to ongoing challenges in oncology—such as the unique genetic fingerprint of each patient, identifying new molecular targets and designing drugs for overabundant molecular targets—a single scientific discipline cannot overcome the hurdles alone. It is the goal of this thesis to show that at the end it is the collaboration among a wide range of experts (including physicists, chemists, biochemists and engineers) that can stimulate creativity and foster innovation to overcome cancer and other complex diseases in our lifetime.

My project focuses on a novel drug delivery strategy known as ultrasound microbubble (USMB) treatment. In order to better illustrate the necessity for the utilization of more advanced delivery strategies, the next chapter will focus on describing the parameters that limit drug efficacy in the body and advancements in the field that address these challenges.

1.2 Pharmacokinetics and drug efficacy

Pharmacokinetics is the study of the absorption, distribution, metabolism and excretion of therapeutic compounds. These four processes together affect the pharmacological responses of drugs inside the body, and determine the target site's actual exposure to drugs following administration (Turner & Agatonovic-Kustrin, 2007). On the other hand, pharmacodynamics describe the relation between the concentration of drugs at the site of action, and the resulting therapeutic response (Pacey, Workman, & Sarker, 2011). Understanding the relationship between these two principles is an essential part of any pharmacological research as it helps to shape part of the successful transition of drugs into clinical practice following initial discovery. Although the clinical transition of drugs does not entirely depend on physiochemical properties, as the therapeutic profile is also influenced by factors including the patient's condition (e.g. renal failure, obesity, dehydration, etc.) as well as individual physiology (including sex, age, genetic makeup) (Le, 2017). Therefore, a clear grasp of the pharmacological properties of drugs, as well as the patient's related features, is necessary in anticipating the pharmacokinetic and pharmacodynamic parameters required for effective therapeutic management of drugs based on individual patient needs (Turfus, Delgoda, Picking, & Gurley, 2017).

In pharmacokinetics, bioavailability describes the total drug exposure or the rate by which the active drug ingredient reaches systemic circulation (Chow, 2014). One of the factors that can significantly influence the bioavailability of a drug is the choice of the appropriate administration route for the delivery of the therapeutic compound to the body. The goal is to employ methods that can maximize the bioavailability with high efficiency and limited toxicity (Wen, Jung, & Li, 2015).

Current routes of administration are broadly categorized into: the enteral and the parenteral routes. The enteral route of drug delivery involves the absorption of the drug via the gastrointestinal tract—it includes oral, gastric, duodenal and rectal administration (Bardal, Waechter, & Martin, 2011). Among the possible enteral routes, oral administration is the most frequently used method due to simplicity, convenience and patient compliance. However, the limitations of this route exceed its advantages, as the bioavailability of orally administered drugs can vary significantly for a number of reasons. The two most important reasons include the need to bypass added biological barriers such as the intestinal epithelium and the exposure to first-pass metabolism in the liver prior to distribution in the systemic circulation (Hale & Abbey, 2017; Hebert, 2013). Other factors that can affect the absorption of orally administered drugs include: stability of the drug to gastric acid, gastric emptying time, intestinal motility, intestinal transit time, the effect of food consumption on the rate of absorption, and intestinal metabolism (Perrie & Rades, 2012).

Parenteral administration refers to any route of administration that does not involve drug absorption via the gastrointestinal tract. It includes the intravenous (IV), intramuscular (IM), subcutaneous (SC or SQ), and transdermal routes. Parenteral is preferred over enteral route for administration of water-soluble drugs with low oral bioavailability, or when fast action is required (Perrie & Rades, 2012). Normally, the direct injection of drugs into the bloodstream results in 100% bioavailability, while the extent of the drug's availability when administered via extravascular routes can be influenced by factors such as enzymatic activity, gastric acidity, hepatic blood flow, intestinal residence time, and protein binding (Hebert, 2013).

The distribution of the drug at the site of action involves its transfer between the systemic circulation and tissues. The pharmacological effects and the intensity of drug actions are directly

related to the concentration of the drug at the target area (Campbell & Cohall, 2017). Since it is challenging to measure the drug concentration at the site of action, the concentration of the drug in the blood or in plasma is taken as the direct representation of tissue distribution, and is referred to as drug-plasma concentration (Mittal, 2017). In order to achieve therapeutic success, the desired drug-plasma concentration must be within the therapeutic window, which is a defined range between minimum effective concentration and maximum safe concentration (Hebert, 2013). Once the drug's rate of exchange between the circulation system and the tissues equals the rate of elimination, the plasma concentration reaches the maximum level or peak plasma concentration—a point that corresponds to the maximum pharmacological response of a drug (Jambhekar & Breen, 2012). Mainly, drug distribution to tissues is affected by factors such as blood perfusion, plasma protein binding, regional pH and the permeability of the cell membrane (Lu & Xue, 2019). The extent of drug distribution to tissues can also be expressed as volume distribution, which refers to a theoretical volume that the administered dose must be diluted in to give the desired concentration in plasma. Volume distribution is assessed as the ratio of the administered dose over its concentration in the plasma, and it is a useful parameter for estimating the dose required to achieve a desired plasma concentration (Lu & Xue, 2019). The volume distribution is directly influenced by the physiochemical properties of the drug. For example, small hydrophilic drugs or drugs that exhibit significant tissue protein binding (e.g. binding to carriers and transporter) can distribute extensively in the body, and therefore have high volume distribution values, while drugs with low lipid solubility or significant plasma protein binding display limited distribution and have low volume distribution values (Davis et al., 2011; Hebert, 2013).

The mode of delivery is not the only factor influencing the pharmacological profile of drugs. Following delivery, drugs must be absorbed through one more layer of epithelial cells to reach their target sites. Drugs cross the cell membrane via either passive diffusion, facilitated passive diffusion or endocytosis (Perrie & Rades, 2012). Passive diffusion is the movement of molecules down the concentration gradient, and it depends on the physiochemical characteristics of the drug, such as lipophilicity, size, degree of ionization, partition coefficient as well as the area of absorption (Backes, 2007; Le, 2017; Sultatos, 2007; Turfus et al., 2017). For small molecules that can penetrate membranes, the rate of diffusion is dictated by the ionization degree of the drug, which corresponds to the solubility of the drug in lipid versus aqueous phases. Since most drugs are weak acids or bases, the pH of the environment highly influences their ionization state, and consequently, the degree of the penetration of a drug through membranes. As an example, aspirin is a weakly acidic drug, and thus predominantly exists in its non-ionic form in the acidic environment of the stomach, which favours its diffusion through the gastric mucosa (Forrester et al., 2016).

For facilitated passive diffusion, drugs utilize carriers to cross the plasma membrane down a concertation gradient, while active transporters rely on ATP hydrolysis to transport drugs against their concentration gradient (Perrie & Rades, 2012). The utilization of transport systems can significantly increase the accumulation of drugs in the cell. For instance, pirarubicin which is a pyranyl derivative of doxorubicin uses the glucose (pyranose) transport system and as such has a 3- to 4-fold faster cellular uptake than doxorubicin (another anthracycline) (Fang, Nakamura, & Maeda, 2011). For carrier-mediated transport, drugs must have specific molecular configurations in order to properly interact with transport systems of cells. Additionally, the rate of entry is limited by the availability of carriers and transporters, and can be significantly

reduced with the presence of competing substances. Different endocytic mechanisms such as receptor-mediated (through binding to specific receptors on the plasma membrane) or non-receptor-mediated mechanisms provide another route for the entry of drugs into cells (Bardal et al., 2011; Perrie & Rades, 2012). Endocytic pathways will be covered in greater detail in later sections.

Aside from tissue-related characteristics that lead to drug uptake into target cells, drug distribution is also affected by drug clearance from the body through both hepatic metabolism and renal excretion. Knowing the rate of clearance for any particular drug is essential for predicting the dosing schedule and the plasma membrane steady-state concentration for a given dose (Kenakin, 2009). For most drugs, the clearance begins by the process of biotransformation, when portions or the entire drug undergoes chemical modification. The liver is the main but not the sole site of biotransformation, as metabolism can also occur at other sites, including the gastrointestinal mucosa, lungs and kidneys (Liu, Wang, Liang, & Roberts, 2017). Biotransformation usually involves two phases: in the first phase (reaction of functionalization), the existing functional group is modified or a new functional group is created by oxidation, reduction or hydrolysis reaction, and in the second phase (reaction of conjugation), the modified drug gets conjugated to an endogenous molecule such as glucuronic acid, sulfuric acid, acetic acid, glutathione, etc. (Tillement & Tremblay, 2007). Generally, drugs undergo biotransformation to form metabolites that are less lipophilic than the parent drug, in order to assist with their elimination in urine or bile. However, there are exceptions, as some drugs can get excreted without undergoing modification, or the parent drug must undergo biotransformation in order to activate the prodrug (Liu et al., 2017).

The kidneys are the primary organs responsible for processing the excretion of drugs or their metabolites from the body. Renal excretion occurs through glomerular filtration, active tubular secretion, and passive tubular reabsorption (Lu & Xue, 2019). Once unchanged (not having undergone biotransformation) or modified drugs (having undergone biotransformation) arrive at the kidneys, free hydrophilic drugs with low molecular weights filter through the pores of the glomerulus epithelial cells into the renal tubes. On the other hand, charged or protein-bound drugs are transported from the peritubular capillaries to the tubular lumen via the action of organic anion transporter and the organic cation transporter families. Once in the renal tube, the non-ionized, lipophilic drugs are reabsorbed back through passive diffusion in the distal tube and must undergo biotransformation prior to renal excretion (Bardal et al., 2011). Aside from the physiochemical properties of the drug or its secondary metabolites, the pH of the urine can also affect the rate of excretion through influencing the ionization state of the drug. Accordingly, the acidification of the urine increases reabsorption of weak acids and increases the renal excretion of weak bases (Aldred, Buck, & Vall, 2009). Other factors that can influence the rate of clearance include renal blood flow, glomerular filtration rate, concentration of drug, as well as the patient's physiology such as age or kidney diseases (Aldred et al., 2009; Bardal et al., 2011). The secondary route of excretion, especially for polar lipophilic drugs with molecular weights larger than 300 Dalton, is the bile system (Lu & Xue, 2019). These drugs or their metabolites are actively secreted from hepatocyte into the bile, and then transported with the bile to the gut for secretion (Bardal et al., 2011). Excretion of drugs can also occur through the lungs, sweat, saliva, or any other bodily fluids. However, compared to kidneys and bile, the contributions of other systems are minimal (Lu & Xue, 2019).

The aim of this last section was to emphasize that both drug delivery and elimination shape the pharmacological responses of drugs in the body. However, this project only focuses on strategies that increase the intracellular delivery of drugs, and does not address the contribution of drug elimination on therapeutic efficacy.

1.3 Drug delivery strategies to improve pharmacokinetics

Drug delivery strategies can play vital roles in determining the success of drug treatments by influencing the pharmacokinetic profiles of therapeutics. Over the past few years, advances in drug delivery strategies have been focused on optimizing basic approaches to control the rate, duration and the site of the drug's action with the goal of enhancing the therapeutic effects of drugs. The conventional methods of drug delivery—also known as immediate release systems—allow for the fast onset of drug action with no deliberate effort to improve the absorption or distribution of therapeutics in the body, which for some drugs results in poor treatment outcome (Ummadi, Shravani, Raghavendra Rao, Reddy, & Nayak, 2013). Despite some of its disadvantageous, the immediate release systems are the preferred route when a fast-acting response is required, such as relieving pain by administration of painkillers (Perrie & Rades, 2012). On the other hand, modified release delivery systems aim to achieve a better therapeutic objective by enhancing the safety, efficacy and bioavailability of drugs especially for those with narrow therapeutic windows or short half-lives. The modified release delivery system can be broadly differentiated into three categories: delayed release, extended release, and site-specific targeting (Wen et al., 2015). Delayed release refers to a system that modifies the onset time of pharmacological response through altering the timing of the drug release. The delayed-release strategy is the preferred route for orally administered tablets and capsules that must release their contents after a time lag following ingestion, and only when they reach specific regions of the

gastrointestinal tract such as the small intestine or colon (Perrie & Rades, 2012). As an example, delayed formulation is widely used for the treatment of inflammatory bowel diseases. In this case, an anti-inflammatory drug such as budesonide is coated with gastric-resistant polymers such as EUDRAGIT® L to activate the release of the drug only after stomach transit (Bhatt, Naik, & Dharamsi, 2014).

Extended release refers to a strategy that allows for the slow release of drugs over an extended period of time, in order to maintain a uniform blood levels and reduce dose-related adverse effects. This system is especially useful in treatment of chronic diseases or for drugs with short half-lives that require repeated administration at frequent intervals (Andrade, 2015). Extended release can be further categorized into the sustained and controlled systems—in both strategies, the rate of drug release is maintained over a period of time. However, the major difference between the sustained and controlled strategies is that the former is restricted to oral administration, whereas the controlled strategy can be used for a variety of administration methods. Furthermore, compared to the sustained method, controlled strategy maintains steady plasma concentration, and thus the rate of release is the rate-determining step for drug absorption (Perrie & Rades, 2012). Notably, both of these modified release strategies are not able to achieve targeted delivery to diseased tissue.

Targeted delivery refers to strategies that control and limit the release of drugs to specific locations in order to maximize specificity and reduce the toxicity of therapeutics as would occur when drugs are administered systematically and broadly across all tissues. Targeted delivery can be achieved using different strategies, from encapsulating drugs inside proper vehicles to developing therapeutic agents with specific interactions that direct them to a particular location. The next generation of drug delivery systems aims to combine temporal and spatial control of

drug release while improving permeability across cell membranes. Some examples of next generation formulation and delivery systems include liposomal, nanoparticles, microbubbles, and antibody-drug conjugates.

1.3.1 Biopharmaceuticals

Antibody-drug conjugates are an important subclass of biopharmaceuticals. The class of biopharmaceutical encompasses drugs that are developed from biological sources and includes a number of subclasses such as therapeutic monoclonal antibodies, peptides, recombinant therapeutic proteins, and polymer of nucleotides (Jozala et al., 2016). Thanks to their specificity and potency, biopharmaceutical drugs have gained considerable attentions in the last three decades and have extensively contributed to providing new angles for therapeutic interventions across a wide range of diseases. Unfortunately, the structural complexity that results in site-specific delivery comes at the expense of substantial delivery challenges, such as poor membrane permeation (Mitragotri, Burke, & Langer, 2014). In fact, the formulation and delivery of biopharmaceuticals have been the biggest limitations in making them a suitable replacement for conventional drugs in the market. One of the biggest challenges has been the structural modification and subsequent inactivation of biopharmaceuticals in the body, caused by aggregation, deamidation, isomerization, hydrolysis, oxidation and denaturation (Cleland, Powell, & Shire, 1993). Although rational approaches have been used to address the stability of biopharmaceuticals, the risk of potential toxicity and immunogen reactions through the addition of stabilizing agents remains one of the biggest concerns in the effective clinical use of biopharmaceutical drugs (Allison, Chang, Randolph, & Carpenter, 1999; Kerwin, 2008; Rajagopal, Wood, Tran, Patapoff, & Nivaggioli, 2013; Sasahara, McPhie, & Minton, 2003).

Therapeutic monoclonal antibodies demonstrate a great example of the challenges faced in the routine clinical use of biopharmaceutical drugs. Despite their successful and promising introduction to the market, the limitations associated with their delivery in clinical use has negatively affected their performance profile. Therapeutic monoclonal antibodies require particular dosing frequency to achieve the desired therapeutic effects. This poses a particular challenge, as their intravenous delivery requires a long administration time or frequent dosage regimen. Furthermore, due to the Food and Drug Administration's (FDA) volume restrictions on drugs administered via subcutaneous and intramuscular injections, therapeutic monoclonal antibodies are usually administered intravenously, which makes the choice of administration limited (Mitragotri et al., 2014). Increasing the concentration of the dose to achieve the desired effect faces separate issues, such as high viscosity, which negatively impacts the injection capabilities of the formulation. Although approaches such as the addition of inorganic and hydrophobic salts can help in lowering the viscosity, injectability remains a concern as the need for an appropriate needle and a longer injection time strongly impacts patient acceptance and compliance (Du & Klibanov, 2011; Liu, Nguyen, Andya, & Shire, 2005). An alternative solution for the delivery of both biopharmaceuticals as well as small conventional drugs is the use of drug delivery vehicles such as liposomes, nanoparticles, and microbubbles, which I will discuss below.

1.3.2 Liposomal drug delivery systems

The liposomal-based delivery system is one of the most well studied drug vehicles thanks to its promising potential to improve therapeutic safety and efficacy. Liposomes are vesicles consisting of a lipid bilayer that encapsulates an aqueous center (Sercombe et al., 2015). The unique characteristics of liposomes—such as the large aqueous center, biocompatible lipid exterior, and

their ability to self-assemble—permit the encapsulation of molecules (Kulkarni & Shaw, 2016; Rooijen, 1998). In fact, thanks to the ease of modification of liposomes' physical properties including chain length, degree of saturation of acyl chains, composition and size, liposomes can act as vehicles for a wide range of macromolecules such as hydrophobic and hydrophilic drugs, DNA, and proteins (Abbina & Anilkumar, 2018; Monteiro, Martins, Reis, & Neves, 2014).

The first generation liposomal-based delivery system aimed to encapsulate drugs inside delivery vehicles to prevent their early activation and degradation, and increase their residence time in the body (Hua & Wu, 2013; Sercombe et al., 2015; Ulrich, 2002)**.** Later generations were introduced to address the rapid elimination of liposomes by coating the surface with hydrophilic polymer (polyethylene glycol (PEG)), in order to prolong circulation time and reduce the elimination rate from systemic circulation (Northfelt et al., 1996; Torchilin et al., 1992). In recent years, the site-specific delivery of liposomes has been achieved through coupling antibodies, peptides, and carbohydrates on the surface of the liposome to deliver drugs to cells or tissues that express or over-express specific ligands (Sercombe et al., 2015; Willis & Forssen, 1998). Among the possible ligands, the attachment of monoclinal antibodies to PEG liposome to create long-circulating immunoliposomes has been the most effective strategy in enhancing the stability, efficacy and targeted delivery of therapeutics (Bendas, 2001; Puri et al., 2009).

As with any system, liposome delivery faces biological challenges in the body, including accumulation in the reticuloendothelial system (RES), opsonization, and immunogenicity (Sercombe et al., 2015). Among the challenges, the accumulation of liposomes in RES, particularly in the liver and spleen, is one of the biggest factors in limiting the effectiveness of the system (Chrai, Murari, & Ahmad, 2002). The large pore diameters in the capillaries of these organs allow for the extravasation and subsequent removal of drug-loaded liposomes from the

circulation, thus sequestering them from target sites (Sapra & Allen, 2003). Following removal from circulation, liposomes undergo phagocytosis by resident macrophages, which also raises the concern as to whether macrophage saturation could lead to immunosuppression and increase the risk of infection (Chrai et al., 2002). Indeed, the administration of liposomal doxorubicin in mice reduced the clearance of bacteria from the blood due to macrophage suppression (Storm, ten Kate, Working, & Bakker-Woudenberg, 1998). Aside from liposome accumulation, opsonization of liposomes and accelerated blood clearance caused by the production of antibodies against liposomes are among other factors that can contribute to the limitation of the system in enhancing the therapeutic index of drugs (Cullis, Chonn, & Semple, 1998; Dams et al., 2000; Ishida, Harashima, & Kiwada, 2001).

1.3.3 Nanoparticle drug delivery systems

Nanoparticle-based delivery is an emerging targeting strategy for the safe and efficient delivery of drugs, particularly in the field of oncology. Nanoparticles are solid colloidal structures with at least one dimension smaller than 100 nm (Wilczewska, Niemirowicz, Markiewicz, & Car, 2012). The small size of the nanoparticles makes them suitable candidates as drug carriers due to the ease of penetration via both passive and active delivery systems that allow the particles to enter even the most impermeable membranes such as the blood brain barrier (Saraiva et al., 2016). To create an optimum vehicle for drug delivery, the size and the biochemical properties must be carefully adjusted. An ideal nanoparticle for the application of drug delivery must have a hydrodynamic diameter of 10-100 nm since these structure are small enough to be easily taken up by cells and at the same time not large enough to undergo opsonization and removal from blood (Cole, Yang, & David, 2011).

Over the years, to accommodate biomedical applications, four main groups of nanoparticles have been designed and categorized based on their chemical compositions: 1) carbon-based, 2) inorganic-based (including metal and metal oxide), 3) organic-based (such as dendrimers, micelles, and polymers), and 4) composite-based nanoparticles (Jeevanandam, Barhoum, Chan, Dufresne, & Danquah, 2018). The polymeric nanoparticles are among the most ideal carriers for drug delivery, and are named nanospheres or nanocapsules depending on their architecture (Wilczewska et al., 2012). Nanospheres are made with biodegradable, biocompatible and synthetic polymers that are dispersed in an organic phase and then cross-linked to form a spherical structure (Gref et al., 1994; McMillan, Batrakova, & Gendelman, 2011). On the other hand, nanocapsules are vesicle-like structures consisting of a polymeric matrix that encloses a cavity (Kothamasu et al., 2012). The delivery of nanoparticles can be achieved through both passive and active targeting. In passive targeting, the physiological environment of tumours such as vasculature permeability and retention of tumour tissue, pH, temperature or enzymatic activity can dictate the site of drug release. On the other hand, active targeting involves the attachment of recognition ligands to the surface or the use of magnetic fields to force magnetic nanoparticles to the target site (Wilczewska et al., 2012).

1.3.3.1 Active targeting of nanoparticles using magnetic force

Nanotechnology is a far-reaching branch of science, with magnetic nanoparticles being the most well accepted and widely used subset. Nanomagnetic particles are used in a variety of biomedical applications, such as tissue repair, magnetic resonance imaging, and targeted gene and drug delivery (Arbab et al., 2003; Berry & Curtis, 2003; Kalish et al., 2003; McBain, Yiu, & Dobson, 2008). The magnetic properties, biocompatibility and suitable surface characteristic of these particles have made them attractive candidates as carriers of drugs for site-specific

delivery. Structurally, magnetic nanoparticles are comprised of an iron oxide core that is coated with biocompatible materials such as polysaccharide, lipid or protein. Due to the unique nature of the core, the magnetic particles can align themselves in the direction of an external magnetic field and deliver particles to the target site dictated by the direction of the magnetic field (Kwon et al., 2007). Despite the numerous advantages of magnetic nanoparticles, particles face similar challenges as liposomes in the body—such as opsonization, accumulation in the RES and elimination by phagocytotic cells (Cole et al., 2011).

Regardless of the composition, the objective of any nanoparticle-based technology is to use these microscopic carriers as vehicles for the delivery of drugs. The mechanism of delivery varies based on the structural composition of the nanocarriers, as drugs can be entrapped in the polymer matrix of the nanosphere, dispersed inside the inner cavity of the nanocapsule, or covalently attached on the nanoparticle surface (Guterres, Alves, & Pohlmann, 2007).

Liposome and nanoparticle-based delivery systems are a few examples of advancements in drug delivery strategies. Most of these strategies are designed to increase therapeutic efficacy by protecting the drug from degradation and thus increasing the residence time in the body, but absorption to target cells remains a major challenge. As mentioned previously, both free drugs and the carriers encapsulating them use intrinsic pathways such as endocytosis to enter cells. Finding targeted delivery strategies that can overcome obstacles to cellular and tissue uptake by selectively modulating these pathways can influence the therapeutic efficacy of drugs in clinical practice. Ultrasound in combination with microbubbles (USMB) is an emerging strategy for targeted intracellular delivery of drug molecules. The nature of USMB and the mechanisms of drug delivery will be covered in detail below.

1.3.4 Ultrasound and microbubbles

1.3.4.1 Ultrasound

The development of the diagnostic application of ultrasound in medicine goes back to the late 19th century, when Paul-Jacques and Pierre Curie discovered that certain materials can transform electrical currents into mechanical vibrations. Forty years after the Curie brothers' discovery, the first experimental study using piezoelectricity was conducted by Paul Langevin for detection of submarines through echo location (O'Brien Jr., 2007). Langevin's experiment was the beginning of decades of human fascination with ultrasound, and provided the basis for years of research leading to the development of both diagnostic and therapeutic applications of ultrasound in medicine.

Ultrasound is the repeating of mechanical pressure waves or sound waves with frequencies greater than 20 kHz, which lie above the limit of human hearing. Similar to all waves, ultrasound has physical characteristics such as frequency, wavelength and amplitude. As the sound waves propagate through a medium, they introduce mechanical disturbances leading to the oscillation of particles in the medium, creating areas of compression and expansion. Compression occurs when the particles are pushed together, corresponding to positive pressure, followed by a period of expansion where the particles are drawn apart, corresponding to negative pressure. The repeated compression and expansion can be portrayed as a sinusoidal curve, which represents the pressure fluctuation as sound waves travel through a medium over time.

The wavelength of the sound is the distance between one complete wave cycle, and is measured in distance units (millimetres). The wavelength depends on the velocity of the sound in the medium and is inversely related to frequency—or the number of waves that pass a point per unit time (measured in Hertz). The maximal pressure variation above or below the baseline is

known as the amplitude and is measured in pressure units—megapascal (MPa). The power of an ultrasonic beam is the flow of energy transferred through the cross-sectional area of the beam per unit time (expressed in watts, W) and the energy within a unit area is represented by the average intensity (W/cm^2). The mode of ultrasonic wave propagation depends on the direction of the wave as it is travelling relative to the direction of the particles' oscillation. The longitudinal wave occurs when the particles move in the same direction as the wave propagation, while the transverse wave is characterized by particle vibration at a right angle to the direction of propagation. Compared to longitudinal waves, which can travel through soft tissues, transverse waves are only transmitted through solid materials, such as bone.

The advances in the field of imaging have popularized ultrasound as an effective imaging modality as well as a non-invasive tool for therapeutic procedures. Diagnostic ultrasound employs frequencies in the 1-10 MHz range to provide 2D or 3D images with the purpose of confirming, assessing and documenting the courses of many diseases (Martini, 2013). The use of ultrasound in diagnostic imaging provides exceptional advantages due to real-time imaging capabilities, availability, cost effectiveness, and most importantly, safety (Shung, 2011). Understanding the behaviour of ultrasonic waves and the acoustic impendence of different tissues in the body are required for forming ultrasound images. Although further discussion would be necessary to explain the physical parameters influencing image formation, the focus of this research is not on the diagnostic angle but on the therapeutic applications of ultrasound—specifically the use of ultrasound for the intracellular delivery of drugs.

Aside from its diagnostic application, ultrasound can also be used as an effective tool in non-invasive therapeutic interventions. Examples of therapeutic applications of ultrasound include lithotripsy procedure to fragment kidney stones, physiotherapy to accelerate the healing

of a fracture, as well as exciting new applications such as drug delivery, gene therapy and tumour therapy (Miller et al., 2012). In both diagnostic and therapeutic applications, the interaction between the ultrasound wave and tissues produces heating and mechanical bioeffects. Tissue heating occurs as the result of absorption of the ultrasound energy by the surrounding tissue, and is assessed by the thermal index (IT), which is the ratio of applied acoustic power over the estimated acoustic power required to raise the temperature of the tissue by 1°C (S.-L. Huang & McPherson, 2014). The mechanical bioeffect is represented by the mechanical index (MI), and is the measure of the power of the ultrasound beam needed to cause non-thermal bioeffects, such as cavitation and streaming. The MI depends on the maximum value of peak negative pressure and the pulse center frequency of the ultrasound field, and can be used as a safety guide for ultrasound exposure to the body. For MIs <0.3, the acoustic amplitude is considered low, while MIs >0.3 and <0.7 may cause minor damage, and MIs >0.7 may have major bioeffects such as cavitation (Huang & McPherson, 2014; Sen, Tufekcioglu, & Koza, 2015). The mechanical effects on cells and tissues can elicit biological responses, one of which is the delivery of molecules across biological barriers. The mechanical bioeffects will be discussed in detail in the following sections.

1.3.4.2 Transducers

Transducers are devices composed of piezoelectric elements encapsulated in plastic cases that convert electric currents into ultrasound. Piezoelectric elements change dimensions cyclically in response to an applied electric charge, allowing them to convert electrical energy into mechanical waves and vice versa. Modern transducers are composite of a non-piezoelectric polymer with ferroelectric ceramics manufactured by mixing lead, zirconate and titanate (commonly referred to as PZT) to offer high electrical-to-mechanical coupling efficiencies and

low acoustic impedance (Swallow, Siores, Dodds, & Luo, 2010). To improve the transfer of energy and sensitivity, matching layers are placed at the front of the piezoelectric element to reduce the impedance difference between the transducer and the second medium. The element is also backed with a damping material, such as rubber, to stop backward propagation of waves and to prevent interference with the reflected waves (Cochran, 2012). The optimal frequency of the transducers is determined by the resonance frequency of the piezoelectric element, which occurs when the thickness of the element reaches half the wavelength (Mikla & Mikla, 2014).

Today, manufactured transducers offer a broad range of frequencies with interchangeable focal depths according to user needs. Transducers can generate ultrasound waves in two modes: continuous or pulsed. In continuous application, the transducer generates continuous pulses over time. In pulsed mode, the transducer generates successive pulses at a specific time interval and switches off until the next pulse. The number of successive ultrasound pulses over a designated period of time is called the pulse repetition frequency, which is measured in terms of cycle per second or Hertz. The time between pulses is known as the pulse repetition interval (Parker, 2017).

1.3.4.3 Natural cavitation

Cavitation occurs when the ultrasound negative pressure causes the distance between the molecules in a liquid to exceed the critical molecular distance necessary to hold the liquid intact. Naturally occurring cavitation bubbles arise when ultrasound with MIs>0.7 is applied to spots with lower tensile strength that contain gas nuclei capable of supporting the cavitation process (Huang & McPherson, 2014). These nuclei are in the form of gas pockets, gas bubbles or interfacial gaseous voids located at water-solid interface, and are transformed into cavitation bubbles during the exposure to acoustic pressure (Mørch, 2015; Junru Wu & Nyborg, 2008).

The benefits of acoustic cavitation came to light upon the surprising discovery that the formation of ultrasonic cavitation in the body could drastically enhance the contrast of ultrasound images (Gramiak & Shah, 1968; Ignee, Atkinson, Schuessler, & Dietrich, 2016). However, despite the benefits of cavitation bubbles in ultrasound imaging, the long exposure of high-intensity focused ultrasound required for their formation could damage the surrounding tissues. The contrast-enhanced images produced by natural cavitation motivated scientists to develop ultrasound contrast agents known as microbubbles to safely mimic the cavitation bioeffects.

Microbubbles are gas filled spherical structures, ranging 1-10 μm in diameter, that are designed to mimic the natural cavitation phenomenon. Since their initial development, the composition of microbubbles has improved to better accommodate their increasing applications in both diagnostic and therapeutic procedures. The first generation of contrast agents was composed of air stabilized with an albumin shell that made them extremely fragile (de Jong, Emmer, van Wamel, & Versluis, 2009; Morin, Lim, Cobbold, & Taylor-Robinson, 2007). In the second generation, gases with higher molecular weight replaced air to stabilize the functional microbubble in the targeted region (e.g., perfluorocarbon gas) (de Jong et al., 2009). Finally, a third generation of ultrasound contrast agents, such as Definity®, was created with a complex lipid shell (composed of dipalmitoylphosphatidic acid, methylPEG dipalmitoylphosphatidyl-ethanolamine, and dipalmitoylphosphatidylcholine) to counter the effect of surface tension and increase bubble longevity (Decato & Mecozzi, 2014). Research on contrast agents is ongoing, and more advanced agents with improved longevity, efficacy and site-specific localization are now on the horizon.

1.3.4.4 Microbubble responses in the acoustic field

Naturally occurring cavitation bubbles and manufactured microbubbles are not stationary, and exhibit dynamic behaviours that are the keystone of this novel approach for the delivery of drugs across biological barriers. Microbubble responses can vary in the acoustic field depending on the pressure and frequency of the transmitted ultrasound, and can be roughly categorized into non-inertial and inertial cavitation. In acoustic fields, bubbles expand and contract during each refraction and compression cycle via a process called rectified diffusion, a phenomenon in which gas diffusion into the bubble during refraction exceeds the efflux during the compression period, allowing for the growth of the bubble (Leong, Ashokkumar, & Kentish, 2015). Under low acoustic pressure, microbubbles volumetrically oscillate around their equilibrium radius over many oscillations (resembling a breathing motion), a behaviour known as non-inertial cavitation (Bakhtiari-Nejad & Shahab, 2018). In stable cavitation, microbubbles will respond linearly or non-linearly in relation to the amplitude of the applied external pressure field (de Jong, Bouakaz, & Frinking, 2002). At low acoustic pressure, the microbubble radius expands linearly in relation to the amplitude of applied external pressure field. At higher amplitudes of external pressure, the expansion and contraction of the microbubbles become asymmetric as they exhibit either an unlimited expansion or compression-only behaviour, a response known as non-linear oscillation. The oscillation of microbubbles depends on parameters such as shell properties, size of the bubble resonance frequencies and damping coefficient (de Jong et al., 2009). As an example, the presence of lipid shells increases the stiffness and favours the non-linear oscillation regimen of microbubbles. During non-inertial cavitation, microbubbles grow through rectified diffusion with each pressure cycle until they reach their resonant size, which is determined by the physical

properties of the fluid (surface tension, viscosity, density, frequency of ultrasound) at which point they collapse (Schafer, 2015).

If a microbubble is positioned near the plasma membrane of a cell, the oscillation of the bubble exerts mechanical forces by pushing and pulling against the cell surface with each compression and expansion cycle. In this close proximity, the oscillation of the bubbles against the water molecules between the bubble-membrane interface can exert shear force on the cells (Kooiman, Vos, Versluis, & de Jong, 2014). Furthermore, the stable cavitation regime of the microbubble will set the surrounding fluid into motion, creating a microstreaming flow in the vicinity of the pulsating bubble. The formation of these microscale flow patterns generates shear stress onto the surrounding cells, and thus has a profound contribution to the activation of mechanically-induced signalling cascades (Ellens & Hynynen, 2015; Wu, 2002). Aside from non-inertial cavitation, acoustic radiation forces can also contribute to the biomechanical stimulation of cells. The primary radiation force, such as 'bubble bullets,' are produced when microbubbles absorb the momentum of the passing ultrasound waves and are pushed toward surrounding cells (Miller, Thomas, & Williams, 1991; Starritt, Duck, & Humphrey, 1991). Microbubbles are also affected by secondary radiation force, known as the mirroring effect, which describes the attraction force of microbubbles to surfaces that reflect their emitted energy, such as the surfaces of neighbouring microbubbles, which may cause them to move toward each other and form aggregates (Leighton, 1994; Miller, Nyborg, & Whitcomb, 1978). These acoustic radiation forces can augment the initial microbubble responses, such as cavitation microstreaming, thereby enhancing the bioeffects in vivo (Stride & Saffari, 2003).

Inertial cavitation refers to the violent behaviour of the microbubble at high acoustic pressure, at which point the bubble expands to twice its equilibrium radius, followed by its rapid

and sudden collapse (Ellens & Hynynen, 2015). The destruction of bubbles results in the formation of bubble fragments as well as the generation of various post-collapse outcomes such as heat, microjet and shock waves, all of which can act as avenues for potential bioeffects by exerting mechanical forces on adjacent cells (Chomas, Dayton, May, & Ferrara, 2001; Collis et al., 2010; Z Fan, Chen, & Deng, 2014; Lauterborn & Ohl, 1997; Marmottant & Hilgenfeldt, 2003; Suslick & Flannigan, 2008). The rapid symmetrical collapse of the bubbles can give rise to a pressure gradient that can generate shock waves sufficient to drive the formation of fluid microjets in the direction of the propagating shock wave. The fluid microjets can also be formed by the compression of gas bubbles by a passing shock wave. Regardless of how they are formed, the tip of fluid microjets carry high pressure, allowing them to act as a micro-syringe with enough power to penetrate the plasma membrane (Dear, Field, & Walton, 1988; Ohl & Ikink, 2003; Prentice, Cuschieri, Dholakia, Prausnitz, & Campbell, 2005).

Additionally, the fragmented pieces produced from the inertial cavitation can potentially act as bubble nuclei, and in turn undergo inertial cavitation themselves, thus contributing to jet-induced cell damage (Stride & Saffari, 2003). The outcome of the rapid volume reduction during inertial cavitation is an increase in temperature of up to a thousand degrees Kelvin at the core of the bubble (Stride & Saffari, 2003). However, due to the small radius of the bubble and the cooling effect of the circulation fluid surrounding the bubble, the thermal fluctuation of the fluid away from the centre is negligible and the risk of thermal effects is quite low (Hilgenfeldt, Lohse, & Zomack, 2000).

Initially used for conventional diagnostic imaging, microbubbles are now being exploited for their potential use in therapeutic intervention in vascular permeability, thrombolysis, and lithotripsy (Hitchcock & Holland, 2010; Neisius et al., 2014; Vykhodtseva, McDannold, &

Hynynen, 2008). Perhaps the most significant therapeutic application of microbubbles could be their potential to be used as vehicles for the delivery of drugs to cells. An improvement in drug delivery efficacy can be achieved through several mechanisms, including 1) encapsulating and targeting drugs, thus increasing the concentration of therapeutics in the vascular compartment of the targeted area, 2) altering the permeability of endothelial cells and increasing the delivery of therapeutics through blood vessels (Miller et al., 2012). The potential use of microbubbles for drug delivery will be discussed in detail in the following sections.

1.3.4.5 Microbubble safety

The associated side effects of microbubble injection to the body are mild and transient, with individual cases of vomiting, nausea, chest pain, hypo and hypertension, as well as discomfort around the vicinity of injection sites having been reported (Dalecki, 2005). The bubbles can be injected as a bolus or slow infusion. Shortly after injection, the microbubbles present an intravascular distribution in the peripheral circle (Correas et al., 2001). Due to their nature, the clearance of microbubbles is fast, as the gas content is eliminated through the lungs after just a few minutes and the phospholipid shell enters the metabolic pathway (Morel et al., 2000). Consequently, fast clearance from the body reduces the risk of liver, renal or cerebral toxicity associated with microbubbles and such incidents have not been reported (Dalecki, 2005).

The large size of microbubbles compared to the capillaries could have potential effects on microvascular circulation. Fortunately, the entrapment of bubbles in the capillaries is resolved within 9 to 18 seconds after their retention, as the bubbles shrink in size due to the dissolution of their gas, and the capillary flow normalizes. Therefore, the risk of capillary blockage by the injected microbubbles is minimal (Braide, Rasmussen, Albrektsson, & Bagge, 2006). With respect to endothelial integrity, it has been reported that ultrasound-exposed microbubbles can

induce a significant increase in the number of intercellular gaps, but integrity is restored within 30 minutes, after which the number of intercellular gaps return to control (Juffermans et al., 2009). The breach in the endothelial integrity following USMB treatment can be used for the localized delivery of drugs to specific tissues.

As the field of ultrasound-microbubbles is rapidly evolving and new applications are emerging, the associated risks and safety considerations must be closely regulated. Today, the general guidelines from FDA provide risk assessment, regulations and recommendations for the safe use of microbubbles in clinics. In the future, these guidelines will be updated to reflect the rapid advances and forthcoming information in this field.

1.3.4.6 The biomedical applications of microbubbles

Best known as contrast agents, the reflective nature of the microbubbles compared to rigid body tissues allows for the production of scattered waves that are proportional to the sixth power of the microbubble diameters as they undergo oscillation. Such enhancement in reflection offers an increase in the intensity of backscattered ultrasound waves, which translates to contrast enhancement that allows for the detection of previously undetectable lesions (Blomley, Cooke, Unger, Monaghan, & Cosgrove, 2001). The acoustic backscattering properties of microbubbles provide echogenicity and make them promising candidates in diagnostic applications, such as ultrasound imaging. Studies have shown that the use of contrast agents can improve sensitivity to metastasis detection by 88%, which has meant that the mean size of the smallest lesions detected by the bubbles has decreased by 50% to under 1 cm (Blomley et al., 2001). Microbubbles can also increase detection sensitivity of echocardiography by highlighting the left ventricular cavity and blood-tissue boundary (Blomley et al., 2001; Cheng, Dy, & Feinstein, 1998).

The targeted gene and drug deliveries are perhaps the most exciting emerging application of microbubbles. In general, USMB drug delivery can be classified into two broad areas: 1) use of microbubbles as carriers for site-specific targeting, and 2) enhancement in cell membrane permeability (Tsutsui, Xie, & Porter, 2004). One strategy for targeted delivery involves linking, adsorbing or incorporating DNA or drug compounds within the lipid shells of microbubbles (Borden, Caskey, Little, Gillies, & Ferrara, 2007; Panje et al., 2012; Wang et al., 2012). The utilization of microbubbles as drug delivery vehicles improves the specificity, and the therapeutic index of drugs (Sirsi & Borden, 2009).

There are several approaches that can be taken to deliver drugs using ultrasound and microbubble interaction. The first approach involves the loading of drugs inside microbubbles followed by focusing the ultrasound beam on the target area to trigger acoustic cavitation of the microbubbles and release of their therapeutic payload at the intended site (Fritz, Unger, Sutherland, & Sahn, 1997; Miller, 2000; Tsutsui et al., 2004; Unger, McCreery, Sweitzer, Caldwell, & Wu, 1998). The second approach to targeted drug delivery via USMB involves the attachment of ligands to the surface of the microbubbles in order to direct them to cells that differentially express disease-specific markers, such as vascular endothelial growth factor receptor 2 (VEGFR2) and integrin $\alpha_v\beta_3$ (Abou-Elkacem, Bachawal, & Willmann, 2015; Anderson et al., 2011; Bachawal et al., 2013; Lindner et al., 2001; Mullick Chowdhury et al., 2017; Weller et al., 2003). The third approach involves co-injecting the drug alongside microbubbles into the blood stream (Mullick Chowdhury et al., 2017). Following injection, the behaviour of the microbubbles in an acoustic field can cause the perturbation of vascular endothelium at the target site, which would allow the passage of drugs through the plasma membrane, thus increasing the intracellular delivery of therapeutics (Deng, Sieling, Pan, & Cui,

2004; Mukherjee et al., 2000; Taniyama et al., 2002). Through selectively enhancing the permeability of the plasma membrane at particular sites, USMB has the potential to improve the therapeutic index of clinically approved drugs by increasing the delivery of therapeutics across the plasma membranes (Boissenot, Bordat, Fattal, & Tsapis, 2016; Mullick Chowdhury et al., 2017). As an example, doxorubicin is an antineoplastic chemotherapy drug widely used against extracranial malignant tumours but has limited success against malignancies within the brain due to its poor accumulation. Treat et al. successfully demonstrated that concurrent intravenous injection of doxorubicin and microbubbles can significantly delay tumour growth and increase survival rate in rats with implanted brain glioma tumours, suggesting that USMB has potential to increase therapeutic efficacy and improve treatment outcomes (Treat, McDannold, Zhang, Vykhodtseva, & Hynynen, 2012).

Despite being well defined in theory, in reality, the successful implementation of USMB involves a complex interplay between ultrasound parameters, the composition of the bubbles, as well as the biophysical properties of the therapeutics (Tsutsui et al., 2004). In particular, utilizing microbubbles as drug carriers faces challenges in effective clinical execution. To reach the enormous clinical potential that microbubbles have as drug carriers, an optimal drug-loading efficiency must be achieved during the preparation process. The drug-loading content and efficiency is dictated by a number of factors, such as the loading capacity, microbubble composition, and loading strategies (Mullick Chowdhury et al., 2017). The interplay between these factors can yield less than desirable loading efficiency results, and produce inconsistent treatment outcomes.

The composition of the microbubbles is one of the important determining factors in the amount and the type of therapeutics that can get incorporated in the bubble. Hydrophobic-fat

soluble drugs can get incorporated in lipid microbubbles, while water-soluble compounds require a polymeric microbubble shell. However, the perfluoropentane core of polymeric microbubbles is not a good solvent for hydrophilic drug substances, which limits the spectrum of drug compounds that can utilize microbubbles as carriers (Hernot & Klibanov, 2008). Aside from the loading efficiency, it is still unclear if loading drugs into microbubbles changes the acoustic behaviours of the bubbles. As an example, the addition of an oil-based drug reservoir between the lipid coating and perfluorobutane gas core alters the coating properties, which drastically changes the acoustic behaviour of the bubble (Kooiman et al., 2014). Furthermore, identifying optimal acoustic parameters to achieve drug delivery requires more in-depth in vitro and in vivo investigations, as the optimal payload release requires adjusting the ultrasound parameters based on the type of compound. To better illustrate this point, Phillips et al. found that the effective release of rapamycin from the microbubble shell requires an ultrasound exposure of 1MHz at 0.5% duty cycle, with a peak negative pressure of up to 400 kPa and a pulse length of more than 10 cycles (Phillips, Klibanov, Wamhoff, & Hossack, 2011). On the other hand, the maximal transfection of smooth muscle cells with microbubbles carrying plasmid DNA occurred using 50 cycles of 1MHz pulses at 300 kPa (Phillips, Klibanov, Wamhoff, & Hossack, 2010).

The challenges in microbubble targeting is not limited to drug encapsulation, as the technique of coupling ligands to the surface of microbubbles is still in its infancy due to limited research in the field. Currently, the only molecularly-targeted contrast agent is manufactured through binding one of the main markers of neoangiogenesis in breast and ovarian cancer (known as the kinase insert domain receptor (KDR)) to the surface of microbubbles (Deshpande, Ren, Foygel, Rosenberg, & Willmann, 2011; Pysz et al., 2010; Willmann et al., 2017). As of the date of publication of this thesis, there is still substantial work to be done to reach clinical potential and

gain widespread acceptance of USMB as an effective drug delivery strategy, especially in the treatment of cancer and vascular diseases. Although more can be done to optimize microbubbles as high-capacity drug-loaded carriers, for now the best approach for enhancing the intracellular delivery of drugs is to co-inject drugs along with microbubbles. It is the goal of this thesis to clearly demonstrate the efficacy of microbubble and drug co-injection followed by ultrasound treatment on the enhancement of drug delivery in vitro.

1.3.4.7 Ultrasound and microbubble mechanisms of drug delivery

Drug delivery into cells by microbubbles in the presence of ultrasound can occur via two uptake routes: pore formation and endocytosis. Depending on the acoustic pressure and applied frequency, the behaviour of microbubbles can vary from stable oscillation to rapid collapse, which consequently affects the magnitude of shear forces exerted on neighbouring cells through the generation of secondary effects such as acoustic streaming patterns and shockwaves (Kooiman et al., 2014). The mechanical stress generated from the microbubble oscillations and collapse, combined with the shear stress caused by the surrounding fluid motions, forms transient perforations on the plasma membrane that permit the diffusion of molecules across cell membranes, a phenomenon known as sonoporation (Chen, Wan, & Yu, 2013; Karshafian, Bevan, Williams, Samac, & Burns, 2009; Mehier-humbert, Bettinger, Yan, & Guy, 2005; Meijering et al., 2009; Schlicher et al., 2006; Tran, Roger, Le Guennec, Tranquart, & Bouakaz, 2007).

Given the mixed responses of microbubbles in the acoustic field, the degree of pore formation varies, with sizes ranging from 1 nm to as large as >100 μm^2 (Fan, Liu, Mayer, & Deng, 2012; Hu, Wan, & Yu, 2013; van Wamel et al., 2006; Yang et al., 2008). Studying the membrane dynamics of cells during the acoustic cavitation process has shown the formation of

pores on the plasma membrane within an instant of the ultrasound wave's pulsing, followed by the rapid resealing of pores between milliseconds to several seconds (depending on the pore size) of the onset of sonoporation (Hu et al., 2013). The magnitude of the mechanical stress generated by microbubbles can have varying effects, which impacts the post-sonoporation recovery of membranes as pores bigger than 100 μm cannot reseal properly (Hu et al., 2013; Mehier-humbert et al., 2005). Therefore, to fully exploit the potential of USMB-mediated sonoporation as a gateway for the intracellular delivery of drugs, the ultrasound parameters must be optimized to form pores that can accommodate drug uptake without irreversibly damaging the plasma membrane. Unfortunately, the exact mechanism of sonoporation, as well as the specific bubble behaviour that favours the formation of pores and drug uptake are not well understood (Forbes, Steinberg, O'Brien, & Jr., 2008; Hallow, Mahajan, McCutchen, & Prausnitz, 2006; M. Kinoshita & Hynynen, 2007; Lai, Wu, Chen, & Li, 2006; Qiu et al., 2010). More detailed experimental and theoretical studies are required to better understand the relation between microbubble behaviour and sonoporation to better utilize USMB for the intracellular delivery of drugs in vitro.

Aside from uptake, the transient permeabilization of plasma membranes has other consequences, including the influx of ions and the generation of reactive oxygen species, which can act as secondary messengers to regulate signal transduction pathways involved in cytoskeletal reorganization, endocytosis, and apoptosis (Fan, Kumon, Park, & Deng, 2010; Juffermans, Dijkmans, Musters, Visser, & Kamp, 2006; Meijering et al., 2009). Using high-speed cameras during the application of ultrasound and microbubbles, it has been shown that cells adjacent to a microbubble experience an immediate increase in Ca^{2+} concentration of up to 1200 nM, which correlates with intracellular delivery of molecules. Aside from the immediate Ca^{2+} transient in sonoporated cells, neighbouring cells not exposed to USMB also exhibit a

delayed increase in intracellular Ca^{2+}, with distance from the treated cells directly affecting the concentration of the intracellular calcium (Fan, Kumon, Park, & Deng, 2010). Studying the dynamics of pore closure has clearly demonstrated that the arrival of a calcium wave through perforations is crucial for the activation of the signalling cascade that mediates the plasma membrane repair, as the removal of extracellular calcium inhibits the resealing of sonoporation sites (Hu et al., 2013).

Notably, the rapid resealing of the plasma membrane following sonoporation suggests that the transient pores alone cannot accommodate sufficient passage of drugs into cells. In fact, aside from pore formation, the activation of endocytic pathways significantly contributes to uptake of molecules following USMB treatment (Fekri, Delos Santos, Karshafian, & Antonescu, 2016; Meijering et al., 2009) . The contribution of endocytosis to USMB-induced delivery of molecules was first observed by Meijering et al., who reported that the acoustic parameters required for sonoporation also activate different endocytic pathways (Meijering et al., 2009). However, Meijering et al. did not identify the mechanisms that regulate USMB-induced endocytic pathways, and they remain to be explained.

1.4 Endocytosis as the entry pathway of drugs to cells upon USMB treatment

Endocytosis is a dynamic and highly regulated process characterized by the internalization of extracellular materials, ligands, and plasma membrane proteins that are enclosed within a portion of the plasma membrane that forms vesicles. There are several intrinsic endocytic mechanisms that operate within higher eukaryotes, each with their own unique and complex molecular machinery that functions to localize specific cargoes on regions of the plasma membrane and sculpt these flat regions into cargo-carrying vesicles. These pathways can be distinguished based on the molecular characteristics of key proteins that are involved in the cargo selection, vesicle

formation and budding. Some pathways might require specific coating proteins, such as clathrin, for vesicle formation while others can coordinate the formation of vesicles from non-coated invaginations. Furthermore, these pathways can share common features—such as the requirement for dynamin or actin for vesicle scission—or might require distinct proteins for this process. Regardless of the mode of entry, upon internalization the vesicle is transported to the endosomal compartment, where cargo-specific sorting signals direct the cargo to the late endosomes and lysosomes for degradation, the trans-Golgi network (TGN), or to recycling endosomal compartments (Grant & Donaldson, 2009).

The endocytic machinery can be roughly divided into clathrin-dependent and clathrin-independent pathways. Clathrin-mediated endocytosis (CME) involves the coating protein clathrin, and > 50 accessory and adaptor proteins that coordinate to package cargoes such as receptors for iron-bound transferrin (Tfn) and low-density lipoprotein (LDL) into clathrin-coated vesicles (Chen, Goldstein, & Brown, 1990; Conner & Schmid, 2003; Mayle, Le, & Kamei, 2012). The vesicle is then cleaved from the plasma membrane by the GTPase dynamin, and is transposed to the endosomal compartment (Grant & Donaldson, 2009). Compared to the detailed mechanistic insights that are available for CME, the molecular identity and the exact molecular mechanisms of clathrin-independent endocytosis (CIE) are far less understood. It is worth mentioning that CIE is a term used to describe a number of pathways with a high capacity for the internalization of membrane portions and fluids that do not require clathrin for cargo internalization. These include but are not limited to macropinocytosis, caveolae-mediated endocytosis, flotillin-mediated endocytosis, fast endophilin-mediated endocytosis and Rho-dependent endocytosis (Sandvig, Pust, Skotland, & van Deurs, 2011). Given the importance of

these endocytic pathways for the delivery of therapeutics into cells upon USMB treatment, I will describe each pathway in detail below.

1.5 Clathrin-mediated endocytosis

As the most extensively studied and best understood endocytic pathway, CME has been a topic of fascination ever since the "vesicle in a basket" was first described by Kanaseki and Kadota in 1969 (Kanaseki & Kadota, 1969). Thanks to years of research, as well as improvements in imaging technologies and computational image analysis, our understanding of the molecular basis and key events of clathrin-mediated endocytosis is now better than ever, though it is still far from complete. As the best characterized receptor-mediated pathway, CME is responsible for the internalization of a diverse range of ligand-receptor complexes such as transferrin receptors (TfRs), receptor tyrosine kinases (RTKs), and LDL receptors (McMahon & Boucrot, 2011).

The modes of receptor internalization via CME can be divided into constitutive or stimulated entry. Some receptors, such as TfRs and LDL receptors, constitutively internalize through CME to carry iron and cholesterol into cells (Anderson, Brown, & Goldstein, 1977; Spencer, Diego, Diego, & Kensington, 1990). On the other hand, recruitment of RTKs and G protein-coupled receptors (GPCRs) to site of clathrin-vesicle assembly requires structural changes, such as dimerization and conformational changes mediated by ligand binding (Kim & Benovic, 2002; Wang, Villeneuve, & Wang, 2005). Upon ligand binding, the activated receptor initiates a cascade of signalling events that translate into major cellular functions and physiological responses, ranging from cell growth, division and differentiation to synaptic transmission (Sorkin & von Zastrow, 2002). Therefore, by clustering or physically removing receptors from the cell surface, CME can influence various receptor-based signalling pathways, with the succeeding outcome depending on the type of receptor (Murphy, Padilla, Hasdemir,

Cottrell, & Bunnett, 2009). The rapid internalization of receptors from the cell surface and trafficking to lysosomes leads to the termination of the signal, while trafficking of some receptors to endosomal compartments leads to an amplification or change in the nature of the signal transduction pathway (Murphy et al., 2009). For example, epidermal growth factor receptors (EGFRs) can continue signalling from the endosome to sustain the phosphoinositide 3-kinase (PI3K)/AKT signalling pathway (Wang et al. 2002). On the other hand, nerve growth factor binding to the tropomyosin receptor kinase A (TrkA) receptor activates Ras at the plasma membrane, but leads to persistent mitogen-activated protein kinase (MAPK) activation upon the trafficking of receptors to endosomes (Wu, Lai, and Mobley 2001).

Named after its main structural component, the CME machinery is composed of more than 50 proteins that exhibit distinct dynamic heterogeneity based on their recruitment hierarchy, working to orchestrate the formation of coated vesicles. As the pathway's main component, clathrin was first visualized by negative-stain electron microscopy in 1969, and reconstructed later using cryogenic-electron microscopy (cryo-EM) in 1986 to reveal the three-dimensional (3D) arrays of triskelia (Vigers, Crowther, & Pearse, 1986). The improved resolution of cryo-EM from 50 Å to 21 Å in 1998 and finally 8 Å in 2004 has provided new insights into the structure of the clathrin cage (Fotin et al., 2004; Kanaseki & Kadota, 1969; Vigers et al., 1986). Each triskelion is made of three 190-kDa clathrin heavy chains (CHCs) and three 25–29-kDa clathrin light chains (CLCs), and has an approximately three-fold rotational symmetry (Fotin et al., 2004). Following initiation, clathrin triskelia assemble to form lattice-like coats around the growing membrane buds. Interestingly, clathrin does not directly bind to cargo or the membrane, and relies on the activity of different adaptors and accessory proteins for cargo selection (McMahon & Boucrot, 2011).

The formation of clathrin-coated vesicles (CCVs) follows five stages: initiation, cargo selection, coat assembly, scission and un-coating (McMahon & Boucrot, 2011). During the initiation stage, the clathrin triskelia bend membranes to form specialized regions known as clathrin-coated pits (CCPs). The receptors, along with adaptors and accessory proteins, cluster inside CCPs and together with clathrin sculpt the membrane into CCVs (Goldstein, Anderson, & Brown, 1979). Despite the use of sophisticated imagining techniques and analytical tools, our current understanding of the early events in CCP formation is limited (Haucke & Kozlov, 2018). Conventionally believed to be initiated by the recruitment and binding of adaptor protein complex 2 (AP-2) to the cytoplasmic tail of receptors, the model was later replaced by two current hypotheses that describe distinct molecular events during the initiation phase of coated pit formation (Cocucci, Aguet, Boulant, & Kirchhausen, 2012; Henne et al., 2010). The most recent initiation model proposed by Cocucci et al. suggests that the recruitment and coordinated binding of two AP-2s to clathrin triskelia and phosphatidylinositol (4,5)-bisphosphate (PtdIns(4,5)P_2) constitute the early events in CCP formation. Using live-cell total internal reflection fluorescence (TIRF) imaging with single-molecule GFP-clathrin sensitivity and high temporal resolution along with unbiased object detection and trajectory tracking of TIRF images, Cocucci et al. provided molecular descriptions of the sequence of initial events leading to CCP formation. According to the aforementioned study, AP-2 constantly samples the membrane and binds to PtdIns(4,5)P_2 and clathrin, with weak affinity and a comparably short lifetime (<1 s). The arrival and the association of the second AP-2 with PtdIns(4,5)P_2 can successfully anchor one clathrin triskelion to the membrane with a much longer residence time at the site of the coated pit-initiation. The subsequent addition of more clathrin triskelia and the resulting clathrin-

to-clathrin contact increases the stability and residence time, providing nucleation sites for the sequential addition of clathrin triskelia and adaptors to form the CCVs (Cocucci et al., 2012).

CME machinery is comprised of a number of membrane sculpting proteins, each with its own unique curvature sensitivity and membrane shaping mechanisms, which coordinate the architecture of invaginated clathrin-coated structures (Haucke & Kozlov, 2018). Some structural proteins directly sense the curvature of the membrane surface to which they bind, and induce membrane bending by merely scaffolding forces (McMahon & Gallop, 2005; Zimmerberg & Kozlov, 2006). Proteins such as members of Bin/amphiphysin/Rvs (BAR) domain superfamily (amphiphysin and endophilin) as well as F-BAR domain only protein 1 or 2 (FCHo1 or FCHo2), F-box protein 7 (FBP17, also known as FNBP1) and syndapin belong to the scaffolding family, meaning that they generate membrane curvature by polymerizing on the membrane (Da Costa et al., 2003; Daumke, Roux, & Haucke, 2014; Henne et al., 2010; Henne et al., 2007; Shimada et al., 2007). On the other hand, some endocytic effectors generate membrane bending forces through hydrophobic insertions. The proteins that use hydrophobic insertion forces include AP180 N-terminal homology (ANTH) and Epsin N-terminal homology (ENTH) domain containing proteins, clathrin assembly lymphoid myeloid leukemia (CALM) and epsin-1 and 2 (Ford et al. 2002; Messa et al. 2014; Miller et al. 2015). The hydrophobic insertion of these proteins enables the relaxation of intra-membrane stresses caused by scaffolding proteins. Therefore, binding and the subsequent intra-membrane stress created by scaffolding proteins enhance the membrane binding affinity of membrane inserting domains, providing the driving force necessary to shape the large curvatures that form the dome-like parts of CCVs (Kozlov et al., 2014). Lastly, the polymerization of clathrin itself contributes to deforming the plasma membrane into coated vesicles (Haucke & Kozlov, 2018).

Since structural proteins are an essential component of coated vesicle formation, an alternative theory argues that it is the arrival of membrane sculpting proteins—specifically FCHo1 or FCHo2—that initiates the coated pits' formation (Henne et al., 2010). The dynamics of FCHo1 and FCHo2 at the site of CCPs formation are due to their unique structural properties, which enable them to sense less extreme positive curvatures. Structurally, both FCHo1 and FCHo2 are shallow arcs whose concave faces interact with negatively charged phospholipids and polymerize into a helical coat (Haucke & Kozlov, 2018). FCHo1 and FCHo2's abilities to accommodate the slightest membrane bending result in the formation of arc-like FCHo1/2 on the membrane, which marks the site of CCPs' assembly. Following the formation of FCHo arcs on the membrane, EPS15 and intersectin are recruited, and together the complex recruits and engages AP-2s to direct clathrin assembly. The FCHo1/2 arc continues to polymerize and form a ring that defines the neck of the vesicle with clathrin assembling inside the FCHo1/2 ring. The subsequent recruitment of other sculpting proteins capable of binding to clathrin and adaptors, such as epsin and CALM, modulates protein crowding and the growth of membrane invagination into the vesicle (Henne et al., 2010; Jarsch, Daste, & Gallop, 2016).

One of the most important features of CME machinery is its ability to selectively localize receptors into small regions of the plasma membrane prior to their internalization, highlighting the specificity of this pathway for the delivery of certain cargoes. The process of cargo selection heavily relies on the activity of cargo specific adaptor proteins (Popova, Deyev, & Petrenko, 2013). The most well-known adaptor protein and the major interaction hub in the maturing CCP is AP-2 (McMahon & Boucrot, 2011). AP-2 belongs to the family of APs, which are divided into two classes: monomeric (AP180/CALM), and heterotetrameric (AP1-AP4). All APs have two large subunits of 100–130 kDa—α and β2 in AP-2, wherein the α-subunit is homologous to the

γ-, δ- and ε-subunits in AP-1, AP3- and AP-4, respectively, while β2 is homologous to β1, β3 and β4 in AP-1, AP-3 and AP-4, respectively. APs also contain a medium-sized subunit of ~50 kDa (μ subunit) and a small subunit of ~20 kDa (σ subunit) (Edeling, Smith, & Owen, 2006). Each AP complex can trigger the formation of clathrin lattices at distinct membrane compartments, but AP-2 is the only member of the family that localizes at the cell surface and contributes to internalization. On the plasma membrane AP-2 binds PtdIns(4,5)P_2 via its α subunit, clathrin via β2 subunits, and interacts with motifs in the cytoplasmic tails of transmembrane receptors through its μ-subunit and σ-subunit to mediate cargo selection (Puertollano, 2004). The μ_2 subunit recognizes and binds to YXXΦ motifs on the cargo receptor (in which X represents any amino acid and Φ represents a large hydrophobic residue) while the σ_2 subunit interacts with [D/E] XXXL[L/I] 'acidic dileucine' motifs, at least one of which is present in all the cargo proteins of CCVs (Kozik, Francis, Seaman, & Robinson, 2010).

AP-2 only recognizes a specific subset of cargoes directly. For others, the selection starts by the recruitment of the cargo's specific adaptor proteins to the site of CCP formation. As an example, the FXNPXY sorting motif in the LDL receptor is recognized by the N-terminal phosphotyrosine-binding (PTB) domains of disabled homolog 2 (Dab2) and ARH (autosomal recessive hypercholesterolemia), both of which are cargo-specific adaptor proteins (Mettlen, Loerke, Yarar, Danuser, & Schmid, 2010). These cargo specific adaptors indirectly anchor LDL receptors to phosphoinositides, clathrin and AP-2, thus simultaneously promote receptor clustering and triskelia assembly (Mishra et al., 2002).

Once the maturation is completed, scission is mediated by the mechanochemical activity of dynamin (Hinshaw & Schmid, 1995). The recruited dynamin polymerizes around the neck of the vesicle by interacting with the Src homology 3 (SH3) domain of BAR-domain containing

proteins, such as amphiphysin, endophilin and sorting nexin 9 (SNX9) (Itoh et al., 2005; Rao et al., 2010; Yoshida et al., 2004). Dynamin assembles a spiral collar around the neck of the vesicle, and then undergoes GTP hydrolysis to constrict the collar and promote vesicle scission (Hinshaw & Schmid, 1995). Aside from the direct role of dynamin, other accessory proteins such as intersectin also contribute to vesicle scission by promoting F-actin assembly through recruiting Cdc42 and N-WASP (Gubar et al., 2013). However, the role of actin has been subject to much debate, as different studies provide contradicting evidence as to whether actin plays a fundamental structural role in CME or not (Durrbach, Louvard, & Coudrier, 1996; Fujimoto, Roth, Heuser, & Schmid, 2000; Christophe Lamaze, Fujimoto, Yin, & Schmid, 1997; Lunn et al., 2000).

Once the vesicle internalizes, the chaperone Hsc70 and the J domain protein auxilin (or cyclin G-associated kinase (GAK) in non-neuronal tissues) together disassemble the clathrin coat from the neck where the vesicle was attached. Synaptojanin-1 also contributes to the un-coating process through dephosphorylating PtdIns(4,5)P_2, which weakens the attachment of dynamin, AP-2s, and clathrin triskelia from the vesicle (Cremona et al., 1999; Kim et al., 2002). The vesicle is then carried to the endosomal compartment, where cargo-specific sorting determines the fate of the receptor—the receptor can recycle back to the plasma membrane for another round of trafficking, or be routed to lysosomes for degradation (Elkin, Lakoduk, & Schmid, 2016).

The important physiological relevance of CME in cells, especially its potential to be utilized as a mode of entry for receptor-targeting of selective drugs, has made CME a topic of continuous interest. Given that USMB treatment holds a significant promise for the targeted delivery and uptake of therapeutics, I became interested in the effect of USMB on the rate of

CME. Our goal was to better understand the mechanism of pathway activation in response to USMB and exploit this route for drug delivery, hoping that one day our findings could enhance the delivery of receptor-targeting drugs using the USMB approach. The potential regulation of CME by USMB is examined in chapter 3.

1.6 Clathrin-independent endocytosis

CIE is a term to describe a number of different endocytic pathways, each with its own unique molecular machinery for cargo selection, vesicle formation, budding and cargo destination (Boucrot et al., 2015; Lamaze et al., 2001; Mayor & Pagano, 2007; Mayor, Parton, & Donaldson, 2014; Sabharanjak, Sharma, Parton, & Mayor, 2002). The wide variety of cargoes that utilize clathrin-independent machineries reflects the diversity and complexity of pathways in the CIE class. Compared to CME, our understanding of CIE pathway-specific molecular machinery and the spatiotemporal distributions of proteins that coordinate the movement of cargoes into cells remains unclear. In this section, I will discuss challenges associated with studying clathrin-independent pathways and summarize our current understanding of the molecular machinery of several CIE pathways, including Rho-dependent, GEEC, caveolin-dependent, macropinocytosis, flotillin-dependent and MEND.

Some might question why the same lessons that were learned from the study of CME could not applied to the study of CIE pathways. In fact, over the years attempts have been made to define CIE subclasses by discovering specific key molecular players (analogous to clathrin and adaptor proteins in CME) that solely associate with a particular pathway. Unfortunately, in most cases the key proteins in the pathways are too transient to be captured by subjecting cells to different manipulation steps. The transient nature and heterogeneity of these proteins, as well as the existence of redundant pathways, contribute to a lack of clear understanding of the precise

mechanistic details required for the generation of vesicles. Moreover, the existence of CME's signature cargoes, such as TfR and LDL, in clathrin-coated vesicles has contributed to much of our understanding of the detailed sequential functions of proteins involved in the pathway. On the other hand, the absence of well-defined endocytic markers and cargoes or the internalization of one cargo via multiple routes makes identifying the type of CIE pathways challenging (Sandvig et al., 2011). As an example, interleukin 2 receptors (IL-2R) are widely known as Rho-specific cargoes but have been shown to rapidly internalize via fast endophilin-mediated endocytosis (FEME) pathways as well (Basquin et al., 2013; Boucrot et al., 2015; Lamaze et al., 2001). Another part of the challenge in studying CIE pathways is the high dependency of these mechanisms on cellular context (Sandvig, Kavaliauskiene, & Skotland, 2018). As an example, the apical uptake of ricin in MDCK cells depends on Rho-GTPase without affecting the basolateral side (Garred, Rodal, van Deurs, & Sandvig, 2001). Aside from cell context, CIE pathways are also highly cell-type dependent, as different regulators of the same pathway might be involved in the formation of endocytic vesicles based on the cell type (Donaldson, Porat-Shliom, & Cohen, 2009). Lastly, due to the interconnected network of protein interaction in distinct CIE routes, manipulation studies may lead to the compensatory effects on other endocytic pathways in the cell. As such, the crosstalk between the key proteins in different CIE pathways and even between CIE and CME adds an extra layer of complexity to the challenges in studying different endocytic routes (D'Souza-Schorey, Li, Colombo, & Stahl, 1995; Kumari & Mayor, 2008; Naslavsky, Weigert, & Donaldson, 2003; Palacios, Schweitzer, Boshans, & D'Souza-Schorey, 2002).

A great example of a protein that is involved in both CME and CIE is ARF6, a multi-functional protein known to participate in clathrin-independent trafficking and recycling of

different cargoes, such as fibrinogen-stimulated internalization of integrin $\alpha_{IIb}\beta_3$ and acetylcholine-muscarinic type 2 receptor (Houndolo, Boulay, & Claing, 2005; Huang et al., 2016). ARF6 also participates in clathrin assembly through the stimulation of phosphatidylinositol 4-phosphate 5-kinase to generate PtdIns(4,5)P_2 at the plasma membrane (Tanabe et al., 2005). Consequently, any manipulation of ARF6 to study its functionality in CIE pathways can affect the uptake of CME cargoes, producing non-physiological cellular responses (D'Souza-Schorey et al., 1995). The crosstalk between the key players of different CIE routes can also negatively regulate other pathways—for example, the key players of caveolae-mediated endocytosis, cavin-1 and cavin-3, can inhibit the CLIC/GEEC pathway by down-regulating Cdc42 (Chaudhary et al., 2014). Furthermore, Cdc42 regulates a number of clathrin-independent pathways including macropinocytosis, FEME and the CLIC/GEEC (Ferreira & Boucrot, 2018; Howes et al., 2010; Sabharanjak, Sharma, Parton, & Mayor, 2002). The existence of crosstalk and parallel pathways makes inhibition studies challenging, since blocking one route may up-regulate compensatory mechanisms that do not contribute to uptake in normal physiological conditions (Sandvig et al., 2011).

1.6.1 Complexity in defining CIE highlighted by GPI-APs studies

One of the best examples of the complexity and difficulty in defining CIE pathways comes from studies on glycosylphosphatidylinositol (GPI)-anchored proteins (GPI-APs) (Rajendran, Knölker, & Simons, 2010). In general, GPI-linked proteins have a long half-life on the plasma membrane, varying from min to hours. Once internalized, GPI-APs can be detected in a population of GPI-enriched endosomal compartments (GEECs) that are void of CME markers such as TfRs (Bhagatji, Leventis, Comeau, Refaei, & Silvius, 2009; Kumari & Mayor, 2008; Sabharanjak et al., 2002).

The clathrin-independent and membrane-raft mediated uptake of GPI-APs has provided the basic rationale for a number of studies to use GPI-APs as an endocytic marker for different CIE pathways (Johannes & Mayor, 2010; Satyajit Mayor & Riezman, 2004; Sharma et al., 2004). Interestingly, years of research on the topic has yielded uncertainty over the extent of CIE pathways' contribution to the uptake of GPI-APs. At first thought to be a caveolae-specific cargo, the involvement of the pathway was later dismissed as it was discovered that the enrichment in the caveolae structures was the artefact of fixation conditions (Mayor & Maxfield, 1995;Mayor, Rothberg, & Maxfield, 1994; Sabharanjak et al., 2002). Multiple studies have independently verified GPI-APs to be the cargo of different endocytic pathways, such as Cdc42 and flotillin-mediated pathways (Ait-Slimane, Galmes, Trugnan, & Maurice, 2009; Kumari, MG, & Mayor, 2010; Sabharanjak et al., 2002). It is most likely that each of these pathways are involved in the differential regulation of GPI-AP uptake on different domains of the plasma membrane or at different times, depending on the upstream signal or the cell line.

1.6.2 Diversity of the molecular mechanisms of CIE subclasses

Despite having different subclasses, the majority of CIE pathways are highly dependent on membrane rafts for internalization. Membrane rafts are specialized microdomains on the plasma membrane that are characterized by the presence of cholesterol and sphingolipids, and directly participate in lateral compartmentalization of molecules at the cell surface (Lajoie & Nabi, 2010). These highly dynamic raft domains constitute the liquid-ordered phase of the plasma membrane and provide signalling and sorting platforms, thereby regulating various signalling and protein trafficking events (Simons & Ehehalt, 2002). It has been shown that the partitioning of CIE cargoes (such as GPI-APs, bacterial toxins, and the cytokine receptor γ chain (γc)) into membrane rafts facilitates membrane invaginations followed by progressive growth into

spherical buds or tubes that finally undergo membrane scission to release the vesicle (Lamaze et al., 2001; Sabharanjak et al., 2002; Sauvonnet, Dujeancourt, & Dautry-Varsat, 2005; Wolf et al., 1998).

Over the years, several pathway-specific cargo selection mechanisms have been identified for different CIE pathways. A few of these mechanisms include the partitioning of cargoes into membrane rafts as seen in the uptake of GM1 ganglioside receptor bound to cholera toxin B subunit (CTxB), the recognition of a specific internalization sequence on the γc subunit of IL-2R, as well as the clustering of cargo by caveolin (Kirkham et al., 2005; Lajoie et al., 2009; Pelkmans, Kartenbeck, & Helenius, 2001; Yu, Olosz, Choi, & Malek, 2000). Based on the type of pathway, the initial curvature can be induced by a variety of mechanisms. The local membrane curvature can be initiated by the binding of membrane proteins such as flotillins, the recruitment of amphipathic proteins such as GRAF-1, or the regulation of plasma membrane dynamics by Rho GTPases through modulation of cytoskeleton (de Curtis & Meldolesi, 2012; Frick et al., 2007; Lundmark et al., 2008; Wang et al., 2009). Regardless of the mechanism, the bending of the membrane forms pathway-specific vesicles that can vary from small, uncoated vesicular structures to larger tubulovesicular compartments (Ferreira & Boucrot, 2018). Similar to other stages, the mechanism behind the vesicle fission is also pathway specific, and can be dynamin dependent, as seen in the Rho-dependent uptake of IL-2R and FEME, or can occur independently of dynamin as seen in CLIC/GEEC (Boucrot et al., 2015; Du Toit, 2015; Lamaze et al., 2001; Sabharanjak et al., 2002). Despite the challenges mentioned above, the mechanisms and kinetics of vesicle formation of different CIE pathways broadly reflects the stages of CME that were described earlier. Many studies have identified the specific molecular components of

these stages, which has allowed us to distinguish different CIE subclasses. In the next section, we will cover different classes of CIE pathways.

1.6.3 Endocytic pathway mediated by Rho family of GTPases

The human Rho GTPases family includes 23 members that act as important biological switches in a variety of intracellular activities, such as cytoskeleton dynamics, cell movement and organelle development (Manneville & Hall, 2002). The three most studied members of the family—Rac1, RhoA and Cdc42—have been primarily associated with the regulation of actin dynamics in cells (Spiering & Hodgson, 2011). Their unique function as master regulators of the actin cytoskeleton, as well as the well-accepted link between actin dynamics and membrane-associated processes provided the rationale to investigate whether Rho GTPases can define a unique subclass of CIE. Perhaps, one of the best understood examples of Rho GTPase-mediated endocytosis came from studies on the mechanisms of IL-2R uptake from plasma membrane of lymphocytes (Basquin et al., 2013;Basquin & Sauvonnet, 2013; Grassart, Dujeancourt, Lazarow, Dautry-Varsat, & Sauvonnet, 2008; Lamaze et al., 2001).

Initially reported by Lamaze et al. in 2001, Baquin et al. dissected the molecular mechanisms of this process a few years later, and confirmed the coordinated involvement of Rac1 in sequestering IL-2Rs in small non-coated invaginations. According to the aforementioned studies, IL-2Rs localize to cholesterol-rich membrane rafts on the plasma membrane and are internalized via an actin-based machinery that is initiated by a PI3K cascade (Basquin et al., 2013a; Lamaze et al., 2001). IL-2R activates Class I PI3K via its regulatory subunit p85, to produce PtdIns(3,4,5)P_3 at the site where receptors are localized. The enrichment of PtdIns(3,4,5)P_3 leads to the activation of Vav2 and the recruitment of Rac1 through the BH domain of p85. The activated Rac1 phosphorylates downstream p21-activated kinase 1 (PAK1).

PAK1 then activates cortactin-N-WASP-Arp2/3 cascade to regulate actin polymerization, and promote F-actin and dynamin-dependent uptake of IL-2Rs (Basquin et al., 2013; Basquin & Sauvonnet, 2013; Grassart et al., 2008).

The studies on the Rho/dynamin-mediated pathway have largely been performed to understand the molecular regulation of IL-2R trafficking, which then questions if Rho-mediated uptake is an exclusive mechanism responsible for shaping immune responses in lymphocytes. Given the universal role of Rho GTPases in the regulation of actin cytoskeleton, it is difficult to imagine that Rho-regulated endocytosis could be exclusive to a specific cell-type. In fact, it has been shown that the intracellular accumulation of amyloid B-peptide, the primary component of amyloid plaques, occurs in a dynamin- and RhoA-dependent manner (Yu, Nwabuisi-Heath, Laxton, & Ladu, 2010). Exploring this pathway can provide avenues for identifying therapeutic targets in Alzheimer's disease.

1.6.4 GEEC pathway

Endocytosis of GPI-APs occurs through a distinct clathrin-independent machinery characterized by clathrin-independent tubulovesicular carriers (CLICs) and the presence of GPI-AP-enriched endosomal compartments (GEECs) as the primary sorting hubs for the incoming cargoes (Kirkham et al., 2005b; Sabharanjak et al., 2002). Ongoing research has further characterized the GEEC pathway to be a dynamin-independent, cholesterol and Cdc42-dependent process that can internalize GPI-APs as well as a number of other cargoes, including CD44, Thy-1, and dysferlin (Chadda et al., 2007; Hernández-Deviez et al., 2008; Howes et al., 2010; Kirkham et al., 2005; Sabharanjak et al., 2002). Given the unique characteristics of its tubulovesicular carriers, the pathway can also accommodate the uptake of a large bulk of fluid-phase along with cargoes, reflecting its role as one of the highest capacity CIE pathway in some cells. Thus, thanks to its

unique morphology, CLICs provide substantial capacity for the internalization of large plasma membrane surface area, and mediate rapid membrane turnover under specific conditions such as plasma membrane repair (Howes et al., 2010; Kirkham et al., 2005; Sabharanjak et al., 2002). The mechanisms of cargo selection are unknown, but the sensitivity to GPI-anchored tails and cholesterol removal suggests that cargo selection might rely on a lipid-based sorting mechanism (Chadda et al., 2007). In fact, the ability of GPI-APs to partition into cholesterol and sphingolipid-enriched rafts can provide a possible explanation for the selective recruitment and the subsequent uptake of the GPI-APs via the GEEC pathway (Sabharanjak et al., 2002).

For the GEEC pathway, the mechanistic details of CLIC biogenesis are not well understood, but it is known that GEEC relies heavily on Cdc42-mediated actin polymerization to mediate the internalization of cargoes (Gupta et al., 2009; Kumari & Mayor, 2008). Following cargo selection, the GEEC internalization pathway progresses by the recruitment of GBF1, a guanine nucleotide exchange factor (GEF) for ARF1 (Gupta et al., 2009). The activated ARF1 then recruits the Rho GTPase-activating-protein (GAP) known as ARHGAP10 to modulate the activity of Cdc42 (Kumari & Mayor, 2008). It has recently been proposed that aside from ARF1, cell surface Cdc42 dynamics are also modulated by a second Rho-GAP, known as GTPase regulator associated with focal adhesion kinase1 (GRAF1) (Lundmark et al., 2008). GRAF1 is a multi-domain protein—comprised of a Rho-GAP, C-terminal SH3 and N-terminal BAR domain—that localizes to PtdIns(4,5)P_2-enriched tubular membranes that have the characteristic morphology of CLICs. Thanks to the multi-domain structure, GRAF1 can simultaneously provide the GAP activity necessary for Cdc42 cycling and sculpt plasma membrane to form tubulovesicular structures (Lundmark et al., 2008). Following endocytosis, CLICs are transported to GEEC endosomes, where cargo sorting takes place.

1.6.5 Caveolae-mediated endocytosis

First observed by Palade in 1953, the flask-shaped plasma membrane microdomains later termed caveolae are now believed to constitute one of the most well-known subclasses of CIE pathways. Caveolae define distinct and abundant cholesterol- and sphingolipid-enriched microdomains that are characterized by the presence of oligomeric caveolin proteins (Kovtun, Tillu, Ariotti, Parton, & Collins, 2015; Parton & del Pozo, 2013). The expression of these specialized microdomains is cell-type specific, as it can heavily decorate the plasma membrane in endothelial, adipocytes and muscle cells, while being completely absent in other cell types (Parton & del Pozo, 2013).

The key structural component responsible for the classical invaginated topology of caveolae are a family of integral proteins known as caveolins. Of the three caveolin members, caveolin-1 and caveolin-2 oligomerize together in cells other than skeletal muscle, and caveolin-3 is predominantly expressed in striated muscle (Williams & Lisanti, 2004). In cultured cells and animal systems, caveolins alone are not sufficient for the formation of caveolae as they require the cooperation of putative caveolar coat proteins, known as cavin, to stabilize the architecture of caveolae on the membrane. The four cavin family members are all cytoplasmic proteins with trimeric coiled-coil architectures, which are recruited to caveolae through interaction with caveolin and phosphatidylserine in order to stabilize the caveolae-domain on the membrane (Bastiani et al., 2009; Fairn et al., 2011; Hill et al., 2008; Kovtun et al., 2015; Liu et al., 2008). Aside from two structural components, other regulators of caveolar machinery—EHD2 (EPS-15 homology domain-containing protein 2), a negative regulator for caveolae endocytosis, as well as PACSIN2 (PKC and casein kinase substrate in neurons 2), a member of BAR-domain proteins—have been shown to associate with mature caveolae at the plasma membrane (Hansen, Howard, & Nichols, 2011; Senju, Itoh, Takano, Hamada, & Suetsugu, 2011; Stoeber et al., 2012).

The tissue-specific expression profile and heterogeneous density of caveolae in cells suggest that these structures serve highly specialized functions in cells. Over the years, diverse biological functions have been associated with caveolae, including as a plasma membrane sensor of extracellular stresses, a fast-acting membrane reservoir to repair membrane damage, a signalling platform to dynamically transmit signals to the cell interior and a regulator of membrane trafficking (Echarri & Del Pozo, 2015; Harvey & Calaghan, 2012; Parton & del Pozo, 2013). Despite being morphologically equivalent to CCPs, the idea of caveolae as a true uptake mechanism is a topic of much debate. The idea that caveolae can only be considered stationary components of the plasma membrane was first demonstrated through fluorescence recovery after photobleaching (FRAP) analysis of GFP-tagged caveolin-1, which revealed that the trafficking of caveolin-1 from the trans-Golgi network to the plasma membrane significantly reduces the mobile fraction to as low as 20-50% (Thomsen, Roepstorff, Stahlhut, & van Deurs, 2002).

The steady-state distribution of caveolae on the membrane is achieved through the interaction of caveolin with actin cytoskeleton and cavin, which together anchor caveolae-raft domains and negatively regulate its internalization (Stahlhut & van Deurs, 2000). The limited mobility of caveolae compared to the dynamic nature of CCPs, makes them incompatible candidates as endocytic carriers. However, despite the observed static nature of caveolae, an increasing number of ligands—such as albumin, autocrine motility factor, and alkaline phosphatase—and pathogens—such as ganglioside-bound cholera toxin, simian virus 40 (SV40), HIV, polyoma virus, and respiratory syncytial virus—have been identified to internalize via the caveolae-dependent pathway (Benlimame, Le, & Nabi, 1998; Mergia, 2017; Parton, Joggerst, & Simons, 1994; Pelkmans et al., 2001; Richterova et al., 2001; Rothberg, Ying, Kolhouse, Kamen, & Anderson, 1990; Schnitzer, Oh, Pinney, & Allard, 1994; Werling et al., 1999).

The development of live cell TIRF microscopy (TIRF-M) made it possible to gain insight into the unique membrane dynamics of caveolae as endocytic carriers of cargoes. Analysis of TIRF images confirmed the existence of two distinct populations of caveolae on the membrane: a major immobilized caveolae fraction and a minor transport-competent fraction capable of constitutive kiss-and-run interaction with the plasma membrane. The constitutive transient fusion occurs over a short distance underneath the plasma membrane and without the complete collapse of the vesicle (Pelkmans & Zerial, 2005). The trafficking of the transport-competent fraction is regulated by the synchronized function of kinases and phosphatases that act as switches for the short to long range cycling between cell surface and intracellular organelles (Botos et al., 2007; Glenney & Zokas, 1989; Kiss, Botos, Turi, & Müllner, 2004; Lee et al., 2000; S. Li, Seitz, & Lisanti, 1996; Sowa, Pypaert, Fulton, & Sessa, 2003).

Once the caveolae vesicles are formed, scission from the membrane is mediated by dynamin GTPase activity at the neck of the vesicle (Henley, Krueger, Oswald, & McNiven, 2000). Following internalization, the intracellular route of caveolae depends on the cargo, as the vesicle can follow the classical endosomal pathway in a Rab5-dependent manner (Pelkmans et al., 2001; Richards, Stang, Pepperkok, & Parton, 2002).

1.6.6 Macropinocytosis

As the oldest and best-understood pathway in the CIE class, the discovery of macropinocytosis goes back to 1931 when it was first observed by Warren Lewis. The formation of distinct membrane ruffles that fuse to form phase bright vesicles allowed for the visualization of macropinocytosis under the light microscope and led to the discovery of the pathway. In most cells, macropinocytosis is induced in response to growth factor stimulation, such as macrophage colony-stimulating factor-1 (CSF-1), epidermal growth factor (EGF) and platelet-derived growth

factor (Davies & Ross, 1978; Lou, Low-Nam, Kerkvliet, & Hoppe, 2014; West, Bretscher, & Watts, 1989). An alternative constitutive form of macropinocytosis contributes to innate immune responses by antigen presenting cells that utilize macropinocytosis as a surveillance mechanism to continuously sample their environments (Doodnauth, Grinstein, & Maxson, 2019). Aside from specialized cells, the aberrant activation of macropinocytosis is a key determinant in the pathology of diseases such as cancer, neurodegenerative diseases, atherosclerosis and renal dysfunction (Amyere et al., 2000; Chung et al., 2015; Kruth et al., 2005; Veithen, Cupers, Baudhuin, & Courtoy, 1996; West et al., 1989; Zeineddine & Yerbury, 2015).

The general process of macropinocytosis involves the rearrangement of the actin cytoskeleton and the formation of plasma membrane ruffles known as lamellipodia or dorsal ruffles in some cells (Pollard & Borisy, 2003). Once the actin cytoskeleton collapses, a portion of the lamellipodium retracts back into the cell, while the other portion fuses with the plasma membrane, creating irregular shaped non-coated vesicles knows as macropinosomes (Araki, Egami, Watanabe, & Hatae, 2007; Swanson & Watts, 1995). The heterogeneous size of macropinosomes—ranging from 0.2 to 5 μm—distinguishes this pathway from other endocytic routes, and allows for the non-specific internalization of large quantities of solutes and fluid (Araki et al., 2007).

Macropinocytosis is regulated by a minor but vital lipid component of membranes known as phosphoinositides, which play critical roles in cell membrane dynamics, membrane trafficking and cellular signalling (Maffucci & Falasca, 2014). Indeed, each stage of macropinocytosis is modulated by the sequential activation of key phosphoinositide metabolising enzymes that control the concentration of different phosphoinositide species, specifically, PtdIns(4,5)P_2, PtdIns(3,4,5)P_3 and PtdIns(3)P (Araki, Johnson, & Swanson, 1996; Araki et al., 2007; Yoshida,

Hoppe, Araki, & Swanson, 2009). The sequential change in the abundance of these phosphoinositide species regulates the stages of macropinocytosis through regulating actin remodeling—from formation of cell surface ruffles that close into open cups (ruffle closure) to the subsequent formation of macropinosomes following cup closure (Yoshida et al., 2009).

Upon activation of receptors such as EGFR, the concentration of PtdIns(4,5)P_2 transiently increases during ruffle formation and reaches its highest level in the membrane ruffles. The increase in PtdIns(4,5)P_2 leads to the recruitment and activation of various actin cytoskeleton modulating-effectors required for the formation of membrane ruffles (Araki et al., 2007). The process is initiated by the recruitment and activation of Rac1 and Cdc42 to the site of membrane protrusion (Araki, Hamasaki, Egami, & Hatae, 2006; Fujii, Kawai, Egami, & Araki, 2013; Patel & Galán, 2006; Yoshida et al., 2009). Following recruitment, Rac1 mediates the activation of WAVE2, while Cdc42 promotes the activation N-WASP (Miki, Yamaguchi, Suetsugu, & Takenawa, 2000; Pollitt & Insall, 2009; Rohatgi, Ho, & Kirschner, 2000). Together, WAVE2 and N-WASP regulate the activity of the Arp2/3 complex to nucleate the branched network actin filaments required for membrane ruffle formation (Machesky et al., 1999; Machesky & Insall, 1998; Rohatgi et al., 2000). Around the time of ruffle closure, Class I PI3K phosphorylates the D3 position of PtdIns(4,5)P_2, leading to the transient increase of PtdIns(3,4,5)P_3 which mediates the recruitment of the next set of protein effectors to promote the turnover of actin filaments during ruffle closure (Yoshida et al., 2009).

Following the PtdIns(3,4,5)P_3 spike within the circular domain of the plasma membrane, Rac1 activity increases again to mediate ruffle closure (Yoshida et al., 2009). During ruffle closure, Rac1 directly phosphorylates PAK1 to activate C-terminal-binding protein-1/Brefeldin A-ADP–ribosylated substrate (CtBP1/BARS), a protein involved in macropinocytic fission and

internalization (Liberali et al., 2008). The cup closure proceeds 40-100 seconds after the deactivation of Rac1 and Class I PI3K, which coincides with the formation of PtdIns(3)P by Class III PI3K as well as the recruitment of effectors (including Rab5 and EEA-1) to mediate homotypic fusion of early macropinosome (Hamasaki, Araki, & Hatae, 2004; Yoshida et al., 2009).

The mechanistic description provided above was a short summary of events leading to macropinosome formation. In reality, macropinocytosis is a complex process that involves the sequential signalling of other proteins such as ARF, Ras and other Rab GTPases involved in macropinosome formation (Kruth et al., 2004).

1.6.7 Flotillin-dependent endocytosis

The flotillin family is composed of two highly homologous members: flotillin-1/reggie-2 and flotillin-2/reggie-1. Both members of the family are ubiquitously expressed, conserved among species and share 50% amino acid sequence identity (Grant & Benjamin, 2011; Meister & Tikkanen, 2014). The two proteins bind to each other and can be efficiently co-immunoprecipitated from the cell extract with their expression and stability depending on one another. However, it appears that flotillin-1 is more dependent on flotillin-2 than vice versa (Solis et al., 2007).

Structurally, both flotillins are composed of 1) N-terminal prohibition homology (PHB) domain also known as SPFH (stomatin/prohibitin/flotillin/HflK/C) domain, which contains key conserved cysteine residue for acylation, 2) phosphorylatable tyrosine residue, and 3) C-terminal alpha-helix folding characterized by the presence of 25 glutamate-alanine enriched heptad tandem arrays, which mediate oligomerization (Babuke et al., 2009; Grant & Benjamin, 2011; Solis et al., 2007). The PHB/SPFH domain is evolutionary conserved and is shared among

several eukaryotic and prokaryotic membrane proteins. The PHB domain is found within a diverse array of proteins that exhibit tendencies to localize to different membrane compartments, from mitochondria to the Golgi and the plasma membrane, and thus can hold diverse functions (Morrow & Parton, 2005). Indeed, all PHB domain-carrying proteins are integral membrane proteins and can associate with the membrane through oligomerization, acylation, or direct insertion into the inner leaflet of the membrane through a hydrophobic hairpin (Morrow and Parton, 2005). In agreement with their PHB feature, flotillins can constitutively associate with the plasma membrane to form highly detergent-resistant microdomains through the insertion of two hydrophobic hairpins, acylation (covalent attachment of a single palmitate in flotillin-1, or a myristate and three palmitates in flotillin-2), oligomerization, and cholesterol binding (Babuke et al., 2009; Li, Martin, Cravatt, & Hofmann, 2012; Morrow et al., 2002; Neumann-Giesen et al., 2004; Strauss et al., 2010). The phosphorylation of tyrosine residues (Y160 and Y163 in flotillin-1 and flotillin-2, respectively) by Fyn and potentially other Src family kinases is essential for flotillin internalization (Babuke et al., 2009; Neumann-Giesen et al., 2007; Riento et al., 2009).

First believed to be a cargo of caveolae-mediated endocytosis or the substitute for caveolae in different cell types and tissues, it is now well-established that flotillins are involved in the formation of non-caveolar microdomains. In fact, their association with detergent-resistant rafts and their ability to form dynamic endocytic structures on the plasma membrane have supported their role as a structural component in membrane trafficking (Frick et al., 2007; Glebov, Bright, & Nichols, 2006). Furthermore, the discovery of flotillin-specific cargoes such as CD59, CTxB, cationic molecules and polyplexes, proteoglycans, and the Niemann-Pick C1-like 1 protein (NPC1L1), have further supported the role of flotillins as carriers of endocytosis

(Al Soraj et al., 2012; Frick et al., 2007; Liang Ge et al., 2011; Glebov et al., 2006; Meister & Tikkanen, 2014; Payne, Jones, Chen, & Zhuang, 2007; Vercauteren et al., 2011).

1.6.7.1 Flotillin's role in endocytosis

The idea that flotillins could participate in clathrin and caveolae-independent uptake of specific cargoes was first proposed by Glebov et al., who used live TIRF imaging and particle tracking software to follow the dynamic behaviour of flotillin-1-GFP on the plasma membrane. According to the aforementioned study, flotillin-1-GFP exhibited distinct punctate distributions along the plasma membrane and colocalized with endocytic markers such as CTxB (but not with transferrin or caveolae) and disappeared overtime, which was indicative of internalization events. Furthermore, they reported that flotillin-1-positive microdomains exhibited more dynamic behaviour compared to CPPs, as they had higher mean velocity and internalized at a frequency that was less than one third of CCPs, emphasizing the dynamic nature of flotillin-1 microdomains (Glebov et al., 2006). Similarly, Frick and colleagues sought to confirm whether flotillins could be considered a distinct class of CIE, by tracking flotillin-1-GFP and flotillin-2-GFP dynamics on the membrane over time. In agreement with Glebov's observations, they reported that flotillin-1-GFP and flotillin-2-GFP co-assembled to generate de novo membrane microdomains with the ability to undergo transient membrane invagination and fission (Frick et al., 2007). Furthermore, they established that flotillin-positive microdomains had a similar morphology as CCPs and interacted with CIE markers such as GPA-APs and subsequently drove them to accumulate in flotillin-positive vesicles. The above studies concomitantly concluded that flotillins define highly dynamic microdomains on the plasma membrane, which can actively participate in membrane trafficking events, and thus act as the determinant of a distinct CIE subclass in cells (Frick et al., 2007; Glebov et al., 2006).

Parallel to the idea of flotillin-dependent endocytosis, there is also evidence for the indirect involvement of flotillins in membrane trafficking. As such, flotillins might also be involved in the pre-endocytic clustering of cargoes that are destined for other endocytic routes such as CME, rather than directly participating in the internalization process (Amaddii et al., 2012a; Schneider et al., 2008; Sorkina, Caltagarone, & Sorkin, 2013). As an example, flotillin-1 is the requisite intermediary of PKC-triggered dopamine transporter (DAT) endocytosis as it facilitates the clustering of the transporters in the plasma membrane prior to their internalization via CME (Cremona et al., 2011; Sorkina, Hoover, Zahniser, & Sorkin, 2005).

Another example of the indirect role of flotillins in endocytosis has been reported in studies of NPC1L1 membrane trafficking (Ge et al., 2011). The NPC1L1 receptor mediates cellular cholesterol uptake and cycles between the plasma membrane and recycling endosomes (Ge et al., 2011; Liang Ge et al., 2008). Upon cholesterol binding, the receptor is internalized with the help of clathrin machinery, while cholesterol depletion induces the recycling of the receptor to the cell surface in a myosin Vb, Rab11a, Rab11-FIP2-dependent manner (Betters & Yu, 2010; Chu et al., 2009). Recent findings have established the role of flotillins in clathrin-mediated internalization of NPC1L1 and cholesterol uptake. Given their propensity to undergo oligomerization, it has been suggested that flotillins act upstream of clathrin by promoting the pre-endocytic clustering of receptors within cholesterol-enriched membrane microdomains to trigger NPC1L1-mediated cholesterol uptake (Liang Ge et al., 2008).

In line with observations about the indirect role of flotillins in DAT and NPC1L1 endocytosis, it was also observed that knocking down flotillin-1 influenced EGFR clustering at the plasma membrane upon EGF stimulation, but it did not affect EGFR internalization (Amaddii et al., 2012). Reflecting on the literatures about flotillins, it can be proposed that a specific subset

of cargoes cluster in flotillin microdomains prior to internalization via CME (Meister & Tikkanen, 2014). This could provide an explanation for recent data showing that some subsets of clathrin-coated vesicles are devoted solely to specific cargoes (Delos Santos et al., 2017). Based on the body of evidence presented above, it is clear that flotillins play a functional role in various membrane trafficking events: from defining an essential structural component that accounts for a significant fraction of clathrin-independent endocytosis, to forming clusters of cargoes prior to their endocytosis by clathrin machinery.

1.6.7.2 Flotillins as a signalling platform

As a marker of membrane rafts, flotillins are important structural raft components for the clustering of key regulators of signal transduction pathways (Grant & Benjamin, 2011). The most famous case in supporting the role of flotillins in the formation of active signalling platforms is their association with insulin-receptor signalling pathway. Following insulin stimulation, CBL and CBL-associated proteins (CAPs) dissociate from the insulin receptor and translocate to membrane rafts. The association of the CBL and CAPs complex to membrane rafts is mediated through the binding of flotillins to the sorbin homology domain of CAPs, which leads to the activation of Rho GTPase, RhoQ, and the trafficking of GLUT4 to the plasma membrane (Baumann et al., 2000; Kimura, Baumann, Chiang, & Saltiel, 2001). Aside from the insulin pathway, flotillins also positively modulate Gαq-coupled GPCR-mediated activation of p38 MAPK signalling pathway through directly interacting and sequestering Gαq in membrane rafts (Sugawara et al., 2007). Finally, flotillins act as assembly sites for the activation of T-cell receptors, as it has been shown that the recruitment of the linker for the activation of T-cells (LAT) to flotillin microdomains is required for the activation of the protein by Src family kinase Lck, and for the regulation of downstream signalling pathways (Slaughter et al., 2010).

1.6.8 Calcium-induced massive endocytosis

Neurons are specialized cells that can process and transmit both electrical and chemical signals. The induction of synaptic vesicle endocytosis in response to an increase in local calcium concentration is a well-known event (Cousin, 2000). An emerging theory suggests the existence of calcium-induced endocytic pathway in non-neuronal cells. The massive endocytic events (MEND) following sudden increases in cytosolic calcium concentration in fibroblast cells were first reported by Hilgemann and colleagues. MEND is a non-conventional clathrin-independent pathway that is responsible for the uptake of large plasma membrane and bulk fluid into cells. Hilgemann and colleagues argue that the MEND pathway is centred on the activity of a member of palmitoyl acyl transferases (PAT) known as DHHC5. Calcium influx initiates the signalling cascades that lead to the activation of DHHC5 and the subsequent palmitoylation of membrane proteins, leading to the lipid reengagement that can potentially activate an endocytic event. However, they did not successfully identify the proteins that are palmitoylated following calcium entry (Hilgemann, Fine, Linder, Jennings, & Lin, 2013).

My goal was to accurately identify the class of CIE pathway—of all those mentioned above—that was stimulated by USMB as a mechanism for targeted drug delivery. My initial observation confirmed that USMB treatment can stimulate the uptake of fluid-phase markers through clathrin-independent machinery, but the molecular identity of the pathway or the mechanism of the activation remained to be resolved. In the third chapter, I simply labelled the clathrin-independent pathway as fluid-phase uptake to distinguish the route from CME and to highlight the non-receptor-based nature of the pathway. The fourth chapter and two years of my PhD studies were invested in finding the exact molecular identity of the “fluid-phase” route,

which I discovered to share similarities with MEND pathways. In the next section the major components of the MEND pathway will be discussed.

1.6.8.1 DHHC5, a key regulator of MEND pathways

Protein lipidation is a type of post-translational modification that involves the attachment of a variety of lipids—such as octanoic acid, myristic acid, palmitic acid, stearic acid, farnesyl or geranylgeranyl group—to specific sequences of a diverse array of proteins that range from soluble to polytopic transmembrane proteins (Aicart-ramos, Valero, & Rodriguez-crespo, 2011). Lipidation can occur at different stages of the protein life cycle to regulate protein function and localization, from immediately after synthesis in ER, during sorting in the Golgi apparatus or even at the plasma membrane (Aicart-ramos et al., 2011). Furthermore, proteins can undergo single or sequential modification with the same or different lipid moiety to promote stable membrane attachment or partition into a specific membrane microdomain. As an example, Ras C-terminal farnesylation and Src-family N-terminal myristoylation promote the palmitoylation of their cysteine residues, while H-Ras can get palmitoylated on either or both Cyst181 and Cyst184. The differential palmitoylation of H-Ras cysteine residues can influence the Golgi to plasma membrane anterograde transport and dictate the lateral segregation of H-Ras in cholesterol-dependent versus independent microdomains (Aicart-ramos et al., 2011; Roy et al., 2005).

Palmitoylation refers to the reversible attachment of 16-carbon palmitate to the cysteine residues of proteins (Aicart-ramos et al., 2011). In most cases, the fatty acid attachment is formed through a thioester linkage (S-palmitoylation)—however, in some cases, palmitate is added to a cysteine residue at the N-terminus of a protein forming a thioester intermediate that is rearranged immediately to a stable amide linkage (N-palmitoylation) (Charollais & Van Der

Goot, 2009). In contrast to the conventional view of palmitoylation as a one-time event for the initial sorting of proteins following translation, the more recent view proposes that palmitoylation is a highly dynamic and reversible process that can influence the function of proteins (Conibear & Davis, 2010). Due to its reversible nature, palmitoylation can alter the subcellular localization of peripheral membrane proteins and govern protein association with different membrane compartments (Rocks et al., 2010). In other words, palmitoylation alters global cellular functions through changing protein-protein interaction, dictating subcellular trafficking, mediating signal transduction and promoting the partitioning into specific membrane microdomains (Choy et al., 1999; Conibear & Davis, 2010; Deschenes, 2013; García-Cardeña, Oh, Liu, Schnitzer, & Sessa, 1996; Resh, 1999; Salaun, Greaves, & Chamberlain, 2010).

Over the past several decades, since the discovery of palmitoylation in cells, a variety of proteins have been identified to undergo dynamic palmitoyl modification—these proteins include Gα subunits of GPCRs, Src family kinases, Ras proteins, endothelial nitric oxide synthase (eNOS), soluble N-ethlymaleimide-sensitive factor attachment protein receptor (SNARE) membrane fusion proteins and many more (Chen & Manning, 2001; Eisenberg et al., 2013; Goddard & Watts, 2012; Koegl, Zlatkine, Ley, Courtneidge, & Magee, 1994; Jianwei Liu, García-Cardeña, & Sessa, 1996; Prescott, Gorleku, Greaves, & Chamberlain, 2009; Wedegaertner, 1998). Despite lacking a clear consensuses sequence, the cysteine residues of all proteins that undergo palmitoylation share some common characteristics: 1) the surrounding amino acids are basic or hydrophobic, 2) the cysteine residues are adjacent to myristoylation or prenylation sites, 3) and they are frequently located in the cytoplasmic region adjacent to transmembrane domain (Popova et al., 2013). Overall, the palmitoylation of cysteine residues of proteins uniquely regulates their localization, and consequently their function.

First identified in yeast, 23 members of the PAT family have been identified in mammals (Linder, 2004; Mitchell, Vasudevan, Linder, & Deschenes, 2006). All members of the family are multi-pass transmembrane proteins with four to six transmembrane domains, and are characterized by the presence of DHHC (aspartate-histidine-histidine-cysteine) motif in their active site (Korycka et al., 2012; Mitchell et al., 2006). These so-called DHHC proteins localize to different organelles—for example, DHHC1, 6, 10, 11, 11,13,14, and 19 localize at ER, DHHC3, 4, 7, 8, 15, 17 and 18 at Golgi while DHHC5, 20, and 21 reside at the plasma membrane (Yaxiao Li & Qi, 2017; Ohno, Kihara, Sano, & Igarashi, 2006). The large number of DHHC enzymes coupled with their localization to distinct membrane compartments could imply that the cellular palmitoylation machinery is highly regulated and can modify protein localization and function at different stages of the protein life cycle (Aicart-ramos et al., 2011).

The large number of DHHC enzymes and the diversity in palmitoylated proteins could suggest enzyme preference for a specific substrate. However, the substrate specificity of DHHCs has not been resolved due to conflicting studies on both the indispensability and the exchangeability of the enzymes for a specific substrate. As an example, H-Ras has been known to be the substrate of DHHC9, and yet knocking down DHHC9 by siRNA gene silencing does not affect the proper localization of H-Ras, suggesting that palmitoylation is not restricted by substrate recognition (Rocks et al., 2010). On the other hand, SNAP25b but not SNAP23 is specifically recognized and palmitoylated by DHHC15. Designing a SNAP23 point mutant (C79F) that mimics SNAP25b can promote its palmitoylation by DHHC15. Furthermore, mutating proline-117, 25 residues downstream of the palmitoylated cysteine-rich domain, can promote palmitoylation by of mutant SNAP25 by DHHC3 but not DHHC17 (Greaves et al., 2009; Greaves, Gorleku, Salaun, & Chamberlain, 2010). Hence, it is possible that the

differential specificity of the DHHC family for a particular substrate is determined by both substrate structure and the sequence surrounding the palmitoylated cysteine (Tabaczar, Czogalla, Podkalicka, Biernatowska, & Sikorski, 2017).

Unlike other DHHCs that reside on ER and Golgi to constitutively palmitoylate proteins for intracellular sorting to the proper membrane compartments, DHHC5, 20 and 21 reside on the cell surface to mediate dynamic palmitoylation that regulates a plethora of physiological processes, from endocytosis to synaptic plasticity (Korycka et al., 2012). The idea that reversible lipid modification can change the localization of proteins at the plasma membrane and alter proteins' activities has been previously investigated in neurons. In fact, dynamic changes in lipid modification have been shown to play an important role in neuronal functions, and disruption in this process can cause a variety of neurodevelopmental conditions (Fukata & Fukata, 2010). Among the members of the DHHC family, DHHC5/8 have been implicated to play physiological roles in higher brain functions, as mice with lower DHHC5 activity exhibited deficit in memory functions and DHHC8 knockout mice had reduced density of dendritic spines and glutaminergic synapses (Li et al., 2010; Mukai et al., 2008). In addition, genome-wide association studies have linked both DHHC5 and 8 to neuropsychiatric conditions. The occurrence of mutations in chromosome 11 containing the *ZDHHC5* gene have been reported in patients with bipolar disorder, while microdeletion in the region of chromosome 22 where *ZDHHC8* lies has been linked to schizophrenia (Fallin et al., 2004; Mukai et al., 2004; Thomas, Hayashi, Chen, Chiu, & Huganir, 2013).

In accordance with its localization at the synaptic cleft, DHHC5 has been shown to play a crucial role in mediating the trafficking and proper localization of a number of synaptic signalling proteins such Grip1b, δ-catenin, flotillin-2, somatostatin receptor 5, and Ankyrin-G

(Brigidi, Santyr, Shimell, Jovellar, & Bamji, 2015; He, Abdi, & Bennett, 2014; Kokkola et al., 2011; Li et al., 2012; Thomas et al., 2013). Moreover, the dynamic palmitoylation of synaptic proteins in response to neuronal activity has been shown to mediate synaptic plasticity. According to Brigidi et al., under basal conditions DHHC5 localizes at the synaptic membrane through interaction with palmitoylated PSD-95 as well as direct phosphorylation of its tyrosine-533 by Fyn kinase. Neuronal activity and an increase in Ca^{2+} concentration disrupt the DHHC5/PSD95/Fyn complex at the membrane, causing the internalization and trafficking of DHHC5 to the recycling endosomes, where it palmitoylates δ-catenin. Following palmitoylation, δ-catenin and DHHC5 move to the synaptic membrane, where palmitoylated δ-catenin localization to the membrane stabilizes cadherin, to promote AMPA-type glutamate receptor recruitment to the membrane and stimulate synaptic plasticity (Brigidi et al., 2015).

Beyond the role of DHHC5 in neurons, dynamic and reversible control of protein palmitoylation is emerging as an important regulator of membrane traffic in epithelial cells. As an example, the membrane traffic of flotillins is controlled by the reversible palmitoylation at Cys34 of flotillin-1 and Cyst4, Cyst19 and Cys20 of flotillin-2 (Jun Liu, DeYoung, Zhang, Dold, & Saltiel, 2005; Morrow et al., 2002; Neumann-Giesen et al., 2004). Recently, Li et al. proposed that flotillin-1 can undergo dynamic palmitoylation at the plasma membrane in response to insulin-like growth factor 1 (IGF-1) stimulation, an event independent of initial palmitoylation which is required for ER exit and the plasma membrane localization. Jang et al. established that flotillin-1 palmitoylation turnover at the plasma membrane was essential in prolonging IGF-1R-activated PI3K/Akt signalling pathway to promote cancer cell proliferation (Jang, Kwon, Jeong, Lee, & Pak, 2015). However, they did not identify which DHHC enzyme is involved in the regulation of dynamic changes in the palmitoylation of flotillin-1 on the

plasma membrane. Given that DHHC5 localizes at the plasma membrane, and the Ca^{2+}-induced massive endocytosis relies on the activity of DHHC5, I hypothesized that USMB treatment promotes the DHHC5-dependent palmitoylation turnover of key plasma membrane proteins that participate in membrane trafficking, such as flotillins.

Parallel to the palmitoylation hypothesis is the idea that USMB might enhance the rate of endocytosis through the activation of the membrane repair pathway as a direct result of transient pore formation. It has been previously shown that injury-induced endocytosis is activated in response to Ca^{2+}-regulated lysosome exocytosis following membrane damage. Given that USMB treatment induces pores on the plasma membrane, I hypothesized that the rapid endocytosis following USMB treatment is triggered as a consequence of membrane damage. The involvement of the membrane repair pathway in the activation of endocytosis following USMB treatment will be examined in Chapter 3. In the next section, the membrane repair pathway will be discussed in greater detail.

1.7 Membrane repair following injury activates endocytosis

The plasma membrane is a dynamic organelle that encloses, defines boundaries, and acts as the primary contact point between the cell and the extracellular environment. As the first barrier, the plasma membrane is exposed to a variety of physical and chemical stresses that can damage its integrity. To withstand mechanically challenging environments, cells have evolved mechanisms that dynamically respond to membrane disruption events (Blazek, Paleo, & Weisleder, 2015). Indeed, the remarkable capacity of cells to respond to membrane damage suggests that resealing is a fundamental biological process. The discovery that sea urchin eggs have the inherent capacity to repair their membranes was the beginning of a long journey to understand the

sophisticated array of repair mechanisms employed by cells to respond to membrane damage (Chambers & Chambers, 1961; Heilbrunn, 1956).

The concentration of calcium in extracellular fluid is 10,000 fold greater than in cytosol, and the concentration difference is maintained by elegant mechanisms that regulate the movement of calcium across membrane compartments (Carafoli & Krebs, 2016). In fact, it is the sensitivity of cells to slight changes in calcium concentration that has turned this ion into an excellent messenger for modulating normal cellular processes such as the secretion of insulin or the contraction of smooth muscle cells, as well as initiating stress responses (Adelstein & Sellers, 1987; Cerella, Diederich, & Ghibelli, 2010; Draznin, 1988). Upon plasma membrane injury, the influx of calcium initiates signalling cascades to modulate membrane-mediated processes, such as exocytosis of intracellular vesicles and organelles, caveolae-mediated wound constriction, outward budding of injured sites, and endocytosis (Bi, Alderton, & Steinhardt, 1995; Cai et al., 2009; Defour et al., 2014; Miyake & McNeil, 1995; Tam et al., 2010). Out of the mechanisms mentioned above, the type of injury-induced membrane process is determined in a context-dependent fashion, and is influenced by wound size, type of cell, and the nature of the stress (Blazek et al., 2015).

When it comes to membrane damage, response time is the most critical factor in determining the fate of the cell, as continuous calcium influx beyond the normal physiological threshold can have detrimental consequences. The observation of barrier formation within 30s after significant membrane disruption suggests the existence of a patching mechanism in cells. The fast speed of membrane replacement at the site of injury suggests that the lipid bilayer is getting delivered from already existing membrane compartments (Bi et al., 1995; Miyake & McNeil, 1995).

Early evidence of the involvement of Ca^{2+}-dependent exocytosis in repairing membrane damage came from the pioneering work of Steinhardt et al. who studied the resealing of disrupted cell membranes in fibroblasts and sea urchin eggs treated with proteases against SNARE proteins. The inactivation of SNAREs using botulinum or tetanus 60 min prior to a wounding event prevented membrane resealing, confirming that exocytosis was required for membrane repair (Steinhardt, Bi, & Alderton, 1994). Based on the initial observation, Whaley et al. used confocal microscopy with cell-impermeant lipophilic fluorescent dyes (such as FM 1-43), and confirmed the exocytosis of intracellular vesicles in sea urchin eggs following membrane damage. But perhaps the most important finding of this study was establishing for the first time that the damage-induced exocytosis occurred as a direct consequence of elevated intracellular calcium concentration (Whalley, Terasaki, Cho, & Vogel, 1995).

Naturally, it was intriguing to identify the population of vesicles that have evolved to undergo rapid exocytosis in response to calcium influx during membrane damage. Studies in sea urchin eggs identified yolk granules as the fusion machinery that undergoes Ca^{2+}-induced exocytosis during membrane resealing (McNeil, Vogel, Miyake, & Terasaki, 2000). The observation of the yolk granules' ability to undergo Ca^{2+}-triggered fusion suggested that the yolk's counterpart in mammalian cells—lysosomes—could follow a similar path. Detection of the lysosomal resident protein, such as lysosomal-associated membrane protein-1 (LAMP-1), on the plasma membrane of wounded cells helped in confirming the identity of the membrane reservoir capable of exocytosis at the injured site (Reddy, Caler, & Andrews, 2001). Moreover, the presence of calcium-sensing synaptotagmins on lysosomes provided strong evidence for the involvement of these organelles as the major resealing component of injured membrane, thus

challenging the traditional view that conventional lysosomes could only act as the terminal compartments of endocytosis (Mcneil & Terasaki, 2001; McNeil, 2002).

Synaptotagmins are a family of proteins composed of a N-terminal transmembrane domain, a central linker and two cytoplasmic calcium binding domains (Südhof, 2002). Initially discovered as an abundant constituent of synaptic vesicles in neurons, there are now 17 isoforms that have been identified in mammals—each with their own tissue-specific distribution and distinct subcellular localization (Chen & Jonas, 2017). The membrane fusion process is initiated through the binding of calcium to the C2 domains of synaptotagmin, which promotes a strong interaction between both the C2A and C2B domains and PtdIns(4,5)P_2 in the target membrane. Upon penetrating the bilayer, the vesicular SNARE interacts with the target membrane SNARE to form a trans-SNARE complex. The complex brings the two membranes into close proximity to trigger the formation of hemifusion intermediate, in which a fusion pore is opened, and the two membranes begin to fuse. As the pore expands, the vesicle collapses, completing the fusion of the vesicle with the target membrane (Chapman, 2002). The structural similarity and the distinct localization of synaptotagmin VII to LAMP-1 positive lysosomes further support the theory that conventional lysosomes can act as secretory organelles in response to elevated calcium concentrations upon membrane injury (Reddy et al., 2001).

For decades, Ca^{2+}-mediated exocytosis was regarded as the only component of the membrane repair pathway (McNeil, Miyake, & Vogel, 2003; McNeil, 2002; Reddy et al., 2001; Rodríguez, Webster, Ortego, & Andrews, 1997; Steinhardt et al., 1994). Yet, there was a possibility that the complete restoration of cellular function following membrane damage might require additional processes. In recent years, the model of membrane repair was revisited and the idea of exocytosis of lysosomes as an end point of the resealing mechanism was challenged for a

number of reasons. First, cells might experience more than one plasma membrane disruption event in their lifetimes—as such, the extra lipid bilayer added via fusion must be retrieved following exocytosis. Otherwise, the surface area of the plasma membrane would increase after each time that the membrane continuity was restored. Secondly, in some cases where membrane integrity is disrupted by chemical agents (such as pore-forming toxin streptolysin O (SLO)), the microbial toxin must be physically removed from the plasma membrane to restore the plasma membrane integrity (Idone et al., 2008; Tam et al., 2010).

This persuaded Tame et al. to revisit the membrane repair mechanism, and provide a more detailed mechanistic insight into the complete sequence of events that occurs following membrane injury. In the new membrane repair model, a consequent compensatory endocytosis response is required for proper membrane resealing. According to this model, the exocytosis of lysosomes triggered by Ca^{2+} entry through SLO-induced membrane injury results in the release of lysosomal acid-sphingomyelinase (A-SMase) to the outer leaflet of the plasma membrane, which promotes ceramide-induced endocytosis (Tam et al., 2010). It is important to note that the compensatory endocytic response in not restricted to SLO treatment, as the injury-induced endocytosis also occurs in mechanically wounded cells (Idone et al., 2008). Given the above, Tam et al. proposed that injury-induced endocytosis is the direct consequence of sphingomyelin turnover in the outer leaflet of the plasma membrane. It is not known whether the same sequence of events that trigger compensatory endocytosis upon membrane damage are responsible for rapid endocytic responses following USMB treatment. In Chapter 3, the contribution of the membrane repair pathway in the activation of USMB-induced endocytosis will be examined.

1.7.1 Ceramide as a modulator of endocytosis

Sphingomyelin is the most abundant sphingolipid in the plasma membrane of mammalian cells. The biosynthesis of sphingomyelin involves the transfer of a phosphocholine headgroup from phosphatidylcholine to a ceramide backbone, a reaction that is mediated by sphingomyelin synthase-1 and 2 in the trans-Golgi network and at the cell surface (Subathra, Qureshi, & Luberto, 2011). The metabolism of sphingomyelin by sphingomyelinase (SMase) releases ceramide and phosphocholine in response to a number of stress stimuli (such as cytokines, death receptor ligands, chemotherapeutics, membrane damage or other environmental stresses), and has been shown to play a significant role in the activation of stress-induced signalling pathways (Van Blitterswijk, Van Der Luit, Veldman, Verheij, & Borst, 2003). Indeed, the plasma membrane contains a pool of sphingomyelin that can undergo rapid turnover to release ceramide in response to stress stimuli. Upon sphingomyelin breakdown, the generated ceramide then activates signal transduction pathways that shape cellular functions, particularly plasma membrane-related processes and apoptosis (Kolesnick & Krönke, 1998).

In line with the membrane repair theory, it has been shown that the elevated Ca^{2+} concentration upon plasma membrane damage and the subsequent membrane addition by lysosome exocytosis indirectly triggers endocytic responses through A-SMase-induced ceramide generation (Tam et al., 2010). Independent of injury-induced endocytosis, the role of ceramide as a second messenger in shaping membrane structure and dynamics had been previously investigated. It has been shown that the asymmetric application of SMase to the outer or inner leaflet of phosphatidylcholine-sphingomyelin liposomes, and the subsequent generation of ceramide, is sufficient for inward membrane invagination and vesicle budding (Holopainen, Angelova, & Kinnunen, 2000). Similarly, the treatment of ATP-depleted macrophages and

fibroblasts with SMase induces the formation of endocytic vesicles within 10 min after treatment (Zha et al., 1998). These studies collectively confirmed that the generation of ceramide on the plasma membrane can promote membrane curvature and vesicle formation, signifying the involvement of ceramide in the modulation of membrane trafficking events in response to stress stimuli.

The effect of ceramide on the spontaneous inward bending of membrane can be attributed to its unique structure. Once generated through sphingomyelin breakdown, ceramide self-segregates to promote the formation of stable, tightly-packed membrane microdomains (Andrews, Almeida, & Corrotte, 2014). The tendency to self-aggregate is a spontaneous response, since as little as 5 mol% ceramide is sufficient for the formation of ceramide-enriched microdomains, and these microdomains can spontaneously fuse to form larger structures with a diameter of up to several micrometers (Veiga, Arrondo, Goñi, & Alonso, 1999). Plus, ceramide has a smaller, less hydrophobic head-group compared to sphingomyelin, and occupies a smaller area within the leaflet compared to other membrane lipids (Andrews et al., 2014). Consequently, the self-aggregation of ceramide into microdomains combined with the asymmetric area difference caused by its small head-group provide the driving force for inward curvature and vesicle formation (López-Montero, Vélez, & Devaux, 2007).

Of course, the sphingomyelin-ceramide signal transduction pathway is not exclusive to membrane damage, as ceramide acts as an important lipid second messenger in eliciting cellular responses ranging from proliferation, differentiation to apoptosis (Hannun, 1994; Hannun & Luberto, 2000). In fact, the existence of multiple physiological sources of ceramide could suggest that ceramide can play a wide range of functions in the cell—from changing the biophysical properties of the membrane, to providing membrane platforms for receptor

signalling, modulating cytosolic enzymes or even regulating ion channels (Grassmé, Riethmüller, & Gulbins, 2007). It is well known that ceramide-enriched membrane platforms participate in signal transduction pathways following the stimulation of cytokine receptors CD95, CD40, or after exposure to environmental stresses such as UV-light and gamma-irradiation (Bionda et al., 2007; Charruyer et al., 2005; Grassmé et al., 2001; Grassmé, Jendrossek, Bock, Riehle, & Gulbins, 2002; Santana et al., 1996). In general, ceramide-microdomains act to initiate or maintain signalling cascades through different mechanisms, such as trapping receptors to stabilize ligand-receptor interaction, excluding inhibitory molecules, and clustering signalling molecules (Yang Zhang, Li, Becker, & Gulbins, 2009).

One of the best described roles of ceramide in mediating stress responses pertains to its involvement in modulating Fas-induced apoptosis. It has been reported that Fas ligation triggers the translocation of A-SMase to the cell surface, where it hydrolyzes sphingomyelin to ceramide. The formation of ceramide microaggregates on the membrane is essential for the oligomerization of preassembled Fas trimers to transmit signals for the activation of caspase-dependent apoptosis (Miyaji et al., 2005). Aside from providing signalling platforms, the generation of ceramide on the cytosolic side of the plasma membrane can initiate signalling cascades by activating several intracellular proteins including cathepsin D, phospholipase A2, kinase suppressor of Ras (KSR—identical to ceramide-activated protein kinase), ceramide-activated protein serine–threonine (CAPP), protein kinase C isoforms and c-Raf-1 (Dobrowsky & Hannun, 1993; Heinrich et al., 1999; Huwiler, Johansen, Skarstad, & Pfeilschifter, 2001; Mathias, Dressler, & Kolesnick, 1991; Müller et al., 1995; Wolff, Dobrowsky, Bielawska, Obeid, & Hannun, 1994; Yao et al., 1995; Zhang et al., 1997). The activation of cathepsin D, phospholipase A2 and CAPP occurs via the

direct binding of ceramide to the enzyme (Chalfant, Szulc, Roddy, Bielawska, & Hannun, 2004; Heinrich et al., 1999; Huwiler et al., 2001).

As mentioned before, the generation of ceramide on the outer leaflet of the plasma membrane promotes an inward membrane curvature and vesicle formation. It is possible that lysosome exocytosis to repair USMB-induced sonoporation enhances ceramide formation at the plasma membrane, thus triggering endocytic responses. The key player in the activation of injury-induced endocytosis is lysosomal-A-SMase.

1.7.2 Role of acid-sphingomyelinase in ceramide-induced endocytosis

SMase is a family of enzymes that cleave the phosphodiester bond of sphingomyelin to release ceramide and phosphocholine, thereby playing a critical role in providing a source of ceramide in cells (Schneider & Kennedy, 1967). Based on their pH profile and the divalent metal ion in their active site for the catalysis of the reaction, SMase can be categorized into four different classes: acidic, Mg^{2+}-dependent neutral, Mg^{2+}-independent neutral, and alkaline (Andrieu-Abadie, Gouazé, Salvayre, & Levade, 2001; Goñi & Alonso, 2002; Levade & Jaffrézou, 1999).

Among the members of the family, the role of A-SMase in ceramide-mediated stress responses is the most well understood (Schneider & Kennedy, 1967). Mammalian A-SMase is encoded by the *SMPD1* gene, and translated from a single splice variant into a common protein precursor that undergoes distinct post-translational modifications and differential trafficking to give rise to two unique isoforms: lysosomal and secretory (Jenkins, Canals, & Hannun, 2009; Schuchman, Suchi, Takahashi, Sandhoff, & Desnick, 1991). The lysosomal A-SMase is glycosylated with mannose-rich oligosaccharide and acquires Zn^{2+} prior to trafficking to lysosomes. On the other hand, secreted A-SMase has a complex N-glycosylation pattern, has a

longer half-life, requires exogenous Zn^{2+} for activity, and is released by the secretory pathway (Kornhuber, Rhein, Müller, & Mühle, 2015).

Notably, both enzymes function optimally at pH 5, and are secreted in response to stress stimuli, such as CD95, tumour necrosis factor-alpha (TNFα) or environmental stress, to mediate the hydrolysis of sphingomyelin into ceramide at the plasma membrane (Jenkins et al., 2009). The existence of two A-SMase isoforms in different subcellular compartments suggests that sphingomyelin hydrolysis can have different biological impacts depending on the type of the stimuli. As an example, it has been shown that stimulation of cultured human platelets with thrombin resulted in increased secretory-A-SMase release, but decreased lysosomal-A-SMase activity (Romiti et al., 2000). In a similar manner, IL-1β or TNFα stimulation enhanced secretory-A-SMase activity with no effect on lysosomal-A-SMase activity (Jenkins et al., 2009). Oxidized LDL and oxidized LDL-containing immune complexes can differentially regulate lysosomal-A-SMase activity and secretory-A-SMase release in macrophages (Truman et al., 2012). On the other hand, mechanically induced membrane damage or treatment with reactive oxygen species only induced Ca^{2+}-dependent lysosomal-A-SMase release, as confirmed by the appearance of LAMP-1 on the membrane and the release of lysosomal B-hexosaminidase into extracellular space (Corrotte et al., 2013; Li, Gulbins, & Zhang, 2012). I propose that the release of lysosomal-A-SMase and the consequent change in the biophysical properties of the plasma membrane through the formation of ceramide, trigger rapid endocytosis following USMB treatment.

1.8 Hypothesis

USMB treatment elicits the formation of transient pores in the plasma membrane and increases the rate of endocytosis. However, the molecular mechanisms and intracellular signals by which

USMB enhances the rate of endocytosis and whether this phenomenon can contribute to targeted drug delivery to control cancer cell survival had not been addressed. In the past five years, I aimed to elucidated the effect of USMB on the rate of clathrin-mediated endocytosis, as well as the non-receptor-mediated pathway responsible for bulk movement of fluid into cells (hereon referred to as fluid-phase uptake). I was also interested in providing detailed mechanistic insights by which USMB enhances the rate of CME and fluid-phase uptake. One possible mechanism by which USMB controls the rate of endocytosis is through the formation of transient membrane pores and modulation of Ca^{2+}-induced lysosome exocytosis, which activates compensatory endocytic responses through lysosomal-A-SMase-mediated ceramide production, similar to the repair pathway in SLO-treated cells. Therefore, I examined the role of lysosome exocytosis and A-SMase activity in USMB-mediated clathrin-mediated endocytosis and fluid-phase uptake. Parallel to the membrane repair hypothesis, it is also possible that USMB induces a MEND-like pathway by promoting DHHC5-mediated palmitoylation turnover of surface proteins (such as flotillins) that function in membrane trafficking. I discovered that the increase in rate of CME was prevented by inhibitors of lysosome exocytosis and A-SMase. However, the fluid-phase endocytosis occurred independent of membrane repair pathway. Next, I aimed to define the nature of the clathrin-independent pathway that is activated in response to USMB treatment and establish whether a MEND-like process was involved in the uptake of fluid following USMB stimulation. To test the palmitoylation turnover hypothesis, I studied the involvement of DHHC5 in the regulation of flotillins following USMB treatment. I observed that USMB treatment elicits a novel signalling pathway that utilizes Fyn and DHHC5 to control flotillin-dependent endocytosis and thus enhancing fluid-phase endocytosis. Further, I observed that the enhancement of flotillin-dependent endocytosis by USMB contributes to enhanced cell killing by

cancer drugs, highlighting the potential clinical relevance of USMB in targeted drug delivery by control of flotillin endocytosis.

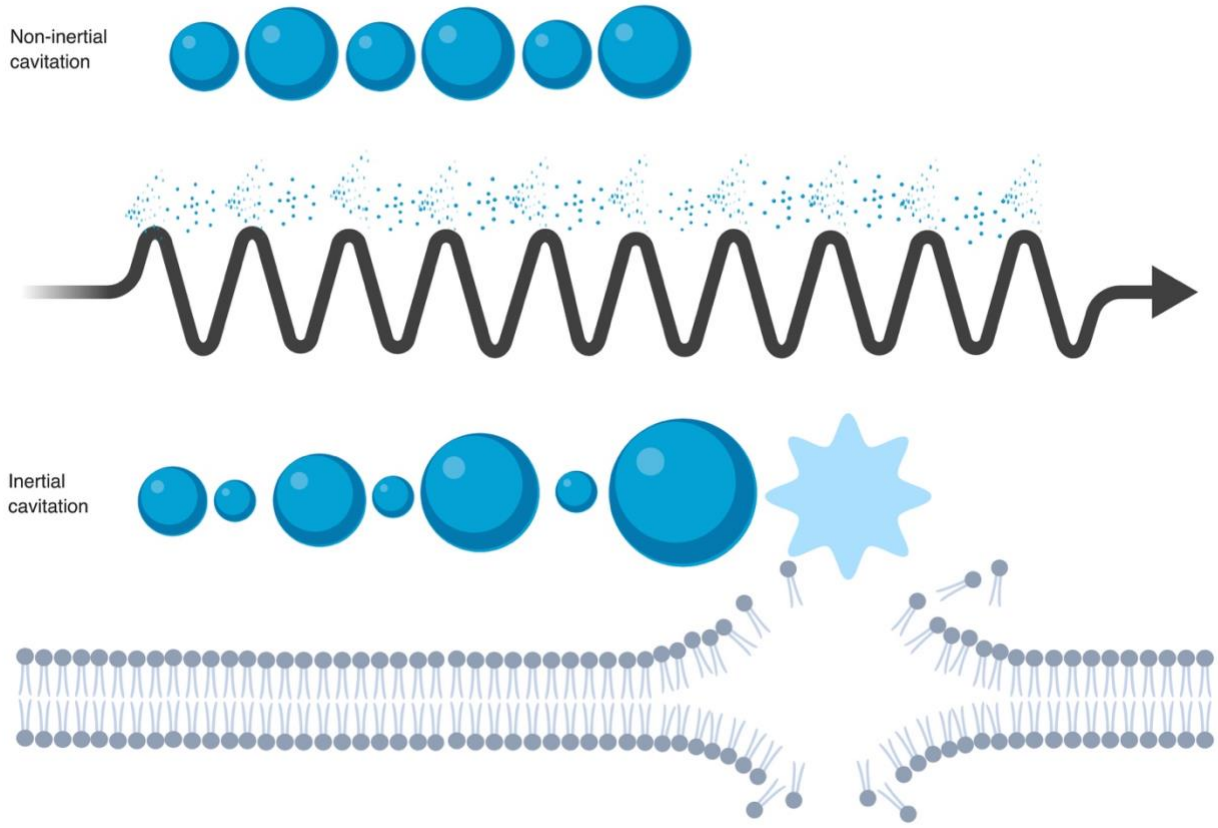

Figure 1.1. Different acoustic behaviours of microbubbles. At lower acoustic pressure, microbubbles stably oscillate with the fluctuations in ultrasound pressure until they break apart, a phenomenon known as non-inertial cavitation. During the non-inertial cavitation, the stable oscillation of the bubbles generates microstreaming of fluids near and around the bubbles, excreting shear stress on the surrounding cells. At high acoustic pressure, the bubbles violently collapse generating microjets and shock waves. Collectively, the acoustical effects of microbubbles can alter the permeability of the plasma membrane to facilitate the intracellular delivery of drugs.

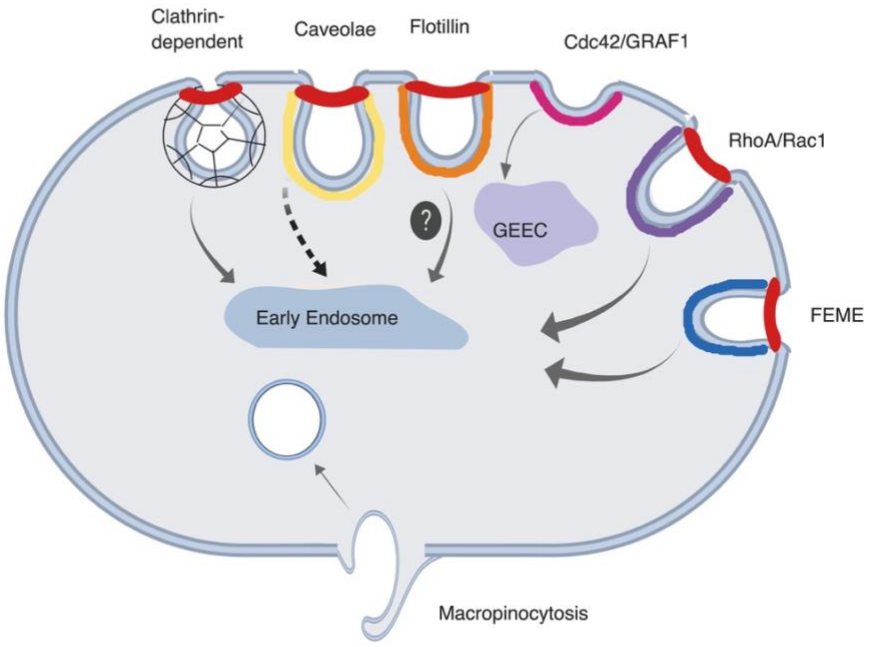

Figure 1.2. Endocytic pathways can be subdivided into two major categories of clathrin-dependent and clathrin-independent pathways in cells. There are a number of clathrin-independent pathways that operate within eukaryotic cells, each requiring different sets of regulators and effectors for the formation of endocytic vesicles. Unlike the ever-increasing details of well-orchestrated clathrin machinery, the exact molecular identity for most of these pathways are not well understood. CIE subclasses can be roughly divided into dynamin-dependents and dynamin-independent pathways (red).

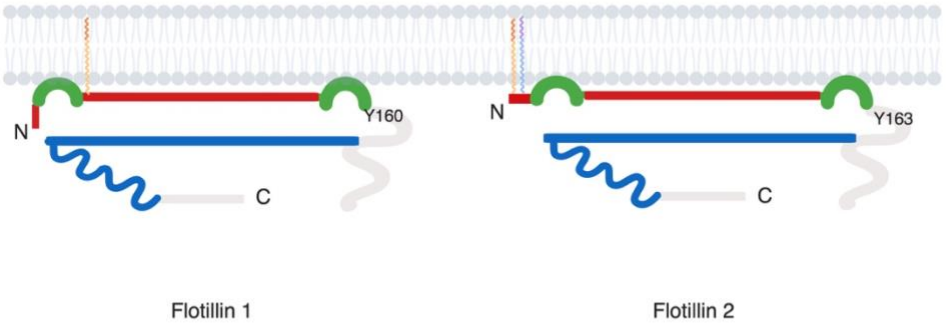

Figure 1.3. Flotillins undergo dynamic rearrangement at the plasma membrane to actively participate in cell signalling and membrane trafficking events. Both flotillins are composed of 1) N-terminal prohibition homology (PHB) domain (in red) which contains two hydrophobic hairpins (green), and key conserved cysteine residues for acylation (Flotillin 2 is myristoylated on Gly2, and palmitoylated while flotillin 1 is palmitoylated on Cys34), tyrosine residues (Y160 in flotillin 1 and Y163 in flotillin 2), and 3) C-terminal alpha-helix folding that mediates oligomerization (blue). Flotillins can constitutively associate with the plasma membrane to form highly detergent-resistant microdomains through the insertion of two hydrophobic hairpins, acylation, oligomerization, and cholesterol binding.

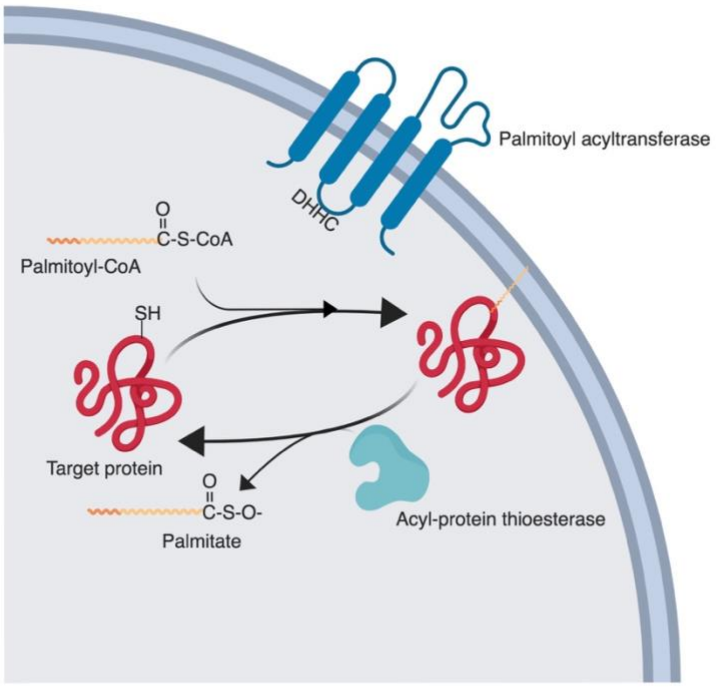

Figure 1.4. Dynamic palmitoylation regulates the localization of proteins at the plasma membrane and can influence membrane-associated processes and signalling events. PAT family constitute 23 enzymes which localize to different membrane compartments and mediate the attachment of 16-carbon palmitate to cysteine residues of proteins. The cell surface resident of PAT family, DHHC5, alters the localization of membrane proteins at the plasma membrane through changing their palmitoylation states. The changes in activity of DHHC5 in response to Ca2+ transient and the subsequent palmitoylation of its substrates have been associated with endocytic responses in neurons and epithelial cells.

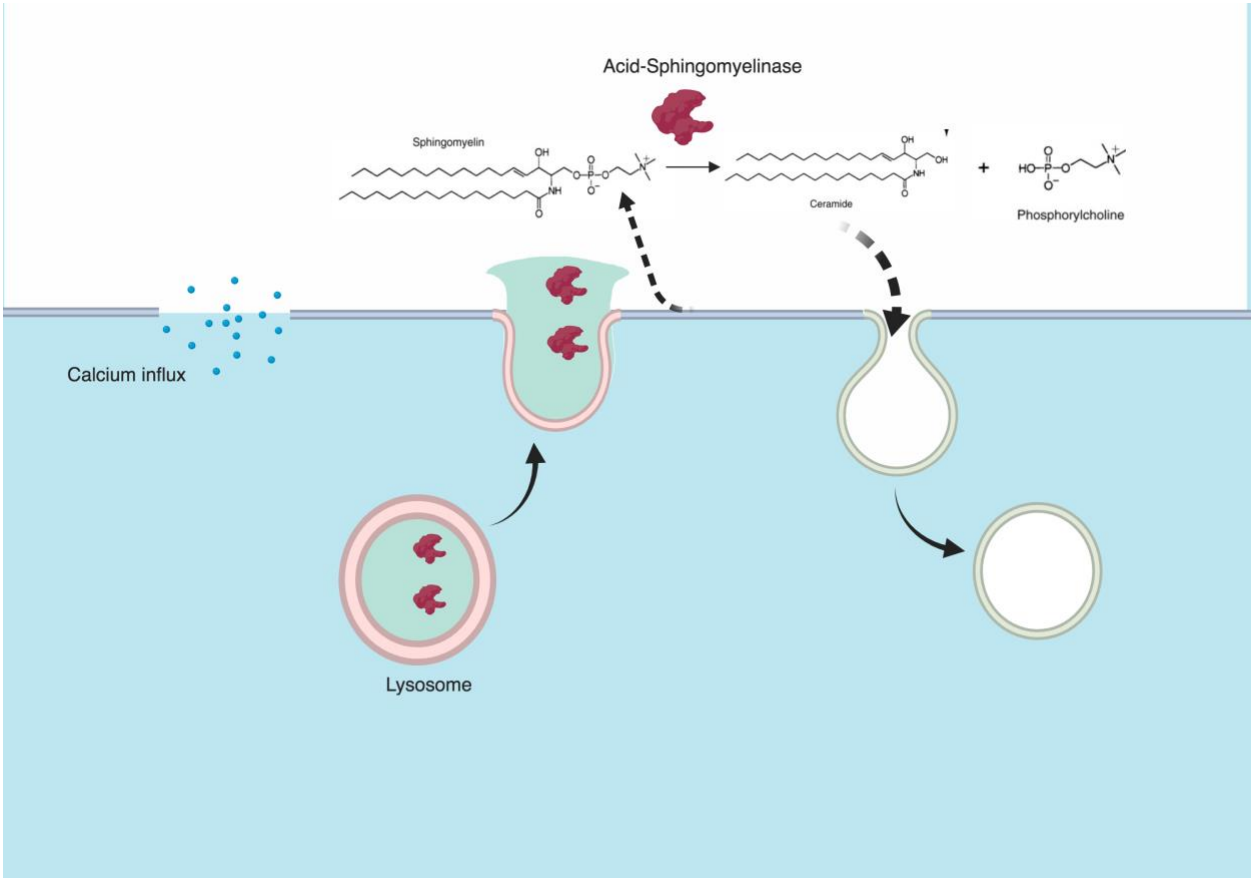

Figure 1.5. Plasma membrane repair pathway involves exocytosis of lysosomes followed by the activation of compensatory endocytosis. Ca^{2+} influx through plasma membrane wounds triggers localized exocytosis of lysosomes and the subsequent release of acid-sphingomyelinase which hydrolyzes sphingomyelin on the outer-leaflet of the plasma membrane to release ceramide and phosphocholine head group. The hydrolysis of sphingomyelin leads to the formation ceramide-enriched microdomains at the plasma membrane that activates endocytosis.

Chapter 2 Materials and Methods

2.1 Materials

Peroxidase from horseradish was obtained from Sigma-Aldrich (Oakville, ON). Antibodies used for immunofluorescence microscopy were as follows: anti-TfR from Santa Cruz Biotechnology (Santa Cruz, CA), anti-EEA-1 from Cell Signaling Technology (Danvers, MA), anti-LAMP-1from Santa Cruz Biotechnology (Santa Cruz, CA), anti-flotillin-1 and anti-γH2AX from Cell Signaling Technologies (Danvers, MA) and anti-flotillin-2 and anti-DHHC5 from Millipore Sigma Canada (Oakville, Ontario). Dynasore and desipramine were obtained from Millipore Sigma Canada. Vacuolin-1 was obtained from Santa Cruz Biotechnology (Santa Cruz, CA). Alexa488-conjugated dextran (A488 dextran, 10000 MW), fluorescein-conjugated dextran (FITC-dextran 70000 MW) and Alexa 555–conjugated Tfn (A555-Tfn) were obtained from Thermo Fisher Scientific (Waltham, MA). For ultrasound treatment, microbubbles were obtained from Definity microbubbles (Lantheus Medical Imaging Inc., Saint-Laurent, QC).

2.2 Cell lines and cell culture

ARPE-19 human retinal pigment epithelial cells (RPE herein) were obtained from American Type Culture Collection (ATCC, Manassas, VA) and cultured in DMEM/F12 media (Gibco, Thermo Fisher Scientific, Waltham, MA) supplemented with 10% fetal bovine serum (FBS) and 5% streptomycin/penicillin in a humidified incubator at 37 ºC and 5% CO_2. MDA-MB-231 cells were obtained from ATCC and cultured with RPMI-1640 media (Gibco) containing 10 % fetal bovine serum, and 5% streptomycin/penicillin and incubated at 37 ºC and 5 % CO_2.

2.3 Ultrasound treatment

Using the monolayer model, cells in six-well plates filled with 13 mL media were exposed to USMB at 500 kHz pulse centre frequency (single element flat transducer with 32 mm element diameter focused at 85 mm and a -6dB beam width of 31 mm at the focal point (IL0509GP,

Valpey-Fisher Inc., Hopkinton, MA, USA), 570 kPa peak negative pressure (Pneg), 32 μs pulse duration (16 cycles tone burst) at 1 kHz pulse repetition frequency (PRF) corresponding to 3.2% duty cycle, for 60 seconds. These ultrasound stimulation conditions were previously optimized and characterized; of note, there was >80% cell viability upon exposure to USMB stimulation (Karshafian, Bevan, Williams, Samac, & Burns, 2009b; Karshafian, Samac, Bevan, & Burns, 2010). Immediately prior to ultrasound treatment of each sample, Definity microbubbles (Lantheus Medical Imaging Inc., Saint-Laurent, QC) were added at a concentration of 10 μL/mL. The Definity microbubbles were activated using a Vialmix for 45 seconds. The setup consisted of an arbitrary waveform generator, connected to a power amplifier (AG series Amplifier., T&C power conversion, Inc., NY), which transmitted the electrical signal to the ultrasound transducer. The transducer was submerged in partially degassed deionized water and focused obliquely at the centre of an acoustic window.

2.4 Inhibitor and drug treatments

For all experiments, some cells were treated with 50 μM desipramine for 1 hour prior to USMB treatment. For the dynamin inhibition experiment (**Figure 4.2E-F**), cells were either treated with 80 μM dynasore or treated in media containing a corresponding volume of dimethyl sulfoxide (DMSO) 30 min prior to USMB treatment. For experiments involving treatment with cisplatin (**Figure 4.7, A4.4A**) or doxorubicin (**Figure A4.4C-D**), following treatment with USMB and/or desipramine, cells were incubated for 2 hours at 37°C in growth media containing either 0.03 mM cisplatin or 0.03 mM doxorubicin, after which time the solution containing these drugs was removed, the cells extensively washed to remove any non-internalized drug, followed by incubation at 37 ºC in regular growth media devoid of any drugs or inhibitors.

2.5 Plasmid and siRNA transfections

DNA plasmid transfection were performed as previously described (Garay et al., 2015). Briefly, cells were incubated with Opti-MEM (Gibco) containing transfection mixture of Fugene HD (Promega, Madison, US) and specific plasmids at a 3:1 ratio. After 4 hours, the transfection mixture was removed, and cells were incubated in fresh cell growth medium at 37 ºC and 5% CO_2 for 16 -24 hours prior to experiments. The cDNA plasmid encoding eGFP-DHHC5 was a kind gift from Dr. Shernaz X. Bamji (University of British Columbia, Vancouver, BC) (Brigidi et al., 2015). This plasmid encoding wild-type eGFP-DHHC5 was used to generate a plasmid encoding eGFP-DHHC5 harbouring a point-mutation corresponding to Y533 by site directed mutagenesis service form BioBasic Inc. (Markham ON). DNA plasmid containing flotillin2-eGFP was a kind gift from Dr. Gregory D. Fairn (University of Toronto, Toronto, ON).

SiRNA transfections were performed as previously described (Bone et al., 2017). Briefly, cells were transfected as previously described with 220 pmol/L of each siRNA sequence mixed with Lipofectamine RNAiMAX (LifeTechnologies, Carlsbad, CA) in Opti-MEM medium (Gibco) for 4 hours at 37 ºC and 5% CO_2, after which cells were washed and replaced in regular growth medium. siRNA transfections were performed twice, 72 hours and 48 hours prior to experiments. The custom-synthesized siRNA transcripts obtained from Dharmacon (Lafayette, CO) were as follows: non-targeting control: CGU ACU GCU UGC GAU ACG GUU (sense strand), and CGT ACT GCT TGC GAT ACG GUU (antisense strand); DHHC5: CUG UGA AGA UCA UGG AUA AUU(sense strand) and UUA UCC AUG AUC UUC ACA GUU (antisense strand); Fyn AGG AAG AGC UCU GAA AUU AUU (sense strand), UAA UUU CAG AGC UCU UCC UUU (antisense strand); flotillin1: UGG CCA AGG CAC AGA GAG AUU (sense strand) and UCU CUC UGU GCC UUG GCC AUU (antisense strand); flotillin2

GGA UGA AGC UCA AGG CAG AUU (sense strand) and UCU GCC UUG AGC UUC AUC CUU (antisense strand).

2.6 CRISPR/Cas9 genome editing

CRISPR/Cas9 genome editing to generate MDA-MB-231 lacking functional flotillin-1 (MBA-MB-231-flot1-KO cells, as in **Figure 4.7**) was performed using the Edit-R CRISPR/Cas9 system from Dharmacon (Lafayette, CO), as per manufacturer instructions. Briefly, 0.75 pmoles of Edit-R crRNA targeting flotillin-1 (catalog CM-010636-04-0002), 0.75 pmoles of Edit-R tracrRNA (catalog no U-002005-20), 200 ng of Edit-R hCMV-mKate2-Cas9 DNA plasmid were combined with 15 μL of Dharmafect Duo (Dharmacon) transfection reagent in 300 μL of Opti-MEM media (Thermo Fisher Scientific) and vortexed. This mixture was added drop-wise to wild-type MDA-MB-231 cells in Opti-MEM media, followed by incubation for 4 hours, prior to washing and incubation of cells in growth media for 48 hours. Single MDA-MB-231 cells expressing mKate2 were isolated using fluorescence-activated cell sorting; each single cell was grown into separate clonal populations, which were then screened for successful knockout of flotillin-1 by immunoblotting and immunofluorescence microscopy.

2.7 HRP and fluorescent dextran fluid-phase internalization assay

RPE or MDA-MB-231 cells grown on coverslips were treated with desipramine for 1 hour prior to USMB treatments. Following USMB stimulation, cells were treated with 10 μg/mL A488-dextran alone or in combination with desipramine at 37 ºC for 30 min. After the incubation time, cells were extensively washed and immediately fixed in 4% PFA. Cells were then mounted on glass slides in fluorescence mounting medium (DAKO, Carpinteria, CA). The uptake of horseradish peroxidase (HRP) was measured by incubating RPE cells with 4mg/ml HRP in PBS containing 20mM HEPES and 0.2% BSA (pH 7.4) for different time points (0, 10 and 20 min) at

37˚C. Following HRP uptake, cells then were detached with a PBS solution containing 0.1% Pronase on ice. Detached cells were washed to remove excess HRP by centrifugation and suspension (all at 4 ºC) and subsequently permeabilized with a PBS solution supplemented with 0.5% Triton-X100. The HRP activity assay was performed in triplicate with o-phenylenediamine dihydrochloride (OPD) as substrate in a 50 mM Na_2HPO_4, 27 mM citrate (pH 5) solution containing the following: 10 mg of OPD and 10 µL of 30% H_2O_2. Following formation of a colored product, the reaction was terminated by adding 50µl of 3M H_2SO_4, followed by measurement of absorbance at 490 nm using an iMark microplate absorbance reader (BioRad, Mississauga, ON).

2.8 Immunofluorescence staining

Endogenous flotillin-1 or -2, DHHC5 or γH2AX were labelled by performing indirect immunofluorescence. Following various treatments as indicated, cells were fixed in a solution of 4% PFA and permeabilized by Triton-X100 (for flotillin labeling experiments) or ice-cold methanol (for DHHC5 labeling experiments), as recommended by antibody manufacturer's instructions. Cells were then blocked in a phosphate-buffered saline (PBS) solution supplemented with 3% bovine serum albumin (BSA), incubated with specific primary antibody solutions, then stained with appropriate fluorophore -conjugated secondary antibody, and finally were mounted on glass slides in fluorescence mounting medium (DAKO, Carpinteria, CA).

2.9 Fluorescent transferrin uptake and EEA1 immunofluorescence staining

To assess the rate of transferrin ligand (Tfn) uptake, RPE cells were treated with USMB or left untreated (control) and incubated with transferrin-Alexa Fluor 555 Conjugate (A555-Tfn, 10 µg/ml) for 7.5 min and fixed. For the USMB-treated condition, A555-Tfn was added 60 seconds following USMB treatment to ensure prior resealing of membrane pores to limit A555-

Tfn uptake to clathrin-mediated endocytosis (see **Figure A3.2**). Following this A555-Tfn uptake and fixation regime, immunofluorescence staining (e.g. of total cellular EEA1) was done as previously described (Camilo Garay et al., 2015). Briefly, cells were subjected to blocking in 3% BSA in PBS for 15 min, followed by labelling with anti-EEA1 and appropriate secondary antibodies. After extensive washing, coverslips were mounted in Dako fluorescent mounting media (Dako, Carpinteria, CA).

2.10 Fluorescence microscopy

For **Figures 3.1, 3.2, 3.5, 3.6 and 3.8**, immunofluorescence microscopy was performed using a 63x (NA 1.49) oil objective on a Leica DM5000 B epifluorescence microscope using a DFC350FX camera (Leica Microsystems, Wetzlar, Germany). Images were acquired using Adobe Photoshop (San Jose, CA) and all exposure times and image scaling were equal within an experiment.

Widefield epifluorescence microscopy of fixed samples, as shown in **Figures 3.9**, **4.1, 4.3C-D, 4.6C-D, 4.7A-B, 4.7D-F, A4.1C, and A4.4B-C** was performed using a 60x (NA 1.35) objective on an Olympus IX83 epifluorescence microscope using a Hamamatsu ORCA FLASH4.0 C11440-22CU camera. Images were acquired using cellSens software (Olympus, Canada, Richmond Hill, ON).

Spinning disk confocal microscopy of fixed samples, as shown in **Figure 4.2G-H** was performed using Quorum (Guelph, ON, Canada) Diskovery combination TIRF and spinning-disc confocal microscope, operating in spinning-disc confocal mode. This instrument is comprised of a Leica DMi8 microscope equipped with a 63×/1.49 NA objective with a 1.8× camera relay (total magnification 108×). Imaging was done using 488, 561 nm laser illumination and 527/30,

630/75 emission filters and acquired using a Zyla 4.2Plus sCMOS camera (Hamamatsu, Bridgewater, NJ).

TIRF-M imaging of fixed samples as shown in **Figures 4.2E-F, 4.3A-B, 4.4C-D, 4.5, 4.6A-B, A4.1B and A4.2B** was performed using Quorum (Guelph, ON, Canada) Diskovery combination total internal reflection fluorescence and spinning -disc confocal microscope, operating in TIRF-M mode. This instrument is comprised of a Leica DMi8 microscope equipped with a 63×/1.49 NA objective with a 1.8× camera relay (total magnification 108×). Imaging was done using 488 -, 561-nm laser illumination and 527/30, 630/75 emission filters and acquired using a Zyla 4.2Plus sCMOS camera (Hamamatsu, Bridgewater, NJ). TIRF-M imaging of live cells (transfected to express flotillin2-eGFP, as in **Figure 4.2A-D**, was performed using the abovementioned Diskovery instrument operating in TIRF mode. During imaging, cells were maintained in temperature (37 ºC) and CO_2-controlled stage. Time-lapse image series were acquired starting at 5 min after USMB treatment, time lapse images were taken every 1 minute for 15 min.

2.11 Image analysis

Cell surface TfR (**Figures 3.1, 3.6, 3.8**), cell surface LAMP1 (**Figure 3.5**), Tfn uptake (**Figure 3.2**) and FITC-dextran uptake (**Figure 3.9**), whole-cell intensity of flotillin-1 (**Figure 4.2F, 4.3B, 4.5B, 4.6B**), DHHC5 (**Figure 4.4C**), internalized fluid-phase A488-dextran (**Figure 4.1B, 4.3D, 4.6D, 4.7B**), or nuclear γH2AX (**Figure 4.7E-F**) was performed as previously described (Bautista et al., 2018; Ross et al., 2015) using ImageJ software (National Institutes of Health, Bethesda, MD) (Schneider, Rasband, & Eliceiri, 2012). Briefly, cell or nuclear outlines were manually delineated in ImageJ, and mean fluorescence intensity within each region of interest

was measured. Background mean fluorescence measured in an area of the coverslip devoid of cells was subtracted from all cellular or nuclear mean fluorescence intensity measurements.

In **Figure 3.2**, the Colocalization Index (between internalized A555-Tfn and EEA1) was determined by Pearson's coefficient, measured using the Just Another Colocalization Plugin (JACoP, (Bolte & Cordelières, 2006)) in ImageJ. Pearson's coefficient values were determined for each cell; these single-cell measurements were used to determine the mean Pearson's coefficient value for each condition in each independent experiment, resulting in Colocalization Index measure for each. Measurements of Colocalization Index for all independent experiments were subjected to a student's t-test, with $p < 0.05$ as a threshold for significant difference among conditions.

Detection and analysis of internalized flotillin-1 puncta (**Figure 4.1G-H**), was performed as previously described for detection of diffraction-limited clathrin structures (Delos Santos et al., 2017; Lucarelli, Delos Santos, & Antonescu, 2017) using custom software developed in Matlab (Mathworks Corporation, Natick, MA), as described in (François Aguet, Antonescu, Mettlen, Schmid, & Danuser, 2013; Garay et al., 2015). Briefly, diffraction-limited flotillin-1 structures were detected using a Gaussian-based modeling method to approximate the point-spread function of flotillin-1 plasma membrane structures or internalized flotillin-1 vesicles. The fluorescence intensity corresponding to A488-dextran within flotillin structures was determined by the amplitude of the Gaussian model for this channel for each flotillin structure. As a result, the measurements of A488-dextran represent their enrichment relative to the local background fluorescence in the immediate vicinity of each detected flotillin structure or vesicle.

Detection, tracking and analysis of cell surface flotillin2-eGFP in time-lapse image series obtained by TIRF-M (**Figure 4.2B-D**) was performed as previously described for cell surface

clathrin structures (François Aguet et al., 2013) using CME analysis custom software developed in Matlab. Briefly, diffraction-limited flotillin2-eGFP structures were detected using a Gaussian-based modeling method to approximate the point-spread function (François Aguet et al., 2013), and trajectories were determined from flotillin2-eGFP structure detections using the u-track software (Jaqaman et al., 2008). CME analysis is a function specialized for tracking and analysis of clathrin-coated pits in cells expressing fluorescently-labelled clathrin, and in particular can identify bona fide clathrin-coated pits from other diffraction-limited clathrin structures based on initial intensity and growth parameters (François Aguet et al., 2013). Here, while CME analysis was used to detect and track flotillin2-eGFP structures, I analyzed all flotillin2-eGFP structures that are detected and tracked, without sorting those that meet the requirements to be classified as clathrin-coated pits since flotillin structures may not display the same initiation and growth characteristics as clathrin structures that form at the plasma membrane. As such, this detection and analysis strategy is unbiased and able to detect, track and analyze all cell surface flotillin structures with limited assumptions of the properties of these flotillin structures. Here we define the 'plateau intensity' of each marker as the mean fluorescence of that protein within each flotillin structure (**Figure 4.2D**), measured within timepoints corresponding to 30% and 70% of the total lifetime of that structure.

2.12 Immunoblotting

Whole cell lysates were prepared in Laemmli sample buffer (LSB; 0.5 M Tris, pH 6.8, glycerol, 5% bromophenol blue, 10% β-mercaptoethanol, 10% SDS) containing phosphatase and protease cocktail (1 mM sodium orthovanadate, 10 nM okadaic acid, and 20 nM protease inhibitor), heated to 65 ºC for 15 min, then passed through with a 27.5-gauge syringe, as previously described (Bautista et al., 2018). Proteins within whole-cell lysates were resolved by Glycine-

Tris SDS-PAGE and then transferred onto a polyvinylidene fluoride (PVDF) membrane, which was then incubated with a solution containing specific primary antibodies. Western blot signal intensity detection corresponding to flotillin-1, DHHC5 or Fyn, and the respective loading controls (e.g. alpha-adaptin) were obtained by signal integration in an area corresponding to the specific lane and band for each condition.

To examine phosphorylation of DHHC5 (**Figure 4.4A**), I used the phos-tag gel system, which results in exaggeration of differences in apparent molecular weight of phosphorylated forms of specific proteins (Kinoshita, Kinoshita-Kikuta, Takiyama, & Koike, 2006). The phos-tag reagent was obtained from Wako (Osaka, Japan), and was used for conjugation within SDS-PAGE polymerization as per the manufacturer's instructions. After SDS-PAGE was completed, gel was submerged in $MnCl_2$ for chelation of remaining phos-tag moieties. Subsequently, protein intensity detection, measurement, and processing for the phos-tag immunoblots are identical to steps mentioned above.

2.13 Cell viability measurements

To perform measurement of cell viability as shown in **Figure 4.7C**, 60,000 MDA-MB-231 cells were seeded per well of a 6-well plate. On the day of experiment (24 hours after seeding), cells were treated with 50 μM desipramine for 1 hour, followed by USMB treatment. To eliminate the contribution of USMB-induced pores to drug uptake, 0.03 mM cisplatin was added to cells 5 min after USMB treatment. After 2 hours, cisplatin was washed off and replaced by fresh-drug free media. After 24 hours, cells were detached using 0.025% trypsin and cells were counted using a Countess II FL Automated Cell Counter (Thermo Fisher Scientific). The number of non-viable cells was determined by the loss of cells from the initial 60,000 cells seeded and expressed as a normalized value.

To perform the cell proliferation/viability assay as shown in **Figure A4.4A**, RPE cells were seeded in 6 well plates. On the day of experiment, cells were treated with 50 μM desipramine for 1 hour, followed by USMB treatment. To eliminate the contribution of USMB-induced pores to drug uptake, 0.03 mM cisplatin was added to cells 5 min after USMB treatment. After 2 hours, cisplatin was washed off and replaced by fresh drug-free media. After 24 hours, cells were stained with crystal violet, then solubilized in a solution of 0.1% SDS, followed by measurement of absorbance at 595 nm. Cell viability was expressed as percentage of the crystal violet signal in control (untreated) cells.

2.14 Statistical analysis

Statistical analysis was performed as previously described (Bautista et al., 2018). Measurements of samples involving one experimental parameter and more than two conditions (**Figures 4.2A-B, 4.2H, A4.4A, A4.4C**) were analyzed by one-way ANOVA, followed by Tukey post-test to compare differences between conditions, with $p < 0.05$ as a threshold for statistically significant difference between conditions. Measurements of samples involving two experimental parameters (**Figures 4.1B, 4.2F, 4.3B, 4.3D, 4.4C, 4.5B, 4.6B, 4.6D, 4.7B, 4.7C, 4.7E**) were analyzed by two-way ANOVA, followed by Tukey post-test to compare differences between conditions, with $p < 0.05$ as a threshold for statistically significant difference between conditions.

Chapter 3 Results: The mechanisms of USMB-induced clathrin-mediated endocytosis

3.1 Chapter 3 rationale

To study the effect of USMB on endocytosis, retinal pigment epithelial cells (ARPE-19 cells, RPE henceforth) or MDA-MB-231 breast cancer cells were treated with USMB in combination with other agents, followed by measurement of various parameters of the membrane traffic of TfR (to measure clathrin-mediated endocytosis), and the uptake of HRP or fluorescent dextran uptake (to measure fluid-phase uptake). Fluid-phase endocytosis occurs by the internalization of soluble molecules from the extracellular milieu by the collective function of several endocytic mechanisms, including those that internalize specific receptors (e.g. clathrin, caveolae) and non-receptor mediated mechanisms (e.g. micropinocytosis). As such, while the fluid-phase uptake markers used in this study (HRP, fluorescent dextran) do not interact with cell-surface receptors, their internalization is mediated by the collective action of a number of internalization mechanisms, although the role of clathrin-mediated endocytosis in fluid-phase uptake is minor (Howes et al., 2010). RPE cells are an emerging model to study the regulation of membrane traffic processes, given their ease of culture and their amenability to TIRF-M to study cell surface phenomena.

3.2 USMB treatment rapidly enhances the rate of clathrin-mediated endocytosis

To investigate whether USMB may regulate the rate of CME, I first examined the cell surface levels of TfR, a well-established cargo of CME, and compared the cell surface levels of TfR in control cells to that of cells 5 min after USMB treatment. After USMB treatment, the cell surface TfR fluorescence intensity was reduced by 35.3 ± 3.9 % compared to cells not exposed to USMB ($n = 3$, $p < 0.05$, **Figure 3.1A-B**). In the presence of US but in the absence of microbubbles, the levels of cell surface TfR were indistinguishable from control cells (**Figure 3.1A-B**), showing that the reduction in the abundance of cell surface TfR was due to the combined effect of US and

microbubbles. Similar results were obtained in MDA-MB-231 cells, in that USMB treatment reduced cell surface TfR levels by 37.28 ± 4.0 % compared to control cells not exposed to USMB (**Figure 3.1C-D**).

TfR undergoes constitutive CME and recycling (Antonescu, McGraw, & Klip, 2013), such that the reduction in cell surface TfR levels upon USMB treatment could arise from an increased rate of endocytosis or a decreased rate of recycling. To resolve this, the uptake of fluorescently conjugated transferrin (A555-Tfn, a ligand of TfR) was measured: RPE cells exposed to USMB exhibited a 67.0 ± 22.2 % increase in the uptake of Tfn compared to control cells ($n = 4$, $p < 0.05$, **Figure 3.2A-B**). To confirm that the enhanced cell-associated Tfn fluorescence reflected enhanced internalization (and not merely increased binding of A555-Tfn to the cell surface), I measured the co-localization of A555-Tfn with the early endosomal marker EEA1. USMB treatment resulted in an increase in colocalization score between A555-Tfn and EEA1 (**Figure 3.2C**). Hence, the increase in fluorescent Tfn labeling in USMB-treated cells during the Tfn uptake assay indeed reflected an increase in Tfn internalization. Moreover, the fact that the extent of co-localization of internalized A555-Tfn with EEA1 increased upon USMB treatment indicated that Tfn uptake was vesicle-mediated and not due to direct cytosolic entry via transient membrane pores, the latter which generally reseal within 30 seconds after USMB treatment (Yang et al., 2008). Hence, the reduction of cell surface TfR upon exposure to USMB resulted from enhanced internalization of TfR, indicating that USMB treatment enhances the rate of CME.

3.3 USMB treatment alters the properties of clathrin-coated pits

Alterations in the rate of TfR endocytosis could result from changes in the availability of cargoes for endocytosis or regulation of CCP formation, assembly, stabilization or scission from the

plasma membrane (François Aguet et al., 2013; Antonescu, Aguet, Danuser, & Schmid, 2011; Antonescu, Danuser, & Schmid, 2010; Loerke et al., 2009; Dinah Loerke, Mettlen, Schmid, & Danuser, 2011; Mettlen et al., 2009, 2010). To determine how USMB may regulate CCPs, I examined these structures in cells stably expressing clathrin light chain fused to green fluorescent protein (GFP-CLCa); these cells were characterized previously (François Aguet et al., 2013) and are henceforth termed RPE GFP-CLC. RPE GFP-CLC cells were first incubated with A555-Tfn (to label surface-exposed TfR) for 3 min followed immediately by fixation and then imaging using TIRF-M. Visual examination of TIRF images revealed that USMB treatment appears to increase the fluorescence intensity of clathrin structures (**Figure 3.3A** and **Figure A3.1**).

In RPE cells, CCPs are diffraction-limited objects; hence, these structures can be detected by estimating the point-spread function using a Gaussian model (François Aguet et al., 2013). This strategy has been previously developed and validated for the systematic detection and analysis of CCPs in fixed images (Camilo Garay et al., 2015) or in time-lapse series (François Aguet et al., 2013). Systematic and automated detection of CCPs in these images revealed that the density of these objects did not change in response to USMB treatment. However, the mean intensity of GFP-CLC within each CCP, determined by the amplitude of the Gaussian model (François Aguet et al., 2013; Camilo Garay et al., 2015) significantly increased in cells treated with USMB compared to control cells ($n > 50$, $p < 0.0001$, **Figure 3.3B**). The increase in GFP-CLC fluorescence within each CCP indicates an increase in clathrin content per CCP upon USMB treatment, which reflects an increase in the size of CCPs (Antonescu et al., 2011). While the fluorescence intensity of GFP-CLC within each CCP was increased by USMB treatment, that of A555-Tfn (and thus TfR) was indistinguishable between control and USMB-treated cells. The

total amount of cell surface TfR was also reduced in USMB-treated cells (**Figure 3.1**). Taken together, these data suggest that the efficiency of the recruitment of cargo receptors (e.g. TfR) to CCPs may also be somewhat increased by USMB treatment or that the proportion of CCPs harbouring TfR that undergo successful endocytosis is increased by USMB stimulation.

These results show that USMB treatment alters the assembly of CCPs at the cell surface, and likely also the efficiency of cargo receptor (TfR) recruitment therein. The vast majority of smaller CCPs are transient structures that undergo abortive turnover without producing an internalized vesicle (François Aguet et al., 2013). Hence, the increase in CCP size upon USMB treatment is consistent with an increased proportion of CCPs leading to the formation of internalized vesicles, and thus an increased rate of TfR endocytosis (**Figure 3.2**).

3.4 USMB-stimulated fluid-phase uptake is delayed relative to the onset of increased CME

To investigate whether the effect of USMB resulted in specific regulation of CME or whether USMB treatment also controlled other endocytic mechanisms, I studied the rate of fluid-phase uptake after USMB treatment. In most cells, CME has a relatively minor contribution to fluid-phase uptake as other, clathrin-independent mechanisms are largely responsible for this phenomenon (Howes et al., 2010). The rate of fluid-phase uptake was monitored by measuring the rate of uptake of extracellular, soluble HRP (Mettlen et al., 2006). Control cells not treated with USMB exhibited a linear accumulation of intracellular HRP as a function of time. In contrast to the rapid regulation of CME (<5 min), there was no effect on the rate of HRP uptake from 0 to 10 min following USMB treatment, compared to control cells (**Figure 3.4**). However, HRP uptake was ~2-fold higher in USMB treated cells than control cells at 20 min following USMB treatment ($n = 5$, $p < 0.005$, **Figure 3.4**). These results indicate that in addition to the rapid, nearly immediate increase in the rate of CME, USMB treatment also triggers a relatively

delayed increase in fluid-phase uptake. Importantly, the fact that the regulation of these two endocytic pathways (CME and fluid-phase endocytosis) occurs at distinct times following USMB treatment (<5 min and >10 min, respectively) suggests that the mechanisms by which USMB controls each pathway are distinct.

3.5 Lysosome exocytosis occurs after USMB treatment

Lysosome exocytosis is triggered following plasma membrane damage by SLO (Reddy et al., 2001) and promotes compensatory endocytic responses (Tam et al., 2010). To investigate whether lysosome exocytosis occurs after USMB treatment, I examined the accumulation of the lysosomal marker protein LAMP-1 at the plasma membrane of intact cells. The cell surface levels of LAMP-1 after USMB treatment increased by 1.53 ± 0.16-fold, compared to that of control cells ($n = 3$, $p < 0.05$, **Figure 3.5A-B**). This suggests that USMB treatment elicits an increase in lysosomal fusion with the plasma membrane. Treatment with vacuolin-1 (an inhibitor of lysosome exocytosis (Cerny et al., 2004)) completely abolished the increase in cell surface LAMP-1 levels elicited by USMB, as evinced by the cell surface LAMP-1 measurements of 1.03 ± 0.05 and 0.80 ± 0.10 in cells treated with vacuolin-1 alone or vacuolin-1 and USMB together, respectively ($n = 3$) (**Figure 3.5A-B**). This establishes that USMB induces an increase in lysosome exocytosis, which can be readily blocked by pre-treatment with vacuolin-1.

3.6 Vacuolin-1 inhibits USMB-stimulated reduction of cell surface TfR without affecting the enhanced fluid-phase uptake

To determine whether lysosome exocytosis contributes to the regulation of CME upon USMB treatment, I examined the effect of vacuolin-1 treatment on the cell surface abundance of TfR following USMB treatment. While in cells not treated with vacuolin-1, USMB treatment resulted in a 38.0 ± 5.1 % reduction in cell surface TfR levels, vacuolin-1 treatment abolished the USMB-

elicited reduction in cell surface TfR levels ($n = 3$, $p < 0.05$, **Figure 3.6A-B**). These results suggest that lysosomal exocytosis may be required for the regulation of TfR by CME upon USMB treatment.

To determine if lysosome exocytosis is also required for the increase in fluid-phase uptake, I examined the effect of vacoulin-1 on USMB-stimulated HRP uptake. In contrast to the effect of vacuolin-1 on the USMB-stimulated reduction of cell surface TfR levels, vacuolin-1 treatment had no effect on HRP uptake, either in control cells or cells stimulated with USMB (**Figure 3.7**). Collectively, these results indicate that lysosome exocytosis contributes to the increase in CME but not that of fluid-phase endocytosis upon USMB treatment.

3.7 Desipramine inhibits USMB-stimulated reduction of cell surface TfR

In response to membrane damage by SLO, cells undergo membrane repair by enhancing the rate of endocytosis, through the release of A-SMase following lysosome exocytosis (Tam et al., 2010). As the reduction of cell surface TfR levels upon USMB treatment was sensitive to inhibition of lysosomal exocytosis by vacuolin-1, I aimed to determine if the control of cell surface TfR levels by USMB also required A-SMase. To do so, cells were treated with the A-SMase inhibitor desipramine (Tam et al., 2010). While control cells (not treated with desipramine) exhibited a $36.3 \pm 0.7\%$ reduction in cell surface TfR levels ($n = 3$, $p < 0.05$), cells treated with desipramine exhibited no detectable change in cell surface TfR levels upon USMB treatment (**Figure 3.8A-B**). This suggests that the USMB-mediated enhancement of CME of TfR requires the activity of A-SMase.

3.8 Desipramine synergizes with USMB treatment to enhance fluid-phase uptake

As inhibition of lysosomal exocytosis by vacuolin-1 treatment did not impact the increase in USMB-induced fluid-phase endocytosis, I tested whether A-SMase activity may also be

dispensable for USMB-dependent regulation of fluid-phase endocytosis. Surprisingly, cells treated with both desipramine and USMB exhibited a robust increase in fluid-phase endocytosis compared to cells that were treated with USMB alone (**Figure 3.9A**). Similar results were obtained when measuring the effect of desipramine and USMB treatment on the fluid-phase uptake of FITC-dextran (**Figure 3.9B-C**). Importantly, desipramine treatment alone had no effect on fluid-phase endocytosis (**Figure 3.9A-C**), suggesting that desipramine synergizes with USMB treatment to enhance fluid-phase endocytosis. Notably and consistent with the lack of inhibition of the USMB-stimulated increase in fluid-phase endocytosis by vacuolin-1 treatment, desipramine also failed to inhibit the effect of USMB treatment on fluid-phase endocytosis. To confirm that USMB effect on the rate of fluid-phase uptake is not exclusive to RPE-WT cells, similar experiments were repeated in MDA-MB-231 breast cancer cells. USMB treatment of MDA-MB-231 cells resulted in a similar increase in FITC-dextran internalization as in RPE cells (**Figure 3.9D-E**). Also consistent with the results obtained in RPE cells, desipramine alone had no effect on FITC-dextran uptake in MDA-MD-231 cells, but dramatically enhanced uptake of this fluid-phase marker in MDA-MB-231 cells treated with USMB (**Figure 3.9D-E**). Hence, the regulation of fluid-phase uptake upon exposure to USMB is not restricted to RPE cells, but also occurs in cancer cells such as MDA-MB-231 cells.

These results further support the observation that lysosomal exocytosis is dispensable for the regulation of fluid-phase endocytosis by USMB treatment. Furthermore, it can be suggested that aside from A-SMase, there are other cellular targets of desipramine that can act as an attractive candidate to improve the ability of USMB to enhance drug delivery by increasing the rate of fluid-phase endocytosis.

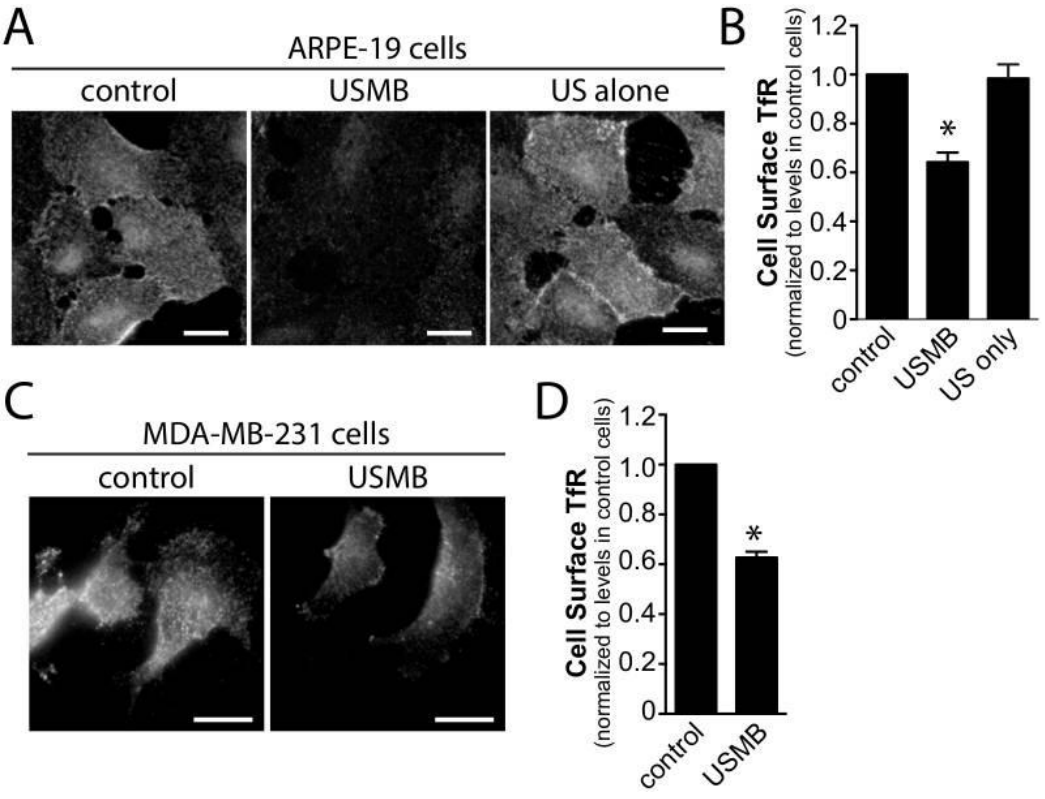

Figure 3.1. USMB treatment rapidly reduces cell surface TfR levels. RPE (A, B) or MDA-MB-231 (C-D) cells grown on glass coverslips were treated with microbubbles and/or ultrasound, as indicated. 5 min following USMB treatment, cells were placed on ice to arrest membrane traffic and subjected to immunofluorescence staining to detect cell surface TfR levels. Shown in (A, C) are representative epifluorescence micrographs of cell surface TfR levels and in (B, D) the mean ± SEM of cell surface TfR fluorescence intensity in each condition (n =3 independent experiments, each experiment >20 cells per condition). Scale = 20 μm. *, $p < 0.05$ relative to the control condition.

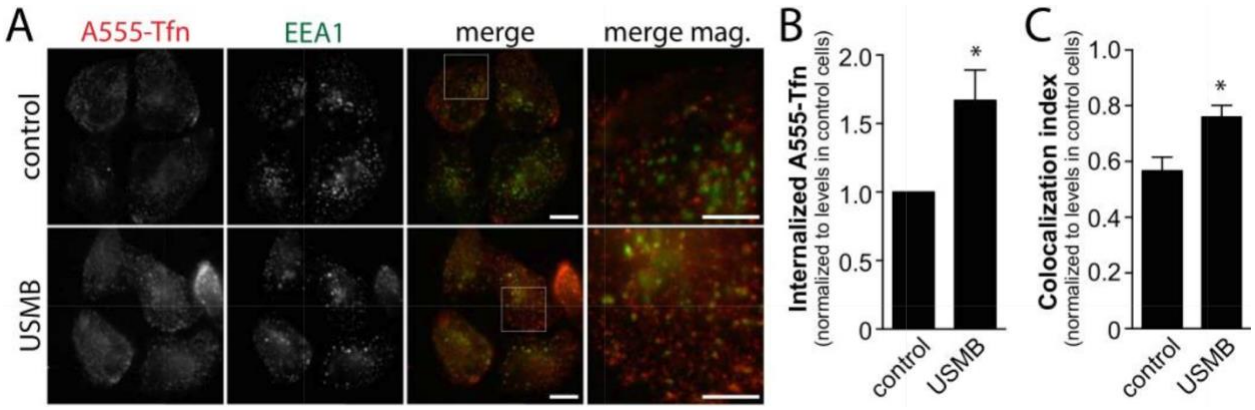

Figure 3.2. USMB treatment enhances the rate of Transferrin uptake. RPE cells grown on glass coverslips were treated with microbubbles and ultrasound (USMB), or left untreated (control), as indicated. Following treatment, cells were incubated with A555-Tfn for 7.5 min, and then immediately placed on ice, washed and fixed, and subjected to staining to detect EEA1. (*A*) Shown are representative epifluorescence micrographs depicting EEA1 and internalized A555-Tfn. (*B*) Shown are mean ± SEM of internalized A555-Tfn intensity in each condition (*C*) Shown are the mean colocalization index between A555-Tfn and EEA1 (determined by Pearson's coefficient). For B, C: n = 3 independent experiments, each experiment >20 cells per condition. Scale = 20 μm, Magnified image scale 10 μm. *, $p < 0.05$ relative to the control condition.

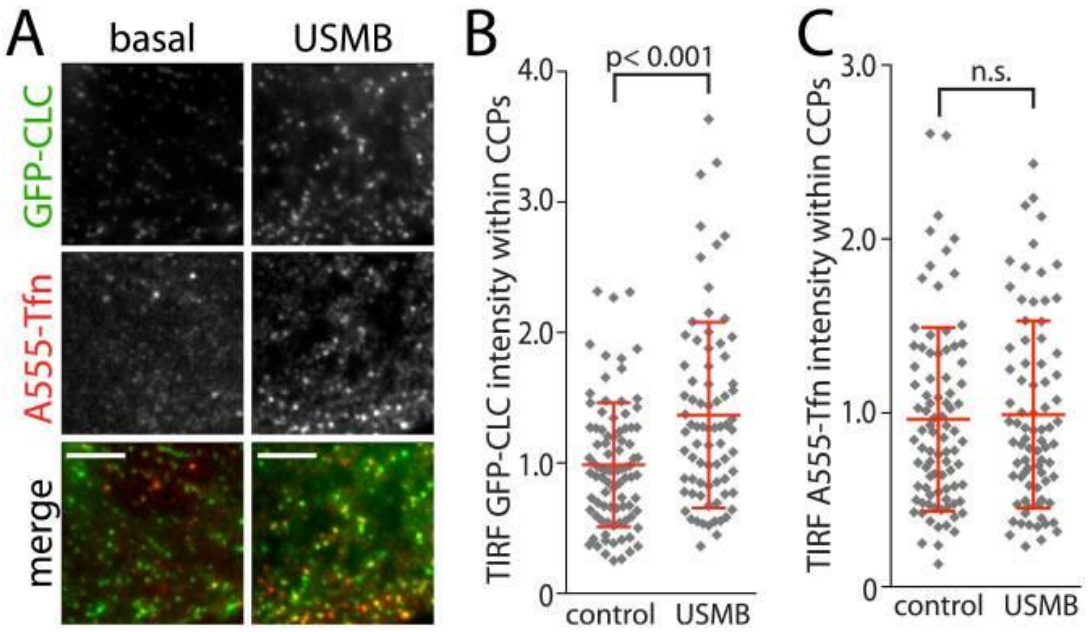

Figure 3.3. USMB treatment alters the properties of clathrin-coated pits. RPE cells stably expressing clathrin light chain fused to green fluorescent protein (RPE GFP-CLC) cells grown on glass coverslips were treated with microbubbles and ultrasound, or left untreated (control), as indicated. Cells were then incubated with A555-Tfn for 3 min to allow labeling of internalizing TfR, and then immediately subjected to fixation and processing for imaging by total internal reflection fluorescence microscopy (TIRF-M). (A) Shown are representative fluorescence micrographs obtained by TIRF-M. Scale = 5 μm. Images are higher magnification insets of larger images shown in Figure A3.1. (B-C) Images obtained by TIRF-M were subjected to automated detection and analysis of clathrin-coated pits (CCPs), as described in Material and Methods. The mean GFP-CLC (B) and A555-Tfn (C) intensity within each detected object (CCP) in each cell are shown. Each diamond symbol represents the mean fluorescence of all objects within a single cell; also shown are the mean of the cellular fluorescence values and interquartile range (red bars). The number of CCPs analyzed (n) and cells (k) from 3 independent experiments for each condition are control: n = 37,762, k = 89; USMB n = 29,897 k = 80.

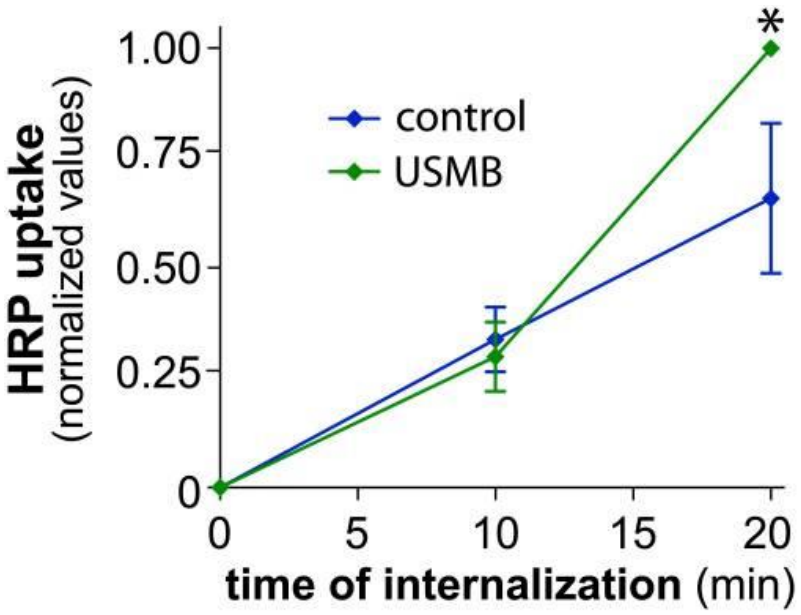

Figure 3.4. USMB treatment results in a delayed increase in fluid-phase internalization. RPE cells were treated with microbubbles and ultrasound, or left untreated (control), as indicated. Following treatment, HRP uptake was measured as described in Materials and Methods. Shown are the mean ± SE of the HRP uptake values at different times following commencement of the assay, which also corresponds to the time following USMB treatment. n = 5, *, $p < 0.05$ relative to the corresponding timepoint of the control condition.

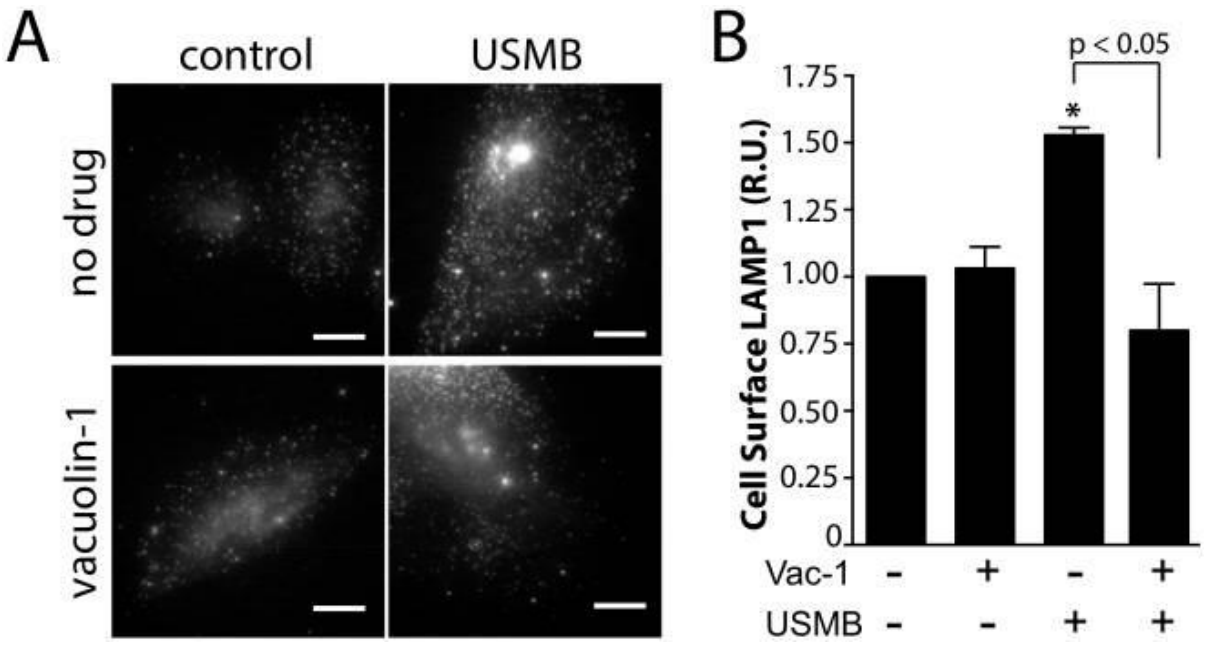

Figure 3.5. USMB treatment increases the cell surface abundance of the lysosomal marker LAMP1. RPE cells grown on glass coverslips were treated with 5.0 μM vacuolin-1 for 60 min, or not treated with this inhibitor (vehicle control). Cells were subsequently treated with USMB or left untreated (control) as indicated. Following treatment, cells were immediately placed on ice to arrest membrane traffic and subjected to immunofluorescence staining to detect cell surface LAMP1 levels. Shown in (A) are representative epifluorescence micrographs of cell surface LAMP1 levels and in (B) the mean ± SEM of cell surface TfR fluorescence intensity in each condition (n =3 independent experiment, each experiment >20 cells per condition). Scale = 20 μm. *, $p < 0.05$ relative to the control, vehicle-treated condition.

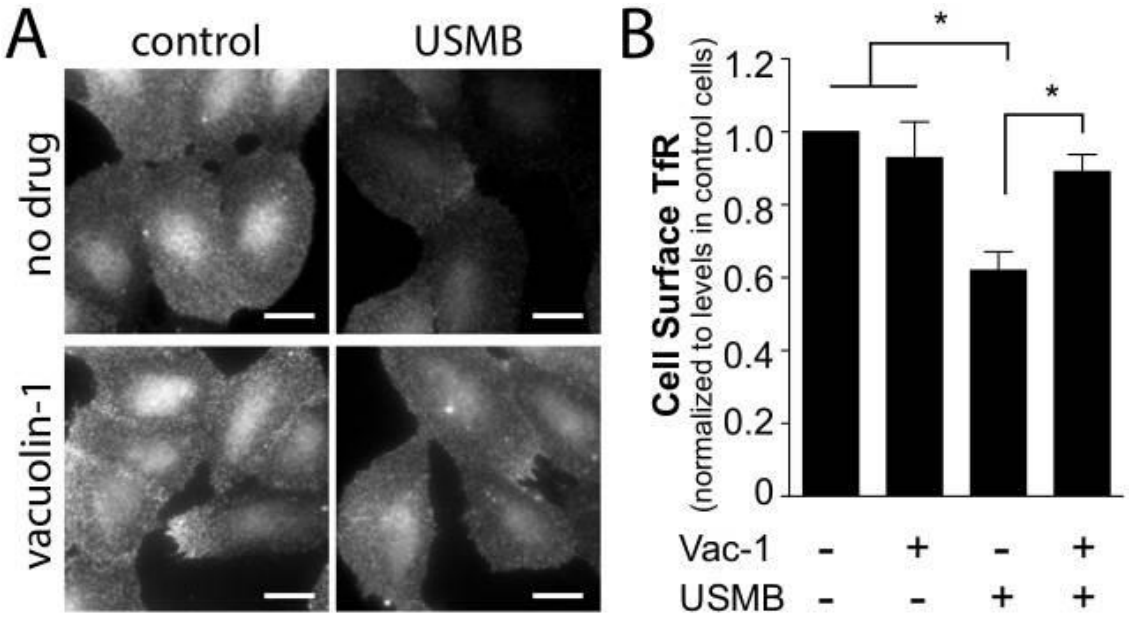

Figure 3.6. Vacuolin-1 treatment impairs the reduction in cell surface TfR levels by USMB treatment. RPE cells grown on glass coverslips were treated with 5.0 μM vacuolin-1 for 60 min, or not treated with this inhibitor (vehicle control). Cells were subsequently treated with USMB or left untreated (control) as indicated. 5 min after USMB treatment, cells were subjected to immunofluorescence staining to detect cell surface TfR levels. Shown in (A) are representative epifluorescence micrographs of cell surface TfR levels and in (B) the mean ± SEM of cell surface TfR fluorescence intensity in each condition (n =3 independent experiments, each experiment >20 cells per condition). Scale = 20 μm. *, $p < 0.05$.

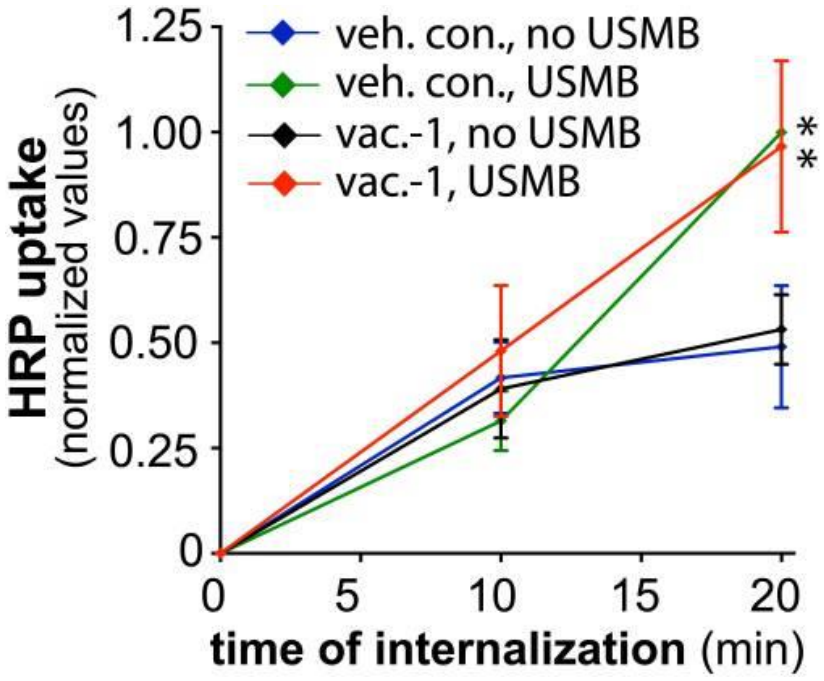

Figure 3.7. Vacuolin-1 treatment does not affect the regulation of fluid-phase endocytosis by USMB treatment. RPE cells were treated with 5.0 μM vacuolin-1 for 60 min, or not treated with this inhibitor (vehicle control). Cells were subsequently treated with USMB or left untreated (control) as indicated. Following treatment, HRP uptake was measured as described in Materials and Methods. Shown are the mean ± SE of the HRP uptake values at different times following commencement of the assay, which also corresponds to the time following USMB treatment. n = 3. *, $p < 0.05$ relative to the corresponding timepoint of the control condition.

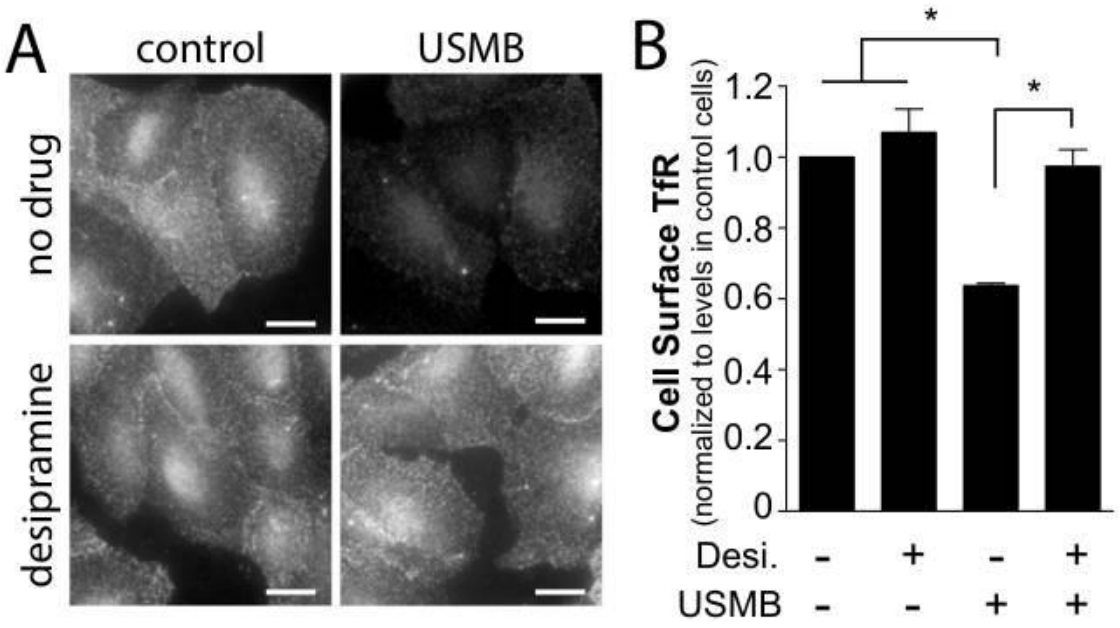

Figure 3.8. Desipramine treatment impairs the reduction in cell surface TfR levels by USMB treatment. RPE cells grown on glass coverslips were treated with 50 μM desipramine for 60 min, or not treated with this inhibitor (vehicle control). Cells were subsequently treated with USMB or left untreated (control) as indicated. 5 min following USMB treatment, cells were subjected to immunofluorescence staining to detect cell surface TfR levels. Shown in (A) are representative epifluorescence micrographs of cell surface TfR levels and in (B) the mean ± SEM of cell surface TfR fluorescence intensity in each condition (n =3 independent experiment, each experiment >20 cells per condition). Scale = 20 μm. *, $p < 0.05$.

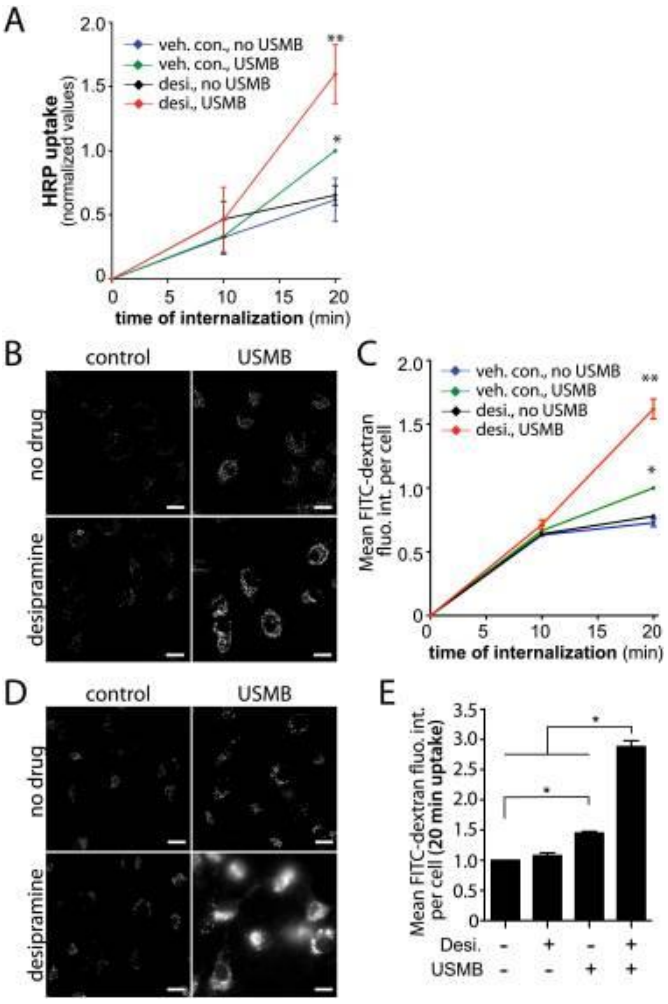

Figure 3.9. Desipramine enhances the rate of fluid-phase uptake in USMB-treated cells. RPE cells or MDA-MB-231 cells were treated with 50 μM desipramine for 60 min, or not treated with this inhibitor (vehicle control). Cells were subsequently treated with USMB or left untreated (control) as indicated. (A) Following treatment, HRP uptake was measured in RPE cells as described in Materials and Methods. Shown are the mean ± SE of the HRP uptake values at different times following commencement of assay, which also corresponds to the time following USMB treatment. n = 4, Following treatment, FITC-dextran was measured in RPE cells (B-C) or MDA-MB-231 cells (D-E) as described in Materials and Methods. Representative fluorescence micrographs of FITC-dextran uptake for 20 min are shown in (B) and (D), scale 20 μm. The mean ± SE of the FITC-dextran values at different times following commencement of the assay, which also corresponds to the time following USMB treatment is shown in (C) and (E) (see Figure A3.2). n = 3. * $p < 0.01$ (relative to vehicle control cells not treated with USMB), ** $p < 0.001$ (relative to vehicle control cells treated with USMB).

Chapter 4 Results: USMB treatment elicits fluid uptake via flotillin-mediated pathway

4.1 Chapter 4 rationale

In the previous chapter, I discovered that the increase in rate of CME was prevented by inhibitors of lysosome exocytosis and A-SMase, while fluid-phase endocytosis was occurring independent of the membrane repair pathway. I then aimed to identify the molecular identity and mechanism of the clathrin-independent pathway that is modulated by USMB and desipramine treatment. This chapter focuses on finding the exact molecular identity of the "fluid-phase" route, which I discovered to share similarities with MEND pathways.

4.2 USMB treatment triggers flotillin-dependent fluid-phase endocytosis

Given the emerging role of flotillins in defining distinct subclasses of clathrin-independent endocytosis, I first investigated the contribution of flotillin-1 and -2 to USMB-induced fluid-phase uptake. To do so, I tracked the internalization of the fluid-phase marker dextran conjugated to Alexa488 for 30 min after USMB treatment in ARPE-19 cells treated with flotillin-1 and flotillin-2 siRNA (**Figure A4.1A**). Consistent with my previous observations (Fekri et al., 2016), RPE cells transfected with non-targeting (control) siRNA exhibited 12.2 ± 0.1 % and 54.0 ± 0.3 % enhancements in fluid-phase endocytosis upon treatment with USMB or USMB+desipramine, respectively, compared to untreated (basal) cells ($n = 3$, $p < 0.05$, **Figure 4.1A-B**). As previously observed (Fekri et al., 2016), desipramine treatment alone had no effect on fluid-phase internalization. Importantly, cells treated with flotillin-1 and -2 siRNA exhibited no change in Alexa488-dextran internalization upon treatment with either USMB or USMB+desipramine (**Figure 4.1A-B**). These results indicate that flotillins are required for USMB-triggered enhancement of fluid uptake.

The functional requirement for flotillins in USMB-stimulated enhancement of fluid-phase internalization suggests that USMB may regulate the assembly or dynamics of flotillin structures at the plasma membrane to directly enhance flotillin-mediated endocytosis, or that flotillins may play a permissive role in cell physiology underlying fluid-phase uptake without being regulated by USMB treatment. To distinguish between these possibilities, I examined the impact of USMB on the dynamics of flotillin2-eGFP in RPE cells, monitored by TIRF-M. Of note, flotillin-1 and -2 exhibited nearly complete overlap as detected by immunostaining and TIRF-M (**Figure A4.1B**), indicating that tracking either flotillin-1 or flotillin-2 reflects the behaviour of virtually all flotillin structures at the plasma membrane. As expected (Glebov et al., 2006), flotillin2-eGFP formed dynamic fluorescent punctate structures at the cell surface in control cells (**Figure 4.2A**), some of which represent endocytic structures and events. The time-lapse image series of cells expressing flotillin2-eGFP and treated with either USMB+desipramine, desipramine alone or no treatment (control) were then subjected to automated detection, tracking and analysis of diffraction-limited flotillin2-eGFP structures, as previously done for clathrin endocytic structures (Aguet, Antonescu, Mettlen, Schmid, & Danuser, 2013). Importantly, USMB+desipramine treatment did not significantly alter the number (**Figure 4.2B**) or lifetime (**Figure 4.2C**) of flotillin2-eGFP structures but resulted in a dramatic decrease in the fluorescence intensity of flotillin2-eGFP structures (**Figure 4.2D**). This indicates that USMB+desipramine treatment regulates flotillin structures at the plasma membrane, which may in turn results in the enhancement of flotillin-dependent endocytosis.

Enhanced flotillin-dependent endocytosis will lead to decreased abundance of flotillins at the plasma membrane, and a concomitant increase of this protein in the intracellular compartments (Riento, Frick, Schafer, & Nichols, 2009). To determine if USMB treatment

indeed enhanced flotillin internalization, the impact of USMB treatment on the plasma membrane localization of flotillins was examined. I first determined that immunofluorescence staining of flotillin-1 was highly specific, given the virtually complete lack of signal in cells subjected to flotillin siRNA (**Figure A4.1C**). The plasma membrane localization of endogenous flotillin-1 was examined by immunofluorescence staining and TIRF-M, which allows selective illumination of plasma membrane-proximal fluorophores. Using this approach, USMB or USMB+desipramine treatments led to a reduction of flotillin-1 fluorescence intensity in the TIRF field by 22.0 ± 0.2 % and 33.5 ± 0.1 %, respectively ($n = 3$, $p < 0.05$, **Figure 4.2E** – top panels, and **Figure 4.2F** – black bars). This reduction in flotillin staining in the TIRF field reflects increased flotillin internalization during this time. Flotillin-mediated endocytosis requires dynamin for vesicle scission (Kurrle, John, Meister, & Tikkanen, 2012). Therefore, to further test whether the loss of cell surface flotillin-1 was indeed the result of flotillin-dependent endocytosis, I treated cells with the dynamin inhibitor dynasore prior to USMB or USMB+desipramine treatment and examined cell surface flotillin-1 levels. Dynasore treatment abolished USMB-elicited reduction in cell surface flotillin-1 compared to control cells ($n = 3$, $p < 0.05$, **Figure 4.2E** – bottom panels, and **Figure 4.2F** – grey bars). These results collectively indicate that USMB treatment triggers enhanced flotillin-dependent endocytosis, consistent with this treatment leading to enhanced flotillin-dependent fluid-phase internalization.

To determine whether the reduction of flotillin-1 from the cell surface indeed contributes to enhanced flotillin-dependent fluid-phase endocytosis, the overlap of flotillin-1 structures with the fluid-phase marker A488-dextran was examined in cells treated with USMB (**Figure 4.2G-H**). Discernable localized enrichment of A488-dextran within flotillin structures would only occur upon sequestration of this fluid-phase marker within the lumen of internalized vesicles,

which is indeed observed in USMB+desipramine treated cells (**Figure 4.2G**). To quantify enrichment of A488-dextran within flotillin structures, images were subjected to automated detection and analysis of diffraction-limited flotillin-1 puncta, followed by quantification of fluorescence intensity of flotillin or A488-dextran within these structures using the amplitude of a Gaussian model of the fluorescence distribution at each structure (François Aguet et al., 2013; Bone et al., 2017; Delos Santos et al., 2017). This analysis allows the measurement of signals enrichment within detected structures and is therefore well suited to measure A488-dextran sequestered within intracellular vesicles, since flotillin structures at the cell surface will have little enrichment of A488-dextran relative to the local extracellular fluid-phase background. USMB+desipramine treatment robustly enhanced the detection of A488-dextran within flotillin structures relative to control samples, or cells only treated with desipramine or USMB alone (**Figure 4.2H**). Collectively, these observations indicate that USMB treatment enhances fluid-phase endocytosis in a flotillin-dependent manner.

4.3 Enhanced flotillin-dependent fluid-phase uptake induced by USMB requires DHHC5

The increase in flotillin-dependent fluid-phase endocytosis triggered by USMB may be related to MEND (Hilgemann et al., 2013), and may thus require the palmitoyltransferase DHHC5, either to broadly modify many cell surface proteins with palmitate, or to target specific endocytic proteins such as flotillins to enhance their endocytic capabilities. To determine if DHHC5 is required for USMB-stimulated gain in flotillin-dependent fluid-phase endocytosis, I next examined the impact of siRNA gene silencing of DHHC5 (**Figure A4.2A**). Cells subjected to siRNA silencing of DHHC5 did not exhibit a reduction in cell surface flotillin-1 levels upon USMB+desipramine treatment (**Figure 4.3A** and **4.3B**, grey bars), while cells subjected to non-targeting (control) siRNA exhibited reduction of 21.5 ± 0.1 % and 45.0 ± 0.1 % in cell surface

flotillin-1 levels upon USMB or USMB+desipramine treatment, respectively (**Figure 4.3B**, black bars). Importantly, DHHC5 silencing also completely prevented the gain in fluid-phase endocytosis elicited by USMB+desipramine treatment that is observed in control siRNA treated cells **(Figure 4.3C-D**). These results indicate that DHHC5 selectively contributes to enhancing flotillin endocytosis and fluid-phase internalization upon treatment with USMB+desipramine.

To determine how USMB may affect the function of DHHC5, I next examined DHHC5 phosphorylation and its cell surface localization. In neurons, DHHC5 localizes at the synaptic membrane through phosphorylation of Y533 in a manner regulated by Fyn (Brigidi et al., 2015). To test the possible regulation of DHHC5 by Fyn and/or phosphorylation upon USMB treatment in epithelial cells, the phosphorylation of DHHC5 was examined using phos-tag gel electrophoresis, a method that exaggerates the apparent molecular weight differences elicited by protein phosphorylation (Bautista et al., 2018). Phos-tag gel revealed that USMB and USMB+desipramine elicited a reduction in the apparent molecular weight of DHHC5 as detected by anti-DHHC5 antibody (**Figure 4.4A**, left lanes), suggesting that USMB induces DHHC5 dephosphorylation. Interestingly, silencing of Fyn (**Figure A4.3A**) impaired the apparent shift in DHHC5 molecular weight induced by USMB and USMB+desipramine (**Figure 4.4A**, right lanes). These results indicate that USMB treatment leads to a reduction of DHHC5 phosphorylation, and that this phenomenon is controlled by Fyn.

I next examined how USMB treatment alters the abundance of DHHC5 at the plasma membrane using TIRF-M. To do so, I used TIRF-M to selectively illuminate cell-surface proximal structures following immunostaining of endogenous DHHC5. Importantly, USMB+desipramine treatment led to an increase in DHHC5 intensity detected in the TIRF field, and this gain in DHHC5 levels was ablated in cells also subjected to Fyn silencing (**Figure**

4.4C). This indicates that Fyn controls both the regulation of DHHC5 phosphorylation as well as the gain in cell surface abundance of DHHC5 triggered by USMB treatment.

Phosphorylation of DHHC5 at Y533 controls its cell surface abundance (Brigidi et al., 2015). To determine how alteration of DHHC5 Y533 phosphorylation by USMB treatment may control flotillin-dependent fluid-phase endocytosis, an eGFP-tagged, phosphorylation deficient Y533A mutant of DHHC5 was obtained. RPE cells were transfected with wild-type eGFP-DHHC5(WT) or eGFP-DHHC5(Y533A) constructs followed by treatment with USMB, USMB+desipramine or desipramine alone. As expected, in cells expressing eGFP-DHHC5(WT), treatment with USMB or USMB+desipramine led to a reduction in flotillin-1 at the cell surface compared to cells not treated with either USMB or desipramine (basal), as detected by intensity of flotillin-1 staining within the TIRF field (**Figure 4.5A-B,** black bars). In contrast, in cells transfected with eGFP-DHHC5(Y533A), treatment with USMB and USMB+desipramine had no significant effect on the cell surface flotillin-1 levels compared to cells not treated with USMB (**Figure 4.5A-B,** grey bars). Collectively these results show a functional requirement for DHHC5 in USMB-stimulated enhancement of flotillin-dependent endocytosis (**Figure 4.3**) and suggest that regulation of phosphorylation of Y533 on DHHC5 is required for the enhanced endocytosis of flotillin-1 following USMB treatment.

4.4 Enhanced flotillin-dependent fluid-phase uptake induced by USMB requires Fyn

Fyn is required for the regulation of DHHC5 phosphorylation (**Figure 4.4A**) and for the subsequent gain in cell surface DHHC5 (**Figure 4.4C**) in response to USMB treatment. To determine whether USMB-mediated reduction of cell surface flotillin-1 requires Fyn, cells were subjected to siRNA gene silencing of Fyn prior to USMB and USMB+desipramine treatment (**Figure A4.3A**). Consistent with previous experiments, USMB or USMB+desipramine

treatment elicited a reduction in flotillin-1 from the plasma membrane in cells transfected with non-targeting (control) siRNA (**Figure 4.6A-B,** black bars). In contrast, cells treated with Fyn siRNA did not exhibit a change in flotillin-1 at cell surface upon USMB or USMB+desipramine treatments (**Figure 4.6A-B,** grey bars), suggesting that Fyn is required for USMB-induced internalization of flotillins.

To determine if Fyn is also important for the stimulation of flotillin-dependent fluid-phase endocytosis upon USMB treatment (**Figure 4.1**), I examined the effect of Fyn silencing on the uptake of A488-dextran. Unlike cells subjected to non-targeting (control) siRNA, treatment of cells with Fyn siRNA prior to USMB or USMB+desipramine treatments blocked A488-dextran uptake (**Figure 4.6C-D**). These results indicate that Fyn is required for the enhanced flotillin-dependent uptake of fluid elicited by USMB treatment.

4.5 Enhanced flotillin-dependent uptake induced by USMB enhances drug uptake and action

USMB treatment, in combination with desipramine, elicits a robust increase in flotillin-dependent fluid-phase endocytosis that also requires DHHC5 and Fyn. To determine if this novel signalling pathway can enhance the uptake of chemotherapeutic drugs, and whether the enhanced delivery of drugs to cells improves the treatment outcome, I first examined this phenomenon in RPE cells. Following treatment with USMB or USMB+desipramine, cells were incubated in a solution containing 0.03 mM cisplatin (CDDP) for 2 h. The drug containing medium was then replaced with fresh drug-free medium and the cell viability was assessed 24 h later (**Figure A4.4A**). This experimental design allowed for the enhanced delivery of cisplatin immediately (for a 2 h period) following USMB treatment, and then assessment of the outcome of this initial effect on viability at a later point (24 h later). Strikingly, cells treated with USMB+desipramine

in combination with cisplatin exhibit a significant reduction of cell viability compared to cells treated with either USMB+desipramine or cisplatin alone (**Figure A4.4A**).

To determine if USMB+desipramine treatment prior to the addition of chemotherapy drugs can enhance the accumulation and retention of drugs at the time of cell viability assessment (24 h post drug exposure), the above experiment was repeated with doxorubicin, a cancer chemotherapy drug that is intrinsically fluorescent. Cells treated with USMB+desipramine prior to 2 h incubation with doxorubicin exhibited a significantly higher level of cellular doxorubicin assessed 24 h subsequent to drug incubation (**Figure A4.4B-C**). Together, these results indicate that USMB+desipramine treatment enhances fluid-phase internalization, and that this synergistic effect has the potential to increase intracellular delivery of drugs and improve the chemotherapeutic efficacy of cancer treatment.

To examine how enhanced fluid-phase endocytosis triggered by USMB+desipramine may contribute to intracellular delivery and action of cisplatin in cancer cells, I next examined the impact of this treatment in MDA-MB-231 cells, a model of triple-negative breast cancer (Chavez, Garimella, & Lipkowitz, 2010). To examine the contribution of flotillins in regulating USMB-induced fluid uptake in these cells, CRISPR/Cas9 genome editing was used to generate an MDA-MB-231 cell line deficient in flotillin-1 (MDA-MB-231-flot1-KO, **Figure A4.4D**). I first examined the effect of USMB+desipramine on the uptake of fluid-phase marker A488-dextran 30 min following treatment. While wild-type MDA-MB-231 cells exhibited a robust increase in fluid-phase internalization upon treatment with USMB+desipramine, MDA-MB-231-flot1-KO cells exhibit no discernable change in fluid-phase internalization upon this treatment (**Figure 4.7A-B**).

Having established that MDA-MB-231 cells exhibit a similar enhancement of flotillin-dependent fluid-phase endocytosis as in RPE cells in response to USMB+desipramine treatment, the impact of this treatment on cisplatin-mediated loss of cell viability was examined. To do so, MDA-MB-231 cells again were treated for 2 h with 0.03 mM cisplatin immediately following the USMB+desipramine treatment, followed by drug washout and measurement of cell viability 24 h later (protocol similar to that used in the experiment shown in **Figure A4.4A**). Using this experimental protocol, wild-type MDA-MB-231 cells treated with cisplatin only (no USMB+desipramine) exhibited a modest decrease in viability compared to control cells (not treated with either USMB+desipramine or cisplatin) (**Figure 4.7C**). Importantly, wild-type MDA-MB-231 cells treated with USMB+desipramine prior to cisplatin treatment exhibited a robust increase in cell death compared to either cells treated only with USMB+desipramine or cisplatin alone. Strikingly, MDA-MB-231-flot1-KO cells exhibited no change in viability upon treatment with either cisplatin, USMB+desipramine, or the two treatments combined (**Figure 4.7C**).

Cisplatin leads to a reduction in cell viability by eliciting DNA damage in the form of double-strand breaks, which first triggers repair mechanisms that can be detected by the presence of γH2AX nuclear puncta, prior to loss of cell viability (Clingen et al., 2008). To further resolve how USMB treatment may enhance the action of cisplatin, I examined the impact of USMB+despiramine treatment on DNA damage induced by exposure to cisplatin for 2 h, a similar protocol as used to study cell viability. As expected, in wild-type MDA-MB-231 cells, cisplatin treatment alone elicited an increase in γH2AX levels, which was significantly enhanced by prior treatment with USMB+desipramine (**Figure 4.7D-E**). Importantly, and consistent with the outcome of cell viability assays, MDA-MB-231-flot-KO cells exhibited no discernable

enhancement of γH2AX levels by cisplatin upon prior treatment with USMB+desipramine (**Figure 4.7D-F**). Collectively, these experiments indicate that the enhanced flotillin-dependent fluid-phase internalization triggered by USMB treatments has potential to enhance drug uptake, DNA damage and cell death by cisplatin.

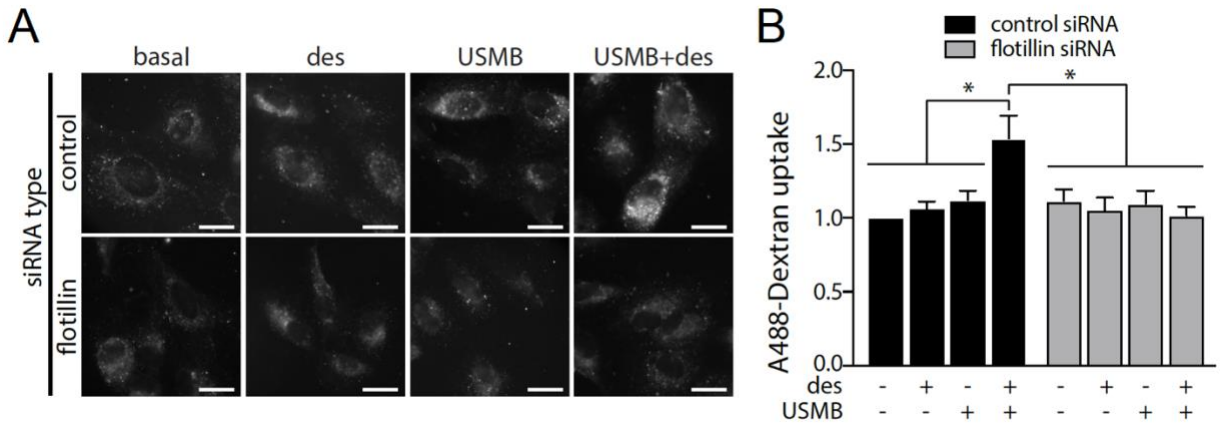

Figure 4.1. Flotillin is required for USMB-induced fluid uptake. RPE cells were transfected with siRNA targeting flotillin-1 and -2 or non-targeting siRNA (control). Following transfection, cells were treated with 50 μM desipramine for 60 min followed by USMB treatment, which was subsequently followed incubation with 10 μg/mL Alexa488-dextran for 30 min, fixation, and imaging by widefield epifluorescence microscopy. (A) Shown are representative fluorescence micrographs showing A488-dextran in cells of each treatment. scale 20 μm. (B) Shown are the mean ± SE of total cellular A488-dextran in teach condition n = 3 independent experiments. *, $p < 0.05$.

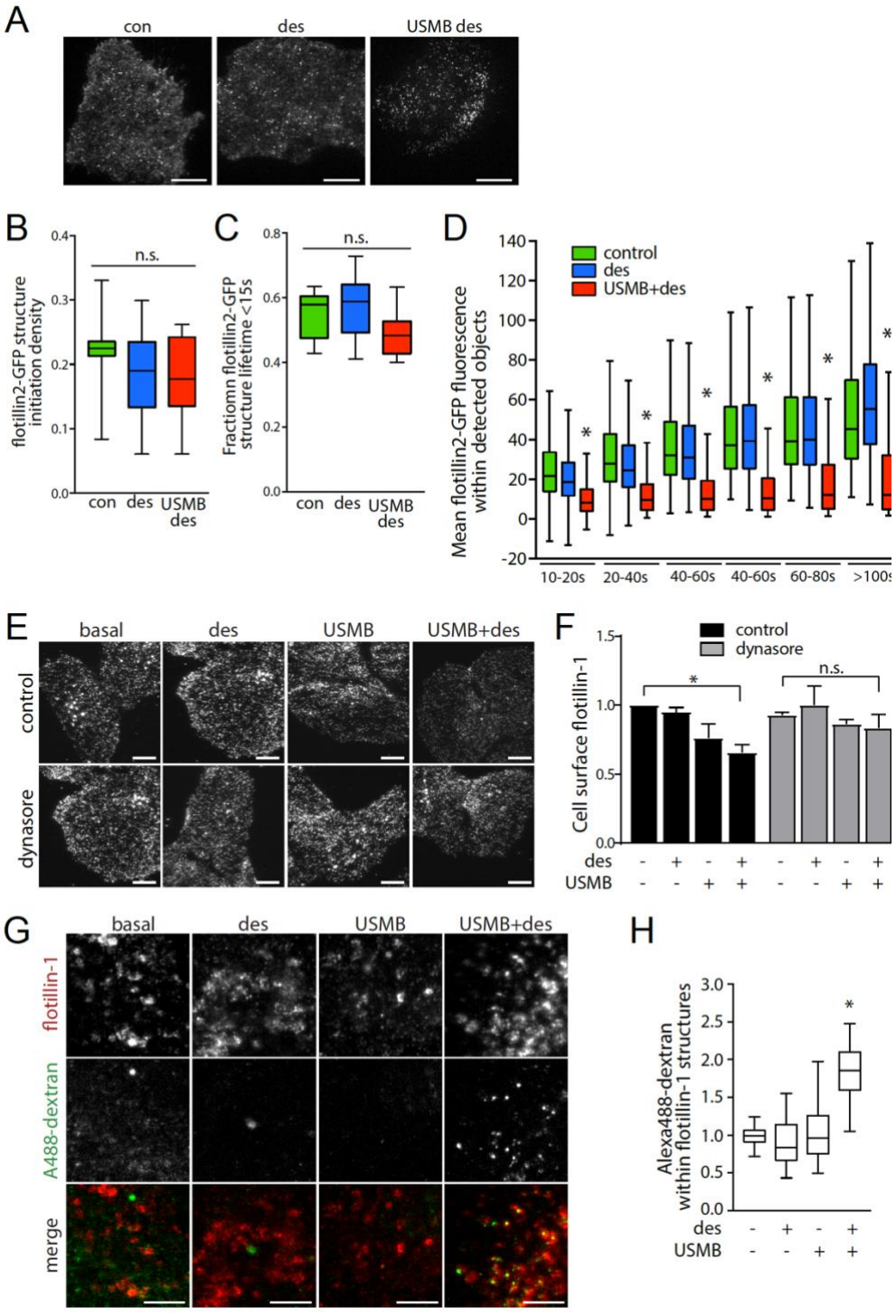

Figure 4.2. USMB treatment regulates flotillin cell surface levels, dynamics and internalization. (A-D) RPE cells were transfected with cDNA encoding flotillin2-eGFP, then treated with 50 μM desipramine (des) for 60 min followed by USMB treatment, of left untreated (control, con.) as indicated. Cells were then subjected to time-lapse imaging by total internal reflection

fluorescence microscopy (TIRF-M), followed by automated detection and analysis of flotillin2-eGFP puncta. Single-frame fluorescence micrographs obtained by TIRF-M are shown in (A). scale 20 μm. The initiation density (B), fraction of structures with lifetimes < 15s and mean intensity (C) of flotillin2-eGFP structures is shown as the median (line) interquartile range (boxes) and full range (whiskers). *, $p < 0.05$, relative to control. The number of cells (k) and flotillin2-eGFP structures (n) in each condition are as follows: control: k = 8, n = 8626; des: k = 12, n = 9757; USMB+des: k = 11, n = 8272. (E-F) RPE cells were treated with 80μM dynasore cotreated with 50 μM desipramine for 60 min, followed by USMB treatment, as indicated. Cells were then fixed and subjected to immunofluorescence staining of flotillin-1, and then imaging by TIRF-M. (E) Shown are representative TIRF-M fluorescence micrographs, scale 10 μm. (F) Flotillin-1 intensity in each cell in TIRF-M images was quantified to determine cell-surface flotillin-1 levels, and these measurements are shown as mean ± SE. n = 3. *, $p < 0.05$ (G-H) Cells were treated with 50 μM desipramine (des) for 60 min followed by USMB treatment, of left untreated (control, con.) as indicated. Subsequently, cells were incubation with 10 μg/mL Alexa488-dextran for 30 min, fixed and subjected to staining to detect flotillin-1, and then imaged by spinning disc confocal microscopy. Shown in (G) are representative fluorescence micrographs, scale 5 μm. (H) Flotillin-1 structures were subjected to automated detection and analysis, shown is the mean cellular A488-dextran intensity detected within flotillin structures in each condition, as median (line), interquartile rand (boxes) and full range (whiskers). The number of cells (k) and flotillin2-eGFP structures (n) in each condition are as follows: control: k = 49, n = 26774, des: k = 49, n = 30701, USMB: k = 49, n = 24796; USMB+des: k = 47, n = 28751. *, $p < 0.05$, relative to control.

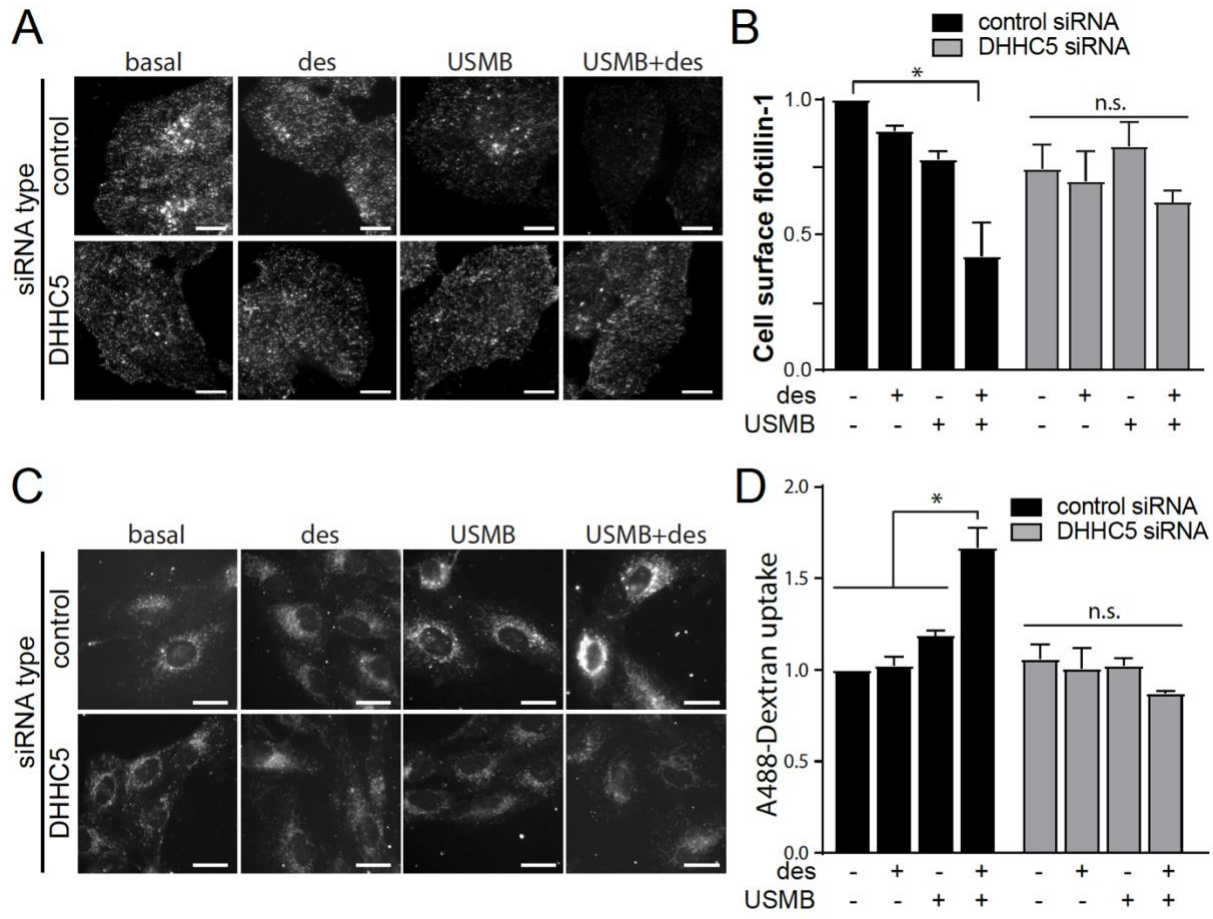

Figure 4.3. DHHC5 is required for USMB-triggered flotillin and fluid-phase internalization.. RPE cells were transfected with siRNA targeting DHHC5 or non-targeting siRNA (control). Following transfection, cells were treated with 50 μM desipramine for 60 min followed by USMB treatment. (A-B) Following treatments and a 30 min incubation, cells were fixed and subjected to immunofluorescence staining of flotillin-1, and then imaged by TIRF-M. Shown in (A) are representative TIRF-M fluorescence micrographs, scale 10 μm. Flotillin-1 intensity in each cell in TIRF-M images was quantified to determine cell-surface flotillin-1 levels, and these measurements are shown in (B) as mean ± SE. n = 3. *, $p < 0.05$ (C-D) Following treatments, cells were incubated with 10 μg/mL Alexa488-dextran for 30 min, fixed, and imaged by widefield epifluorescence microscopy. Shown in (C) are representative fluorescence micrographs showing A488-dextran in cells of each treatment, scale 20 μm. Shown in (D) are the mean ± SE of total cellular A488-dextran in teach condition n = 3. *, $p < 0.05$.

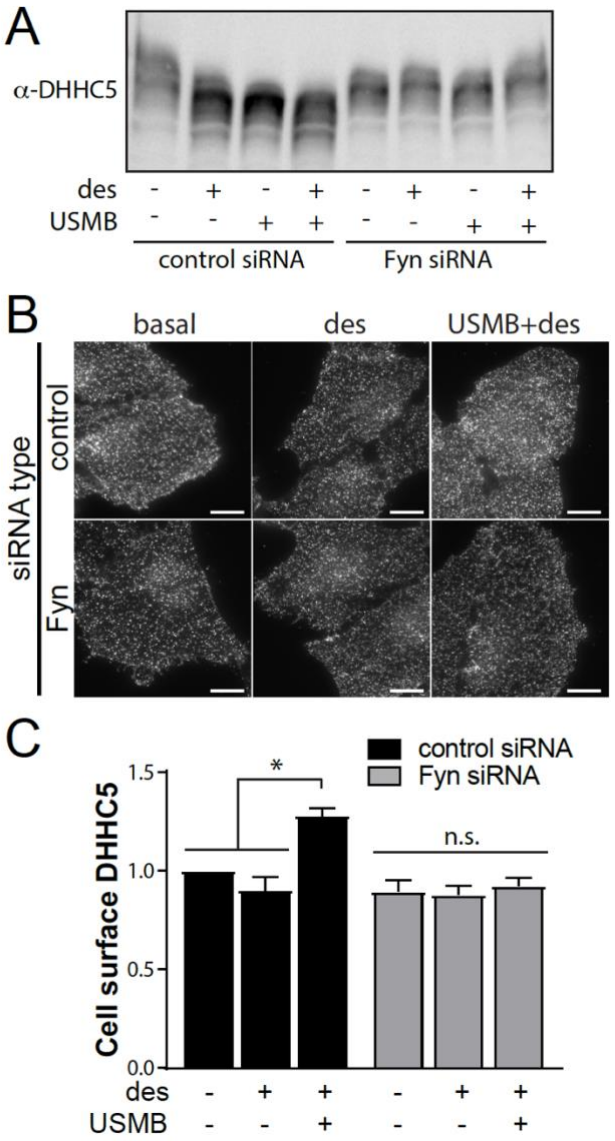

Figure 4.4. USMB treatment regulates DHHC5. RPE cells were transfected with siRNA targeting Fyn or non-targeting siRNA (control). Following transfection, cells were treated with 50 μM desipramine for 60 min followed by USMB treatment. (A) Following treatments, cells were lysed and whole-cell lysates were resolved by phos-tag SDS-PAGE and western blotting to detect DHHC5. Shown is a representative immunoblot showing DHHC5 staining. (B-C) Following treatments and a subsequent 30 min incubation, cells were then fixed and subjected to immunofluorescence staining of DHHC5, and then imaging by TIRF-M. Shown in (B) are representative TIRF-M fluorescence micrographs, scale 10 μm. DHHC5 intensity in each cell in TIRF-M images was quantified to determine cell-surface flotillin-1 levels, and these measurements are shown in (C) as mean ± SE. n = 3. *, $p < 0.05$.

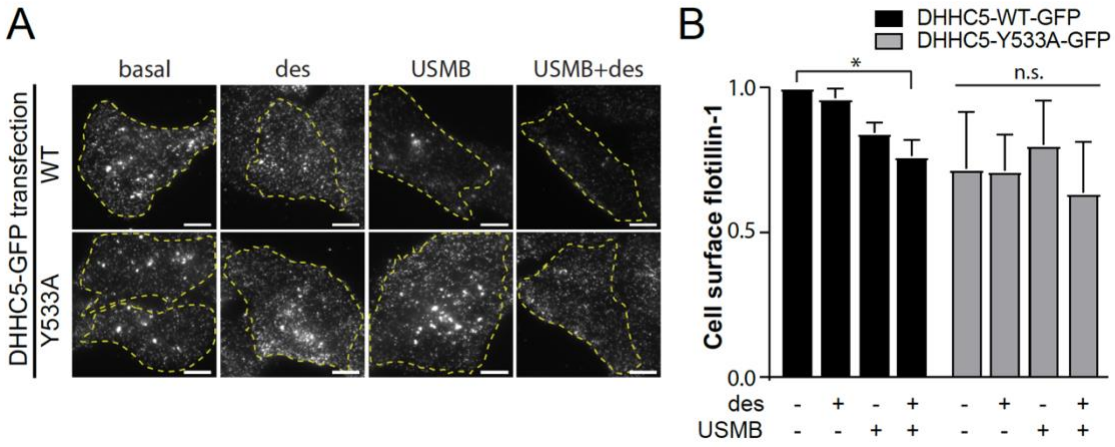

Figure 4.5. Expression of a phosphorylation-defective mutant of DHHC5 impairs flotillin internalization elicited by USMB treatment. RPE cells were transfected with cDNA encoding either wild-type (WT) or Y533A mutant DHHC5, fused to eGFP. Following transfection, cells were treated with 50 μM desipramine for 60 min followed by USMB treatment. Following a subsequent 30 min incubation, cells were then fixed and subjected to immunofluorescence staining of flotillin-1, and then imaging by TIRF-M. (E) Shown are representative TIRF-M fluorescence micrographs, scale 10 μm. Transfected cells are outlined, and GFP-channel images are shown in Figure A2B. (F) Flotillin-1 intensity in each cell in TIRF-M images was quantified to determine cell-surface flotillin-1 levels, and these measurements are shown as mean ± SE. n = 3. *, $p < 0.05$

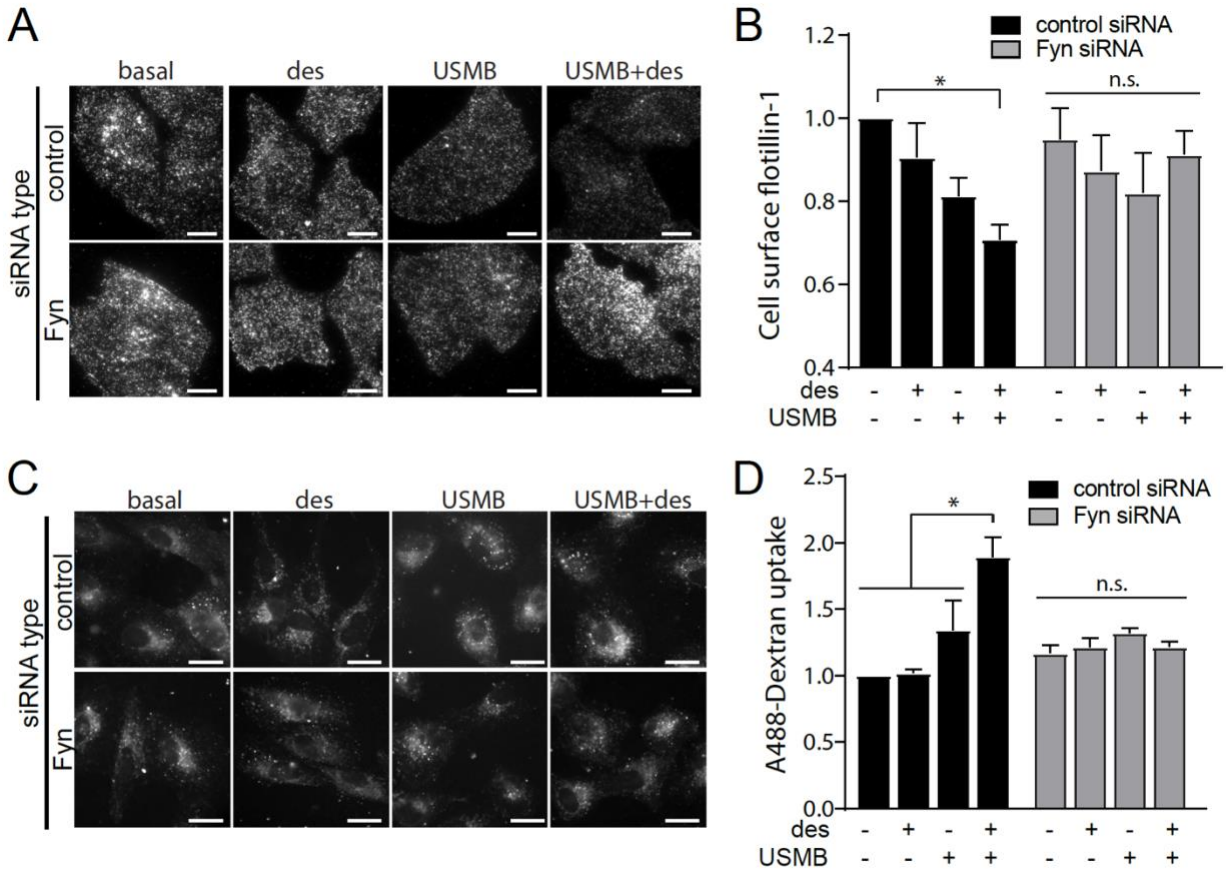

Figure 4.6. Fyn is required for USMB-triggered flotillin and fluid-phase internalization. RPE cells were transfected with siRNA targeting Fyn or non-targeting siRNA (control). Following transfection, cells were treated with 50 μM desipramine for 60 min followed by USMB treatment. (A-B) Following treatments and a 30 min incubation, cells were fixed and subjected to immunofluorescence staining of flotillin-1, and then imaged by TIRF-M. Shown in (A) are representative TIRF-M fluorescence micrographs, scale 10 μm. Flotillin-1 intensity in each cell in TIRF-M images was quantified to determine cell-surface flotillin-1 levels, and these measurements are shown in (B) as mean ± SE. n = 3 independent experiments. *, $p < 0.05$. (C-D) Following treatments, cells were incubated with 10 μg/mL Alexa488-dextran for 30 min, fixed, and imaged by widefield epifluorescence microscopy. Shown in (C) are representative fluorescence micrographs showing A488-dextran in cells of each treatment. scale 10 μm. Shown in (D) are the mean ± SE of total cellular A488-dextran in teach condition n = 3 independent experiments. *, $p < 0.05$.

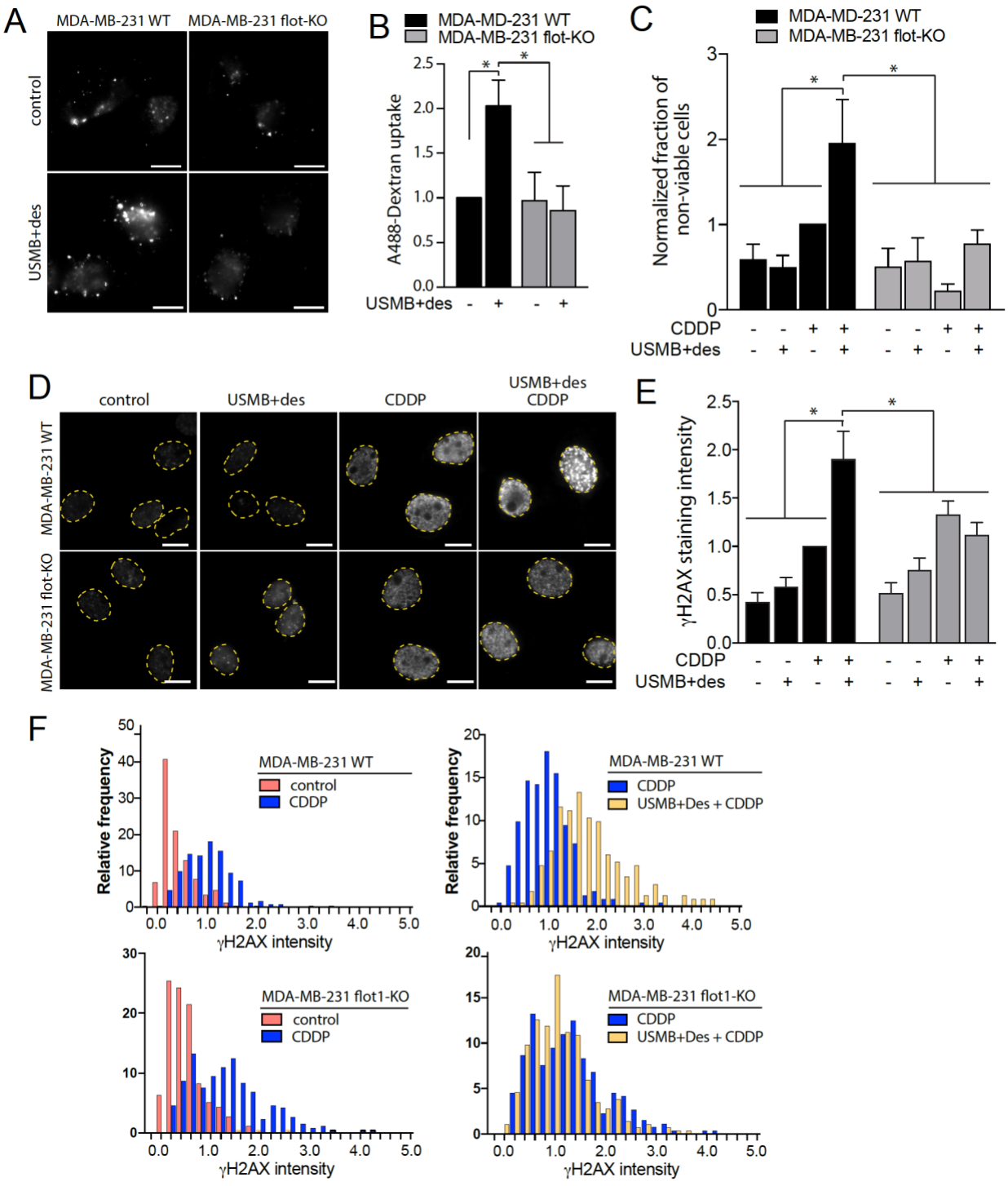

Figure 4.7. USMB treatment enhances cisplatin-mediated DNA damage and death in breast cancer cells in a flotillin-1 dependent manner. MDA-MB-231 wild-type (WT) or flotillin knockout (flot-KO) cells were treated with 50 μM desipramine for 60 min followed by USMB treatment. (A-B) Following treatments, cells were incubated with 10 μg/mL Alexa488-dextran for 30 min, fixed,

and imaged by widefield epifluorescence microscopy. Shown in (A) are representative fluorescencemicrographs showing A488-dextran in cells of each treatment, scale 20 μm. Shown in (B) are the mean ± SE of total cellular A488-dextran in teach condition n = 3 independent experiments. *, $p < 0.05$. (C-F) Following USMB and other treatments, cells were incubated with 0.03 mM cisplatin for 2 h (as shown), followed by washing and incubation in growth media (no drugs) (C) 24 h after USMB and/or cisplatin exposure, cell viability was assessed and shown are the mean ± SE of the fraction of non-viable cells, normalized to that of MDA-MB-231 WT cells treated with cisplatin only. n = 3 independent experiments. *, $p < 0.05$. (D-F) 24 h after USMB and/or cisplatin exposure, cells were fixed and stained to detect γH2AX. Shown in (D) are representative fluorescence micrographs in each condition, scale 10 μm. Shown in (E) is the mean ± SE of γH2AX intensity in each independent experiment. n = 3 independent experiments. *, $p < 0.05$. Also shown in (F) are frequency distribution of γH2AX intensity measurements in individual cells.

Chapter 5 Discussion

5.1 USMB enhances the rate of CME and fluid-phase uptake

I first examined the effect of USMB treatment on the regulation of distinct endocytic processes. Analysis of the cell surface TfR levels (**Figures 3.1, 3.6, 3.8**) and the cellular uptake of the TfR ligand transferrin (**Figure 3.2**), as well as examination of the properties of CCPs using TIRF-M (**Figure 3.3**), revealed that USMB treatment increased the efficiency of CME and altered the assembly of CCPs, resulting in larger structures. These observations indicate that USMB alters the properties of CCP assembly, stability and/or scission from the plasma membrane, suggesting that in addition to TfR, many other cell surface proteins may be regulated by USMB treatment. Importantly, the changes in these parameters occurred within 5 minutes of USMB treatment, indicating a very rapid regulation of CME upon exposure to USMB.

Fluid-phase internalization following USMB treatment was monitored by the uptake of soluble HRP followed by enzymatic detection of HRP activity (**Figure 3.4, 3.7, 3.9**) or uptake of FITC-dextran and detection by fluorescence microscopy (**Figure 3.9**). Using these assays, I found that USMB treatment also increased the uptake of HRP and FITC-dextran. In contrast to the very rapid, acute regulation of CME, the rate of fluid-phase uptake was indistinguishable from the control condition for up to 10 min and was readily observed following 20 min of USMB treatment. These results indicate that USMB-mediated regulation of CME and fluid-phase uptake occurs through partially distinct signalling mechanisms that can be separated based on their response time following USMB treatment.

Treatment with vacuolin-1 (lysosome exocytosis inhibitor) and desipramine (A-SMase inhibitor) prior to USMB treatment inhibited the changes in cell surface TfR levels (**Figure 3.6, 3.8**). In contrast, vacuolin-1 was without effect on the rate of HRP uptake upon USMB treatment (**Figure 3.7**), while desipramine enhanced USMB-stimulated HRP and FITC-dextran uptake

(**Figure 3.9**). These results suggest that while lysosome exocytosis and A-SMase may regulate the rate of USMB-induced CME, these processes are not required for the increase in the rate of USMB-induced fluid-phase endocytosis. Based on the above observations, it can be concluded that USMB regulates the rate of CME and fluid-phase endocytosis through separate mechanisms, as the effect of USMB on the two pathways were separated by time, and the pathways were differentially sensitive to drugs that target lysosome fusion and lysosomal A-SMase.

5.2 Lysosome exocytosis upon USMB treatment

A seminal study by Andrews and colleagues showed that the plasma membrane repair of mechanically induced injuries—by scratch wounding or fibroblast-collagen-matrix contraction assays—involved lysosome exocytosis, measured by staining the intact cells with an antibody for the lysosomal protein LAMP1 (Reddy, Caler, & Andrews, 2001). It was later confirmed that the increase in lysosome exocytosis caused an increase in endocytosis, which was critical for the plasma membrane repair (Tam et al., 2010). Consistent with previous studies, USMB treatment also elicited an increase in cell surface LAMP1 staining, suggesting the occurrence of lysosome-plasma membrane fusion. Importantly, cells treated with vacuolin-1 (an inhibitor of lysosome exocytosis) did not exhibit an increase in cell surface LAMP1 staining following USMB treatment (**Figure 3.5**), which further supports the notion that USMB treatment triggers lysosomal exocytosis.

Furthermore, lysosome exocytosis in response to plasma membrane lesions induced by other mechanical or chemical stresses—such as scratch wounding, fibroblast-collagen-matrix contraction wounding, and SLO treatment—occurs as the direct consequence of an increase in intracellular Ca^{2+} (Reddy et al., 2001; Tam et al., 2010). Comparably, and consistent with my results, Yang et al. reported an increase in intracellular Ca^{2+} and detected higher levels of cell

surface LAMP1 staining upon USMB treatment (Yang et al., 2008), although they did not make use of lysosome exocytosis inhibitors to further confirm the occurrence of lysosome fusion in response to USMB treatment. Therefore, it is possible that USMB-induced sonoporation, and the subsequent influx of extracellular calcium trigger the fusion of lysosomes with the plasma membrane to repair membrane damage, and consequently drive endocytic responses.

5.3 Regulation of CME by USMB treatment

USMB treatment decreased the levels of TfR at the cell surface by ~35-40% % after as little as 5 min of treatment. Given the dynamic nature of TfR membrane traffic, any reduction in the cell surface levels of this receptor may occur as a result of an enhanced rate of TfR endocytosis or a reduced rate of TfR recycling. USMB elicited an increase in the uptake of fluorescent transferrin (**Figure 3.3**). The increase in A555-Tfn internalization and a decrease in cell surface TfR levels, confirmed that USMB can directly increase TfR internalization. The increased colocalization of internalized Tfn with the early endosomal marker EEA1 (**Figure 3.2C**) further supports this conclusion. Therefore, these results collectively show that USMB treatment increases the rate of TfR internalization, which is known to occur entirely via clathrin-mediated endocytosis.

Analysis of TIRF images uncovered that the increase in TfR internalization correlated with the regulation of CCPs. These results suggest that USMB treatment alters the assembly or stabilization of CCPs, leading to an increase in the mean size of CCPs (**Figure 3.3**). An increase in the mean CCP size can indicate two non-mutually exclusive effects of USMB on CCPs: (i) an increase in the rate of clathrin incorporation during the initial assembly phase of CCPs, similar to the effect observed upon increasing the rate of PtdIns(4,5)P_2 synthesis (Antonescu et al., 2011), or (ii) an increase in the proportion of CCPs that are stabilized and become productive for generating vesicles, since these are on average larger than abortive CCPs (François Aguet et al.,

2013; Loerke et al., 2009; Dinah Loerke et al., 2011; Mettlen et al., 2009). While USMB stimulation elicited an increase in CCP size and enhanced TfR and Tfn internalization (**Figure 3.2**), there was no detectable change in A555-Tfn within CCPs. Considered together, these results indicate that USMB treatment may (i) enhance the recruitment of TfR to CCPs, since in the USMB-stimulated condition, similar levels of TfR were being recruited to CCPs from a smaller pool of cell-surface TfR, and/or (ii) enhance the proportion of CCPs harbouring TfR that form vesicles. Distinguishing between these possibilities requires a measurement of CCP lifetimes and thus time-lapse imaging. However, coupling an ultrasound transducer for near-simultaneous treatment with USMB and imaging by TIRF-M is technically challenging and this instrumentation is not readily available, although some coupled ultrasound fluorescence microscopy systems are being developed (Ibsen, Benchimol, & Esener, 2013). Nonetheless, I discovered that USMB treatment alters the properties of CCPs in a manner that is consistent with enhanced endocytosis, suggesting that USMB treatment directly controls the formation, assembly and maturation of CCPs.

Clathrin assembly into CCPs, and accordingly the CCPs sizes, are regulated by many factors, including lipids such as PtdIns(4,5)P_2 (Antonescu et al., 2011), and clathrin-binding adaptor proteins Dab2 and ARH (Mettlen et al., 2010). The inhibitory effect of vacuolin-1 and desipramine treatment on TfR endocytosis (**Figures 3.6, 3.8**) suggests that the delivery of A-SMase via lysosome exocytosis and the subsequent production of ceramide on the plasma membrane might regulate CME, likely by altering the assembly of CCPs. Several studies using a variety of methods have revealed the ability of ceramide to elicit the formation of lipid-ordered domains analogous to membrane rafts (Holopainen, Lehtonen, & Kinnunen, 1997; Silva, Almeida, Fedorov, Matos, & Prieto, 2009; Sot, Bagatolli, Goñi, & Alonso, 2006). In fact, it was

previously reported that the addition of sphingomyelinase to lipid bilayers containing sphingomyelin resulted in the formation of lipid-ordered microdomains capable of promoting membrane curvature in lipid bilayers (Holopainen, Subramanian, & Kinnunen, 1998; Ira & Johnston, 2008). Similarly, ceramide synthesis in the outer leaflet of giant unilamellar vesicles produced internal vesicles (Holopainen et al., 2000), and promoted the transition of the membrane to the non-lamellar phase, an effect consistent with the role of ceramide in promoting vesicle formation (Sot, Aranda, Collado, Goñi, & Alonso, 2005; Stancevic & Kolesnick, 2010; Veiga et al., 1999). Efficient CCP assembly and production of intracellular CCVs require several proteins that induce and stabilize membrane curvature, such as BAR-domain containing proteins (e.g. amphiphysin, endophilin, SNX9) and epsin (which contains an ENTH domain). Although the exact mechanism by which ceramide enhances the rate of CME is not known, one possible explanation could be that ceramide's ability to help curve membranes during the assembly of CCVs permits sufficient curvature with fewer "curvature proteins" required per CCPs, thus allowing the coated-vesicles to grow at a much faster rate.

It has been shown that following SLO-induced membrane injury, annexin A6 translocates to the site of injury and participates in the resealing of plasma membrane by recruiting annexin A1 and A2 to the ceramide-enriched microdomains (Babiychuk, Monastyrskaya, Potez, & Draeger, 2009; Draeger, Monastyrskaya, & Babiychuk, 2011; Potez et al., 2011). Interestingly, both annexin A6 and A2 are known to participate in calcium-regulated coated pit formation, and as such can enhance the internalization of CME cargoes such as LDL receptors (Grewal et al., 2000; Lin, Südhof, & Anderson, 1992; Merrifield, Feldman, Wan, & Almers, 2002; Munksgaard, Futter, & White, 2007). Therefore, an alternative hypothesis could be that the recruitment of

annexins to the site of ceramide-enriched microdomains during membrane repair coordinates the formation of CCVs following Ca^{2+}-dependent lysosome exocytosis.

5.4 Regulation of fluid-phase endocytosis by USMB treatment

In addition to the regulation of CME, USMB enhances the rate of fluid-phase uptake. However, unlike the fast-acting effect of USMB on the rate of CME (within <5 min after treatment), the increase in the rate of fluid-phase uptake occurred >10 min following USMB treatment, suggesting that USMB regulates each endocytic pathway differently. The increase in fluid-phase endocytosis following USMB treatment did not require lysosome exocytosis, since treatment with the lysosome exocytosis inhibitor vacuolin-1, was without an effect on USMB-stimulated HRP uptake (**Figure 3.7**). Moreover, the increase in fluid-phase uptake upon USMB treatment was not reversed by treatment with the A-SMase inhibitor desipramine, indicating that unlike the regulation of CME, the regulation of fluid-phase internalization by USMB treatment did not depend on lysosome exocytosis and A-SMase. Thus, these results collectively confirm that USMB treatment elicits an increase in fluid-phase internalization, and that this increase in fluid-phase internalization is distinct from the compensatory endocytosis in membrane repair pathway.

Interestingly, I observed that pre-treatment with desipramine robustly enhanced the effect of USMB, in a manner independent of the action of desipramine on ASMase. Since desipramine is a clinically approved drug and thus can be considered for therapeutic combination alongside USMB to enhance the intracellular delivery of therapeutics, I based my study on the effects of USMB on fluid-phase endocytosis on the combined use of USMB and desipramine. I aimed to identify the exact molecular identity of the pathway that is activated in response to USMB and desipramine treatment to mediate the vesicular uptake of fluid into cells, as this may represent an important new strategy to design new therapies for targeted drug delivery.

5.5 Palmitoylation of membrane proteins

I identified that flotillin-dependent CIE is an endocytic pathway that can be modulated by USMB and desipramine treatment to mediate the majority of vesicular uptake of fluid into cells. This stimulation of flotillin-dependent endocytosis by USMB treatment may be an effective therapeutic strategy for drug delivery, given the ability to focus ultrasound on small volumes. Moreover, USMB modulation of flotillin-dependent endocytosis involves Fyn-dependent modulation of DHHC5 phosphorylation. These observations led me to propose a signalling pathway that links USMB treatment to stimulation of flotillin-dependent endocytosis that initiates with Fyn engagement and the control of palmitoyltransferase DHHC5 (**Figure 4.8**). Finally, I uncovered that the USMB-stimulated enhancement of flotillin-dependent fluid-phase endocytosis was significant for enhancing drug delivery, as USMB treatment led to an increase in cisplatin drug action in a manner that required flotillin.

5.6 DHHC5-dependent control of fluid-phase endocytosis

The central role of DHHC5 in USMB-induced fluid-phase endocytosis provides evidence that this endocytic mechanism may be similar to the MEND internalization pathway described by Hilgemann (Hilgemann et al., 2013). According to Hilgemann et al., Ca^{2+} entry to the cell stimulates the palmitoylation of membrane proteins by activating the mitochondria-mediated stress response. Aside from being the center of ATP synthesis by oxidative phosphorylation, mitochondria regulate cellular homeostasis by serving as one of major calcium buffer systems and storage alongside the ER, and as such can actively participate in the initiation and regulation of many major signalling pathways that dictate cell fate.

The cross-regulation between endocytosis and mitochondria as described by Hilgemann et al. can be attributed to the mitochondria's role as the reservoir of metabolites and ions. Under

normal and physiological conditions, the movement of ions and metabolites is controlled by the selective permeability of the outer and inner-mitochondrial membranes. However, various stress and apoptotic stimuli can transform the inner and outer mitochondrial membranes' selective permeability by triggering the formation of the mitochondrial permeability transition pore (mPTP). Normally closed, the opening of the pores occurs under a variety of conditions—such as loading calcium into the mitochondrial matrix, depletion of adenine nucleotide, increase in phosphate concentration and oxidative stress—to permit the non-selective passage of solutes up to approximately 1.5 kDa (Kim-Campbell, Gomez, & Bayir, 2019). The pore opening is specifically prominent when the continuous Ca^{2+} loading into mitochondrial matrix is coupled with increased ROS generation, as it occurs in USMB treated cells (Jia et al., 2018). The exact structural composition of mPTP has not been resolved, but throughout the years, several candidates—including adenine nucleotide translocase (ANT) in the inner membrane, the voltage dependent anion channel (VDAC) on the outer membrane, cyclophilin D in the matrix compartment, as well as spastic paraplegia 7 (SPG7), phosphate carrier (PiC), and components of the ATP synthase—have been proposed to coordinately assemble the architecture of the pores (Briston et al., 2017).

Regardless of the structure, the opening of mPTP precedes the release of metabolites and ions, such as pro-apoptotic cytochrome c, to initiate cellular responses including necrotic cell death and apoptosis (Morishita & Watanabe, 1997). Hilgemann & colleagues proposed that the enhancement of protein palmitoylation following Ca^{2+}-induced mPTP opening arises as the direct consequence of the release of mitochondrial metabolic substrates into cytosol, specifically coenzyme A, which acts as an intermediate for the protein acylation reaction. Once in the cytosol, coenzyme A is readily converted into acetyl-CoA by the action of acetyl-coA synthase,

providing the substrate for DHHC5-dependent palmitoylation of cell surface proteins that is required to drive MEND (Hilgemann et al., 2013).

In accordance with the palmitoylation hypothesis, it has been previously shown that the treatment of K562 cells with USMB induces mitochondrial dysfunctions including mitochondrial depolarization and cytochrome c release. Interestingly, these dysfunctions were prevented by treatment with mPTP opening inhibitor, cyclosporin A, suggesting that USMB-induced mitochondrial dysfunctions occur as the result of mPTP opening (Zhao, Feng, Shi, Zong, & Wan, 2015). Furthermore, Hilgemann et al. proposed that the enhanced formation of endocytic carriers upon triggering of MEND favors lipid-ordered membrane domains (Hilgemann et al., 2013). This would be consistent with the observation that USMB stimulation leads to an enhancement of flotillin internalization, as the latter is a resident of lipid-ordered membrane domains (Bryan-Lluka, Bönisch, & Lewis, 2003). Most importantly, DHHC5-dependent MEND is insensitive to the blockage of lysosome exocytosis and lysosomal sphingomyelinases (Lariccia et al., 2011), similar to the insensitivity of USMB-triggered fluid-phase endocytosis to desipramine and vacuolin-1 (Fekri et al., 2016). Therefore, each of these phenomena is distinct from compensatory endocytosis, which follows the lysosome exocytosis step during plasma membrane repair (Idone et al., 2008; Tam et al., 2010). Lastly, MEND triggers internalization that can exceed 50-70% of the cell surface area (Hilgemann et al., 2013). Given that USMB and USMB+desipramine treatment induce ~20-50% enhancement in the formation of plasma membrane-derived fluid containing vesicles over 30 min, the effect of USMB appears to be approximately in line with the magnitude of MEND.

5.7 Flotillin-dependent endocytosis is tuneable by a Fyn and DHHC5 signalling pathway

DHHC5 has several identified substrates—as such, it is possible that USMB triggers the palmitoylation of many cell surface proteins, as was suggested to occur in MEND (Hilgemann et al., 2013). Out of the possible DHHC5 substrates on the plasma membrane, I focused on flotillins for two main reasons. Firstly, the idea of flotillins serving as a major component of CIE carriers for a number of endocytic cargoes has been emerging, which motivated me to look at the contribution of flotillins in the modulation of USMB-induced endocytosis (Meister & Tikkanen, 2014). Secondly, the extent of some proteins' association with the plasma membrane and specifically lipid-ordered domains can be modulated by the addition of palmitoyl moiety. The fact that flotillins can undergo palmitoylation at different stages of their life cycle, makes them attractive candidates as the driver of MEND initiation and progression (Levental, Lingwood, Grzybek, Coskun, & Simons, 2010). Aside from membrane association, palmitoylation can also alter protein-protein interactions, as it has been shown in the case of Rab7, where palmitoylation is required for the recruitment of retromer and efficient endosome-to-TGN trafficking of the lysosomal sorting receptors (Levental et al., 2010). Therefore, it is possible that USMB-induced palmitoylation promotes flotillins interaction with other proteins that facilitate their endocytosis.

In agreement with my hypothesis, it has been previously shown that flotillins themselves are subject to palmitoylation (Jun Liu, DeYoung, et al., 2005; Morrow et al., 2002; Neumann-Giesen et al., 2004), and DHHC5 directly palmitoylates flotillin-2 at Cys4 and Cys20 (Yi Li et al., 2012), suggesting that it is possible that the direct and specific palmitoylation of flotillins by DHHC5 is required for enhanced flotillin-dependent fluid-phase endocytosis upon USMB treatment. More recently, Jang et al. described the effect of the dynamic palmitoylation of flotillins at the plasma membrane. According to the aforementioned study, following IGF-R

activation, flotillin-1undergoes palmitoylation turnover at the plasma membrane (independent of its initial palmitoylation at ER) to regulate the steady-state formation of flotillin-1 positive microdomains, which are required to sustain IGF-R signalling (Jang et al., 2015). Thus, it is possible that USMB triggers DHHC5-dependent palmitoylation turnover of flotillins at the plasma membrane in order to promote the formation of microdomains that are capable of inward budding.

It is not clear how enhanced palmitoylation of flotillins, or more broadly of many cell surface proteins, leads to the enhancement of flotillin-dependent endocytosis. This hypothesis is difficult to test experimentally, as perturbation of flotillin palmitoylation by site-directed mutagenesis of flotillins can result in broader alterations in the membrane traffic of these proteins, as evinced by the arrest of flotillins harbouring mutations that impact Cys43 palmitoylation in the ER (Jang et al., 2015). Nonetheless, whether USMB elicits broad palmitoylation or palmitoylation of only a few key protein(s) to trigger the enhancement of fluid-phase endocytosis, our results strongly indicate that this is flotillin-dependent (**Figure 4.1**), and results in the enhanced formation of flotillin-positive carriers derived from the plasma membrane (**Figure 4.2**).

The tracking of flotillin2-eGFP structures in living cells (**Figure 4.2A-D**) revealed that USMB stimulation leads to a reduction of flotillin2-eGFP intensity in these flotillin structures (**Figure 4.2D**), consistent with USMB stimulation leading to a reduction of flotillin at the cell surface (**Figure 4.2E**). The fact that USMB treatment decreased the intensity of flotillin2-eGFP in flotillin structures suggests that this treatment may either restrict flotillin oligomerization or may selectively enhance endocytic turnover of larger flotillin structures. This DHHC5-dependent regulation of flotillin-dependent endocytosis adds to the known regulation of flotillin-dependent

endocytosis that is mediated by flotillin phosphorylation upon EGF stimulation (Riento et al., 2009). A detailed understanding of the molecular mechanism of flotillin endocytosis is currently lacking, which limits a full comprehension of how USMB treatments and other cues may modulate this process.

It appears that Fyn and DHHC5 act as the upstream regulators of flotillin-dependent endocytosis, as perturbations of either DHHC5 (**Figure 4.3**) or Fyn (**Figure 4.6**) impair the reduction of cell surface flotillin-1 elicited by USMB stimulation, as well as USMB-stimulated enhancement of fluid-phase endocytosis (**Figures 4.4** & **4.6**). Based on the observation that Fyn silencing prevented USMB-stimulated changes in DHHC5 phosphorylation (**Figure 4.4A**) and cell surface DHHC5 levels (**Figure 4.4C**), it can be suggested that Fyn functions upstream of DHHC5 (**Figure 4.8**). Interestingly, previous work in neurons has shown that PSD95 recruits Fyn to the cell surface, where it phosphorylates DHHC5 to impair its endocytosis, thus enhancing DHHC5 levels at the cell surface (Brigidi et al., 2015). In agreement with the neuronal regulation of DHHC5 at the plasma membrane, I discovered that Fyn is also critical for the regulation of DHHC5 in non-neuronal cells (**Figure 4.4A**).

However, in contrast to neurons, Fyn is required for USMB-induced dephosphorylation of DHHC5 in epithelial cells, suggesting the existence of an additional mechanism by which Fyn controls DHHC5. As Fyn is recruited to the cell surface in neurons by PSD95 to act on DHHC5, and PSD95 expression is enriched in neurons, the distinct function of Fyn in these two cell types may be due to distinct modes of association with the plasma membrane. Nonetheless, our results are consistent with previous reports that Y533 on DHHC5 is critical for the regulation of membrane traffic, likely as a result of the phosphorylation of this residue. Notably, none of the perturbations of either Fyn, DHHC5 or flotillin had any effect on fluid-phase uptake in the

absence of USMB stimulation (**Figures 4.1, 4.3 & 4.6**). This suggests that while enhanced fluid-phase endocytosis following USMB treatment occurs via flotillin-dependent endocytosis, other mechanisms predominately sustain constitutive fluid-phase endocytosis.

5.8 Enhanced endocytosis by USMB treatment is an effective strategy for targeted drug delivery

I discovered that flotillin silencing (**Figure 4.1**) or CRISPR/Cas9 knockout (**Figure 4.7**) selectively impair fluid-phase internalization in cells subjected to USMB treatment, but not in resting cells. Previous studies found that flotillin perturbation impairs fluid-phase endocytosis (Glebov et al., 2006), but the contribution of flotillins relative to other forms of clathrin-independent endocytosis varied by cell type and conditions (Mayor et al., 2014). Considered together, these results suggest that other mechanisms—such as other forms of clathrin-independent (or even clathrin-dependent) endocytosis—are largely responsible for constitutive fluid-phase endocytosis in resting cells (i.e. in the absence of USMB treatment). Flotillin-dependent endocytosis can thus be selectively triggered to boost fluid-phase endocytosis upon USMB stimulation, suggesting that this may be an effective strategy for the targeted delivery of drugs.

USMB has been increasingly studied as an attractive and exciting strategy for targeted drug delivery. At the cellular level, USMB treatment elicits the formation of transient pores (De Cock et al., 2015). While sonoporation has been proposed as a strategy for the enhanced delivery of drugs from the extracellular milieu by simple diffusion, these pores are transient and typically re-seal within < 1 minute (Hu et al., 2013). In fact, Fan et al. showed that low intensity (0.17MPa) ultrasound pulse rapidly enhanced cellular uptake of propidium iodide dye from 0 to 1.5 (x10_3 a.u.) within the first minute after USMB exposure, followed by a gradual saturation at

four minutes, indicating a resealing process (Fan, Liu, Mayer, & Deng, 2012). In agreement with Fan's observations, several other studies confirmed that USMB treatment enhances the uptake of different sized molecules up to one minute, although the cytosolic distribution pattern of larger particles are different, and appear to be mediated through mechanisms other than pore formation, particularly endocytosis (Park, Zhang, Vykhodtseva, Akula, & McDannold, 2012; Sheikov, McDannold, Sharma, & Hynynen, 2008; Van Wamel, Bouakaz, & de Jong, 2003). Notably, most experimental strategies that assess the ability of USMB in the enhancement of cellular uptake involve the pre-treatment of cells with the fluorescent dyes or drugs, and then ongoing incubation of cells with dyes/drugs during and following USMB stimulation. As such, these strategies do not distinguish between the delivery of molecules to the cellular interior through transient pores that form and re-seal during or immediately after USMB (<1 min), or the sustained enhancement of fluid-phase endocytosis as I (Fekri et al., 2016) and others (De Cock et al., 2015; Hu et al., 2013; Sennoga et al., 2017; Tardoski et al., 2015) have observed.

The drug treatment protocol that I employed here (**Figure 4.7C** and **Figure A4.4B**) specified the addition of cisplatin for 2 hours, starting at 5 min following USMB stimulation. I was able to exclude direct entry from USMB-induced pores as a mechanism for enhanced cellular uptake of cisplatin and enhanced cisplatin-mediated cell killing in USMB-treated cells. The enhanced uptake via flotillin-dependent endocytosis and not through direct entry via USMB-induced transient pores is further supported by (i) the punctate distribution of fluid-phase markers upon entry into cells (e.g. **Figure 4.1**) and (ii) the fact that USMB enhancement of cisplatin toxicity on cells is completely abrogated in flotillin-1 knockout cells (**Figure 4.7C**), which are selectively defective in flotillin-dependent endocytosis.

The increased flotillin-dependent ability of cisplatin to elicit cell death in cells treated with USMB implies not only that cisplatin is taken up into intracellular vesicles, but also that this treatment results in an uptake with slow recycling of internalized vesicles, leading to the sustained exposure of cells to drugs within the fluid-phase lumen of these vesicles. Consistent with this, doxorubicin was retained in USMB-treated cells to a higher extent than in control cells. Moreover, the increased ability of cisplatin to trigger cell death and DNA damage in USMB-treated cells following flotillin-dependent endocytosis suggests that a significant amount of cisplatin must translocate from the lumen of internalized vesicles to access the nucleus. The mechanism by which this may occur is unclear, and could be due to simple diffusion from the lumen of internalized vesicles retained within the cell. However, the fact that USMB treatment enhances the ability of cisplatin to be taken up via flotillin-dependent endocytosis to cause DNA damage (**Figure 4.7D-E**) indicates that a significant translocation of the drug from internalized vesicles to the cytoplasm/nucleus does indeed occur, leading to an enhancement of drug action.

My work indicates that USMB, in particular in combination with systemic administration of desipramine, may be an effective combination to selectively enhance drug uptake in cancer cells. While the mechanism(s) by which desipramine synergizes with USMB treatment to enhance flotillin-dependent endocytosis remains to be discovered, my results suggest that desipramine, as a clinically approved agent, can form the basis of an effective strategy for targeted drug delivery when administered alongside USMB. These results can at least serve as a proof-of-concept that such a strategy is feasible, and can have important potential implications for the applications of USMB in the targeted enhancement of drug delivery. This selectivity is further supported by the observation that desipramine did not impact fluid-phase endocytosis on

its own but instead only amplified the increase in fluid-phase internalization upon USMB treatment.

Chapter 6 Future direction

6.1 Detailed mechanism of flotillin-dependent endocytosis

Despite establishing the involvement of Fyn and DHHC5 in the regulation of USMB-induced flotillin-mediated endocytosis, the exact hierarchy of interactions is unknown. In post-synaptic neurons, the arrival of the action potential and calcium transient trigger the dissociation of the Fyn, DHHC5, and PSD-95 complex from the plasma membrane, followed by DHHC5 trafficking to the endosomal compartment where it mediates the palmitoylation of its substrates (Brigidi et al., 2015). However, my observations suggest that unlike in neurons, the DHHC5-mediated palmitoylation of membrane proteins is initiated by the recruitment of DHHC5 to the plasma membrane, signifying that the DHHC5 regulation of membrane trafficking might occur via different mechanisms in non-neuronal cells. Furthermore, my findings suggest that Fyn acts upstream of DHHC5, though it is unclear how USMB stimulates and changes Fyn activity or whether the effect of USMB on Fyn arises as the consequence of mechanical or chemical stimulation. Interestingly, the decrease in the phosphorylation levels of DHHC5 following USMB treatment suggests that unlike its recruitment kinetics, the regulation of DHHC5 activity on the plasma membrane might be at least somehow similar to the neuronal pathway, since in both neurons and epithelial cells, the dephosphorylation of DHHC5 triggers the palmitoylation and subsequent membrane trafficking of its substrates. It would be interesting to map out the exact mechanism by which Fyn regulates DHHC5 activity following USMB treatment.

Despite confirming the involvement of flotillins in the regulation of USMB-induced fluid uptake, I did not directly measure changes in the palmitoylation levels of flotillins in response to USMB, nor did I identify the involvement of other palmitoylated proteins in the formation of endocytic vesicles. Confirming the number and nature of plasma membrane proteins that undergo DHHC5-mediated palmitoylation in response to USMB treatment can provide a better

understanding of events that drive the formation of endocytic vesicles. To address this point, acyl-biotin exchange (ABE) reaction on whole-cell lysates can be performed to detect the identity of palmitoylated proteins following USMB treatment. ABE assay relies on the cleavage of covalent thioester linkage between palmitic acid moieties and cysteine residues of target proteins, followed by labelling of newly available thiol groups with biotin. The biotinylated proteins are then pulled down from streptavidin agarose column and analyzed further by proteomics mass spectrometry (Drisdel & Green, 2004).

Lastly, I did not confirm the involvement of the mPTP opening in the initiation of USMB-induced flotillin endocytosis, so it is unclear whether USMB-induced fluid uptake is similar to the MEND response described by Hilgemann & colleagues (Hilgemann et al., 2013). One of the known consequences of mPTP opening is the collapse of mitochondrial membrane potential, which can be detected by using a specific marker, known as JC-1. Following exposure to stress stimuli, mitochondrial depolarization is indicated by a decrease in the red/green fluorescence intensity ratio. Using the same strategy, Zhao et al. demonstrated that USMB treatment results in mitochondrial depolarization which can be completely prevented by treatment of cells with cyclosporin A prior to USMB (Zhao et al., 2015). In order to test the involvement of mPTP in shaping the initial stages of USMB-induced flotillin-mediated endocytosis, cells should be treated with cyclosporin A prior to USMB treatment. If mPTP opening is essential for triggering of flotillin-mediated endocytosis, then inhibition of mPTP opening should abolish the enhanced uptake of fluid and fluid-phase markers, as well as the change in localization of flotillins.

Most experiments were conducted at two time points of 5 min (CME) or 30 min (fluid-phase uptake) after USMB treatment. Interestingly, our analysis of doxorubicin accumulation 24

hours after USMB treatment suggests that aside from endocytosis, drug retention is also altered by USMB treatment. Studying the effects of USMB on CME and flotillin-mediated endocytosis at different time points can provide valuable information on the kinetics of endocytosis and exocytosis, which would collectively determine the extent of drug retention in the cell. A more in-depth understanding of overall kinetics would allow for the modification of the drug's dosage and dose schedule to better complement the utilization of USMB as drug carriers.

6.2 Identifying the intracellular target of desipramine

It is currently unclear which mode of action desipramine uses to synergize with USMB to enhance flotillin-dependent fluid uptake. While desipramine is a known inhibitor of A-SMase, I previously excluded this mode of action on the enhancement of USMB-induced fluid-phase endocytosis (Fekri et al., 2016). Desipramine potently targets a variety of neurotransmitter receptors and transporters, such as the norepinephrine transporter (Bryan-Lluka et al., 2003), suggesting a broad list of possible targets in the context of regulation of fluid-phase endocytosis following USMB treatment. In addition to the inhibition of A-SMase, desipramine triggers the release of Ca^{2+} from ER in a Ca^{2+} and phospholipase C-independent but concentration-dependent manner (Ho, Kuo, Chen, Huang, & Jan, 2005; Huang et al., 2007).

As mentioned before, USMB-induced sonoporation and the subsequent influx of extracellular Ca^{2+} might be involved in the initiation of the signal transduction pathways that impact cellular processes, such as lysosome exocytosis or the opening of mPTP. Hence, desipramine may boost the ability of USMB to enhance flotillin-dependent endocytosis by triggering the release of Ca^{2+} from intracellular stores, thus amplifying the Ca^{2+} signal that is instigated by the influx of extracellular Ca^{2+} through USMB-induced pores. One way to test whether the contribution of desipramine to the rate of USMB-induced flotillin-mediated

endocytosis occurs through Ca^{2+} signalling is to deplete the intracellular calcium stores with thapsigargin (a non-competitive inhibitor of ER Ca^{2+} ATPases) prior to USMB treatment. If the contribution of desipramine to the enhancement of flotillin-dependent endocytosis occurs through amplification of Ca^{2+} signalling, then treatment with thapsigargin prior to USMB treatment should mimic the effect of desipramine on the rate of USMB-induced flotillin-mediated fluid uptake.

The opening of mPTP elicits a wide range of responses, from altering membrane dynamics to more detrimental effects such as the activation of programmed cell death. Naturally, cells have protective mechanisms to negatively regulate the opening of mPTP. A number of studies have highlighted the central role of PKCε in the regulation of the mPTP opening (Baines et al., 2002, 2003; Ping et al., 1997). For years, it was known that the activation of PKCε during reperfusion could protect the heart from reperfusion injury, a phenomenon that was later discovered to be through the PKCε -mediated inhibition of the mPTP opening (Clarke et al., 2008; Shigeru Morishita, 1997). In agreement with the role of PKCε as the negative regulator of the mPTP, Hilgemann et al. also reported that treatment with PKCε activator 1-oleoyl-2- acetyl-sn-glycerol (OAG, 15 μM) prior to the arrival of Ca^{2+} transient can effectively block MEND initiation by inhibiting the opening of mPTP (Hilgemann et al., 2013). Interestingly, the desipramine inhibitory effect on neurotransmitter uptake occurs partially through the inhibition of PKC activity, specifically in the presence of calcium (Morishita & Watanabe, 1997). As such it is possible that the pre-treatment with desipramine inhibits PKCε, thus ensuring the opening of mPTP and the acylation of membrane proteins in response to USMB-induced calcium influx, all of which can collectively augment the magnitude of MEND. To test whether desipramine and USMB synergism occurs as a result of PKCε inhibition, cells should be treated with other known

PKCε inhibitors such as staurosporine prior to USMB stimulation. If desipramine exerts its effect through PKCε inhibition, then the cell surface distribution of flotillins and the rate of Alexa-dextran uptake following USMB should mimic the effect of USMB and desipramine synergism.

Alternatively, the potent inhibitory effect of desipramine on phosphatidic acid phosphatase (PAP) can exaggerate USMB-induced fluid uptake by promoting phosphatidic acid (PA)-mediated endocytosis (Shaughnessy et al., 2014). The idea that PAP inhibition could drive endocytic responses has been previously investigated in the internalization of oncogenic EGFRs in the absence of EGF ligands. Notably, the aforementioned study established that desipramine—by inhibiting PAP—can activate the PA/PDE4/PKA pathway to regulate the endocytic trafficking of EGFR. However, it is not clear whether phosphatidic acid-mediated endocytosis is related to the palmitoylation of membrane proteins or the MEND pathway. It would be interesting to test whether replacing desipramine with other phosphatidic acid phosphatase inhibitors can mimic the effect of USMB and desipramine synergism. Examining the hypothesis mentioned above could potentially identify how desipramine synergises with USMB treatment to trigger enhanced flotillin-dependent endocytosis. Identifying the mechanism can provide venues for developing novel therapeutic agents that can mimic the effect of desipramine but with a higher specificity.

6.3 Increasing the delivery of trastuzumab using USMB and desipramine treatment

The receptor tyrosine kinase ErbB2, also known as the human epidermal growth factor receptor 2 (HER2), is a member of the epidermal growth factor receptor family (EGFR/ErbB family). The activation kinetic of the receptor involves the ligand-independent heterodimerization of HER2 with other ligand-activated members of the family (EGFR/ErbB1, ErbB3, ErbB4). This is followed by the autophosphorylation of tyrosine residues within the cytoplasmic domain, and the

recruitment of signalling molecules to initiate downstream signalling pathways that modulate proliferation and migration (Wolf-Yadlin et al., 2006).

Given the profound role of the EGFR family in cell proliferation, any dysregulation in the signalling network can trigger the uncontrolled cell division that correlates with cancer development and progression. In fact, HER2 gene amplification and overexpression is present in 20-30% of human breast tumours and is known to extensively contribute to tumour aggressiveness, poor prognosis and higher recurrence rate (Meric-Bernstam & Hung, 2006; Mitri, Constantine, & O'Regan, 2012; Slamon et al., 1987, 1989). Indeed, the detection of HER2 by histology in tumor biopsies results in classification of the tumor as HER2-positive, a specific subset of breast tumors with specific targeted treatment plans and strategies. Therefore, the indisputable involvement of the HER2 receptor in tumourigenesis makes this receptor an appropriate target for the therapeutic treatment of HER2-positive breast cancer. Over the years, a number of approaches have been developed for the treatment of HER2-positive breast cancer, including monoclonal antibodies such as trastuzumab, tyrosine kinase inhibitors and active immunotherapy (Mènard, Tagliabue, Campiglio, & Pupa, 2000).

Normally, the endocytosis of an activated receptor and its subsequent degradation in lysosome helps to attenuate the receptor-activated signal transduction pathway. However, the pathogenic role of HER2 in tumour progression is sustained by the retention of the receptor in actin- and flotillin-enriched membrane microdomains, which augment the threshold of HER2 signalling. Retention of HER2 at the cell surface is achieved through colocalization of the receptor with calcium ATPase2 (PMCA2), HSP90, and flotillins, allowing the HER2 to resist internalization and continue signalling at the plasma membrane (Jeong, Kim, Kim, VanHouten, & Wysolmerski, 2017). As one of the main components of the membrane rafts and a possible

endocytic carrier, the association of flotillins with the altered signalling and trafficking of HER2 in breast cancer cells has been previously investigated. Immunohistochemistry analyses of 171 breast cancer samples have confirmed that flotillin-2 is overexpressed in 82 of 171 breast cancer specimens which corresponded to 47.7% cumulative 5-year survival rate, whereas the rate was 87.3% for patients with low FLOT2 expression levels (Wang et al., 2013). Furthermore, the assessment of 282 samples of gastric carcinoma has revealed that the positive correlation between flotillin-2 and HER2 is required for the localization and retention of HER2 at the plasma membrane, and is directly related to the low survival rate of gastric cancer patients (Zhu et al., 2013). The unique property of HER2 to resist internalization also affects the therapeutic efficacy of HER2 targeting drugs. For example, the treatment of SKBr3 cells with trastuzumab blunts their proliferation through the recruitment of PTEN-dependent dephosphorylation of Akt, but it cannot promote HER2 internalization and receptor degradation (Longva, Pedersen, Haslekås, Stang, & Madshus, 2005).

Previously our lab confirmed that HER2 strongly localizes to flotillin structures, and my findings have established that USMB and desipramine can selectively enhance the internalization of flotillins from the plasma membrane. I propose that the treatment of HER2-positive cancer cells in combination with trastuzumab can promote the endocytic downregulation of HER2, and increase trastuzumab's anti-proliferative effect by inducing receptor internalization and degradation, as well as inhibiting the constitutive phosphorylation of the Akt signalling pathway. The selective and targeted modulation of receptor internalization along with the inhibition of signalling pathways can improve the pharmacologic responses of anti-HER2-monoclonal antibodies.

Conclusion

USMB has the potential to produce incredibly effective drug delivery outcomes, thanks to its targeted nature and its ability to enhance the delivery of therapeutics across biological barriers. The aim of this project was to study the effect of USMB on membrane-associated processes, particularly endocytosis. I discovered that USMB can extrinsically modulate the rate of intrinsic endocytic pathways that function as gatekeepers of the plasma membrane for the entry of molecules into cells, a phenomenon that can be particularly useful for the intracellular delivery of therapeutics. I identified that USMB treatment specifically increases internalization by two distinct mechanisms: CME and fluid-phase endocytosis. I found that the increase in CME was prevented by inhibitors of lysosome exocytosis and A-SMase, suggesting that the production of ceramide on the plasma membrane may enhance CME upon USMB treatment. Unlike CME, USMB-induced fluid-phase uptake occurred independently of lysosome exocytosis and A-SMase activity, but required the contribution of flotillins to promote the endocytic response.

Furthermore, I discovered that USMB modulation of flotillins' distribution and endocytosis requires the activity of DHHC5 and Fyn, though the exact interaction hierarchy remains to be discovered. I also made the surprising discovery that pre-treatment with drugs such as desipramine prior to USMB can synergistically enhance the rate of flotillin-mediated endocytosis. Lastly, I established that USMB and desipramine synergism could be useful for the delivery of chemotherapeutic drugs—such as cisplatin into cancer cells—and can positively affect drug efficacy and treatment outcome. Although the mechanism of action is not known, I propose that the clinical application of desipramine (or similar compounds) along with USMB could improve the intracellular delivery of drugs. This highlights the potential usefulness of USMB in developing more effective therapies to treat cancer, as it drives targeted delivery and drug uptake into tumours or other diseased tissues. However, as of now, our grasp on the effects

of USMB on membrane dynamics or even global cellular responses is still at its infancy. Continuing on this path could shape a more in-depth understanding of the mechanisms that drive membrane responses, and possibly open new venues for designing therapeutic strategies that can achieve efficient drug delivery across the most impermeable membranes.

Appendices

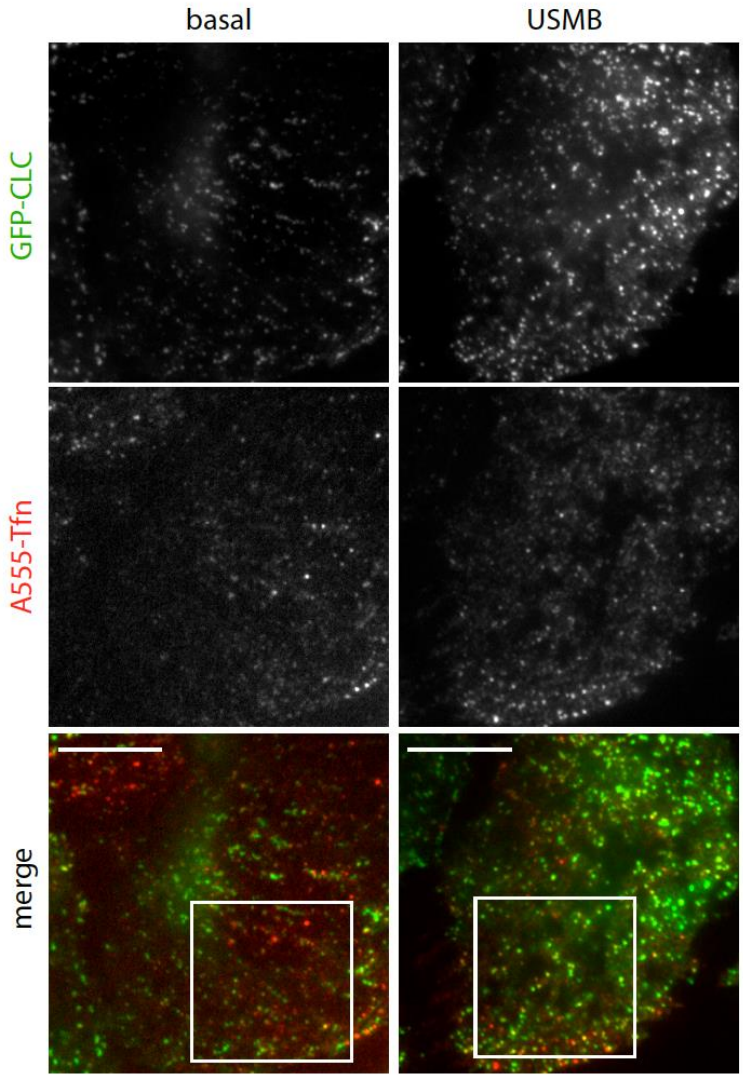

Figure A3.1. Full image panels for TIRF-M images shown in Figure 3.1. To allow visualization of clathrin structures the images shown in Figure 3.1 are magnified insets of larger images. Shown in this figure are the full images obtained by TIRF-M corresponding to the magnified image insets (shown by the white boxes) shown in Figure 3.1. Scale = 20 μm.

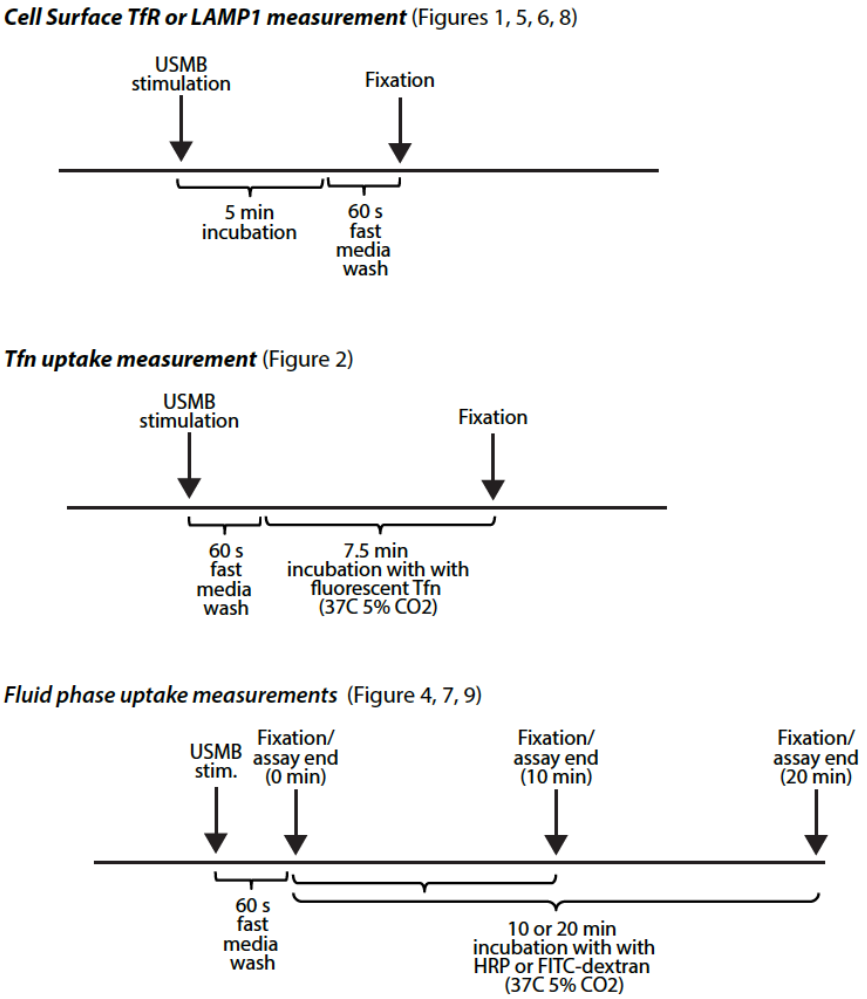

Figure A3.2. Diagram depicting the timing of measurements of membrane traffic used in this study. Shown are diagrams of the timing of the experimental manipulations, starting with the USMB stimulation in each case. Top panel: For cell-surface TfR level measurement, USMB stimulation is followed by a 5 min incubation, followed by rapid washing and fixation. Middle panel: For A555-Tfn uptake experiments (except for TIRF experiments), USMB stimulation is followed by rapid washes, then by incubation in media with A555-Tfn for 7.5 min, followed by immediate fixation. For TIRF experiments in RPE GFP-CLC cells (Figure 3.2), A555-Tfn is added for only 3 min prior to fixation. Lower panel: For fluid-phase uptake measurements, USMB stimulation is followed by a rapid wash, then by incubation with media containing wither HRP or FITC-dextran for 10 or 20 min, followed by immediate assay end or fixation.

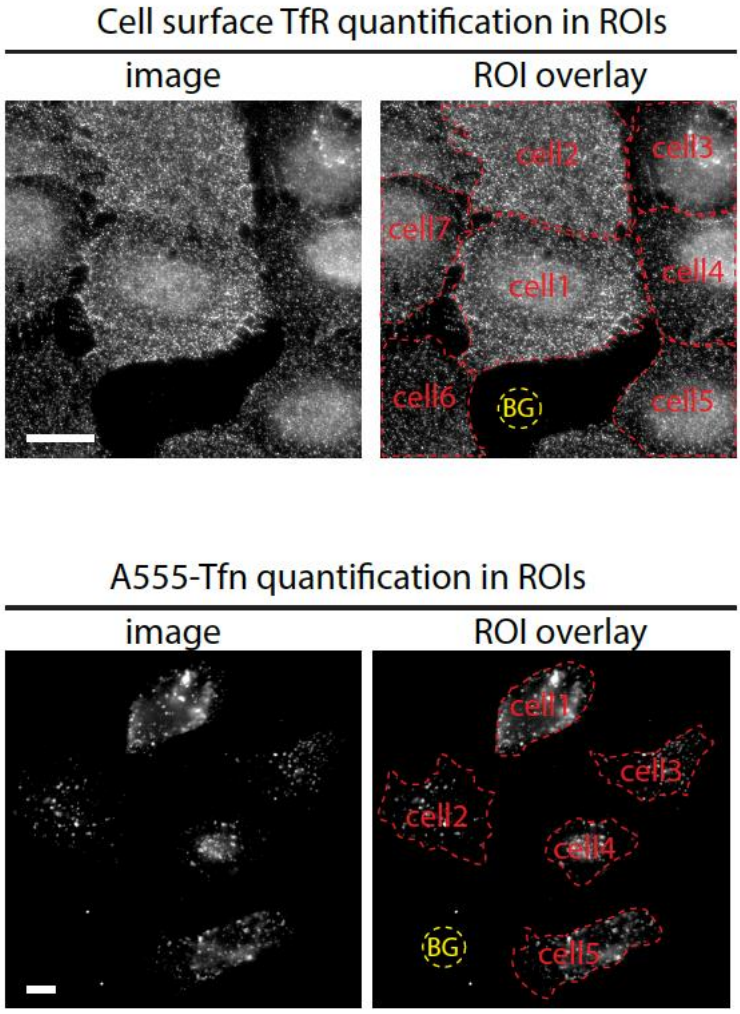

Figure A3.3. Quantification of cellular fluorescence intensity, used for measurement of cell surface TfR and LAMP1, Tfn uptake and FITC-dextran uptake. RPE cells were subjected to detection of cell surface TfR levels (*top panels*, as per Figure 3.1, 3.6 and and 3.8) or uptake of A555-Tfn (bottom panels, as per Figure 3.2. Shown are representative fluorescence micrographs (left images), scale 20 μm. Shown in the right images are overlays of the fluorescence micrographs with manually selected regions of interest (ROI, red dashed lines) corresponding to the entire cell area of all visible cells in each image, as well as a standard ROI corresponding to coverslip background (BG, yellow dashed lines). As described in *Materials and Methods*, cell surface Tfn, LAMP1 or total internalized Tfn or FITC-dextran was measured by quantification of mean pixel intensity within ROIs (corresponding to visible cells) in each image, followed by subtraction of mean pixel intensity of the BG ROI, in order to obtain the net mean pixel intensity for each cell in each image.

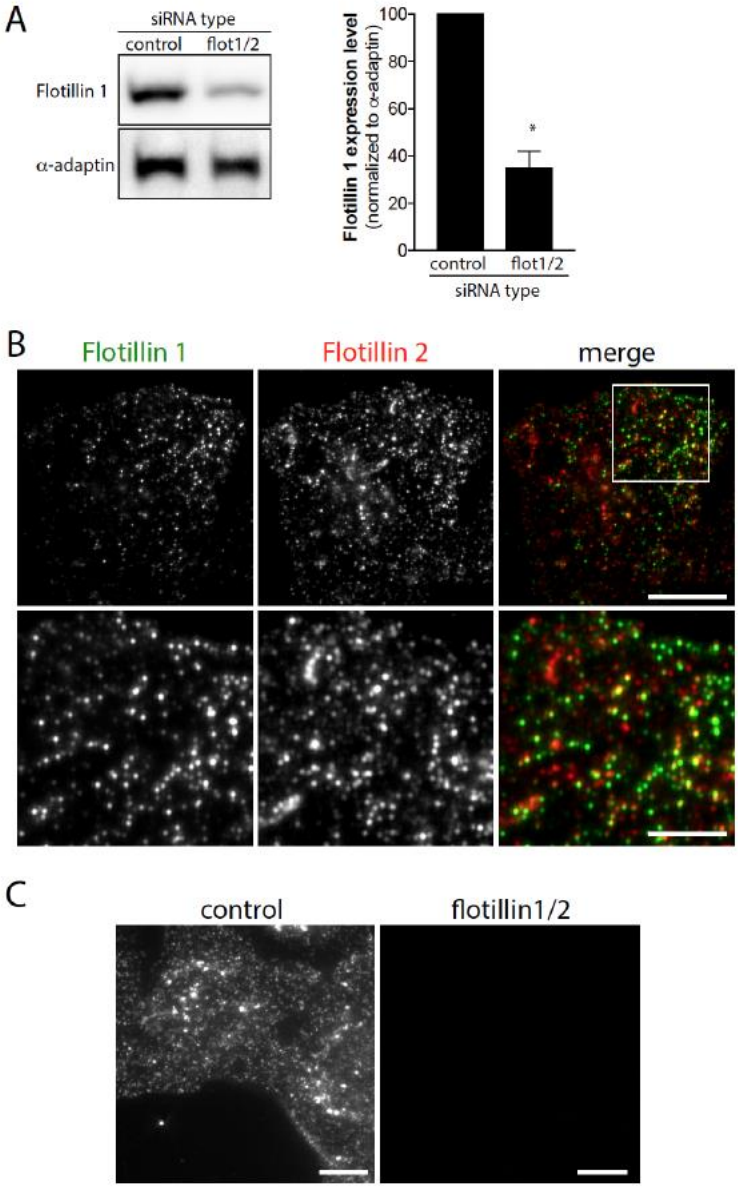

Figure A4.1. Flotillin knockdown and immunofluorescence detection. (A) RPE cells were transfected with siRNA targeting flotillin-1 and -2 (flotillin) or non-targeting siRNA (control). Whole cell lysates were resolved by SDS-PAGE and subjected to immunoblotting to detect flotillin-1 or alpha-adaptin (AP2, loading control). Shown (left panels) are representative immunoblot and the mean ± SE of flotillin-1 detected by this method (right panels). This demonstrates effective knockdown of flotillin1 by siRNA silencing. (B) RPE cells were subjected to immunofluorescence staining to detect flotillin-1 and flotillin-2 and then subjected to imaging by total internal reflection fluorescence microscopy (TIRF-M). Shown are representative fluorescence micrographs that show the extensive co-localization of flotillin-1 and flotillin-2, scale 10 μm. This indicates that the vast majority of flotillin structures in these cells are positive for both flotillin-1 and flotillin-

2. (C) RPE cells were transfected with siRNA targeting flotillin-1 and -2 (flotillin) or non-targeting siRNA (control), followed by immunofluorescence staining to detect flotillin-1, then subjected to imaging by TIRF-M. Shown are representative fluorescence micrographs, scale 10 μm, which indicate the specificity of flotillin-1 staining for flotillin-1.

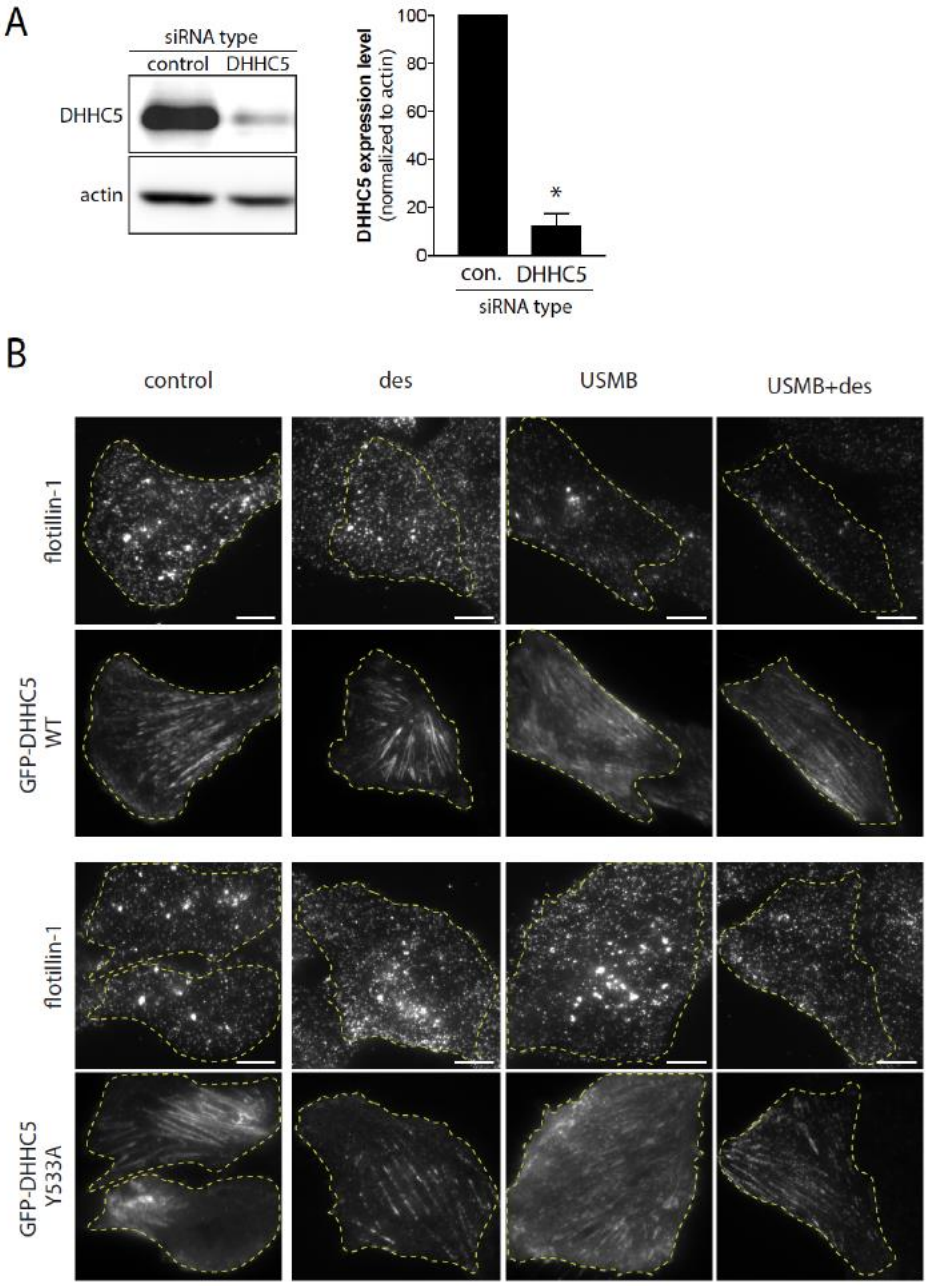

Figure A4.2. DHHC5 knockdown and transfection. (A) RPE cells were transfected with siRNA targeting DHHC5 or non-targeting siRNA (control). Whole-cell lysates were resolved by SDSPAGE and subjected to immunoblotting to detect DHHC5 or actin (loading control). Shown (left panels) are representative immunoblot and the mean ± SE of DHHC5 detected by this method (right panels). This demonstrates effective knockdown of DHHC5 by siRNA silencing. (B) RPE cells were transfected with cDNA encoding either wild-type (WT) or Y533A mutant DHHC5,

fused to eGFP. Following transfection, some cells were treated with 50 μM desipramine for 60 min followed by USMB treatment, as indicated. Following a subsequent 30 min incubation, cells were then fixed and subjected to immunofluorescence staining of flotillin-1, and then imaging by TIRFM. Shown are representative TIRF-M fluorescence micrographs, scale 10 μm. Transfected cells are outlined, based on GFP signal. These images show the eGFP-DHHC5 expression of cells shown in Figure 5.

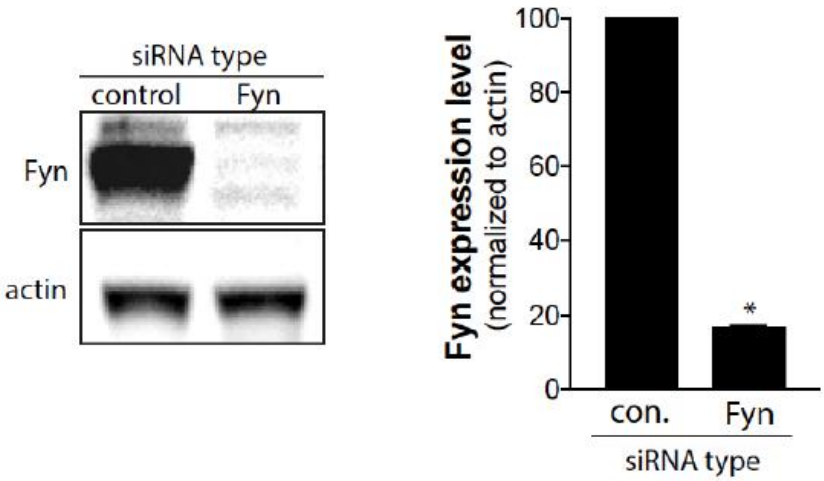

Figure A4.3. Fyn knockdown. RPE cells were transfected with siRNA targeting Fyn or nontargeting siRNA (control). Whole-cell lysates were resolved by SDS-PAGE and subjected by immunoblotting to detect Fyn or actin (loading control). Shown (left panels) are representative immunoblot and the mean ± SE of Fyn detected by this method (right panels). This demonstrates effective knockdown of Fyn by siRNA silencing.

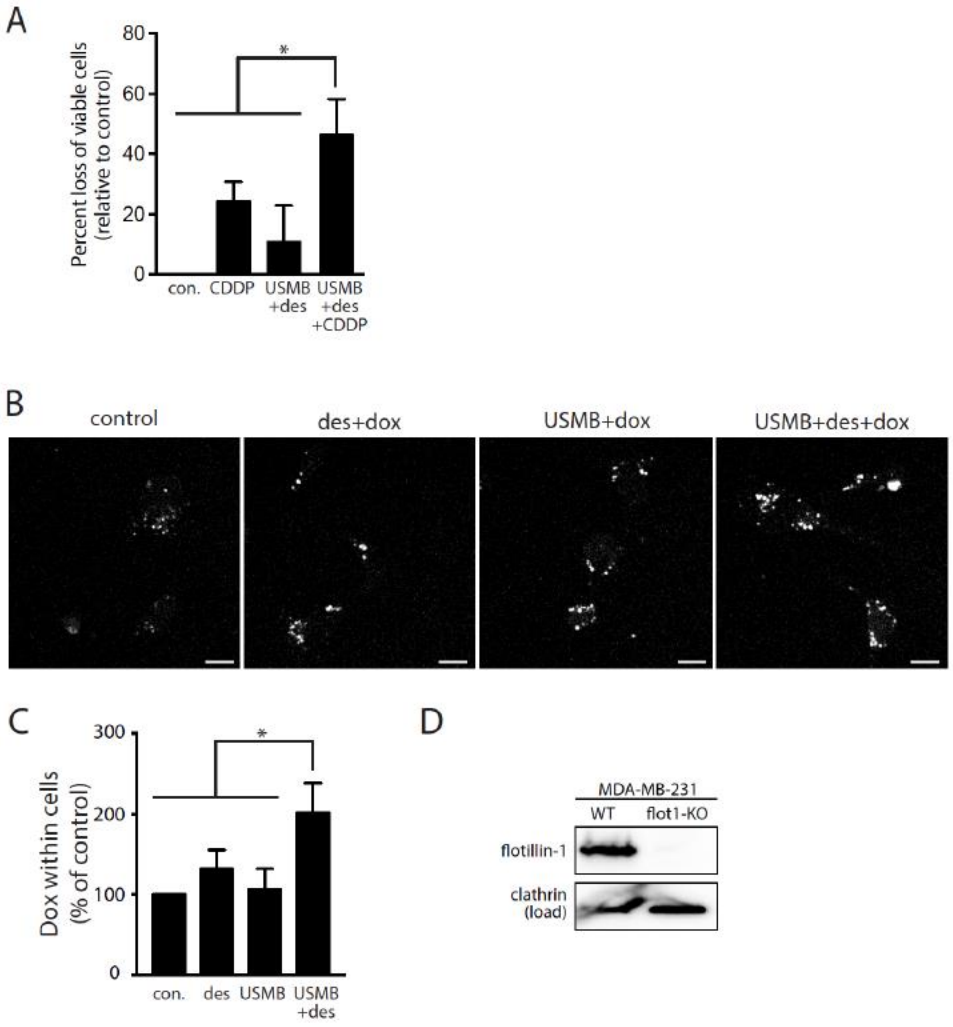

Figure A4.4. Flotillin knockout cells and contribution of flotillin to cell viability in USMB treated cells. (A) RPE cells were treated with 50 μM desipramine for 60 min followed by USMB treatment, as indicated. Following treatments, some cells were incubated with 0.03 mM cisplatin (CDDP) for 2 h, as indicated, followed by washing and incubation in growth media (no drugs). 24 h after USMB and/or cisplatin exposure, cell viability was assessed by crystal violet assay, and shown are the mean ± SE of the percent reduction in the total viable cells, relative to that of control (not treated with CDDP, USMB or desipramine). n = 3 independent experiments. *, $p < 0.05$. (BC) RPE cells were treated with 50 μM desipramine for 60 min followed by USMB treatment, as indicated. Following treatments, cells were incubated with 0.03 mM doxorubicin for 2 h (as shown), followed by washing and incubation in growth media (no drugs) for 24 h, after which cells were subjected to widefield epifluorescence microscopy to detect doxorubicin fluorescence within cells. Shown in (B) are representative fluorescence micrographs of doxorubicin fluorescence, and in (C) the mean ± SE of cellular doxorubicin fluorescence. n = 3 independent experiments. *, $p < 0.05$. This indicates that cells treated with USMB+desipramine

retain more chemotherapeutic drugs 24 h after exposure to these drugs compared to control cells (cells not treated with USMB+desipramine). (D) Whole cell lysates from MDA-MB-231 wild-type (WT) cells or MDAMB- 231 cells subjected to CRISR/Cas9 genome editing (to knock out flotillin-1) were resolved by SDS-PAGE and subjected by immunoblotting to detect flotillin-1 or clathrin heavy chain (loading control). Shown are representative immunoblots demonstrates effective knockout of flotillin in MDA-MB-231-flot-KO cells.

Bibliography

Abbina, S., & Anilkumar, P. (2018). PEGylation and its alternatives: A summary. In P. Anilkumar (Ed.), *Engineering of Biomaterials for Drug Delivery Systems* (pp. 363–376). Cambridge: Woodhead Publishing. https://doi.org/10.1016/B978-0-08-101750-0.00014-3

Abou-Elkacem, L., Bachawal, S. V., & Willmann, J. K. (2015). Ultrasound molecular imaging: Moving toward clinical translation. *European Journal of Radiology*, *84*(9), 1685–1693. https://doi.org/10.1016/j.ejrad.2015.03.016

Adelstein, R. S., & Sellers, J. R. (1987). Effects of calcium on vascular smooth muscle contraction. *The American Journal of Cardiology*, *59*(3), 4B–10B. Retrieved from http://www.ncbi.nlm.nih.gov/pubmed/3028118

Aguet, F., Antonescu, C., Mettlen, M., Schmid, S., & Danuser, G. (2013). Advances in analysis of low signal-to-noise images link dynamin and AP2 to the functions of an endocytic checkpoint. *Developmental Cell*, *26*(3). https://doi.org/10.1016/j.devcel.2013.06.019

Aicart-ramos, C., Valero, R. A., & Rodriguez-crespo, I. (2011). Protein palmitoylation and subcellular trafficking. *Biochimica et Biophysica Acta*, *1808*, 2981–2994. https://doi.org/10.1016/j.bbamem.2011.07.009

Ait-Slimane, T., Galmes, R., Trugnan, G., & Maurice, M. (2009). Basolateral Internalization of GPI-anchored Proteins Occurs via a Clathrin-independent Flotillin-dependent Pathway in Polarized Hepatic Cells. *Molecular Biology of the Cell*, *20*(17), 3792–3800. https://doi.org/10.1091/mbc.E09-04-0275

Al Soraj, M., He, L., Peynshaert, K., Cousaert, J., Vercauteren, D., Braeckmans, K., … Jones, A. T. (2012). siRNA and pharmacological inhibition of endocytic pathways to characterize the differential role of macropinocytosis and the actin cytoskeleton on cellular uptake of dextran and cationic cell penetrating peptides octaarginine (R8) and HIV-Tat. *Journal of*

Controlled Release, *161*(1), 132–141. https://doi.org/10.1016/j.jconrel.2012.03.015

Aldred, E. M., Buck, C., & Vall, K. (2009). Drug excretion. In *Pharmacology A Handbook for Complementary Healthcare Professionals* (pp. 133–136). London: Churchill Livingstone. https://doi.org/10.1016/B978-0-443-06898-0.00018-9

Allison, S. D., Chang, B., Randolph, T. W., & Carpenter, J. F. (1999). Hydrogen Bonding between Sugar and Protein Is Responsible for Inhibition of Dehydration-Induced Protein Unfolding. *Archives of Biochemistry and Biophysics*, *365*(2), 289–298. https://doi.org/10.1006/abbi.1999.1175

Amaddii, M., Meister, M., Banning, A., Tomasovic, A., Mooz, J., Rajalingam, K., & Tikkanen, R. (2012a). Flotillin-1/reggie-2 protein plays dual role in activation of receptor-tyrosine kinase/mitogen-activated protein kinase signaling. *The Journal of Biological Chemistry*, *287*(10), 7265–78. https://doi.org/10.1074/jbc.M111.287599

Amyere, M., Payrastre, B., Krause, U., Smissen, P. Van Der, Veithen, A., & Courtoy, P. J. (2000). Constitutive Macropinocytosis in Oncogene-transformed Fibroblasts Depends on Sequential Permanent Activation of Phosphoinositide 3-Kinase and Phospholipase C. *Molecular Biology of the Cell*, *11*(10), 3453–3467. https://doi.org/10.1091/mbc.11.10.3453

Anderson, C. R., Hu, X., Zhang, H., Tlaxca, J., Declèves, A.-E., Houghtaling, R., … Rychak, J. J. (2011). Ultrasound Molecular Imaging of Tumor Angiogenesis With an Integrin Targeted Microbubble Contrast Agent. *Investigative Radiology*, *46*(4), 215–224. https://doi.org/10.1097/RLI.0b013e3182034fed

Anderson, R. G. W., Brown, M. S., & Goldstein, J. L. (1977). Role of the coated endocytic vesicle in the uptake of receptor-bound low density lipoprotein in human fibroblasts. *Cell*, *10*(3), 351–364. https://doi.org/10.1016/0092-8674(77)90022-8

Andrade, C. (2015). Sustained-Release, Extended-Release, and Other Time-Release Formulations in Neuropsychiatry. *The Journal of Clinical Psychiatry*, *76*(08), 995–999. https://doi.org/10.4088/JCP.15f10219

Andrews, N. W., Almeida, P. E., & Corrotte, M. (2014). Damage control: cellular mechanisms of plasma membrane repair. *Trends in Cell Biology*, *24*(12), 734–42. https://doi.org/10.1016/j.tcb.2014.07.008

Andrieu-Abadie, N., Gouazé, V., Salvayre, R., & Levade, T. (2001). Ceramide in apoptosis signaling: relationship with oxidative stress. *Free Radical Biology & Medicine*, *31*(6), 717–28. Retrieved from http://www.ncbi.nlm.nih.gov/pubmed/11557309

Antonescu, C. N., Aguet, F., Danuser, G., & Schmid, S. L. (2011). Phosphatidylinositol-(4,5)-bisphosphate regulates clathrin-coated pit initiation, stabilization, and size. *Molecular Biology of the Cell*, *22*(14), 2588–600. https://doi.org/10.1091/mbc.E11-04-0362

Antonescu, C. N., Danuser, G., & Schmid, S. L. (2010). Phosphatidic acid plays a regulatory role in clathrin-mediated endocytosis. *Molecular Biology of the Cell*, *21*(16), 2944–2952. https://doi.org/10.1091/mbc.E10-05-0421

Antonescu, C. N., McGraw, T. E., & Klip, A. (2013). Reciprocal regulation of endocytosis and metabolism. *Cold Spring Harbor Perspectives in Biology*, *in press*(7), a016964. https://doi.org/10.1101/cshperspect.a016964

Araki, N., Egami, Y., Watanabe, Y., & Hatae, T. (2007). Phosphoinositide metabolism during membrane ruffling and macropinosome formation in EGF-stimulated A431 cells. *Experimental Cell Research*, *313*(7), 1496–1507. https://doi.org/10.1016/j.yexcr.2007.02.012

Araki, N., Hamasaki, M., Egami, Y., & Hatae, T. (2006). Effect of 3-methyladenine on the

fusion process of macropinosomes in EGF-stimulated A431 cells. *Cell Structure and Function*, *31*(2), 145–57. Retrieved from http://www.ncbi.nlm.nih.gov/pubmed/17146146

Araki, N., Johnson, M. T., & Swanson, J. A. (1996). A role for phosphoinositide 3-kinase in the completion of macropinocytosis and phagocytosis by macrophages. *The Journal of Cell Biology*, *135*(5), 1249–60. Retrieved from http://www.ncbi.nlm.nih.gov/pubmed/8947549

Arbab, A. S., Bashaw, L. A., Miller, B. R., Jordan, E. K., Lewis, B. K., Kalish, H., & Frank, J. A. (2003). Characterization of Biophysical and Metabolic Properties of Cells Labeled with Superparamagnetic Iron Oxide Nanoparticles and Transfection Agent for Cellular MR Imaging. *Radiology*, *229*(3), 838–846. https://doi.org/10.1148/radiol.2293021215

Babiychuk, E. B., Monastyrskaya, K., Potez, S., & Draeger, A. (2009). Intracellular Ca2+ operates a switch between repair and lysis of streptolysin O-perforated cells. *Cell Death & Differentiation*, *16*(8), 1126–1134. https://doi.org/10.1038/cdd.2009.30

Babuke, T., Ruonala, M., Meister, M., Amaddii, M., Genzler, C., Esposito, A., & Tikkanen, R. (2009). Hetero-oligomerization of reggie-1/flotillin-2 and reggie-2/flotillin-1 is required for their endocytosis. *Cellular Signalling*, *21*(8), 1287–1297. https://doi.org/10.1016/j.cellsig.2009.03.012

Bachawal, S. V., Jensen, K. C., Lutz, A. M., Gambhir, S. S., Tranquart, F., Tian, L., & Willmann, J. K. (2013). Earlier Detection of Breast Cancer with Ultrasound Molecular Imaging in a Transgenic Mouse Model. *Cancer Research*, *73*(6), 1689–1698. https://doi.org/10.1158/0008-5472.CAN-12-3391

Backes, W. L. (2007). Passive Diffusion of Drugs Across Membranes. In S. J. Enna & D. B. Bylund (Eds.), *xPharm: The Comprehensive Pharmacology Reference* (pp. 1–5). Elsevier. https://doi.org/10.1016/B978-008055232-3.60067-4

Baines, C. P., Song, C.-X., Zheng, Y.-T., Wang, G.-W., Zhang, J., Wang, O.-L., … Ping, P. (2003). Protein Kinase Cε Interacts With and Inhibits the Permeability Transition Pore in Cardiac Mitochondria. *Circulation Research*, *92*(8), 873–880. https://doi.org/10.1161/01.RES.0000069215.36389.8D

Baines, C. P., Zhang, J., Wang, G.-W., Zheng, Y.-T., Xiu, J. X., Cardwell, E. M., … Ping, P. (2002). Mitochondrial PKCepsilon and MAPK form signaling modules in the murine heart: enhanced mitochondrial PKCepsilon-MAPK interactions and differential MAPK activation in PKCepsilon-induced cardioprotection. *Circulation Research*, *90*(4), 390–7. Retrieved from http://www.ncbi.nlm.nih.gov/pubmed/11884367

Bakhtiari-Nejad, M., & Shahab, S. (2018). Effects of Nonlinear Propagation of Focused Ultrasound on the Stable Cavitation of a Single Bubble. *Acoustics*, *1*(1), 14–34. https://doi.org/10.3390/acoustics1010003

Bardal, S. K., Waechter, J. E., & Martin, D. S. (2011). Pharmacokinetics. In *Applied Pharmacology* (1st ed., p. 470). Missouri: Elsevier/Saunders. Retrieved from https://www.sciencedirect.com/book/9781437703108/applied-pharmacology

Basquin, C., Malarde, V., Mellor, P., Anderson, D. H., Meas-Yedid, V., Olivo-Marin, J.-C., … Sauvonnet, N. (2013a). The signalling factor PI3K is a specific regulator of the clathrin-independent dynamin-dependent endocytosis of IL-2 receptors. *Journal of Cell Science*, *126*(5), 1099–1108. https://doi.org/10.1242/jcs.110932

Basquin, C., & Sauvonnet, N. (2013). Phosphoinositide 3-kinase at the crossroad between endocytosis and signaling of cytokine receptors. *Communicative & Integrative Biology*, *6*(4), e24243. https://doi.org/10.4161/cib.24243

Bastiani, M., Liu, L., Hill, M. M., Jedrychowski, M. P., Nixon, S. J., Lo, H. P., … Parton, R. G.

(2009). MURC/Cavin-4 and cavin family members form tissue-specific caveolar complexes. *The Journal of Cell Biology*, *185*(7), 1259–1273. https://doi.org/10.1083/jcb.200903053

Baumann, C. a, Ribon, V., Kanzaki, M., Thurmond, D. C., Mora, S., Shigematsu, S., … Saltiel, a R. (2000). CAP defines a second signalling pathway required for insulin-stimulated glucose transport. *Nature*, *407*(6801), 202–207. https://doi.org/10.1038/35025089

Bautista, S. J., Boras, I., Vissa, A., Mecica, N., Yip, C. M., Kim, P. K., & Antonescu, C. N. (2018). mTOR complex 1 controls the nuclear localization and function of glycogen synthase kinase 3β. *Journal of Biological Chemistry*, *293*, 14723–14739. https://doi.org/10.1074/jbc.RA118.002800

Bendas, G. (2001). Immunoliposomes: a promising approach to targeting cancer therapy. *BioDrugs*, *15*(4), 215–224. https://doi.org/10.2165/00063030-200115040-00002

Benlimame, N., Le, P. U., & Nabi, I. R. (1998). Localization of autocrine motility factor receptor to caveolae and clathrin-independent internalization of its ligand to smooth endoplasmic reticulum. *Molecular Biology of the Cell*, *9*(7), 1773–86. Retrieved from http://www.ncbi.nlm.nih.gov/pubmed/9658170

Berry, C. C., & Curtis, A. S. G. (2003). Functionalisation of magnetic nanoparticles for applications in biomedicine. *Journal of Physics D: Applied Physics*, *36*(13), R198–R206. https://doi.org/10.1088/0022-3727/36/13/203

Betters, J. L., & Yu, L. (2010). NPC1L1 and cholesterol transport. *FEBS Letters*, *584*(13), 2740–2747. https://doi.org/10.1016/j.febslet.2010.03.030

Bhagatji, P., Leventis, R., Comeau, J., Refaei, M., & Silvius, J. R. (2009). Steric and not structure-specific factors dictate the endocytic mechanism of glycosylphosphatidylinositol-

anchored proteins. *The Journal of Cell Biology*, *186*(4), 615–628. https://doi.org/10.1083/jcb.200903102

Bhatt, H., Naik, B., & Dharamsi, A. (2014). Solubility Enhancement of Budesonide and Statistical Optimization of Coating Variables for Targeted Drug Delivery. *Journal of Pharmaceutics*, *2014*, 262194. https://doi.org/10.1155/2014/262194

Bi, G. Q., Alderton, J. M., & Steinhardt, R. A. (1995). Calcium-regulated exocytosis is required for cell membrane resealing. *The Journal of Cell Biology*, *131*(6 Pt 2), 1747–58. Retrieved from http://www.ncbi.nlm.nih.gov/pubmed/8557742

Bionda, C., Hadchity, E., Alphonse, G., Chapet, O., Rousson, R., Rodriguez-Lafrasse, C., & Ardail, D. (2007). Radioresistance of human carcinoma cells is correlated to a defect in raft membrane clustering. *Free Radical Biology and Medicine*, *43*(5), 681–694. https://doi.org/10.1016/j.freeradbiomed.2007.04.031

Blazek, A. D., Paleo, B. J., & Weisleder, N. (2015). Plasma Membrane Repair: A Central Process for Maintaining Cellular Homeostasis. *Physiology*, *30*(6), 438–448. https://doi.org/10.1152/physiol.00019.2015

Blomley, M. J., Cooke, J. C., Unger, E. C., Monaghan, M. J., & Cosgrove, D. O. (2001). Microbubble contrast agents: a new era in ultrasound. *BMJ (Clinical Research Ed.)*, *322*(7296), 1222–5. Retrieved from http://www.ncbi.nlm.nih.gov/pubmed/11358777

Boissenot, T., Bordat, A., Fattal, E., & Tsapis, N. (2016). Ultrasound-triggered drug delivery for cancer treatment using drug delivery systems: From theoretical considerations to practical applications. *Journal of Controlled Release*, *241*, 144–163. https://doi.org/10.1016/j.jconrel.2016.09.026

Bolte, S., & Cordelières, F. P. (2006). A guided tour into subcellular colocalization analysis in

light microscopy. *Journal of Microscopy*, *224*(Pt 3), 213–32. https://doi.org/10.1111/j.1365-2818.2006.01706.x

Bone, L. N., Dayam, R. M., Lee, M., Kono, N., Fairn, G. D., Arai, H., … Antonescu, C. N. (2017). The acyltransferase LYCAT controls specific phosphoinositides and related membrane traffic. *Molecular Biology of the Cell*, *28*(1), 161–172.

Borden, M. A., Caskey, C. F., Little, E., Gillies, R. J., & Ferrara, K. W. (2007). DNA and Polylysine Adsorption and Multilayer Construction onto Cationic Lipid-Coated Microbubbles. *Langmuir*, *23*(18), 9401–9408. https://doi.org/10.1021/la7009034

Botos, E., Turi, Á., Müllner, N., Kovalszky, I., Tátrai, P., & Kiss, A. L. (2007). Regulatory role of kinases and phosphatases on the internalisation of caveolae in HepG2 cells. *Micron*, *38*(3), 313–320. https://doi.org/10.1016/j.micron.2006.03.012

Boucrot, E., Ferreira, A. P. A., Almeida-Souza, L., Debard, S., Vallis, Y., Howard, G., … McMahon, H. T. (2015). Endophilin marks and controls a clathrin-independent endocytic pathway. *Nature*, *517*(7535), 460–465. https://doi.org/10.1038/nature14067

Braide, M., Rasmussen, H., Albrektsson, A., & Bagge, U. (2006). Microvascular Behavior and Effects of Sonazoid Microbubbles in the Cremaster Muscle of Rats After. *Ultrasound*, 883–890.

Brigidi, G. S., Santyr, B., Shimell, J., Jovellar, B., & Bamji, S. X. (2015). Activity-regulated trafficking of the palmitoyl-acyl. *Nature Communications*, *6*, 1–17. https://doi.org/10.1038/ncomms9200

Briston, T., Roberts, M., Lewis, S., Powney, B., M. Staddon, J., Szabadkai, G., & Duchen, M. R. (2017). Mitochondrial permeability transition pore: sensitivity to opening and mechanistic dependence on substrate availability. *Scientific Reports*, *7*(1), 10492.

https://doi.org/10.1038/s41598-017-10673-8

Bryan-Lluka, L. J., Bönisch, H., & Lewis, R. J. (2003). χ-Conopeptide MrIA Partially Overlaps Desipramine and Cocaine Binding Sites on the Human Norepinephrine Transporter. *Journal of Biological Chemistry*, *278*(41), 40324–40329. https://doi.org/10.1074/jbc.M213101200

Cai, C., Weisleder, N., Ko, J.-K., Komazaki, S., Sunada, Y., Nishi, M., … Ma, J. (2009). Membrane Repair Defects in Muscular Dystrophy Are Linked to Altered Interaction between MG53, Caveolin-3, and Dysferlin. *Journal of Biological Chemistry*, *284*(23), 15894–15902. https://doi.org/10.1074/jbc.M109.009589

Campbell, J. E., & Cohall, D. (2017). Pharmacodynamics—A Pharmacognosy Perspective. In S. Badal & R. Delgoda (Eds.), *Pharmacognosy Fundamentals, Applications and Strategies* (pp. 513–525). London: Academic Press. https://doi.org/10.1016/B978-0-12-802104-0.00026-3

Carafoli, E., & Krebs, J. (2016). Why Calcium? How Calcium Became the Best Communicator. *The Journal of Biological Chemistry*, *291*(40), 20849–20857. https://doi.org/10.1074/jbc.R116.735894

Cerella, C., Diederich, M., & Ghibelli, L. (2010). The dual role of calcium as messenger and stressor in cell damage, death, and survival. *International Journal of Cell Biology*, *2010*, 546163. https://doi.org/10.1155/2010/546163

Cerny, J., Feng, Y., Yu, A., Miyake, K., Borgonovo, B., Klumperman, J., … Kirchhausen, T. (2004). The small chemical vacuolin-1 inhibits Ca(2+)-dependent lysosomal exocytosis but not cell resealing. *EMBO Reports*, *5*(9), 883–8. https://doi.org/10.1038/sj.embor.7400243

Chadda, R., Howes, M. T., Plowman, S. J., Hancock, J. F., Parton, R. G., & Mayor, S. (2007). Cholesterol-Sensitive Cdc42 Activation Regulates Actin Polymerization for Endocytosis via

the GEEC Pathway. *Traffic*, *8*(6), 702–717. https://doi.org/10.1111/j.1600-0854.2007.00565.x

Chalfant, C. E., Szulc, Z., Roddy, P., Bielawska, A., & Hannun, Y. A. (2004). The structural requirements for ceramide activation of serine-threonine protein phosphatases. *Journal of Lipid Research*, *45*(3), 496–506. https://doi.org/10.1194/jlr.M300347-JLR200

Chambers, R., & Chambers, E. L. (1961). The Dynamics of Living Protoplasm. *Journal of Medical Education*, *36*(8), 966. https://doi.org/10.1097/ACM.0000000000001197

Chapman, E. R. (2002). SYNAPTOTAGMIN: A Ca 2+ SENSOR THAT TRIGGERS EXOCYTOSIS? *NATURE REVIEWS | MOLECULAR CELL BIOLOGY*, *3*. https://doi.org/10.1038/nrm855

Charollais, J., & Van Der Goot, F. G. (2009). Palmitoylation of membrane proteins (Review). *Molecular Membrane Biology*, *26*(1–2), 55–66. https://doi.org/10.1080/09687680802620369

Charruyer, A., Grazide, S., Bezombes, C., Müller, S., Laurent, G., & Jaffrézou, J.-P. (2005). UV-C Light Induces Raft-associated Acid Sphingomyelinase and JNK Activation and Translocation Independently on a Nuclear Signal. *Journal of Biological Chemistry*, *280*(19), 19196–19204. https://doi.org/10.1074/jbc.M412867200

Chaudhary, N., Gomez, G. A., Howes, M. T., Lo, H. P., McMahon, K.-A., Rae, J. A., … Parton, R. G. (2014). Endocytic Crosstalk: Cavins, Caveolins, and Caveolae Regulate Clathrin-Independent Endocytosis. *PLoS Biology*, *12*(4), e1001832. https://doi.org/10.1371/journal.pbio.1001832

Chavez, K. J., Garimella, S. V, & Lipkowitz, S. (2010). Triple negative breast cancer cell lines: one tool in the search for better treatment of triple negative breast cancer. *Breast Disease*,

32(1–2), 35–48. https://doi.org/10.3233/BD-2010-0307

Chen, C. A., & Manning, D. R. (2001). Regulation of G proteins by covalent modification. *Oncogene*, *20*(13), 1643–1652. https://doi.org/10.1038/sj.onc.1204185

Chen, C., & Jonas, P. (2017). Synaptotagmins: That's Why So Many. *Neuron*, *94*(4), 694–696. https://doi.org/10.1016/j.neuron.2017.05.011

Chen, W. J., Goldstein, J. L., & Brown, M. S. (1990). NPXY, a sequence often found in cytoplasmic tails, is required for coated pit-mediated internalization of the low density lipoprotein receptor. *The Journal of Biological Chemistry*, *265*(6), 3116–23. Retrieved from http://www.ncbi.nlm.nih.gov/pubmed/1968060

Chen, X., Wan, J. M. F., & Yu, A. C. H. (2013). Sonoporation as a Cellular Stress: Induction of Morphological Repression and Developmental Delays. *Ultrasound in Medicine & Biology*, *39*(6), 1075–1086. https://doi.org/10.1016/j.ultrasmedbio.2013.01.008

Cheng, S. C., Dy, T. C., & Feinstein, S. B. (1998). Contrast echocardiography: review and future directions. *The American Journal of Cardiology*, *81*(12A), 41G–48G. Retrieved from http://www.ncbi.nlm.nih.gov/pubmed/9662227

Chomas, J. E., Dayton, P., May, D., & Ferrara, K. (2001). Threshold of fragmentation for ultrasonic contrast agents. *Journal of Biomedical Optics*, *6*(2), 141. https://doi.org/10.1117/1.1352752

Chow, S.-C. (2014). Bioavailability and Bioequivalence in Drug Development. *Wiley Interdisciplinary Reviews. Computational Statistics*, *6*(4), 304–312. https://doi.org/10.1002/wics.1310

Choy, E., Chiu, V. K., Silletti, J., Feoktistov, M., Morimoto, T., Michaelson, D., … Philips, M. R. (1999). Endomembrane trafficking of ras: the CAAX motif targets proteins to the ER and

Golgi. *Cell*, *98*, 69–80. Retrieved from http://ac.els-cdn.com/S0092867400806078/1-s2.0-S0092867400806078-main.pdf?_tid=306fc48a-3a4d-11e7-a9e6-00000aab0f26&acdnat=1494949065_213473ab27fa93daaea216da04e8fbfe

Chrai, S. S., Murari, M. R., & Ahmad, I. (2002). *Liposomes (a Review) Part Two: Drug Delivery Systems*. Retrieved from www.delsyspharma.com.

Chu, B. B., Ge, L., Xie, C., Zhao, Y., Miao, H. H., Wang, J., … Song, B. L. (2009). Requirement of myosin Vb·Rab11a·Rab11-FIP2 complex in cholesterol-regulated translocation of NPC1L1 to the cell surface. *Journal of Biological Chemistry*, *284*(33), 22481–22490. https://doi.org/10.1074/jbc.M109.034355

Chung, J.-J., Huber, T. B., Gödel, M., Jarad, G., Hartleben, B., Kwoh, C., … Shaw, A. S. (2015). Albumin-associated free fatty acids induce macropinocytosis in podocytes. *Journal of Clinical Investigation*, *125*(6), 2307–2316. https://doi.org/10.1172/JCI79641

Clarke, S. J., Khaliulin, I., Das, M., Parker, J. E., Heesom, K. J., & Halestrap, A. P. (2008). Inhibition of mitochondrial permeability transition pore opening by ischemic preconditioning is probably mediated by reduction of oxidative stress rather than mitochondrial protein phosphorylation. *Circulation Research*, *102*(9), 1082–90. https://doi.org/10.1161/CIRCRESAHA.107.167072

Cleland, J. L., Powell, M. F., & Shire, S. J. (1993). The development of stable protein formulations: a close look at protein aggregation, deamidation, and oxidation. *Critical Reviews in Therapeutic Drug Carrier Systems*, *10*(4), 307–77. Retrieved from http://www.ncbi.nlm.nih.gov/pubmed/8124728

Clingen, P. H., Wu, J. Y., Miller, J., Mistry, N., Chin, F., Wynne, P., … Hartley, J. A. (2008). Histone H2AX phosphorylation as a molecular pharmacological marker for DNA

interstrand crosslink cancer chemotherapy. *Biochemical Pharmacology*, *76*, 19–27. https://doi.org/10.1016/j.bcp.2008.03.025

Cochran, S. (2012). Piezoelectricity and basic configurations for piezoelectric ultrasonic transducers. In K. Nakamura (Ed.), *Ultrasonic Transducers* (pp. 3–35). Cambridge: Woodhead Publishing. https://doi.org/10.1533/9780857096302.1.3

Cocucci, E., Aguet, F., Boulant, S., & Kirchhausen, T. (2012). The First Five Seconds in the Life of a Clathrin-Coated Pit. *Cell*, *150*(3), 495–507. https://doi.org/10.1016/j.cell.2012.05.047

Cole, A. J., Yang, V. C., & David, A. E. (2011). Cancer theranostics: the rise of targeted magnetic nanoparticles. *Trends in Biotechnology*, *29*(7), 323–32. https://doi.org/10.1016/j.tibtech.2011.03.001

Collis, J., Manasseh, R., Liovic, P., Tho, P., Ooi, A., Petkovic-Duran, K., & Zhu, Y. (2010). Cavitation microstreaming and stress fields created by microbubbles. *Ultrasonics*, *50*(2), 273–279. https://doi.org/10.1016/j.ultras.2009.10.002

Conibear, E., & Davis, N. G. (2010). Palmitoylation and depalmitoylation dynamics at a glance. *Journal of Cell Science*, *123*(23), 4007–4010. https://doi.org/10.1242/jcs.059287

Conner, S. D., & Schmid, S. L. (2003). Regulated portals of entry into the cell. *Nature*, *422*(6927), 37–44.

Correas, J. M., Bridal, L., Lesavre, A., Méjean, A., Claudon, M., & Hélénon, O. (2001). Ultrasound contrast agents: Properties, principles of action, tolerance, and artifacts. *European Radiology*, *11*(8), 1316–1328. https://doi.org/10.1007/s003300100940

Corrotte, M., Almeida, P. E., Tam, C., Castro-Gomes, T., Fernandes, M. C., Millis, B. A., … Andrews, N. W. (2013). Caveolae internalization repairs wounded cells and muscle fibers. *ELife*, *2*, e00926. https://doi.org/10.7554/eLife.00926

Cousin, M. A. (2000). Synaptic Vesicle Endocytosis. *Molecular Neurobiology*, *22*(1–3), 115–128. https://doi.org/10.1385/MN:22:1-3:115

Cremona, M. L., Matthies, H. J. G., Pau, K., Bowton, E., Speed, N., Lute, B. J., … Yamamoto, A. (2011). Flotillin-1 is essential for PKC-triggered endocytosis and membrane microdomain localization of DAT. *Nature Neuroscience*, *14*(4), 469–477. https://doi.org/10.1038/nn.2781

Cremona, O., Di Paolo, G., Wenk, M. R., Lüthi, A., Kim, W. T., Takei, K., … De Camilli, P. (1999). Essential role of phosphoinositide metabolism in synaptic vesicle recycling. *Cell*, *99*(2), 179–88. Retrieved from http://www.ncbi.nlm.nih.gov/pubmed/10535736

Cullis, Chonn, & Semple. (1998). Interactions of liposomes and lipid-based carrier systems with blood proteins: Relation to clearance behaviour in vivo. *Advanced Drug Delivery Reviews*, *32*(1–2), 3–17. Retrieved from http://www.ncbi.nlm.nih.gov/pubmed/10837632

D'Souza-Schorey, C., Li, G., Colombo, M. I., & Stahl, P. D. (1995). A regulatory role for ARF6 in receptor-mediated endocytosis. *Science (New York, N.Y.)*, *267*(5201), 1175–8. Retrieved from http://www.ncbi.nlm.nih.gov/pubmed/7855600

Da Costa, S. R., Sou, E., Xie, J., Yarber, F. A., Okamoto, C. T., Pidgeon, M., … Hamm-Alvarez, S. F. (2003). Impairing actin filament or syndapin functions promotes accumulation of clathrin-coated vesicles at the apical plasma membrane of acinar epithelial cells. *Molecular Biology of the Cell*, *14*(11), 4397–413. https://doi.org/10.1091/mbc.e03-05-0315

Dalecki, D. (2005). Biological Effects of Microbubble-Based Ultrasound Contrast Agents BT - Contrast Media in Ultrasonography: Basic Principles and Clinical Applications. In E. Quaia (Ed.) (pp. 77–85). Berlin, Heidelberg: Springer Berlin Heidelberg. https://doi.org/10.1007/3-540-27214-3_6

Dams, E. T., Laverman, P., Oyen, W. J., Storm, G., Scherphof, G. L., van Der Meer, J. W., … Boerman, O. C. (2000). Accelerated blood clearance and altered biodistribution of repeated injections of sterically stabilized liposomes. *The Journal of Pharmacology and Experimental Therapeutics*, *292*(3), 1071–9. Retrieved from http://www.ncbi.nlm.nih.gov/pubmed/10688625

Daumke, O., Roux, A., & Haucke, V. (2014). BAR Domain Scaffolds in Dynamin-Mediated Membrane Fission. *Cell*, *156*(5), 882–892. https://doi.org/10.1016/j.cell.2014.02.017

Davies, P. F., & Ross, R. (1978). Mediation of pinocytosis in cultured arterial smooth muscle and endothelial cells by platelet-derived growth factor. *The Journal of Cell Biology*, *79*(3), 663–71. Retrieved from http://www.ncbi.nlm.nih.gov/pubmed/103882

Davis, P. J., Cladis, F. P., Motoyama, E. K., Davis, P. J., Bosenberg, A., Davidson, A., … Woelfel, S. (2011). Pharmacology of Pediatric Anesthesia. In P. J. Davis & F. P. Cladis (Eds.), *Smith's Anesthesia for Infants and Children* (8th ed., pp. 179–261). Philadelphia: Elsevier. https://doi.org/10.1016/B978-0-323-06612-9.00007-9

De Cock, I., Zagato, E., Braeckmans, K., Luan, Y., de Jong, N., De Smedt, S. C., & Lentacker, I. (2015). Ultrasound and microbubble mediated drug delivery: acoustic pressure as determinant for uptake via membrane pores or endocytosis. *Journal of Controlled Release : Official Journal of the Controlled Release Society*, *197*, 20–8. https://doi.org/10.1016/j.jconrel.2014.10.031

de Curtis, I., & Meldolesi, J. (2012). Cell surface dynamics - how Rho GTPases orchestrate the interplay between the plasma membrane and the cortical cytoskeleton. *Journal of Cell Science*, *125*(19), 4435–4444. https://doi.org/10.1242/jcs.108266

de Jong, N., Bouakaz, A., & Frinking, P. (2002). Basic acoustic properties of microbubbles.

Echocardiography (Mount Kisco, N.Y.), *19*(3), 229–40. https://doi.org/10.1046/j.1540-8175.2002.00229.x

de Jong, N., Emmer, M., van Wamel, A., & Versluis, M. (2009). Ultrasonic characterization of ultrasound contrast agents. *Medical & Biological Engineering & Computing*, *47*(8), 861–873. https://doi.org/10.1007/s11517-009-0497-1

Dear, J. P., Field, J. E., & Walton, A. J. (1988). Gas compression and jet formation in cavities collapsed by a shock wave. *Nature*, *332*(6164), 505–508. https://doi.org/10.1038/332505a0

Decato, S., & Mecozzi, S. (2014). Highly fluorinated colloids in drug delivery and imaging. In H. Ohshima & K. Makino (Eds.), *Colloid and Interface Science in Pharmaceutical Research and Development* (pp. 319–345). Elsevier. https://doi.org/10.1016/B978-0-444-62614-1.00016-8

Defour, A., Van der Meulen, J. H., Bhat, R., Bigot, A., Bashir, R., Nagaraju, K., & Jaiswal, J. K. (2014). Dysferlin regulates cell membrane repair by facilitating injury-triggered acid sphingomyelinase secretion. *Cell Death & Disease*, *5*(6), e1306–e1306. https://doi.org/10.1038/cddis.2014.272

Delos Santos, R., Bautista, S., Bone, L., Lucarelli, S., Dayam, R., Botelho, R., & Antonescu, C. (2017). Selective control of clathrin- mediated endocytosis and clathrin-dependent signaling by phospholipase C and Ca2+ signals. *Molecular Biology of the Cell*, *28*, 2802–2818.

Deng, C. X., Sieling, F., Pan, H., & Cui, J. (2004). Ultrasound-induced cell membrane porosity. *Ultrasound in Medicine & Biology*, *30*(4), 519–526. https://doi.org/10.1016/j.ultrasmedbio.2004.01.005

Deschenes, R. J. (2013). Protein Palmitoylation. *Encyclopedia of Biological Chemistry: Second Edition*, *40*(2), 645–647. https://doi.org/10.1016/B978-0-12-378630-2.00022-0

Deshpande, N., Ren, Y., Foygel, K., Rosenberg, J., & Willmann, J. K. (2011). Tumor Angiogenic Marker Expression Levels during Tumor Growth: Longitudinal Assessment with Molecularly Targeted Microbubbles and US Imaging. *Radiology*, *258*(3), 804–811. https://doi.org/10.1148/radiol.10101079

Dobrowsky, R. T., & Hannun, Y. A. (1993). Ceramide-activated protein phosphatase: partial purification and relationship to protein phosphatase 2A. *Advances in Lipid Research*, *25*, 91–104. Retrieved from http://www.ncbi.nlm.nih.gov/pubmed/8396314

Donaldson, J., Porat-Shliom, N., & Cohen, L. (2009). Clathrin-independent endocytosis: A unique platform for cell signaling and PM remodeling. *Cellular Signalling*, *21*(1), 1–6. https://doi.org/10.1016/j.cellsig.2008.06.020

Doodnauth, S. A., Grinstein, S., & Maxson, M. E. (2019). Constitutive and stimulated macropinocytosis in macrophages: roles in immunity and in the pathogenesis of atherosclerosis. *Philosophical Transactions of the Royal Society B: Biological Sciences*, *374*(1765), 20180147. https://doi.org/10.1098/rstb.2018.0147

Draeger, A., Monastyrskaya, K., & Babiychuk, E. B. (2011). Plasma membrane repair and cellular damage control: The annexin survival kit. *Biochemical Pharmacology*, *81*(6), 703–712. https://doi.org/10.1016/j.bcp.2010.12.027

Draznin, B. (1988). Intracellular calcium, insulin secretion, and action. *The American Journal of Medicine*, *85*(5A), 44–58. Retrieved from http://www.ncbi.nlm.nih.gov/pubmed/3057895

Drisdel, R. C., & Green, W. N. (2004). Labeling and quantifying sites of protein palmitoylation. *BioTechniques*, *36*(2), 276–285. https://doi.org/10.2144/04362RR02

Du Toit, A. (2015). A new gateway into cells. *Nature Reviews Molecular Cell Biology*, *16*(2), 68–68. https://doi.org/10.1038/nrm3939

Du, W., & Klibanov, A. M. (2011). Hydrophobic salts markedly diminish viscosity of concentrated protein solutions. *Biotechnology and Bioengineering*, *108*(3), 632–636. https://doi.org/10.1002/bit.22983

Durrbach, A., Louvard, D., & Coudrier, E. (1996). Actin filaments facilitate two steps of endocytosis, *465*, 457–465.

Echarri, A., & Del Pozo, M. A. (2015). Caveolae - mechanosensitive membrane invaginations linked to actin filaments. *Journal of Cell Science*, *128*(15), 2747–58. https://doi.org/10.1242/jcs.153940

Edeling, M. A., Smith, C., & Owen, D. (2006). Life of a clathrin coat: insights from clathrin and AP structures. *Nature Reviews Molecular Cell Biology*, *7*(1), 32–44. https://doi.org/10.1038/nrm1786

Eisenberg, S., Laude, A. J., Beckett, A. J., Mageean, C. J., Aran, V., Hernandez-Valladares, M., … Prior, I. A. (2013). The role of palmitoylation in regulating Ras localization and function. *Biochemical Society Transactions*, *41*(1), 79–83. https://doi.org/10.1042/BST20120268

Elkin, S. R., Lakoduk, A. M., & Schmid, S. L. (2016). Endocytic pathways and endosomal trafficking: a primer. *Wiener Medizinische Wochenschrift (1946)*, *166*(7–8), 196–204. https://doi.org/10.1007/s10354-016-0432-7

Ellens, N. P. K., & Hynynen, K. (2015). High-intensity focused ultrasound for medical therapy. In J. A. Gallego-Juárez & K. F. Graff (Eds.), *Power Ultrasonics* (pp. 661–693). Cambridge: Woodhead Publishing. https://doi.org/10.1016/B978-1-78242-028-6.00022-3

Fairn, G. D., Schieber, N. L., Ariotti, N., Murphy, S., Kuerschner, L., Webb, R. I., … Parton, R. G. (2011). High-resolution mapping reveals topologically distinct cellular pools of

phosphatidylserine. *The Journal of Cell Biology*, *194*(2), 257–275. https://doi.org/10.1083/jcb.201012028

Fallin, M. D., Lasseter, V. K., Wolyniec, P. S., McGrath, J. A., Nestadt, G., Valle, D., … Pulver, A. E. (2004). Genomewide linkage scan for bipolar-disorder susceptibility loci among Ashkenazi Jewish families. *Am J Hum Genet*, *75*(2), 204–219. https://doi.org/10.1086/422474

Fan, Z., Chen, D., & Deng, C. X. (2014). Characterization of the dynamic activities of a population of microbubbles driven by pulsed ultrasound exposures in sonoporation. *Journal of Ultrasound in Medicine Impact Factor*, *40*(6), 1260–1272. https://doi.org/10.1007/s11103-011-9767-z.Plastid

Fan, Z., Kumon, R. E., Park, J., & Deng, C. X. (2010a). Intracellular delivery and calcium transients generated in sonoporation facilitated by microbubbles. *Journal of Controlled Release : Official Journal of the Controlled Release Society*, *142*(1), 31–9. https://doi.org/10.1016/j.jconrel.2009.09.031

Fan, Z., Liu, H., Mayer, M., & Deng, C. X. (2012). Spatiotemporally controlled single cell sonoporation. *Proceedings of the National Academy of Sciences of the United States of America*, *109*(41), 16486–91. https://doi.org/10.1073/pnas.1208198109

Fang, J., Nakamura, H., & Maeda, H. (2011). The EPR effect : Unique features of tumor blood vessels for drug delivery , factors involved , and limitations and augmentation of the effect. *Advanced Drug Delivery Reviews*, *63*(3), 136–151. https://doi.org/10.1016/j.addr.2010.04.009

Fekri, F., Delos Santos, R., Karshafian, R., & Antonescu, C. (2016). Ultrasound microbubble treatment enhances clathrin-mediated endocytosis and fluid-phase uptake through distinct

mechanisms. *PLoS ONE*, *11*(6), e0156754.

Ferreira, A. P. A., & Boucrot, E. (2018). Mechanisms of Carrier Formation during Clathrin-Independent Endocytosis. *Trends in Cell Biology*, *28*(3), 188–200. https://doi.org/10.1016/j.tcb.2017.11.004

Forbes, M. M., Steinberg, R. L., O'Brien, W. D., & Jr. (2008). Examination of inertial cavitation of Optison in producing sonoporation of chinese hamster ovary cells. *Ultrasound in Medicine & Biology*, *34*(12), 2009–18. https://doi.org/10.1016/j.ultrasmedbio.2008.05.003

Ford, M. G. J., Mills, I. G., Peter, B. J., Vallis, Y., Praefcke, G. J. K., Evans, P. R., & McMahon, H. T. (2002). Curvature of clathrin-coated pits driven by epsin. *Nature*, *419*(6905), 361–366. https://doi.org/10.1038/nature01020

Forrester, J. V., Dick, A. D., McMenamin, P. G., Roberts, F., Pearlman, E., Forrester, J. V., … Pearlman, E. (2016). General and ocular pharmacology. In *The Eye: Basic Science in Practice* (4th ed., pp. 338–369). W.B. Saunders. https://doi.org/10.1016/B978-0-7020-5554-6.00006-X

Fotin, A., Cheng, Y., Sliz, P., Grigorieff, N., Harrison, S. C., Kirchhausen, T., & Walz, T. (2004). Molecular model for a complete clathrin lattice from electron cryomicroscopy. *Nature*, *432*(7017), 573–579. https://doi.org/10.1038/nature03079

Frick, M., Bright, N. A., Riento, K., Bray, A., Merrified, C., & Nichols, B. J. (2007). Coassembly of Flotillins Induces Formation of Membrane Microdomains, Membrane Curvature, and Vesicle Budding. *Current Biology*, *17*(13), 1151–1156. https://doi.org/10.1016/j.cub.2007.05.078

Fritz, T. A., Unger, E. C., Sutherland, G., & Sahn, D. (1997). Phase I clinical trials of MRX-115. A new ultrasound contrast agent. *Investigative Radiology*, *32*(12), 735–40. Retrieved from

http://www.ncbi.nlm.nih.gov/pubmed/9406013

Fujii, M., Kawai, K., Egami, Y., & Araki, N. (2013). Dissecting the roles of Rac1 activation and deactivation in macropinocytosis using microscopic photo-manipulation. *Scientific Reports*, *3*(1), 2385. https://doi.org/10.1038/srep02385

Fujimoto, L. M., Roth, R., Heuser, J. E., & Schmid, S. L. (2000). Actin Assembly Plays a Variable , but not Obligatory Role in Receptor-Mediated Endocytosis in Mammalian, (6), 161–171.

Fukata, Y., & Fukata, M. (2010). Protein palmitoylation in neuronal development and synaptic plasticity. *Nature Reviews Neuroscience*, *11*(3), 161–175. https://doi.org/10.1038/nrn2788

Garay, C., Judge, G., Lucarelli, S., Bautista, S., Pandey, R., Singh, T., & Antonescu, C. N. (2015). Epidermal growth factor-stimulated Akt phosphorylation requires clathrin or ErbB2 but not receptor endocytosis. *Molecular Biology of the Cell*, *26*, 3504–19. https://doi.org/10.1091/mbc.E14-09-1412

Garay, C., Judge, G., Lucarelli, S., Bautista, S., Pandey, R., Singh, T., & Antonescu, C. N. (2015). Epidermal growth factor-stimulated Akt phosphorylation requires clathrin or ErbB2 but not receptor endocytosis. *Molecular Biology of the Cell*, *26*(19). https://doi.org/10.1091/mbc.E14-09-1412

García-Cardeña, G., Oh, P., Liu, J., Schnitzer, J. E., & Sessa, W. C. (1996). Targeting of nitric oxide synthase to endothelial cell caveolae via palmitoylation: implications for nitric oxide signaling. *Proceedings of the National Academy of Sciences of the United States of America*, *93*(13), 6448–53. Retrieved from http://www.ncbi.nlm.nih.gov/pubmed/8692835

Garred, Ø., Rodal, S. K., van Deurs, B., & Sandvig, K. (2001). Reconstitution of clathrin-independent endocytosis at the apical domain of permeabilized MDCK II cells: requirement

for a Rho-family GTPase. *Traffic (Copenhagen, Denmark)*, *2*(1), 26–36. Retrieved from http://www.ncbi.nlm.nih.gov/pubmed/11208166

Ge, L., Qi, W., Wang, L.-J., Miao, H.-H., Qu, Y.-X., Li, B.-L., & Song, B.-L. (2011). Flotillins play an essential role in Niemann-Pick C1-like 1-mediated cholesterol uptake. *Proceedings of the National Academy of Sciences*, *108*(2), 551–556. https://doi.org/10.1073/pnas.1014434108

Ge, L., Qi, W., Wang, L.-J., Miao, H.-H., Qu, Y.-X., Li, B.-L., & Song, B.-L. (2011). Flotillins play an essential role in Niemann-Pick C1-like 1-mediated cholesterol uptake. *Proceedings of the National Academy of Sciences*, *108*(2), 551–556. https://doi.org/10.1073/pnas.1014434108

Ge, L., Wang, J., Qi, W., Miao, H.-H., Cao, J., Qu, Y.-X., … Song, B.-L. (2008). The Cholesterol Absorption Inhibitor Ezetimibe Acts by Blocking the Sterol-Induced Internalization of NPC1L1. *Cell Metabolism*, *7*(6), 508–519. https://doi.org/10.1016/j.cmet.2008.04.001

Glebov, O. O., Bright, N. A., & Nichols, B. J. (2006). Flotillin-1 defines a clathrin-independent endocytic pathway in mammalian cells. *Nature Cell Biology*, *8*(1), 46–54. https://doi.org/10.1038/ncb1342

Glenney, J. R., & Zokas, L. (1989). Novel tyrosine kinase substrates from Rous sarcoma virus-transformed cells are present in the membrane skeleton. *The Journal of Cell Biology*, *108*(6), 2401–8. https://doi.org/10.1083/JCB.108.6.2401

Goddard, A. D., & Watts, A. (2012). Regulation of G protein-coupled receptors by palmitoylation and cholesterol. *BMC Biology*, *10*, 2–4. https://doi.org/10.1186/1741-7007-10-27

Goldstein, J. L., Anderson, R. G. W., & Brown, M. S. (1979). Coated pits, coated vesicles, and receptor-mediated endocytosis. *Nature*, *279*(5715), 679–685. https://doi.org/10.1038/279679a0

Goñi, F. M., & Alonso, A. (2002). Sphingomyelinases: enzymology and membrane activity. *FEBS Letters*, *531*(1), 38–46. Retrieved from http://www.ncbi.nlm.nih.gov/pubmed/12401200

Gramiak, R., & Shah, P. M. (1968). Echocardiography of the aortic root. *Investigative Radiology*, *3*(5), 356–66. Retrieved from http://www.ncbi.nlm.nih.gov/pubmed/5688346

Grant, B. D., & Donaldson, J. G. (2009). Pathways and mechanisms of endocytotic recycling. *Molecular Cell Biology*, *10*(9), 597–604. https://doi.org/10.1038/nrm2755.Pathways

Grant, P. O., & Benjamin, J. N. (2011). The roles of flotillin microdomains - endocytosis and beyond. *Journal of Cell Science*, *124*(23), 3933–3940. https://doi.org/10.1242/jcs.092015

Grassart, A., Dujeancourt, A., Lazarow, P. B., Dautry-Varsat, A., & Sauvonnet, N. (2008). Clathrin-independent endocytosis used by the IL-2 receptor is regulated by Rac1, Pak1 and Pak2. *EMBO Reports*, *9*(4), 356–62. https://doi.org/10.1038/embor.2008.28

Grassmé, H., Jekle, A., Riehle, A., Schwarz, H., Berger, J., Sandhoff, K., … Gulbins, E. (2001). CD95 Signaling via Ceramide-rich Membrane Rafts. *Journal of Biological Chemistry*, *276*(23), 20589–20596. https://doi.org/10.1074/jbc.M101207200

Grassmé, H., Jendrossek, V., Bock, J., Riehle, A., & Gulbins, E. (2002). Ceramide-rich membrane rafts mediate CD40 clustering. *Journal of Immunology (Baltimore, Md. : 1950)*, *168*(1), 298–307. Retrieved from http://www.ncbi.nlm.nih.gov/pubmed/11751974

Grassmé, H., Riethmüller, J., & Gulbins, E. (2007). Biological aspects of ceramide-enriched membrane domains. *Progress in Lipid Research*, *46*(3–4), 161–170.

https://doi.org/10.1016/j.plipres.2007.03.002

Greaves, J., Gorleku, O. A., Salaun, C., & Chamberlain, L. H. (2010). Palmitoylation of the SNAP25 protein family: Specificity and regulation by DHHC palmitoyl transferases. *Journal of Biological Chemistry*, *285*(32), 24629–24638. https://doi.org/10.1074/jbc.M110.119289

Greaves, J., Prescott, G. R., Fukata, Y., Fukata, M., Salaun, C., & Chamberlain, L. H. (2009). The Hydrophobic Cysteine-rich Domain of SNAP25 Couples with Downstream Residues to Mediate Membrane Interactions and Recognition by DHHC Palmitoyl Transferases. *Molecular Biology of the Cell*, *20*(6), 1845–1854. https://doi.org/10.1091/mbc.e08-09-0944

Gref, R., Minamitake, Y., Peracchia, M. T., Trubetskoy, V., Torchilin, V., & Langer, R. (1994). Biodegradable long-circulating polymeric nanospheres. *Science (New York, N.Y.)*, *263*(5153), 1600–3. Retrieved from http://www.ncbi.nlm.nih.gov/pubmed/8128245

Grewal, T., Heeren, J., Mewawala, D., Schnitgerhans, T., Wendt, D., Salomon, G., … Jäckle, S. (2000). Annexin VI Stimulates Endocytosis and Is Involved in the Trafficking of Low Density Lipoprotein to the Prelysosomal Compartment. *Journal of Biological Chemistry*, *275*(43), 33806–33813. https://doi.org/10.1074/jbc.M002662200

Gubar, O., Morderer, D., Tsyba, L., Croisé, P., Houy, S., Ory, S., … Rynditch, A. (2013). Intersectin : the crossroad between vesicle exocytosis and endocytosis, *4*(August), 1–5. https://doi.org/10.3389/fendo.2013.00109

Gupta, G. D., Swetha, M. G., Kumari, S., Lakshminarayan, R., Dey, G., & Mayor, S. (2009). Analysis of endocytic pathways in Drosophila cells reveals a conserved role for GBF1 in internalization via GEECs. *PLoS ONE*, *4*(8). https://doi.org/10.1371/journal.pone.0006768

Guterres, S. S., Alves, M. P., & Pohlmann, A. R. (2007). Polymeric nanoparticles, nanospheres

and nanocapsules, for cutaneous applications. *Drug Target Insights*, *2*, 147–57. Retrieved from http://www.ncbi.nlm.nih.gov/pubmed/21901071

Hale, T., & Abbey, J. (2017). Drug Transfer During Breast-Feeding. In R. A. Polin, S. H. Abman, D. H. Rowitch, W. E. Benitz, & W. W. Fox (Eds.), *Fetal and Neonatal Physiology* (5th ed., p. 239–248.e5). Elsevier. https://doi.org/10.1016/B978-0-323-35214-7.00023-8

Hallow, D. M., Mahajan, A. D., McCutchen, T. E., & Prausnitz, M. R. (2006). Measurement and correlation of acoustic cavitation with cellular bioeffects. *Ultrasound in Medicine & Biology*, *32*(7), 1111–1122. https://doi.org/10.1016/j.ultrasmedbio.2006.03.008

Hamasaki, M., Araki, N., & Hatae, T. (2004). Association of early endosomal autoantigen 1 with macropinocytosis in EGF-stimulated a431 cells. *The Anatomical Record*, *277A*(2), 298–306. https://doi.org/10.1002/ar.a.20027

Hannun, Y. A. (1994). The sphingomyelin cycle and the second messenger function of ceramide. *The Journal of Biological Chemistry*, *269*(5), 3125–8. Retrieved from http://www.ncbi.nlm.nih.gov/pubmed/8106344

Hannun, Y. A., & Luberto, C. (2000). Ceramide in the eukaryotic stress response. *Trends in Cell Biology*, *10*(2), 73–80. Retrieved from http://www.ncbi.nlm.nih.gov/pubmed/10652518

Hansen, C. G., Howard, G., & Nichols, B. J. (2011). Pacsin 2 is recruited to caveolae and functions in caveolar biogenesis. *Journal of Cell Science*, *124*(16), 2777–2785. https://doi.org/10.1242/jcs.084319

Harvey, R. D., & Calaghan, S. C. (2012). Caveolae create local signalling domains through their distinct protein content, lipid profile and morphology. *Journal of Molecular and Cellular Cardiology*, *52*(2), 366–75. https://doi.org/10.1016/j.yjmcc.2011.07.007

Haucke, V., & Kozlov, M. M. (2018). Membrane remodeling in clathrin-mediated endocytosis.

Journal of Cell Science, *131*(17), jcs216812. https://doi.org/10.1242/jcs.216812

He, M., Abdi, K. M., & Bennett, V. (2014). Ankyrin-G palmitoylation and βII-spectrin binding to phosphoinositide lipids drive lateral membrane assembly. *Journal of Cell Biology*, *206*(2), 273–288. https://doi.org/10.1083/jcb.201401016

Hebert, M. F. (2013). Impact of Pregnancy on Maternal Pharmacokinetics of Medications. In *Clinical Pharmacology During Pregnancy* (pp. 17–39). Academic Press. https://doi.org/10.1016/B978-0-12-386007-1.00003-9

Heilbrunn, L. V. (1956). *The dynamics of living protoplasm.* Academic Press. Retrieved from https://books.google.ca/books/about/The_Dynamics_of_Living_Protoplasm.html?id=tMw3BQAAQBAJ&printsec=frontcover&source=kp_read_button&redir_esc=y#v=onepage&q&f=false

Heinrich, M., Wickel, M., Schneider-Brachert, W., Sandberg, C., Gahr, J., Schwandner, R., … Schütze, S. (1999). Cathepsin D targeted by acid sphingomyelinase-derived ceramide. *The EMBO Journal*, *18*(19), 5252–5263. https://doi.org/10.1093/emboj/18.19.5252

Henley, J. R., Krueger, E. W., Oswald, B. J., & McNiven, M. A. (2000). Dynamin-mediated internalization of caveolae. *The Journal of Cell Biology*, *22*(1), 115–128. Retrieved from http://www.ncbi.nlm.nih.gov/pubmed/9531550

Henne, W. M., Boucrot, E., Meinecke, M., Evergren, E., Vallis, Y., Mittal, R., & McMahon, H. T. (2010). FCHo Proteins Are Nucleators of Clathrin-Mediated Endocytosis. *Science*, *328*(5983), 1281–1284. https://doi.org/10.1126/science.1188462

Henne, W. M., Kent, H. M., Ford, M. G. J., Hegde, B. G., Daumke, O., Butler, P. J. G., … McMahon, H. T. (2007). Structure and Analysis of FCHo2 F-BAR Domain: A Dimerizing and Membrane Recruitment Module that Effects Membrane Curvature. *Structure*, *15*(7),

839–852. https://doi.org/10.1016/j.str.2007.05.002

Hernández-Deviez, D. J., Howes, M. T., Laval, S. H., Bushby, K., Hancock, J. F., & Parton, R. G. (2008). Caveolin regulates endocytosis of the muscle repair protein, dysferlin. *The Journal of Biological Chemistry*, *283*(10), 6476–88. https://doi.org/10.1074/jbc.M708776200

Hernot, S., & Klibanov, A. L. (2008). Microbubbles in ultrasound-triggered drug and gene delivery. *Advanced Drug Delivery Reviews*, *60*(10), 1153–1166. https://doi.org/10.1016/j.addr.2008.03.005

Hilgemann, D. W., Fine, M., Linder, M. E., Jennings, B. C., & Lin, M.-J. (2013). Massive endocytosis triggered by surface membrane palmitoylation under mitochondrial control in BHK fibroblasts. *ELife*, *2*, e01293. https://doi.org/10.7554/eLife.01293

Hilgenfeldt, S., Lohse, D., & Zomack, M. (2000). Sound scattering and localized heat deposition of pulse-driven microbubbles. *The Journal of the Acoustical Society of America*, *107*(6), 3530–9. https://doi.org/10.1121/1.429438

Hill, M. M., Bastiani, M., Luetterforst, R., Kirkham, M., Kirkham, A., Nixon, S. J., … Parton, R. G. (2008). PTRF-Cavin, a Conserved Cytoplasmic Protein Required for Caveola Formation and Function. *Cell*, *132*(1), 113–124. https://doi.org/10.1016/j.cell.2007.11.042

Hinshaw, J. E., & Schmid, S. L. (1995). Dynamin self-assembles into rings suggesting a mechanism for coated vesicle budding. *Nature*, *374*(6518), 190–192. https://doi.org/10.1038/374190a0

Hitchcock, K. E., & Holland, C. K. (2010). Ultrasound-assisted thrombolysis for stroke therapy: Better thrombus break-up with bubbles. *Stroke*, *41*(10 SUPPL. 1). https://doi.org/10.1161/STROKEAHA.110.595348

Ho, C.-M., Kuo, S.-Y., Chen, C.-H., Huang, J.-K., & Jan, C.-R. (2005). Effect of desipramine on Ca2+ levels and growth in renal tubular cells. *Cellular Signalling*, *17*(7), 837–45. https://doi.org/10.1016/j.cellsig.2004.11.005

Holopainen, J. M., Angelova, M. I., & Kinnunen, P. K. (2000). Vectorial budding of vesicles by asymmetrical enzymatic formation of ceramide in giant liposomes. *Biophysical Journal*, *78*(2), 830–8. https://doi.org/10.1016/S0006-3495(00)76640-9

Holopainen, J. M., Lehtonen, J. Y., & Kinnunen, P. K. (1997). Lipid microdomains in dimyristoylphosphatidylcholine-ceramide liposomes. *Chemistry and Physics of Lipids*, *88*(1), 1–13.

Holopainen, J. M., Subramanian, M., & Kinnunen, P. K. (1998). Sphingomyelinase induces lipid microdomain formation in a fluid phosphatidylcholine/sphingomyelin membrane. *Biochemistry*, *37*(50), 17562–70. https://doi.org/10.1021/bi980915e

Houndolo, T., Boulay, P.-L., & Claing, A. (2005). G protein-coupled receptor endocytosis in ADP-ribosylation factor 6-depleted cells. *The Journal of Biological Chemistry*, *280*(7), 5598–604. https://doi.org/10.1074/jbc.M411456200

Howes, M. T., Kirkham, M., Riches, J., Cortese, K., Walser, P. J., Simpson, F., … Parton, R. G. (2010). Clathrin-independent carriers form a high capacity endocytic sorting system at the leading edge of migrating cells. *The Journal of Cell Biology*, *190*(4), 675–691. https://doi.org/10.1083/jcb.201002119

Hu, Y., Wan, J. M. F., & Yu, A. C. H. (2013). Membrane Perforation and Recovery Dynamics in Microbubble-Mediated Sonoporation. *Ultrasound in Medicine & Biology*, *39*(12), 2393–2405. https://doi.org/10.1016/j.ultrasmedbio.2013.08.003

Hua, S., & Wu, S. Y. (2013). The use of lipid-based nanocarriers for targeted pain therapies.

Frontiers in Pharmacology, *4*, 143. https://doi.org/10.3389/fphar.2013.00143

Huang, C.-J., Cheng, H.-H., Chou, C.-T., Kuo, C.-C., Lu, Y.-C., Tseng, L.-L., … Jan, C.-R. (2007). Desipramine-induced Ca2+ movement and cytotoxicity in PC3 human prostate cancer cells. *Toxicology in Vitro*, *21*(3), 449–456. https://doi.org/10.1016/J.TIV.2006.10.011

Huang, S.-L., & McPherson, D. D. (2014). Ultrasound for Drug/Gene Delivery. In X. Chen & S. Wong (Eds.), *Cancer Theranostics* (pp. 269–283). London: Academic Press. https://doi.org/10.1016/B978-0-12-407722-5.00016-5

Huang, Y., Joshi, S., Xiang, B., Kanaho, Y., Li, Z., Bouchard, B. A., … Whiteheart, S. W. (2016). Arf6 controls platelet spreading and clot retraction via integrin IIb 3 trafficking. *Blood*, *127*(11), 1459–1467. https://doi.org/10.1182/blood-2015-05-648550

Huwiler, A., Johansen, B., Skarstad, A., & Pfeilschifter, J. (2001). Ceramide binds to the CaLB domain of cytosolic phospholipase A 2 and facilitates its membrane docking and arachidonic acid release. *The FASEB Journal*, *15*(1), 7–9. https://doi.org/10.1096/fj.00-0370fje

Ibsen, S., Benchimol, M., & Esener, S. (2013). Fluorescent microscope system to monitor real-time interactions between focused ultrasound, echogenic drug delivery vehicles, and live cell membranes. *Ultrasonics*, *53*(1), 178–84. https://doi.org/10.1016/j.ultras.2012.05.006

Idone, V., Tam, C., Goss, J. W., Toomre, D., Pypaert, M., & Andrews, N. W. (2008). Repair of injured plasma membrane by rapid Ca2+-dependent endocytosis. *The Journal of Cell Biology*, *180*(5), 905–14. https://doi.org/10.1083/jcb.200708010

Ignee, A., Atkinson, N. S. S., Schuessler, G., & Dietrich, C. F. (2016). Ultrasound contrast agents. *Endoscopic Ultrasound*, *5*(6), 355–362. https://doi.org/10.4103/2303-9027.193594

Ira, & Johnston, L. J. (2008). Sphingomyelinase generation of ceramide promotes clustering of nanoscale domains in supported bilayer membranes. *Biochimica et Biophysica Acta*, *1778*(1), 185–97. https://doi.org/10.1016/j.bbamem.2007.09.021

Ishida, T., Harashima, H., & Kiwada, H. (2001). Interactions of Liposomes with Cells In Vitro and In Vivo: Opsonins and Receptors. *Current Drug Metabolism*, *2*(4), 397–409. https://doi.org/10.2174/1389200013338306

Itoh, T., Erdmann, K. S., Roux, A., Habermann, B., Werner, H., & De Camilli, P. (2005). Dynamin and the actin cytoskeleton cooperatively regulate plasma membrane invagination by BAR and F-BAR proteins. *Developmental Cell*, *9*(6), 791–804. https://doi.org/10.1016/j.devcel.2005.11.005

Jambhekar, S. S., & Breen, P. J. (2012). Extravascular routes of drug administration. In *Basic Pharmacokinetics* (Second, pp. 106–126). London: Pharmaceutical Press. Retrieved from www.pharmpress.com

Jang, D., Kwon, H., Jeong, K., Lee, J., & Pak, Y. (2015). Essential role of flotillin-1 palmitoylation in the intracellular localization and signaling function of IGF-1 receptor. *Journal of Cell Science*, *128*(11), 2179–90. https://doi.org/10.1242/jcs.169409

Jaqaman, K., Loerke, D., Mettlen, M., Kuwata, H., Grinstein, S., Schmid, S. L., & Danuser, G. (2008). Robust single-particle tracking in live-cell time-lapse sequences. *Nature Methods*, *5*(8), 695–702. https://doi.org/10.1038/nmeth.1237

Jarsch, I. K., Daste, F., & Gallop, J. L. (2016). Membrane curvature in cell biology: An integration of molecular mechanisms. *J Cell Biol*, *214*(4), 375–387. https://doi.org/10.1083/JCB.201604003

Jeevanandam, J., Barhoum, A., Chan, Y. S., Dufresne, A., & Danquah, M. K. (2018). Review on

nanoparticles and nanostructured materials: history, sources, toxicity and regulations. *Beilstein Journal of Nanotechnology*, *9*, 1050–1074. https://doi.org/10.3762/bjnano.9.98

Jenkins, R. W., Canals, D., & Hannun, Y. A. (2009). Roles and regulation of secretory and lysosomal acid sphingomyelinase. *Cellular Signalling*, *21*(6), 836–46. Retrieved from http://www.ncbi.nlm.nih.gov/pubmed/19385042

Jeong, J., Kim, W., Kim, L. K., VanHouten, J., & Wysolmerski, J. J. (2017). HER2 signaling regulates HER2 localization and membrane retention. *PLoS ONE*, *12*(4). https://doi.org/10.1371/JOURNAL.PONE.0174849

Jia, C., Xu, L., Han, T., Cai, P., Yu, A. C. H., & Qin, P. (2018). Generation of Reactive Oxygen Species in Heterogeneously Sonoporated Cells by Microbubbles with Single-Pulse Ultrasound. *Ultrasound in Medicine & Biology*, *44*(5), 1074–1085. https://doi.org/10.1016/j.ultrasmedbio.2018.01.006

Johannes, L., & Mayor, S. (2010). Induced Domain Formation in Endocytic Invagination, Lipid Sorting, and Scission. *Cell*, *142*(4), 507–510. https://doi.org/10.1016/j.cell.2010.08.007

Jozala, A. F., Geraldes, D. C., Tundisi, L. L., Feitosa, V. de A., Breyer, C. A., Cardoso, S. L., … Jr. (2016). Biopharmaceuticals from microorganisms: from production to purification. *Brazilian Journal of Microbiology*, *47 Suppl 1*(Suppl 1), 51–63. https://doi.org/10.1016/j.bjm.2016.10.007

Juffermans, L. J. M., Dijkmans, P. A., Musters, R. J. P., Visser, C. A., & Kamp, O. (2006). Transient permeabilization of cell membranes by ultrasound-exposed microbubbles is related to formation of hydrogen peroxide. *Am J Physiol Heart Circ Physiol*, *291*(4), H1595-601. https://doi.org/01120.2005 [pii]\r10.1152/ajpheart.01120.2005

Juffermans, L., van Dijk, A., Jongenelen, C. A. M., Drukarch, B., Reijerkerk, A., de Vries, H. E.,

… Musters, R. J. P. (2009). Ultrasound and Microbubble-Induced Intra- and Intercellular Bioeffects in Primary Endothelial Cells. *Ultrasound in Medicine and Biology*, *35*(11), 1917–1927. https://doi.org/10.1016/j.ultrasmedbio.2009.06.1091

Kalish, H., Arbab, A. S., Miller, B. R., Lewis, B. K., Zywicke, H. A., Bulte, J. W. M., … Frank, J. A. (2003). Combination of transfection agents and magnetic resonance contrast agents for cellular imaging: Relationship between relaxivities, electrostatic forces, and chemical composition. *Magnetic Resonance in Medicine*, *50*(2), 275–282. https://doi.org/10.1002/mrm.10556

Kanaseki, T., & Kadota, K. (1969). The "vesicle in a basket". A morphological study of the coated vesicle isolated from the nerve endings of the guinea pig brain, with special reference to the mechanism of membrane movements. *Journal of Cell Biology*, *42*(1), 202–220. https://doi.org/10.1083/jcb.42.1.202

Kanavos, P., Sullivan, R., Lewison, G., Schurer, W., Eckhouse, S., & Vlachopioti, Z. (2010). The role of funding and policies on innovation in cancer drug development. *Ecancermedicalscience*, *4*, 164. https://doi.org/10.3332/ecancer.2010.164

Karshafian, R., Bevan, P. D., Williams, R., Samac, S., & Burns, P. N. (2009a). Sonoporation by Ultrasound-Activated Microbubble Contrast Agents: Effect of Acoustic Exposure Parameters on Cell Membrane Permeability and Cell Viability. *Ultrasound in Medicine & Biology*, *35*(5), 847–860. https://doi.org/10.1016/j.ultrasmedbio.2008.10.013

Karshafian, R., Samac, S., Bevan, P. D., & Burns, P. N. (2010). Microbubble mediated sonoporation of cells in suspension: clonogenic viability and influence of molecular size on uptake. *Ultrasonics*, *50*(7), 691–7. https://doi.org/10.1016/j.ultras.2010.01.009

Kenakin, T. P. (2009). Pharmacokinetics. In *A Pharmacology Primer: Theory, Applications, and*

Methods (3rd ed., pp. 179–214). Academic Press. https://doi.org/10.1016/B978-0-12-374585-9.00009-8

Kerwin, B. A. (2008). Polysorbates 20 and 80 Used in the Formulation of Protein Biotherapeutics: Structure and Degradation Pathways. *Journal of Pharmaceutical Sciences*, *97*(8), 2924–2935. https://doi.org/10.1002/jps.21190

Kim-Campbell, N., Gomez, H., & Bayir, H. (2019). Cell Death Pathways: Apoptosis and Regulated Necrosis. In C. Ronco, R. Bellomo, J. A. Kellum, & Z. Ricci (Eds.), *Critical Care Nephrology* (3rd ed., p. 113–121.e2). Content Repository Only! https://doi.org/10.1016/B978-0-323-44942-7.00020-0

Kim, W. T., Chang, S., Daniell, L., Cremona, O., Di Paolo, G., & De Camilli, P. (2002). Delayed reentry of recycling vesicles into the fusion-competent synaptic vesicle pool in synaptojanin 1 knockout mice. *Proceedings of the National Academy of Sciences*, *99*(26), 17143–17148. https://doi.org/10.1073/pnas.222657399

Kim, Y.-M., & Benovic, J. L. (2002). Differential Roles of Arrestin-2 Interaction with Clathrin and Adaptor Protein 2 in G Protein-coupled Receptor Trafficking. *Journal of Biological Chemistry*, *277*(34), 30760–30768. https://doi.org/10.1074/jbc.M204528200

Kimura, a, Baumann, C. a, Chiang, S. H., & Saltiel, a R. (2001). The sorbin homology domain: a motif for the targeting of proteins to lipid rafts. *Proceedings of the National Academy of Sciences of the United States of America*, *98*(16), 9098–9103. https://doi.org/10.1073/pnas.151252898

Kinoshita, E., Kinoshita-Kikuta, E., Takiyama, K., & Koike, T. (2006). Phosphate-binding tag, a new tool to visualize phosphorylated proteins. *Molecular & Cellular Proteomics : MCP*, *5*(4), 749–57. https://doi.org/10.1074/mcp.T500024-MCP200

Kinoshita, M., & Hynynen, K. (2007). Key factors that affect sonoporation efficiency in in vitro settings: the importance of standing wave in sonoporation. *Biochemical and Biophysical Research Communications*, *359*(4), 860–5. https://doi.org/10.1016/j.bbrc.2007.05.153

Kirkham, M., Fujita, A., Chadda, R., Nixon, S. J., Kurzchalia, T. V., Sharma, D. K., … Parton, R. G. (2005a). Ultrastructural identification of uncoated caveolin-independent early endocytic vehicles. *The Journal of Cell Biology*, *168*(3), 465–476. https://doi.org/10.1083/jcb.200407078

Kiss, A. L., Botos, E., Turi, Á., & Müllner, N. (2004). Ocadaic acid treatment causes tyrosine phosphorylation of caveolin-2 and induces internalization of caveolae in rat peritoneal macrophages. *Micron*, *35*(8), 707–715. https://doi.org/10.1016/j.micron.2004.04.003

Koegl, M., Zlatkine, P., Ley, S. C., Courtneidge, S. A., & Magee, A. I. (1994). Palmitoylation of multiple Src-family kinases at a homologous N-terminal motif. *The Biochemical Journal*, *303 (Pt 3*, 749–53. https://doi.org/10.1042/bj3030749

Kokkola, T., Kruse, C., Roy-Pogodzik, E. M., Pekkinen, J., Bauch, C., Hönck, H. H., … Kreienkamp, H. J. (2011). Somatostatin receptor 5 is palmitoylated by the interacting ZDHHC5 palmitoyltransferase. *FEBS Letters*, *585*(17), 2665–2670. https://doi.org/10.1016/j.febslet.2011.07.028

Kolesnick, R. N., & Krönke, M. (1998). REGULATION OF CERAMIDE PRODUCTION AND APOPTOSIS. *Annual Review of Physiology*, *60*(1), 643–665. https://doi.org/10.1146/annurev.physiol.60.1.643

Kooiman, K., Vos, H. J., Versluis, M., & de Jong, N. (2014). Acoustic behavior of microbubbles and implications for drug delivery. *Advanced Drug Delivery Reviews*, *72*, 28–48. https://doi.org/10.1016/j.addr.2014.03.003

Kornhuber, J., Rhein, C., Müller, C. P., & Mühle, C. (2015). Secretory sphingomyelinase in health and disease. *Biological Chemistry*, *396*(6–7). https://doi.org/10.1515/hsz-2015-0109

Korycka, J., Łach, A., Heger, E., Bogusławska, D. M., Wolny, M., Toporkiewicz, M., … Sikorski, A. F. (2012). Human DHHC proteins: A spotlight on the hidden player of palmitoylation. *European Journal of Cell Biology*, *91*(2), 107–117. https://doi.org/10.1016/j.ejcb.2011.09.013

Kothamasu, P., Kanumur, H., Ravur, N., Maddu, C., Parasuramrajam, R., & Thangavel, S. (2012). Nanocapsules: the weapons for novel drug delivery systems. *BioImpacts : BI*, *2*(2), 71–81. https://doi.org/10.5681/bi.2012.011

Kovtun, O., Tillu, V. A., Ariotti, N., Parton, R. G., & Collins, B. M. (2015). Cavin family proteins and the assembly of caveolae. *Journal of Cell Science*, *128*(7), 1269–1278. https://doi.org/10.1242/jcs.167866

Kozik, P., Francis, R. W., Seaman, M. N. J., & Robinson, M. S. (2010). A Screen for Endocytic Motifs. *Traffic*, *11*(6), 843–855. https://doi.org/10.1111/j.1600-0854.2010.01056.x

Kozlov, M. M., Campelo, F., Liska, N., Chernomordik, L. V, Marrink, S. J., & McMahon, H. T. (2014). Mechanisms shaping cell membranes. *Current Opinion in Cell Biology*, *29*, 53–60. https://doi.org/10.1016/j.ceb.2014.03.006

Kruth, H. S., Jones, N. L., Huang, W., Zhao, B., Ishii, I., Chang, J., … Zhang, W.-Y. (2004). Macropinocytosis Is the Endocytic Pathway That Mediates Macrophage Foam Cell Formation with Native Low Density Lipoprotein* □ S. https://doi.org/10.1074/jbc.M407167200

Kruth, H. S., Jones, N. L., Huang, W., Zhao, B., Ishii, I., Chang, J., … Zhang, W.-Y. (2005). Macropinocytosis Is the Endocytic Pathway That Mediates Macrophage Foam Cell

Formation with Native Low Density Lipoprotein. *Journal of Biological Chemistry*, *280*(3), 2352–2360. https://doi.org/10.1074/jbc.M407167200

Kulkarni, V. S., & Shaw, C. (2016). Formulating Creams, Gels, Lotions, and Suspensions. In *Essential Chemistry for Formulators of Semisolid and Liquid Dosages* (pp. 29–41). London: Academic Press. https://doi.org/10.1016/B978-0-12-801024-2.00004-2

Kumari, S., & Mayor, S. (2008a). ARF1 is directly involved in dynamin-indepefile:///Users/Farnaz/Downloads/pone.0096647.pdfndent endocytosis. *Nature Cell Biology*, *10*(1), 30–41. https://doi.org/10.1038/ncb1666

Kumari, S., MG, S., & Mayor, S. (2010). Endocytosis unplugged: multiple ways to enter the cell. *Cell Research*, *20*(3), 256–275. https://doi.org/10.1038/cr.2010.19

Kurrle, N., John, B., Meister, M., & Tikkanen, R. (2012). Function of flotillins in receptor tyrosine kinase signaling and endocytosis: role of tyrosine phosphorylation and oligomerization. *Protein Phosphorylation in Human Health*, (4). https://doi.org/10.5772/48598

Kwon, S. G., Piao, Y., Park, J., Angappane, S., Jo, Y., Hwang, N.-M., … Hyeon, T. (2007). Kinetics of Monodisperse Iron Oxide Nanocrystal Formation by "Heating-Up" Process. *Journal of the American Chemical Society*, *129*(41), 12571–12584. https://doi.org/10.1021/ja074633q

Lai, C.-Y., Wu, C.-H., Chen, C.-C., & Li, P.-C. (2006). Quantitative relations of acoustic inertial cavitation with sonoporation and cell viability. *Ultrasound in Medicine & Biology*, *32*(12), 1931–1941. https://doi.org/10.1016/j.ultrasmedbio.2006.06.020

Lajoie, P., Kojic, L. D., Nim, S., Li, L., Dennis, J. W., & Nabi, I. R. (2009). Caveolin-1 regulation of dynamin-dependent, raft-mediated endocytosis of cholera toxin-B sub-unit

occurs independently of caveolae. *Journal of Cellular and Molecular Medicine*, *13*(9b), 3218–3225. https://doi.org/10.1111/j.1582-4934.2009.00732.x

Lajoie, P., & Nabi, I. R. (2010). Lipid Rafts, Caveolae, and Their Endocytosis. *International Review of Cell and Molecular Biology*, *282*, 135–163. https://doi.org/10.1016/S1937-6448(10)82003-9

Lamaze, C., Dujeancourt, A., Baba, T., Lo, C. G., Benmerah, A., & Dautry-Varsat, A. (2001). Interleukin 2 receptors and detergent-resistant membrane domains define a clathrin-independent endocytic pathway. *Molecular Cell*, *7*(3), 661–71. Retrieved from http://www.ncbi.nlm.nih.gov/pubmed/11463390

Lamaze, C., Fujimoto, L. M., Yin, H. L., & Schmid, S. L. (1997). The Actin Cytoskeleton Is Required for Receptor-mediated Endocytosis in Mammalian Cells *.

Lariccia, V., Fine, M., Magi, S., Lin, M.-J., Yaradanakul, A., Llaguno, M. C., & Hilgemann, D. W. (2011). Massive calcium–activated endocytosis without involvement of classical endocytic proteins. *The Journal of General Physiology*, *137*(1), 111–132. https://doi.org/10.1085/jgp.201010468

Lauterborn, W., & Ohl, C. D. (1997). Cavitation bubble dynamics. *Ultrasonics Sonochemistry*, *4*(2), 65–75. Retrieved from http://www.ncbi.nlm.nih.gov/pubmed/11237047

Le, J. (2017). Overview of Pharmacokinetics - Clinical Pharmacology. Retrieved March 15, 2019, from https://www.merckmanuals.com/professional/clinical-pharmacology/pharmacokinetics/overview-of-pharmacokinetics

Lee, H., Volonte', D., Galbiati, F., Iyengar, P., Lublin, D. M., Bregman, D. B., … Lisanti, M. P. (2000). Constitutive and Growth Factor-Regulated Phosphorylation of Caveolin-1 Occurs at the Same Site (Tyr-14) *in Vivo:* Identification of a c-Src/Cav-1/Grb7 Signaling Cassette.

Molecular Endocrinology, *14*(11), 1750–1775. https://doi.org/10.1210/mend.14.11.0553

Leighton, T. G. (1994). *The acoustic bubble*. Academic Press. Retrieved from https://books.google.ca/books?id=tR-8SNimBuEC&pg=PA404&lpg=PA404&dq=stable+cavitation+rectified+diffusion+to+resonance+radius&source=bl&ots=gXCpru-dMm&sig=ACfU3U2_s_MZFoYvGltxoJ1y1QWZihFy9w&hl=en&sa=X&ved=2ahUKEwilxquB6_jgAhUEO60KHV_gBUYQ6AEwA3oECAEQAQ#v=

Leong, T., Ashokkumar, M., & Kentish, S. (2015). The Growth of Bubbles in an Acoustic Field by Rectified Diffusion. In *Handbook of Ultrasonics and Sonochemistry* (pp. 1–30). Singapore: Springer Singapore. https://doi.org/10.1007/978-981-287-470-2_74-1

Levade, T., & Jaffrézou, J. P. (1999). Signalling sphingomyelinases: which, where, how and why? *Biochimica et Biophysica Acta*, *1438*(1), 1–17. Retrieved from http://www.ncbi.nlm.nih.gov/pubmed/10216276

Levental, I., Lingwood, D., Grzybek, M., Coskun, U., & Simons, K. (2010). Palmitoylation regulates raft affinity for the majority of integral raft proteins. *Proceedings of the National Academy of Sciences*, *107*(51), 22050–22054. https://doi.org/10.1073/pnas.1016184107

Li, S., Seitz, R., & Lisanti, M. P. (1996). Phosphorylation of caveolin by src tyrosine kinases. The alpha-isoform of caveolin is selectively phosphorylated by v-Src in vivo. *The Journal of Biological Chemistry*, *271*(7), 3863–8. Retrieved from http://www.ncbi.nlm.nih.gov/pubmed/8632005

Li, X., Gulbins, E., & Zhang, Y. (2012). Oxidative stress triggers Ca-dependent lysosome trafficking and activation of acid sphingomyelinase. *Cellular Physiology and Biochemistry : International Journal of Experimental Cellular Physiology, Biochemistry, and*

Pharmacology, *30*(4), 815–26. https://doi.org/10.1159/000341460

Li, Y., Hu, J., Höfer, K., Wong, A. M. S., Cooper, J. D., Birnbaum, S. G., … Hofmann, S. L. (2010). DHHC5 Interacts with PDZ Domain 3 of Post-synaptic Density-95 (PSD-95) Protein and Plays a Role in Learning and Memory. *Journal of Biological Chemistry*, *285*(17), 13022–13031. https://doi.org/10.1074/jbc.M109.079426

Li, Y., Martin, B. R., Cravatt, B. F., & Hofmann, S. L. (2012). DHHC5 protein palmitoylates flotillin-2 and is rapidly degraded on induction of neuronal differentiation in cultured cells. *Journal of Biological Chemistry*, *287*(1), 523–530. https://doi.org/10.1074/jbc.M111.306183

Li, Y., & Qi, B. (2017). Progress toward Understanding Protein S-acylation: Prospective in Plants. *Frontiers in Plant Science*, *8*, 346. https://doi.org/10.3389/fpls.2017.00346

Liberali, P., Kakkonen, E., Turacchio, G., Valente, C., Spaar, A., Perinetti, G., … Luini, A. (2008). The closure of Pak1-dependent macropinosomes requires the phosphorylation of CtBP1/BARS. *The EMBO Journal*, *27*(7), 970–981. https://doi.org/10.1038/emboj.2008.59

Lin, H. C., Südhof, T. C., & Anderson, R. G. (1992). Annexin VI is required for budding of clathrin-coated pits. *Cell*, *70*(2), 283–91. Retrieved from http://www.ncbi.nlm.nih.gov/pubmed/1386288

Linder, M. E. (2004). Model organisms lead the way to protein palmitoyltransferases. *Journal of Cell Science*, *117*(4), 521–526. https://doi.org/10.1242/jcs.00989

Lindner, J. R., Song, J., Christiansen, J., Klibanov, A. L., Xu, F., & Ley, K. (2001). Ultrasound assessment of inflammation and renal tissue injury with microbubbles targeted to P-selectin. *Circulation*, *104*(17), 2107–12. Retrieved from http://www.ncbi.nlm.nih.gov/pubmed/11673354

Liu, J., DeYoung, S. M., Zhang, M., Dold, L. H., & Saltiel, A. R. (2005). The stomatin/prohibitin/flotillin/HflK/C domain of flotillin-1 contains distinct sequences that direct plasma membrane localization and protein interactions in 3T3-L1 adipocytes. *Journal of Biological Chemistry*, *280*(16), 16125–16134. https://doi.org/10.1074/jbc.M500940200

Liu, J., García-Cardeña, G., & Sessa, W. C. (1996). Palmitoylation of endothelial nitric oxide synthase is necessary for optimal stimulated release of nitric oxide: Implications for caveolae localization. *Biochemistry*, *35*(41), 13277–13281. https://doi.org/10.1021/bi961720e

Liu, J., Nguyen, M. D. H., Andya, J. D., & Shire, S. J. (2005). Reversible Self-Association Increases the Viscosity of a Concentrated Monoclonal Antibody in Aqueous Solution. *Journal of Pharmaceutical Sciences*, *94*(9), 1928–1940. https://doi.org/10.1002/jps.20347

Liu, L., Brown, D., McKee, M., LeBrasseur, N. K., Yang, D., Albrecht, K. H., … Pilch, P. F. (2008). Deletion of Cavin/PTRF Causes Global Loss of Caveolae, Dyslipidemia, and Glucose Intolerance. *Cell Metabolism*, *8*(4), 310–317. https://doi.org/10.1016/j.cmet.2008.07.008

Liu, X., Wang, H., Liang, X., & Roberts, M. (2017). Hepatic Metabolism in Liver Health and Disease. In P. Muriel (Ed.), *Liver Pathophysiology* (pp. 391–400). Academic Press. https://doi.org/10.1016/B978-0-12-804274-8.00030-8

Loerke, D., Mettlen, M., Schmid, S. L., & Danuser, G. (2011). Measuring the hierarchy of molecular events during clathrin-mediated endocytosis. *Traffic (Copenhagen, Denmark)*. https://doi.org/10.1111/j.1600-0854.2011.01197.x

Loerke, D., Mettlen, M., Yarar, D., Jaqaman, K., Jaqaman, H., Danuser, G., & Schmid, S. L. (2009). Cargo and dynamin regulate clathrin-coated pit maturation. *PLoS Biol*, *7*(3), e57.

Longva, K. E., Pedersen, N. M., Haslekås, C., Stang, E., & Madshus, I. H. (2005). Herceptin-induced inhibition of ErbB2 signaling involves reduced phosphorylation of Akt but not endocytic down-regulation of ErbB2. *International Journal of Cancer*, *116*(3), 359–367. https://doi.org/10.1002/ijc.21015

López-Montero, I., Vélez, M., & Devaux, P. F. (2007). Surface tension induced by sphingomyelin to ceramide conversion in lipid membranes. *Biochimica et Biophysica Acta (BBA) - Biomembranes*, *1768*(3), 553–561. https://doi.org/10.1016/j.bbamem.2007.01.001

Lou, J., Low-Nam, S. T., Kerkvliet, J. G., & Hoppe, A. D. (2014). Delivery of CSF-1R to the lumen of macropinosomes promotes its destruction in macrophages. *Journal of Cell Science*, *127*(Pt 24), 5228–39. https://doi.org/10.1242/jcs.154393

Lu, J.-D., & Xue, J. (2019). Poisoning: Kinetics to Therapeutics. In C. Ronco, R. Bellomo, J. A. Kellum, & Z. Ricci (Eds.), *Critical Care Nephrology* (3rd ed., pp. 600–629). Elsevier. https://doi.org/10.1016/B978-0-323-44942-7.00101-1

Lucarelli, S., Delos Santos, R. C., & Antonescu, C. N. (2017). Measurement of Epidermal Growth Factor Receptor-Derived Signals Within Plasma Membrane Clathrin Structures. In *Methods in molecular biology (Clifton, N.J.)* (Vol. 1652, pp. 191–225). https://doi.org/10.1007/978-1-4939-7219-7_15

Lundmark, R., Doherty, G. J., Howes, M. T., Cortese, K., Vallis, Y., Parton, R. G., & McMahon, H. T. (2008). The GTPase-Activating Protein GRAF1 Regulates the CLIC/GEEC Endocytic Pathway. *Current Biology*, *18*(22), 1802–1808. https://doi.org/10.1016/j.cub.2008.10.044

Lunn, J. A., Wong, H., Rozengurt, E., Walsh, J. H., Adrian, J., Wong, H., … Walsh, J. H. (2000). Requirement of cortical actin organization for bombesin , endothelin , and EGF receptor internalization, *1792*(June), 2019–2027.

M. Resh. (1999). Fatty acylation of proteins: new insights into membrane targeting of myristylated and palmitoylated proteins. *Biochimica et Biophysica Acta - Molecular Cell Research*, *1451*(1), 1–16. https://doi.org/10.1016/S0167-4889(99)00075-0

Machesky, L. M., & Insall, R. H. (1998). Scar1 and the related Wiskott-Aldrich syndrome protein, WASP, regulate the actin cytoskeleton through the Arp2/3 complex. *Current Biology : CB*, *8*(25), 1347–56. Retrieved from http://www.ncbi.nlm.nih.gov/pubmed/9889097

Machesky, L. M., Mullins, R. D., Higgs, H. N., Kaiser, D. A., Blanchoin, L., May, R. C., … Pollard, T. D. (1999). Scar, a WASp-related protein, activates nucleation of actin filaments by the Arp2/3 complex. *Proceedings of the National Academy of Sciences of the United States of America*, *96*(7), 3739–44. https://doi.org/10.1073/PNAS.96.7.3739

Maffucci, T., & Falasca, M. (2014). Analysis, Regulation, and Roles of Endosomal Phosphoinositides. *Methods in Enzymology*, *535*, 75–91. https://doi.org/10.1016/B978-0-12-397925-4.00005-5

Manneville, S. E.-, & Hall, A. (2002). Rho GTPases in cell biology. *Nature*, *420*(December), 629–635.

Marmottant, P., & Hilgenfeldt, S. (2003). Controlled vesicle deformation and lysis by single oscillating bubbles. *Nature*, *423*(6936), 153–156. https://doi.org/10.1038/nature01613

Martini, S. (2013). An Overview of Ultrasound. In *Sonocrystallization of Fats* (pp. 7–16). New York, NY: Springer New York. https://doi.org/10.1007/978-1-4614-7693-1_2

Mathias, S., Dressler, K. A., & Kolesnick, R. N. (1991). Characterization of a ceramide-activated protein kinase: stimulation by tumor necrosis factor alpha. *Proceedings of the National Academy of Sciences of the United States of America*, *88*(22), 10009–13. Retrieved from

http://www.ncbi.nlm.nih.gov/pubmed/1946418

Mayle, K. M., Le, A. M., & Kamei, D. T. (2012). The intracellular trafficking pathway of transferrin. *Biochimica et Biophysica Acta*, *1820*(3), 264–81. https://doi.org/10.1016/j.bbagen.2011.09.009

Mayor, S., & Maxfield, F. R. (1995). Insolubility and redistribution of GPI-anchored proteins at the cell surface after detergent treatment. *Molecular Biology of the Cell*, *6*(7), 929–44. Retrieved from http://www.ncbi.nlm.nih.gov/pubmed/7579703

Mayor, S., & Pagano, R. E. (2007). Pathways of clathrin-independent endocytosis. *Nature Reviews Molecular Cell Biology*, *8*(8), 603–612. https://doi.org/10.1038/nrm2216

Mayor, S., Parton, R. G., & Donaldson, J. G. (2014). Clathrin-independent pathways of endocytosis. *Cold Spring Harbor Perspectives in Biology*, *6*(6), 1–20. https://doi.org/10.1101/cshperspect.a016758

Mayor, S., & Riezman, H. (2004). Sorting GPI-anchored proteins. *Nature Reviews Molecular Cell Biology*, *5*(2), 110–120. https://doi.org/10.1038/nrm1309

Mayor, S., Rothberg, K. G., & Maxfield, F. R. (1994). Sequestration of GPI-anchored proteins in caveolae triggered by cross-linking. *Science (New York, N.Y.)*, *264*(5167), 1948–51. Retrieved from http://www.ncbi.nlm.nih.gov/pubmed/7516582

McBain, S. C., Yiu, H. H. P., & Dobson, J. (2008). Magnetic nanoparticles for gene and drug delivery. *International Journal of Nanomedicine*, *3*(2), 169–80. Retrieved from http://www.ncbi.nlm.nih.gov/pubmed/18686777

McMahon, H. T., & Boucrot, E. (2011). Molecular mechanism and physiological functions of clathrin-mediated endocytosis. *Nature Reviews. Molecular Cell Biology*, *12*(8), 517–33. https://doi.org/10.1038/nrm3151

McMahon, H. T., & Gallop, J. L. (2005). Membrane curvature and mechanisms of dynamic cell membrane remodelling. *Nature*, *438*(7068), 590–596. https://doi.org/10.1038/nature04396

McMillan, J., Batrakova, E., & Gendelman, H. E. (2011). Cell Delivery of Therapeutic Nanoparticles. *Progress in Molecular Biology and Translational Science*, *104*, 563–601. https://doi.org/10.1016/B978-0-12-416020-0.00014-0

McNeil, P. L. (2002). Repairing a torn cell surface: make way, lysosomes to the rescue. *Journal of Cell Science*, *115*(Pt 5), 873–879.

McNeil, P. L., Miyake, K., & Vogel, S. S. (2003). The endomembrane requirement for cell surface repair. *Proceedings of the National Academy of Sciences*, *100*(8), 4592–4597. https://doi.org/10.1073/pnas.0736739100

Mcneil, P. L., & Terasaki, M. (2001). *Coping with the inevitable: how cells repair a torn surface membrane*. *NATURE CELL BIOLOGY* (Vol. 3). Retrieved from http://cellbio.nature.come124

McNeil, P., Vogel, S. S., Miyake, K., & Terasaki, M. (2000). Patching plasma membrane disruptions with cytoplasmic membrane. *Journal of Cell Science*, *113 (Pt 1*, 1891–902. Retrieved from http://www.ncbi.nlm.nih.gov/pubmed/10806100

Mehier-humbert, S., Bettinger, T., Yan, F., & Guy, R. H. (2005). Plasma membrane poration induced by ultrasound exposure : Implication for drug delivery GENE DELIVERY, *104*, 213–222. https://doi.org/10.1016/j.jconrel.2005.01.007

Meijering, B. D. M., Juffermans, L. J. M., van Wamel, A., Henning, R. H., Zuhorn, I. S., Emmer, M., … Kamp, O. (2009). Ultrasound and Microbubble-Targeted Delivery of Macromolecules Is Regulated by Induction of Endocytosis and Pore Formation. *Circulation Research*, *104*(5), 679–687. https://doi.org/10.1161/CIRCRESAHA.108.183806

Meister, M., & Tikkanen, R. (2014). Endocytic trafficking of membrane-bound cargo: A flotillin point of view. *Membranes*, *4*(3), 356–371. https://doi.org/10.3390/membranes4030356

Mènard, S., Tagliabue, E., Campiglio, M., & Pupa, S. M. (2000). Role of HER2 gene overexpression in breast carcinoma. *Journal of Cellular Physiology*, *182*(2), 150–162. https://doi.org/10.1002/(SICI)1097-4652(200002)182:2<150::AID-JCP3>3.0.CO;2-E

Mergia, A. (2017). The Role of Caveolin 1 in HIV Infection and Pathogenesis. *Viruses*, *9*(6). https://doi.org/10.3390/v9060129

Meric-Bernstam, F., & Hung, M.-C. (2006). Advances in Targeting Human Epidermal Growth Factor Receptor-2 Signaling for Cancer Therapy. *Clinical Cancer Research*, *12*(21), 6326–6330. https://doi.org/10.1158/1078-0432.CCR-06-1732

Merrifield, C. J., Feldman, M. E., Wan, L., & Almers, W. (2002). Imaging actin and dynamin recruitment during invagination of single clathrin-coated pits. *Nature Cell Biology*, *4*(9), 691–698. https://doi.org/10.1038/ncb837

Messa, M., Fernández-Busnadiego, R., Sun, E. W., Chen, H., Czapla, H., Wrasman, K., … De Camilli, P. (2014). Epsin deficiency impairs endocytosis by stalling the actin-dependent invagination of endocytic clathrin-coated pits. *ELife*, *3*. https://doi.org/10.7554/eLife.03311

Mettlen, M., Loerke, D., Yarar, D., Danuser, G., & Schmid, S. L. (2010). Cargo- and adaptor-specific mechanisms regulate clathrin-mediated endocytosis. *Journal of Cell Biology*, *188*(6), 919–933. https://doi.org/10.1083/jcb.200908078

Mettlen, M., Platek, A., Van Der Smissen, P., Carpentier, S., Amyere, M., Lanzetti, L., … Courtoy, P. J. (2006). Src triggers circular ruffling and macropinocytosis at the apical surface of polarized MDCK cells. *Traffic (Copenhagen, Denmark)*, *7*(5), 589–603. https://doi.org/10.1111/j.1600-0854.2006.00412.x

Mettlen, M., Stoeber, M., Loerke, D., Antonescu, C. N., Danuser, G., & Schmid, S. L. (2009). Endocytic accessory proteins are functionally distinguished by their differential effects on the maturation of clathrin-coated pits. *Molecular Biology of the Cell*, *20*(14), 3251–60. https://doi.org/10.1091/mbc.E09-03-0256

Miki, H., Yamaguchi, H., Suetsugu, S., & Takenawa, T. (2000). IRSp53 is an essential intermediate between Rac and WAVE in the regulation of membrane ruffling. *Nature*, *408*(6813), 732–735. https://doi.org/10.1038/35047107

Mikla, V. I., & Mikla, V. V. (2014). Ultrasound Imaging. In *Medical Imaging Technology* (pp. 113–128). Elsevier. https://doi.org/10.1016/B978-0-12-417021-6.00007-1

Miller, D. L., Nyborg, W. L., & Whitcomb, C. C. (1978). In Vitro Clumping of Platelets Exposed to Low Intensity Ultrasound. In *Ultrasound in Medicine* (pp. 545–553). Boston, MA: Springer US. https://doi.org/10.1007/978-1-4613-4021-8_120

Miller, D. L., Smith, N. B., Bailey, M. R., Czarnota, G. J., Hynynen, K., & Makin, I. R. S. (2012). Overview of therapeutic ultrasound applications and safety considerations. *Journal of Ultrasound in Medicine : Official Journal of the American Institute of Ultrasound in Medicine*, *31*(4), 623–34. https://doi.org/10.1016/j.biotechadv.2011.08.021.Secreted

Miller, D. L., Thomas, R. M., & Williams, A. R. (1991). Mechanisms for hemolysis by ultrasonic cavitation in the rotating exposure system. *Ultrasound in Medicine & Biology*, *17*(2), 171–8. Retrieved from http://www.ncbi.nlm.nih.gov/pubmed/2053213

Miller, M. W. (2000). Gene transfection and drug delivery. *Ultrasound in Medicine & Biology*, *26*, S59–S62. https://doi.org/10.1016/S0301-5629(00)00166-6

Miller, S. E., Mathiasen, S., Bright, N. A., Pierre, F., Kelly, B. T., Kladt, N., … Owen, D. J. (2015). CALM regulates clathrin-coated vesicle size and maturation by directly sensing and

driving membrane curvature. *Developmental Cell*, *33*(2), 163–75. https://doi.org/10.1016/j.devcel.2015.03.002

Mishra, S. K., Keyel, P. A., Hawryluk, M. J., Agostinelli, N. R., Watkins, S. C., & Traub, L. M. (2002). Disabled-2 exhibits the properties of a cargo-selective endocytic clathrin adaptor. *EMBO Journal*, *21*(18), 4915–4926. https://doi.org/10.1093/emboj/cdf487

Mitchell, D. A., Vasudevan, A., Linder, M. E., & Deschenes, R. J. (2006). Protein palmitoylation by a family of DHHC protein S-acyltransferases. *Journal of Lipid Research*, *47*(6), 1118–1127. https://doi.org/10.1194/jlr.R600007-JLR200

Mitragotri, S., Burke, P. A., & Langer, R. (2014). Overcoming the challenges in administering biopharmaceuticals: formulation and delivery strategies. *Nature Publishing Group*, *13*. https://doi.org/10.1038/nrd4363

Mitri, Z., Constantine, T., & O'Regan, R. (2012). The HER2 Receptor in Breast Cancer: Pathophysiology, Clinical Use, and New Advances in Therapy. *Chemotherapy Research and Practice*, *2012*, 743193. https://doi.org/10.1155/2012/743193

Mittal, B. (2017). Pharmacokinetics and Preformulation. In M. Levin (Ed.), *How to Develop Robust Solid Oral Dosage Forms from Conception to Post-Approval* (pp. 17–37). London: Academic Press. https://doi.org/10.1016/B978-0-12-804731-6.00002-9

Miyaji, M., Jin, Z.-X., Yamaoka, S., Amakawa, R., Fukuhara, S., Sato, S. B., … Umehara, H. (2005). Role of membrane sphingomyelin and ceramide in platform formation for Fas-mediated apoptosis. *The Journal of Experimental Medicine*, *202*(2), 249–59. https://doi.org/10.1084/jem.20041685

Miyake, K., & McNeil, P. L. (1995). Vesicle accumulation and exocytosis at sites of plasma membrane disruption. *The Journal of Cell Biology*, *131*(6 Pt 2), 1737–45. Retrieved from

http://www.ncbi.nlm.nih.gov/pubmed/8557741

Monteiro, N., Martins, A., Reis, R. L., & Neves, N. M. (2014). Liposomes in tissue engineering and regenerative medicine. *Journal of The Royal Society Interface*, *11*(101), 20140459–20140459. https://doi.org/10.1098/rsif.2014.0459

Mørch, K. A. (2015). Cavitation inception from bubble nuclei. *Interface Focus*, *5*(5), 20150006. https://doi.org/10.1098/rsfs.2015.0006

Morin, S.-H., Lim, A.-K., Cobbold, J.-F., & Taylor-Robinson, S. D. (2007). Use of second generation contrast-enhanced ultrasound in the assessment of focal liver lesions. *World Journal of Gastroenterology*, *13*(45), 5963–70. https://doi.org/10.3748/WJG.V13.45.5963

Morishita, S. (1997). *Effect of the tricyclic antidepressant desipramine on protein kinase C in rat brain and rabbit platelets in vitro*. *Psychiafry and Clinical Neurosciences* (Vol. 51). Retrieved from https://onlinelibrary.wiley.com/doi/pdf/10.1111/j.1440-1819.1997.tb02592.x

Morishita, S., & Watanabe, S. (1997). Effect of the tricyclic antidepressant desipramine on protein kinase C in rat brain and rabbit platelets in vitro. *Psychiatry and Clinical Neurosciences*, *51*(4), 249–52. Retrieved from http://www.ncbi.nlm.nih.gov/pubmed/9316173

Morrow, I. C., & Parton, R. G. (2005). Flotillins and the PHB Domain Protein Family: Rafts, Worms and Anaesthetics. *Traffic*, *6*(9), 725–740. https://doi.org/10.1111/j.1600-0854.2005.00318.x

Morrow, I. C., Rea, S., Martin, S., Prior, I. A., Prohaska, R., Hancock, J. F., … Parton, R. G. (2002). Flotillin-1/reggie-2 traffics to surface raft domains via a novel Golgi-independent pathway. Identification of a novel membrane targeting domain and a role for palmitoylation.

Journal of Biological Chemistry, *277*(50), 48834–48841. https://doi.org/10.1074/jbc.M209082200

Mukai, J., Dhilla, A., Drew, L. J., Stark, K. L., Cao, L., MacDermott, A. B., … Gogos, J. A. (2008). Palmitoylation-dependent neurodevelopmental deficits in a mouse model of 22q11 microdeletion. *Nature Neuroscience*, *11*(11), 1302–1310. https://doi.org/10.1038/nn.2204

Mukai, J., Liu, H., Burt, R. A., Swor, D. E., Lai, W. S., Karayiorgou, M., & Gogos, J. A. (2004). Evidence that the gene encoding ZDHHC8 contributes to the risk of schizophrenia. *Nature Genetics*, *36*(7), 725–731. https://doi.org/10.1038/ng1375

Mukherjee, D., Wong, J., Griffin, B., Ellis, S. G., Porter, T., Sen, S., & Thomas, J. D. (2000). Ten-fold augmentation of endothelial uptake of vascular endothelial growth factor with ultrasound after systemic administration. *Journal of the American College of Cardiology*, *35*(6), 1678–86. Retrieved from http://www.ncbi.nlm.nih.gov/pubmed/10807476

Müller, G., Ayoub, M., Storz, P., Rennecke, J., Fabbro, D., & Pfizenmaier, K. (1995). PKC zeta is a molecular switch in signal transduction of TNF-alpha, bifunctionally regulated by ceramide and arachidonic acid. *The EMBO Journal*, *14*(9), 1961–9. Retrieved from http://www.ncbi.nlm.nih.gov/pubmed/7744003

Mullick Chowdhury, S., Lee, T., & Willmann, J. K. (2017). Ultrasound-guided drug delivery in cancer. *Ultrasonography (Seoul, Korea)*, *36*(3), 171–184. https://doi.org/10.14366/usg.17021

Munksgaard, B., Futter, C. E., & White, I. J. (2007). Annexins and Endocytosis. *The Authors Journal Compilation #*. https://doi.org/10.1111/j.1600-0854.2007.00590.x

Murphy, J. E., Padilla, B. E., Hasdemir, B., Cottrell, G. S., & Bunnett, N. W. (2009). Endosomes: a legitimate platform for the signaling train. *Proceedings of the National*

Academy of Sciences of the United States of America, *106*(42), 17615–22. https://doi.org/10.1073/pnas.0906541106

Naslavsky, N., Weigert, R., & Donaldson, J. G. (2003). Convergence of Non-clathrin- and Clathrin-derived Endosomes Involves Arf6 Inactivation and Changes in Phosphoinositides. *Molecular Biology of the Cell*, *14*(2), 417–431. https://doi.org/10.1091/mbc.02-04-0053

Neisius, A., Lipkin, M. E., Rassweiler, J. J., Zhong, P., Preminger, G. M., & Knoll, T. (2014). Shock wave lithotripsy: The new phoenix? *World Journal of Urology*, *33*(2), 213–221. https://doi.org/10.1007/s00345-014-1369-3

Neumann-Giesen, C., Falkenbach, B., Beicht, P., Claasen, S., Luers, G., Stuermer, C. A., … Tikkanen, R. (2004). Membrane and raft association of reggie-1/flotillin-2: role of myristoylation, palmitoylation and oligomerization and induction of filopodia by overexpression. *Biochem J*, *378*(Pt 2), 509–518. https://doi.org/10.1042/BJ20031100

Northfelt, D. W., Martin, F. J., Working, P., Volberding, P. A., Russell, J., Newman, M., … Kaplan, L. D. (1996). Doxorubicin encapsulated in liposomes containing surface-bound polyethylene glycol: pharmacokinetics, tumor localization, and safety in patients with AIDS-related Kaposi's sarcoma. *Journal of Clinical Pharmacology*, *36*(1), 55–63. Retrieved from http://www.ncbi.nlm.nih.gov/pubmed/8932544

O'Brien Jr., W. (2007). Ultrasound–biophysics mechanisms. *Progress in Biophysics and Molecular Biology*, *93*(1–3), 212–255. https://doi.org/10.1016/j.pbiomolbio.2006.07.010

Ohl, C. D., & Ikink, R. (2003). Shock-Wave-Induced Jetting of Micron-Size Bubbles. *Physical Review Letters*, *90*(21), 214502. https://doi.org/10.1103/PhysRevLett.90.214502

Ohno, Y., Kihara, A., Sano, T., & Igarashi, Y. (2006). Intracellular localization and tissue-specific distribution of human and yeast DHHC cysteine-rich domain-containing proteins.

Biochimica et Biophysica Acta (BBA) - Molecular and Cell Biology of Lipids, *1761*(4), 474–483. https://doi.org/10.1016/j.bbalip.2006.03.010

Pacey, S., Workman, P., & Sarker, D. (2011). Pharmacokinetics and Pharmacodynamics in Drug Development. In *Encyclopedia of Cancer* (pp. 2845–2848). Berlin, Heidelberg: Springer Berlin Heidelberg. https://doi.org/10.1007/978-3-642-16483-5_4501

Palacios, F., Schweitzer, J. K., Boshans, R. L., & D'Souza-Schorey, C. (2002). ARF6-GTP recruits Nm23-H1 to facilitate dynamin-mediated endocytosis during adherens junctions disassembly. *Nature Cell Biology*, *4*(12), 929–936. https://doi.org/10.1038/ncb881

Panje, C. M., Wang, D. S., Pysz, M. A., Paulmurugan, R., Ren, Y., Tranquart, F., … Willmann, J. K. (2012). Ultrasound-Mediated Gene Delivery with Cationic Versus Neutral Microbubbles: Effect of DNA and Microbubble Dose on *In Vivo* Transfection Efficiency. *Theranostics*, *2*(11), 1078–1091. https://doi.org/10.7150/thno.4240

Park, J., Zhang, Y., Vykhodtseva, N., Akula, J. D., & McDannold, N. J. (2012). Targeted and Reversible Blood-Retinal Barrier Disruption via Focused Ultrasound and Microbubbles. *PLoS ONE*, *7*(8), e42754. https://doi.org/10.1371/journal.pone.0042754

Parker, M. (2017). Automotive Radar. In *Digital Signal Processing 101* (2nd ed., pp. 253–276). Newnes. https://doi.org/10.1016/B978-0-12-811453-7.00020-2

Parton, R. G., & del Pozo, M. A. (2013). Caveolae as plasma membrane sensors, protectors and organizers. *Nature Reviews Molecular Cell Biology*, *14*(2), 98–112. https://doi.org/10.1038/nrm3512

Parton, R. G., Joggerst, B., & Simons, K. (1994). Regulated internalization of caveolae. *The Journal of Cell Biology*, *127*(5), 1199–215. Retrieved from http://www.ncbi.nlm.nih.gov/pubmed/7962085

Patel, J. C., & Galán, J. E. (2006). Differential activation and function of Rho GTPases during *Salmonella*– host cell interactions. *The Journal of Cell Biology*, *175*(3), 453–463. https://doi.org/10.1083/jcb.200605144

Payne, C. K., Jones, S. A., Chen, C., & Zhuang, X. (2007). Internalization and trafficking of cell surface proteoglycans and proteoglycan-binding ligands. *Traffic*, *8*(4), 389–401. https://doi.org/10.1111/j.1600-0854.2007.00540.x

Pelkmans, L., Kartenbeck, J., & Helenius, A. (2001). Caveolar endocytosis of simian virus 40 reveals a new two-step vesicular-transport pathway to the ER. *Nature Cell Biology*, *3*(5), 473–483. https://doi.org/10.1038/35074539

Pelkmans, L., & Zerial, M. (2005). Kinase-regulated quantal assemblies and kiss-and-run recycling of caveolae. *Nature*, *436*(7047), 128–133. https://doi.org/10.1038/nature03866

Perrie, Y., & Rades, T. (2012). Controlling drug delivery. In *Pharmaceutics: Drug Delivery and Targeting* (2nd ed., pp. 1–24). London: Pharmaceutical Press. Retrieved from https://books.google.ca/books/about/FASTtrack_Pharmaceutics.html?id=F9DNMYOG7IoC&redir_esc=y

Phillips, L. C., Klibanov, A. L., Wamhoff, B. R., & Hossack, J. A. (2010). Targeted gene transfection from microbubbles into vascular smooth muscle cells using focused, ultrasound-mediated delivery. *Ultrasound in Medicine & Biology*, *36*(9), 1470–80. https://doi.org/10.1016/j.ultrasmedbio.2010.06.010

Phillips, L. C., Klibanov, A. L., Wamhoff, B. R., & Hossack, J. A. (2011). Localized ultrasound enhances delivery of rapamycin from microbubbles to prevent smooth muscle proliferation. *Journal of Controlled Release*, *154*(1), 42–49. https://doi.org/10.1016/j.jconrel.2011.04.020

Ping, P., Zhang, J., Qiu, Y., Tang, X. L., Manchikalapudi, S., Cao, X., & Bolli, R. (1997).

Ischemic preconditioning induces selective translocation of protein kinase C isoforms epsilon and eta in the heart of conscious rabbits without subcellular redistribution of total protein kinase C activity. *Circulation Research*, *81*(3), 404–14. Retrieved from http://www.ncbi.nlm.nih.gov/pubmed/9285643

Pollard, T. D., & Borisy, G. G. (2003). Cellular motility driven by assembly and disassembly of actin filaments. *Cell*, *112*(4), 453–65. Retrieved from http://www.ncbi.nlm.nih.gov/pubmed/12600310

Pollitt, A. Y., & Insall, R. H. (2009). WASP and SCAR/WAVE proteins: the drivers of actin assembly. *Journal of Cell Science*, *122*(Pt 15), 2575–8. https://doi.org/10.1242/jcs.023879

Popova, N. V., Deyev, I. E., & Petrenko, A. G. (2013). Clathrin-mediated endocytosis and adaptor proteins. *Acta Naturae*, *5*(18), 62–73.

Potez, S., Luginbühl, M., Monastyrskaya, K., Hostettler, A., Draeger, A., & Babiychuk, E. B. (2011). Tailored protection against plasmalemmal injury by annexins with different Ca2+ sensitivities. *The Journal of Biological Chemistry*, *286*(20), 17982–91. https://doi.org/10.1074/jbc.M110.187625

Prentice, P., Cuschieri, A., Dholakia, K., Prausnitz, M., & Campbell, P. (2005). Membrane disruption by optically controlled microbubble cavitation. *Nature Physics*, *1*(2), 107–110. https://doi.org/10.1038/nphys148

Prescott, G. R., Gorleku, O. A., Greaves, J., & Chamberlain, L. H. (2009). Palmitoylation of the synaptic vesicle fusion machinery. *Journal of Neurochemistry*, *110*(4), 1135–1149. https://doi.org/10.1111/j.1471-4159.2009.06205.x

Puertollano, R. (2004). Clathrin-mediated transport: assembly required. *EMBO Reports*, *5*(10), 942–946. https://doi.org/10.1038/sj.embor.7400249

Puri, A., Loomis, K., Smith, B., Lee, J.-H., Yavlovich, A., Heldman, E., & Blumenthal, R. (2009). Lipid-Based Nanoparticles as Pharmaceutical Drug Carriers: From Concepts to Clinic. *Critical Reviews™ in Therapeutic Drug Carrier Systems*, *26*(6), 523–580. https://doi.org/10.1615/CritRevTherDrugCarrierSyst.v26.i6.10

Pysz, M. A., Foygel, K., Rosenberg, J., Gambhir, S. S., Schneider, M., & Willmann, J. K. (2010). Antiangiogenic Cancer Therapy: Monitoring with Molecular US and a Clinically Translatable Contrast Agent (BR55). *Radiology*, *256*(2), 519–527. https://doi.org/10.1148/radiol.10091858

Qiu, Y., Luo, Y., Zhang, Y., Cui, W., Zhang, D., Wu, J., … Tu, J. (2010). The correlation between acoustic cavitation and sonoporation involved in ultrasound-mediated DNA transfection with polyethylenimine (PEI) in vitro. *Journal of Controlled Release : Official Journal of the Controlled Release Society*, *145*(1), 40–8. https://doi.org/10.1016/j.jconrel.2010.04.010

Rajagopal, K., Wood, J., Tran, B., Patapoff, T. W., & Nivaggioli, T. (2013). Trehalose Limits BSA Aggregation in Spray-Dried Formulations at High Temperatures: Implications in Preparing Polymer Implants for Long-Term Protein Delivery. *Journal of Pharmaceutical Sciences*, *102*(8), 2655–2666. https://doi.org/10.1002/jps.23634

Rajendran, L., Knölker, H.-J., & Simons, K. (2010). Subcellular targeting strategies for drug design and delivery. *Nature Reviews Drug Discovery*, *9*(1), 29–42. https://doi.org/10.1038/nrd2897

Rao, Y., Ma, Q., Vahedi-Faridi, A., Sundborger, A., Pechstein, A., Puchkov, D., … Haucke, V. (2010). Molecular basis for SH3 domain regulation of F-BAR-mediated membrane deformation. *Proceedings of the National Academy of Sciences*, *107*(18), 8213–8218.

https://doi.org/10.1073/pnas.1003478107

Reddy, A., Caler, E. V., & Andrews, N. W. (2001). Plasma membrane repair is mediated by Ca2+-regulated exocytosis of lysosomes. *Cell*, *106*(2), 157–169. https://doi.org/10.1016/S0092-8674(01)00421-4

Richards, A. A., Stang, E., Pepperkok, R., & Parton, R. G. (2002). Inhibitors of COP-mediated transport and cholera toxin action inhibit simian virus 40 infection. *Molecular Biology of the Cell*, *13*(5), 1750–64. https://doi.org/10.1091/mbc.01-12-0592

Richterova, Z., Liebl, D., Horak, M., Palkova, Z., Stokrova, J., Hozak, P., … Forstova, J. (2001). Caveolae Are Involved in the Trafficking of Mouse Polyomavirus Virions and Artificial VP1 Pseudocapsids toward Cell Nuclei. *Journal of Virology*, *75*(22), 10880–10891. https://doi.org/10.1128/JVI.75.22.10880-10891.2001

Riento, K., Frick, M., Schafer, I., & Nichols, B. J. (2009). Endocytosis of flotillin-1 and flotillin-2 is regulated by Fyn kinase. *Journal of Cell Science*, *122*(Pt 7), 912–8. https://doi.org/10.1242/jcs.039024

Rocks, O., Gerauer, M., Vartak, N., Koch, S., Huang, Z. P., Pechlivanis, M., … Bastiaens, P. I. H. (2010). The palmitoylation machinery is a spatially organizing system for peripheral membrane proteins. *Cell*, *141*(3), 458–471. https://doi.org/10.1016/j.cell.2010.04.007

Rodríguez, A., Webster, P., Ortego, J., & Andrews, N. W. (1997). Lysosomes Behave as Ca 2. *Cell*, *137*(1), 93–104.

Rohatgi, R., Ho, H. Y., & Kirschner, M. W. (2000). Mechanism of N-WASP activation by CDC42 and phosphatidylinositol 4, 5-bisphosphate. *The Journal of Cell Biology*, *150*(6), 1299–310. Retrieved from http://www.ncbi.nlm.nih.gov/pubmed/10995436

Romiti, E., Vasta, V., Meacci, E., Farnararo, M., Linke, T., Ferlinz, K., … Bruni, P. (2000).

Characterization of sphingomyelinase activity released by thrombin-stimulated platelets. *Molecular and Cellular Biochemistry*, *205*(1/2), 75–81. https://doi.org/10.1023/A:1007041329052

Rooijen, N. va. (1998). Liposomes. In P. J. Delves (Ed.), *Encyclopedia of Immunology* (2nd ed., pp. 1588–1592). London: Academic Press. https://doi.org/10.1006/RWEI.1999.0407

Ross, E., Ata, R., Thavarajah, T., Medvedev, S., Bowden, P., Marshall, G., & Antonescu, C. N. (2015). AMP-Activated Protein Kinase Regulates the Cell Surface Proteome and Integrin Membrane Traffic, 1–29. https://doi.org/10.1371/journal.pone.0128013

Rothberg, K. G., Ying, Y. S., Kolhouse, J. F., Kamen, B. A., & Anderson, R. G. (1990). The glycophospholipid-linked folate receptor internalizes folate without entering the clathrin-coated pit endocytic pathway. *The Journal of Cell Biology*, *110*(3), 637–49. Retrieved from http://www.ncbi.nlm.nih.gov/pubmed/1968465

Roy, S., Plowman, S., Rotblat, B., Prior, I. A., Muncke, C., Grainger, S., … Hancock, J. F. (2005). Individual palmitoyl residues serve distinct roles in H-Ras. *Molecular and Cellular Biology*, *25*(15), 6722–6733. https://doi.org/10.1128/MCB.25.15.6722

Sabharanjak, S., Sharma, P., Parton, R. G., & Mayor, S. (2002). GPI-Anchored Proteins Are Delivered to Recycling Endosomes via a Distinct cdc42-Regulated, Clathrin-Independent Pinocytic Pathway. *Developmental Cell*, *2*(4), 411–423. https://doi.org/10.1016/S1534-5807(02)00145-4

Salaun, C., Greaves, J., & Chamberlain, L. H. (2010). The intracellular dynamic of protein palmitoylation. *Journal of Cell Biology*, *191*(7), 1229–1238. https://doi.org/10.1083/jcb.201008160

Sandvig, K., Kavaliauskiene, S., & Skotland, T. (2018). Clathrin-independent endocytosis: an

increasing degree of complexity. *Histochemistry and Cell Biology*, *150*(2), 107–118. https://doi.org/10.1007/s00418-018-1678-5

Sandvig, K., Pust, S., Skotland, T., & van Deurs, B. (2011). Clathrin-independent endocytosis: Mechanisms and function. *Current Opinion in Cell Biology*, *23*(4), 413–420. https://doi.org/10.1016/j.ceb.2011.03.007

Santana, P., Peña, L. A., Haimovitz-Friedman, A., Martin, S., Green, D., McLoughlin, M., … Kolesnick, R. (1996). Acid sphingomyelinase-deficient human lymphoblasts and mice are defective in radiation-induced apoptosis. *Cell*, *86*(2), 189–99. Retrieved from http://www.ncbi.nlm.nih.gov/pubmed/8706124

Sapra, P., & Allen, T. M. (2003). Ligand-targeted liposomal anticancer drugs. *Progress in Lipid Research*, *42*(5), 439–62. Retrieved from http://www.ncbi.nlm.nih.gov/pubmed/12814645

Saraiva, C., Praça, C., Ferreira, R., Santos, T., Ferreira, L., & Bernardino, L. (2016). Nanoparticle-mediated brain drug delivery: Overcoming blood–brain barrier to treat neurodegenerative diseases. *Journal of Controlled Release*, *235*, 34–47. https://doi.org/10.1016/J.JCONREL.2016.05.044

Sasahara, K., McPhie, P., & Minton, A. P. (2003). Effect of dextran on protein stability and conformation attributed to macromolecular crowding. *Journal of Molecular Biology*, *326*(4), 1227–37. Retrieved from http://www.ncbi.nlm.nih.gov/pubmed/12589765

Sauvonnet, N., Dujeancourt, A., & Dautry-Varsat, A. (2005). Cortactin and dynamin are required for the clathrin-independent endocytosis of γc cytokine receptor. *The Journal of Cell Biology*, *168*(1), 155–163. https://doi.org/10.1083/jcb.200406174

Schafer, M. E. (2015). Ultrasonic surgical devices and procedures. In J. A. Gallego-Juárez & K. F. Graff (Eds.), *Power Ultrasonics* (pp. 633–660). Cambridge: Woodhead Publishing.

https://doi.org/10.1016/B978-1-78242-028-6.00021-1

Schlicher, R. K., Radhakrishna, H., Tolentino, T. P., Apkarian, R. P., Zarnitsyn, V., & Prausnitz, M. R. (2006). Mechanism of intracellular delivery by acoustic cavitation. *Ultrasound in Medicine & Biology*, *32*(6), 915–924. https://doi.org/10.1016/j.ultrasmedbio.2006.02.1416

Schneider, A., Rajendran, L., Honsho, M., Gralle, M., Donnert, G., Wouters, F., … Simons, M. (2008). Flotillin-Dependent Clustering of the Amyloid Precursor Protein Regulates Its Endocytosis and Amyloidogenic Processing in Neurons. *Journal of Neuroscience*, *28*(11), 2874–2882. https://doi.org/10.1523/JNEUROSCI.5345-07.2008

Schneider, C. A., Rasband, W. S., & Eliceiri, K. W. (2012). NIH Image to ImageJ: 25 years of image analysis. *Nature Methods*, *9*(7), 671–5.

Schneider, P. B., & Kennedy, E. P. (1967). Sphingomyelinase in normal human spleens and in spleens from subjects with Niemann-Pick disease. *Journal of Lipid Research*, *8*(3), 202–9. Retrieved from http://www.ncbi.nlm.nih.gov/pubmed/4962590

Schnitzer, J. E., Oh, P., Pinney, E., & Allard, J. (1994). Filipin-sensitive caveolae-mediated transport in endothelium: reduced transcytosis, scavenger endocytosis, and capillary permeability of select macromolecules. *The Journal of Cell Biology*, *127*(5), 1217–32. Retrieved from http://www.ncbi.nlm.nih.gov/pubmed/7525606

Schuchman, E. H., Suchi, M., Takahashi, T., Sandhoff, K., & Desnick, R. J. (1991). Human acid sphingomyelinase. Isolation, nucleotide sequence and expression of the full-length and alternatively spliced cDNAs. *The Journal of Biological Chemistry*, *266*(13), 8531–9. Retrieved from http://www.ncbi.nlm.nih.gov/pubmed/1840600

Sen, T., Tufekcioglu, O., & Koza, Y. (2015). Mechanical index. *Anadolu Kardiyoloji Dergisi/The Anatolian Journal of Cardiology*, *15*(4), 334–336.

https://doi.org/10.5152/akd.2015.6061

Senju, Y., Itoh, Y., Takano, K., Hamada, S., & Suetsugu, S. (2011). Essential role of PACSIN2/syndapin-II in caveolae membrane sculpting. *Journal of Cell Science*, *124*(12), 2032–2040. https://doi.org/10.1242/jcs.086264

Sennoga, C. A., Kanbar, E., Auboire, L., Dujardin, P. A., Fouan, D., Escoffre, J. M., & Bouakaz, A. (2017). Microbubble-mediated ultrasound drug-delivery and therapeutic monitoring. *Expert Opinion on Drug Delivery*, *14*(9), 1031–1043. https://doi.org/10.1080/17425247.2017.1266328

Sercombe, L., Veerati, T., Moheimani, F., Wu, S. Y., Sood, A. K., & Hua, S. (2015). Advances and Challenges of Liposome Assisted Drug Delivery. *Frontiers in Pharmacology*, *6*, 286. https://doi.org/10.3389/fphar.2015.00286

Sharma, P., Varma, R., Sarasij, R. C., Ira, Gousset, K., Krishnamoorthy, G., … Mayor, S. (2004). Nanoscale organization of multiple GPI-anchored proteins in living cell membranes. *Cell*, *116*(4), 577–89. Retrieved from http://www.ncbi.nlm.nih.gov/pubmed/14980224

Shaughnessy, R., Retamal, C., Oyanadel, C., Norambuena, A., López, A., Bravo-Zehnder, M., … González, A. (2014). Epidermal growth factor receptor endocytic traffic perturbation by phosphatidate phosphohydrolase inhibition: new strategy against cancer. *FEBS Journal*, *281*(9), 2172–2189. https://doi.org/10.1111/febs.12770

Sheikov, N., McDannold, N., Sharma, S., & Hynynen, K. (2008). Effect of focused ultrasound applied with an ultrasound contrast agent on the tight junctional integrity of the brain microvascular endothelium. *Ultrasound in Medicine & Biology*, *34*(7), 1093. https://doi.org/10.1016/J.ULTRASMEDBIO.2007.12.015

Shimada, A., Niwa, H., Tsujita, K., Suetsugu, S., Nitta, K., Hanawa-Suetsugu, K., … Yokoyama,

S. (2007). Curved EFC/F-BAR-domain dimers are joined end to end into a filament for membrane invagination in endocytosis. *Cell*, *129*(4), 761–72. https://doi.org/10.1016/j.cell.2007.03.040

Shung, K. K. (2011). Introduction to biomedical engineering. *Journal of Medical and Biological Engineering*, *31*(6), 371. https://doi.org/10.5405/jmbe.871

Silva, L., Almeida, R. F. M. De, Fedorov, A., Matos, A. P. A., & Prieto, M. (2009). Ceramide-platform formation and -induced biophysical changes in a fluid phospholipid membrane. *Molecular Membrane Biology*.

Simons, K., & Ehehalt, R. (2002). Cholesterol, lipid rafts, and disease. *Journal of Clinical Investigation*, *110*(5), 597–603. https://doi.org/10.1172/JCI200216390

Sirsi, S., & Borden, M. (2009). Microbubble Compositions, Properties and Biomedical Applications. *Bubble Science, Engineering & Technology*, *1*(1–2), 3–17. https://doi.org/10.1179/175889709X446507.Microbubble

Slamon, D. J., Clark, G. M., Wong, S. G., Levin, W. J., Ullrich, A., & McGuire, W. L. (1987). Human breast cancer: correlation of relapse and survival with amplification of the HER-2/neu oncogene. *Science (New York, N.Y.)*, *235*(4785), 177–82. Retrieved from http://www.ncbi.nlm.nih.gov/pubmed/3798106

Slamon, D. J., Godolphin, W., Jones, L. A., Holt, J. A., Wong, S. G., Keith, D. E., … Ullrich, A. (1989). Studies of the HER-2/neu proto-oncogene in human breast and ovarian cancer. *Science (New York, N.Y.)*, *244*(4905), 707–12. Retrieved from http://www.ncbi.nlm.nih.gov/pubmed/2470152

Slaughter, N., Laux, I., Tu, X., Whitelegge, J., Zhu, X., Effros, R., … Andre, N. (2010). The flotillins are integral membrane proteins in lipid rafts that contain TCR-associated signaling

components: implications for T-cell activation. *Clinical Immunology*, *584*(13), 2740–2747. https://doi.org/10.1016/j.febslet.2010.03.030

Solis, G. P., Hoegg, M., Munderloh, C., Schrock, Y., Malaga-Trillo, E., Rivera-Milla, E., & Stuermer, C. A. O. (2007). Reggie/flotillin proteins are organized into stable tetramers in membrane microdomains. *Biochemical Journal*, *403*(2), 313–322. https://doi.org/10.1042/BJ20061686

Sorkin, A., & von Zastrow, M. (2002). Signal transduction and endocytosis: close encounters of many kinds. *Nature Reviews Molecular Cell Biology*, *3*(8), 600–614. https://doi.org/10.1038/nrm883

Sorkina, T., Caltagarone, J., & Sorkin, A. (2013). Flotillins Regulate Membrane Mobility of the Dopamine Transporter but Are Not Required for Its Protein Kinase C Dependent Endocytosis. *Traffic*, *14*(6), 709–724. https://doi.org/10.1111/tra.12059

Sorkina, T., Hoover, B. R., Zahniser, N. R., & Sorkin, A. (2005). Constitutive and protein kinase C-induced internalization of the dopamine transporter is mediated by a clathrin-dependent mechanism. *Traffic*, *6*(2), 157–170. https://doi.org/10.1111/j.1600-0854.2005.00259.x

Sot, J., Aranda, F. J., Collado, M.-I., Goñi, F. M., & Alonso, A. (2005). Different effects of long- and short-chain ceramides on the gel-fluid and lamellar-hexagonal transitions of phospholipids: a calorimetric, NMR, and x-ray diffraction study. *Biophysical Journal*, *88*(5), 3368–80. https://doi.org/10.1529/biophysj.104.057851

Sot, J., Bagatolli, L. A., Goñi, F. M., & Alonso, A. (2006). Detergent-resistant, ceramide-enriched domains in sphingomyelin/ceramide bilayers. *Biophysical Journal*, *90*(3), 903–14. https://doi.org/10.1529/biophysj.105.067710

Sowa, G., Pypaert, M., Fulton, D., & Sessa, W. C. (2003). The phosphorylation of caveolin-2 on

serines 23 and 36 modulates caveolin-1-dependent caveolae formation. *Proceedings of the National Academy of Sciences*, *100*(11), 6511–6516. https://doi.org/10.1073/pnas.1031672100

Spencer, T., Diego, S., Diego, S., & Kensington, S. (1990). Of a Specific Signal Sequence for Internalization, *110*(February), 283–294.

Spiering, D., & Hodgson, L. (2011). Dynamics of the Rho-family small GTPases in actin regulation and motility. *Cell Adhesion & Migration*, *5*(2), 170–80. https://doi.org/10.4161/CAM.5.2.14403

Stahlhut, M., & van Deurs, B. (2000). Identification of filamin as a novel ligand for caveolin-1: evidence for the organization of caveolin-1-associated membrane domains by the actin cytoskeleton. *Molecular Biology of the Cell*, *11*(1), 325–37. https://doi.org/10.1091/mbc.11.1.325

Stancevic, B., & Kolesnick, R. (2010). Ceramide-rich platforms in transmembrane signaling. *FEBS Letters*, *584*(9), 1728–40. https://doi.org/10.1016/j.febslet.2010.02.026

Starritt, H. C., Duck, F. A., & Humphrey, V. F. (1991). Forces acting in the direction of propagation in pulsed ultrasound fields. *Physics in Medicine and Biology*, *36*(11), 1465–1474. https://doi.org/10.1088/0031-9155/36/11/006

Steinhardt, R. A., Bi, G., & Alderton, J. M. (1994). Cell Membrane Resealing by a Vesicular Mechanism Similar to Neurotransmitter Release, *263*(5145), 390–393.

Stoeber, M., Stoeck, I. K., Hänni, C., Bleck, C. K. E., Balistreri, G., & Helenius, A. (2012). Oligomers of the ATPase EHD2 confine caveolae to the plasma membrane through association with actin. *The EMBO Journal*, *31*(10), 2350–2364. https://doi.org/10.1038/emboj.2012.98

Storm, G., ten Kate, M. T., Working, P. K., & Bakker-Woudenberg, I. A. (1998). Doxorubicin entrapped in sterically stabilized liposomes: effects on bacterial blood clearance capacity of the mononuclear phagocyte system. *Clinical Cancer Research : An Official Journal of the American Association for Cancer Research*, *4*(1), 111–5. Retrieved from http://www.ncbi.nlm.nih.gov/pubmed/9516959

Strauss, K., Goebel, C., Runz, H., Möbius, W., Weiss, S., Feussner, I., … Schneider, A. (2010). Exosome secretion ameliorates lysosomal storage of cholesterol in Niemann-Pick type C disease. *Journal of Biological Chemistry*, *285*(34), 26279–26288. https://doi.org/10.1074/jbc.M110.134775

Stride, E., & Saffari, N. (2003). Microbubble ultrasound contrast agents: A review. *Proceedings of the Institution of Mechanical Engineers, Part H: Journal of Engineering in Medicine*, *217*(6), 429–447. https://doi.org/10.1243/09544110360729072

Subathra, M., Qureshi, A., & Luberto, C. (2011). Sphingomyelin Synthases Regulate Protein Trafficking and Secretion. *PLoS ONE*, *6*(9), e23644. https://doi.org/10.1371/journal.pone.0023644

Südhof, T. C. (2002). Synaptotagmins: why so many? *The Journal of Biological Chemistry*, *277*(10), 7629–32. https://doi.org/10.1074/jbc.R100052200

Sugawara, Y., Nishii, H., Takahashi, T., Yamauchi, J., Mizuno, N., Tago, K., & Itoh, H. (2007). The lipid raft proteins flotillins/reggies interact with G??q and are involved in Gq-mediated p38 mitogen-activated protein kinase activation through tyrosine kinase. *Cellular Signalling*, *19*(6), 1301–1308. https://doi.org/10.1016/j.cellsig.2007.01.012

Sultatos, L. (2007). Regional Blood Flow. In S. J. Enna & D. B. Bylund (Eds.), *xPharm: The Comprehensive Pharmacology Reference* (pp. 1–2). Elsevier. https://doi.org/10.1016/B978-

008055232-3.60024-8

Suslick, K. S., & Flannigan, D. J. (2008). Inside a Collapsing Bubble: Sonoluminescence and the Conditions During Cavitation. *Annual Review of Physical Chemistry*, *59*(1), 659–683. https://doi.org/10.1146/annurev.physchem.59.032607.093739

Swallow, L. M., Siores, E., Dodds, D., & Luo, J. K. (2010). Self-Powered Medical Devices for Vibration Suppression. In S. C. Anand, J. F. Kennedy, M. Miraftab, & S. Rajendran (Eds.), *Medical and Healthcare Textiles* (pp. 415–422). Woodhead Publishing. https://doi.org/10.1533/9780857090348.415

Swanson, J. A., & Watts, C. (1995). Macropinocytosis. *Trends in Cell Biology*, *5*(11), 424–8. https://doi.org/10.1016/S0962-8924(00)89101-1

Tabaczar, S., Czogalla, A., Podkalicka, J., Biernatowska, A., & Sikorski, A. F. (2017). Protein palmitoylation: Palmitoyltransferases and their specificity. *Experimental Biology and Medicine*, *242*(11), 1150–1157. https://doi.org/10.1177/1535370217707732

Tam, C., Idone, V., Devlin, C., Fernandes, M. C., Flannery, A., He, X., … Andrews, N. W. (2010). Exocytosis of acid sphingomyelinase by wounded cells promotes endocytosis and plasma membrane repair. *Journal of Cell Biology*, *189*(6), 1027–1038. https://doi.org/10.1083/jcb.201003053

Tanabe, K., Torii, T., Natsume, W., Braesch-Andersen, S., Watanabe, T., & Satake, M. (2005). A novel GTPase-activating protein for ARF6 directly interacts with clathrin and regulates clathrin-dependent endocytosis. *Molecular Biology of the Cell*, *16*(4), 1617–28. https://doi.org/10.1091/mbc.e04-08-0683

Taniyama, Y., Tachibana, K., Hiraoka, K., Namba, T., Yamasaki, K., Hashiya, N., … Morishita, R. (2002). Local delivery of plasmid DNA into rat carotid artery using ultrasound.

Circulation, *105*(10), 1233–9. Retrieved from http://www.ncbi.nlm.nih.gov/pubmed/11889019

Tardoski, S., Gineyts, E., Ngo, J., Kocot, A., Clézardin, P., & Melodelima, D. (2015). Low-Intensity Ultrasound Promotes Clathrin-Dependent Endocytosis for Drug Penetration into Tumor Cells. *Ultrasound in Medicine & Biology*, *41*(10), 2740–54. https://doi.org/10.1016/j.ultrasmedbio.2015.06.006

Thomas, G. M., Hayashi, T., Chen, C.-M., Chiu, S.-L., & Huganir, R. L. (2013). Palmitoylation by DHHC5/8 targets GRIP1 to dendritic endosomes to regulate AMPA-R trafficking. *Magn Reson Imaging*, *31*(3), 477–479. https://doi.org/10.1016/j.immuni.2010.12.017.Two-stage

Thomsen, P., Roepstorff, K., Stahlhut, M., & van Deurs, B. (2002). Caveolae are highly immobile plasma membrane microdomains, which are not involved in constitutive endocytic trafficking. *Molecular Biology of the Cell*, *13*(1), 238–50. https://doi.org/10.1091/mbc.01-06-0317

Tillement, J. P., & Tremblay, D. (2007). Clinical Pharmacokinetic Criteria for Drug Research. In J. B. Taylor & D. J. Triggle (Eds.), *Comprehensive Medicinal Chemistry II* (2nd ed., pp. 11–30). Elsevier. https://doi.org/10.1016/B0-08-045044-X/00117-6

Torchilin, V. P., Klibanov, A. L., Huang, L., O'Donnell, S., Nossiff, N. D., & Khaw, B. A. (1992). Targeted accumulation of polyethylene glycol-coated immunoliposomes in infarcted rabbit myocardium. *FASEB Journal : Official Publication of the Federation of American Societies for Experimental Biology*, *6*(9), 2716–9. Retrieved from http://www.ncbi.nlm.nih.gov/pubmed/1612296

Tran, T. A., Roger, S., Le Guennec, J. Y., Tranquart, F., & Bouakaz, A. (2007). Effect of ultrasound-activated microbubbles on the cell electrophysiological properties. *Ultrasound in*

Medicine & Biology, *33*(1), 158–163. https://doi.org/10.1016/j.ultrasmedbio.2006.07.029

Treat, L. H., McDannold, N., Zhang, Y., Vykhodtseva, N., & Hynynen, K. (2012). Improved anti-tumor effect of liposomal doxorubicin after targeted blood-brain barrier disruption by MRI-guided focused ultrasound in rat glioma. *Ultrasound in Medicine & Biology*, *38*(10), 1716–25. https://doi.org/10.1016/j.ultrasmedbio.2012.04.015

Truman, J.-P., Al Gadban, M. M., Smith, K. J., Jenkins, R. W., Mayroo, N., Virella, G., … Hammad, S. M. (2012). Differential regulation of acid sphingomyelinase in macrophages stimulated with oxidized low-density lipoprotein (LDL) and oxidized LDL immune complexes: role in phagocytosis and cytokine release. *Immunology*, *136*(1), 30–45. https://doi.org/10.1111/j.1365-2567.2012.03552.x

Tsutsui, J. M., Xie, F., & Porter, R. T. (2004). The use of microbubbles to target drug delivery. *Cardiovascular Ultrasound*, *2*, 23. https://doi.org/10.1186/1476-7120-2-23

Turfus, S. C., Delgoda, R., Picking, D., & Gurley, B. J. (2017). Pharmacokinetics. In S. Badal & R. Delgoda (Eds.), *Pharmacognosy Fundamentals, Applications and Strategies* (pp. 495–512). London: Academic Press. https://doi.org/10.1016/B978-0-12-802104-0.00025-1

Turner, J. V., & Agatonovic-Kustrin, S. (2007). In Silico Prediction of Oral Bioavailability. In *Comprehensive Medicinal Chemistry II* (pp. 699–724). Elsevier. https://doi.org/10.1016/B0-08-045044-X/00147-4

Ulrich, A. S. (2002). *Biophysical Aspects of Using Liposomes as Delivery Vehicles*. *Bioscience Reports* (Vol. 22). Retrieved from https://link-springer-com.ezproxy.lib.ryerson.ca/content/pdf/10.1023%2FA%3A1020178304031.pdf

Ummadi, S., Shravani, B. N., Raghavendra Rao, N. G., Reddy, S. M., & Nayak, S. B. (2013). Overview on Controlled Release Dosage Form. *International Journal of Pharma Sciences*,

3(4), 258–269. Retrieved from http://ijps.aizeonpublishers.net/content/2013/4/ijps258-269.pdf

Unger, E. C., McCreery, T. P., Sweitzer, R. H., Caldwell, V. E., & Wu, Y. (1998). Acoustically active lipospheres containing paclitaxel: a new therapeutic ultrasound contrast agent. *Investigative Radiology*, *33*(12), 886–92. Retrieved from http://www.ncbi.nlm.nih.gov/pubmed/9851823

Van Blitterswijk, W. J., Van Der Luit, A. H., Veldman, R. J., Verheij, M., & Borst, J. (2003). *Ceramide : second messenger or modulator of membrane structure and dynamics ? Biochem. J* (Vol. 369). Retrieved from https://www.ncbi.nlm.nih.gov/pmc/articles/PMC1223095/pdf/12408751.pdf

Van Wamel, A., Bouakaz, A., & de Jong, N. (2003). Duration of ultrasound bubbles enhanced cell membrane permeability. *IEEE Symposium on Ultrasonics*, *1*, 917–920. https://doi.org/10.1109/ULTSYM.2003.1293549

van Wamel, A., Kooiman, K., Harteveld, M., Emmer, M., ten Cate, F. J., Versluis, M., & de Jong, N. (2006). Vibrating microbubbles poking individual cells: Drug transfer into cells via sonoporation. *Journal of Controlled Release*, *112*(2), 149–155. https://doi.org/10.1016/j.jconrel.2006.02.007

Veiga, M. P., Arrondo, L. J., Goñi, F. M., & Alonso, A. (1999). *Ceramides in Phospholipid Membranes: Effects on Bilayer Stability and Transition to Nonlamellar Phases*. *Biophysical Journal* (Vol. 76). https://doi.org/10.1016/S0006-3495(99)77201-2

Veithen, A., Cupers, P., Baudhuin, P., & Courtoy, P. J. (1996). v-Src induces constitutive macropinocytosis in rat fibroblasts. *Journal of Cell Science*, *109 (Pt 8)*, 2005–12. Retrieved from http://www.ncbi.nlm.nih.gov/pubmed/8856496

Vercauteren, D., Piest, M., van der Aa, L. J., Al Soraj, M., Jones, A. T., Engbersen, J. F. J., … Braeckmans, K. (2011). Flotillin-dependent endocytosis and a phagocytosis-like mechanism for cellular internalization of disulfide-based poly(amido amine)/DNA polyplexes. *Biomaterials*, *32*(11), 3072–3084. https://doi.org/10.1016/j.biomaterials.2010.12.045

Vigers, G. P., Crowther, R. A., & Pearse, B. M. (1986). Three-dimensional structure of clathrin cages in ice. *The EMBO Journal*, *5*(3), 529–34. Retrieved from http://www.pubmedcentral.nih.gov/articlerender.fcgi?artid=1166794&tool=pmcentrez&rendertype=abstract

Vykhodtseva, N., McDannold, N., & Hynynen, K. (2008). Progress and problems in the application of focused ultrasound for blood-brain barrier disruption. *Ultrasonics*, *48*(4), 279–296. https://doi.org/10.1016/j.ultras.2008.04.004

Wang, D. S., Panje, C., Pysz, M. A., Paulmurugan, R., Rosenberg, J., Gambhir, S. S., … Willmann, J. K. (2012). Cationic versus Neutral Microbubbles for Ultrasound-mediated Gene Delivery in Cancer. *Radiology*, *264*(3), 721–732. https://doi.org/10.1148/radiol.12112368

Wang, Q., Villeneuve, G., & Wang, Z. (2005). Control of epidermal growth factor receptor endocytosis by receptor dimerization, rather than receptor kinase activation. *EMBO Reports*, *6*(10), 942–8. https://doi.org/10.1038/sj.embor.7400491

Wang, X., Yang, Q., Guo, L., Li, X.-H., Zhao, X.-H., Song, L.-B., & Lin, H.-X. (2013). Flotillin-2 is associated with breast cancer progression and poor survival outcomes. *Journal of Translational Medicine*, *11*, 190. https://doi.org/10.1186/1479-5876-11-190

Wang, Y., Pennock, S., Chen, X., & Wang, Z. (2002). Endosomal signaling of epidermal growth factor receptor stimulates signal transduction pathways leading to cell survival. *Mol Cell*

Biol, *22*(20), 7279–7290. https://doi.org/10.1128/MCB.22.20.7279

Wang, Z., Thurmond, D. C., James, D. E., Osman, M. A., Schiavo, G., Bader, M. F., & Gasman, S. (2009). Mechanisms of biphasic insulin-granule exocytosis - roles of the cytoskeleton, small GTPases and SNARE proteins. *Journal of Cell Science*, *122*(Pt 7), 893–903. https://doi.org/10.1242/jcs.034355

Wedegaertner, P. B. (1998). Lipid modifications and membrane targeting of G alpha. *Neurosignals*, *7*(2), 125–135. https://doi.org/10.1159/000014538

Weller, G. E. R., Lu, E., Csikari, M. M., Klibanov, A. L., Fischer, D., Wagner, W. R., & Villanueva, F. S. (2003). Ultrasound Imaging of Acute Cardiac Transplant Rejection With Microbubbles Targeted to Intercellular Adhesion Molecule-1. *Circulation*, *108*(2), 218–224. https://doi.org/10.1161/01.CIR.0000080287.74762.60

Wen, H., Jung, H., & Li, X. (2015). Drug Delivery Approaches in Addressing Clinical Pharmacology-Related Issues: Opportunities and Challenges. *The AAPS Journal*, *17*(6), 1327–40. https://doi.org/10.1208/s12248-015-9814-9

Werling, D., Hope, J. C., Chaplin, P., Collins, R. A., Taylor, G., & Howard, C. J. (1999). Involvement of caveolae in the uptake of respiratory syncytial virus antigen by dendritic cells. *Journal of Leukocyte Biology*, *66*(1), 50–8. Retrieved from http://www.ncbi.nlm.nih.gov/pubmed/10410989

West, M. A., Bretscher, M. S., & Watts, C. (1989). Distinct endocytotic pathways in epidermal growth factor-stimulated human carcinoma A431 cells. *The Journal of Cell Biology*, *109*(6 Pt 1), 2731–9. Retrieved from http://www.ncbi.nlm.nih.gov/pubmed/2556406

Whalley, T., Terasaki, M., Cho, M. S., & Vogel, S. S. (1995). Direct membrane retrieval into large vesicles after exocytosis in sea urchin eggs. *Journal of Cell Biology*, *131*(5), 1183–

1192. https://doi.org/10.1083/jcb.131.5.1183

Wilczewska, A. Z., Niemirowicz, K., Markiewicz, K. H., & Car, H. (2012). Nanoparticles as drug delivery systems. *Pharmacological Reports*, *64*(5), 1020–1037. https://doi.org/10.1016/S1734-1140(12)70901-5

Williams, T. M., & Lisanti, M. P. (2004). The caveolin proteins. *Genome Biology*, *5*(3), 214. https://doi.org/10.1186/gb-2004-5-3-214

Willis, & Forssen. (1998). Ligand-targeted liposomes. *Advanced Drug Delivery Reviews*, *29*(3), 249–271. Retrieved from http://www.ncbi.nlm.nih.gov/pubmed/10837594

Willmann, J. K., Bonomo, L., Testa, A. C., Rinaldi, P., Rindi, G., Valluru, K. S., … Gambhir, S. S. (2017). Ultrasound Molecular Imaging With BR55 in Patients With Breast and Ovarian Lesions: First-in-Human Results. *Journal of Clinical Oncology*, *35*(19), 2133–2140. https://doi.org/10.1200/JCO.2016.70.8594

Wolf-Yadlin, A., Kumar, N., Zhang, Y., Hautaniemi, S., Zaman, M., Kim, H.-D., … White, F. M. (2006). Effects of HER2 overexpression on cell signaling networks governing proliferation and migration. *Molecular Systems Biology*, *2*, 54. https://doi.org/10.1038/msb4100094

Wolf, A. A., Jobling, M. G., Wimer-Mackin, S., Ferguson-Maltzman, M., Madara, J. L., Holmes, R. K., & Lencer, W. I. (1998). Ganglioside structure dictates signal transduction by cholera toxin and association with caveolae-like membrane domains in polarized epithelia. *The Journal of Cell Biology*, *141*(4), 917–27. https://doi.org/10.1083/JCB.141.4.917

Wolff, R. A., Dobrowsky, R. T., Bielawska, A., Obeid, L. M., & Hannun, Y. A. (1994). Role of ceramide-activated protein phosphatase in ceramide-mediated signal transduction. *The Journal of Biological Chemistry*, *269*(30), 19605–9. Retrieved from

http://www.ncbi.nlm.nih.gov/pubmed/8034729

Wu, C., Lai, C. F., & Mobley, W. C. (2001). Nerve growth factor activates persistent Rap1 signaling in endosomes. *The Journal of Neuroscience : The Official Journal of the Society for Neuroscience*, *21*(15), 5406–16. https://doi.org/21/15/5406 [pii]

Wu, J. (2002). Theoretical study on shear stress generated by microstreaming surrounding contrast agents attached to living cells. *Ultrasound in Medicine and Biology*, *28*(1), 125–129. https://doi.org/10.1016/S0301-5629(01)00497-5

Wu, J., & Nyborg, W. L. (2008). Ultrasound, cavitation bubbles and their interaction with cells. *Advanced Drug Delivery Reviews*, *60*(10), 1103–1116. https://doi.org/10.1016/j.addr.2008.03.009

Yang, F., Gu, N., Chen, D., Xi, X., Zhang, D., Li, Y., & Wu, J. (2008a). Experimental study on cell self-sealing during sonoporation. *Journal of Controlled Release : Official Journal of the Controlled Release Society*, *131*(3), 205–10. https://doi.org/10.1016/j.jconrel.2008.07.038

Yao, B., Zhang, Y., Delikat, S., Mathias, S., Basu, S., & Kolesnick, R. (1995). Phosphorylation of Raf by ceramide-activated protein kinase. *Nature*, *378*(6554), 307–310. https://doi.org/10.1038/378307a0

Yoshida, S., Hoppe, A. D., Araki, N., & Swanson, J. A. (2009). Sequential signaling in plasma-membrane domains during macropinosome formation in macrophages. *Journal of Cell Science*, *122*(18), 3250–3261. https://doi.org/10.1242/jcs.053207

Yoshida, Y., Kinuta, M., Abe, T., Liang, S., Araki, K., Cremona, O., … Takei, K. (2004). The stimulatory action of amphiphysin on dynamin function is dependent on lipid bilayer curvature. *The EMBO Journal*, *23*(17), 3483–3491. https://doi.org/10.1038/sj.emboj.7600355

Yu, A., Olosz, F., Choi, C. Y., & Malek, T. R. (2000). Efficient Internalization of IL-2 Depends on the Distal Portion of the Cytoplasmic Tail of the IL-2R Common -Chain and a Lymphoid Cell Environment. *The Journal of Immunology*, *165*(5), 2556–2562. https://doi.org/10.4049/jimmunol.165.5.2556

Yu, C., Nwabuisi-Heath, E., Laxton, K., & Ladu, M. J. (2010). Endocytic pathways mediating oligomeric Abeta42 neurotoxicity. *Molecular Neurodegeneration*, *5*, 19. https://doi.org/10.1186/1750-1326-5-19

Zeineddine, R., & Yerbury, J. J. (2015). The role of macropinocytosis in the propagation of protein aggregation associated with neurodegenerative diseases. *Frontiers in Physiology*, *6*, 277. https://doi.org/10.3389/fphys.2015.00277

Zha, X., Pierini, L. M., Leopold, P. L., Skiba, P. J., Tabas, I., & Maxfield, F. R. (1998). Sphingomyelinase treatment induces ATP-independent endocytosis. *The Journal of Cell Biology*, *140*(1), 39–47. Retrieved from http://www.ncbi.nlm.nih.gov/pubmed/9425152

Zhang, Y., Li, X., Becker, K. A., & Gulbins, E. (2009). Ceramide-enriched membrane domains—Structure and function. *Biochimica et Biophysica Acta (BBA) - Biomembranes*, *1788*(1), 178–183. https://doi.org/10.1016/J.BBAMEM.2008.07.030

Zhang, Y., Yao, B., Delikat, S., Bayoumy, S., Lin, X. H., Basu, S., … Kolesnick, R. (1997). Kinase suppressor of Ras is ceramide-activated protein kinase. *Cell*, *89*(1), 63–72. Retrieved from http://www.ncbi.nlm.nih.gov/pubmed/9094715

Zhao, L., Feng, Y., Shi, A., Zong, Y., & Wan, M. (2015). Apoptosis Induced by Microbubble-Assisted Acoustic Cavitation in K562 Cells: The Predominant Role of the Cyclosporin A-Dependent Mitochondrial Permeability Transition Pore. *Ultrasound in Medicine & Biology*, *41*(10), 2755–2764. https://doi.org/10.1016/j.ultrasmedbio.2015.05.021

Zhu, Z., Wang, J., Sun, Z., Sun, X., Wang, Z., & Xu, H. (2013). Flotillin2 Expression Correlates with HER2 Levels and Poor Prognosis in Gastric Cancer. *PLoS ONE*, *8*(5), e62365. https://doi.org/10.1371/journal.pone.0062365

Zimmerberg, J., & Kozlov, M. M. (2006). How proteins produce cellular membrane curvature. *Nature Reviews Molecular Cell Biology*, *7*(1), 9–19. https://doi.org/10.1038/nrm1784